CRANFIELD UNIVERSITY

ADEYINKA ADEBAYO

CHARACTERISATION OF INTEGRATED WAAM AND MACHINING PROCESSES

SCHOOL OF APPLIED SCIENCES

PhD THESIS

Academic Year: 2010 - 2013

Supervisors:

Dr Jörn Mehnen

Dr Xavier Tonnellier

December 2013

CRANFIELD UNIVERSITY

School of Applied Sciences

PhD Thesis

Academic Year 2010 - 2013

ADEYINKA ADEBAYO

CHARACTERISATION OF INTEGRATED WAAM AND MACHINING PROCESSES

Supervisors:
Dr Jörn Mehnen
Dr Xavier Tonnellier

December 2013

This thesis is submitted in fulfilment of the requirements for the degree of Doctor of Philosophy

© Cranfield University 2013. All rights reserved. No part of this publication may be reproduced without the written permission of the copyright owner.

ABSTRACT

This research describes the process of manufacturing and machining of wire and arc additive manufactured (WAAM) thin wall structures on integrated and non-integrated WAAM systems. The overall aim of this thesis is to obtain a better understanding of deposition and machining of WAAM wall parts through an integrated system. This research includes the study of the comparison of deposition of WAAM wall structures on different WAAM platforms, namely an Integrated SAM Edgetek grinding machine, an ABB robot and a Friction Stir Welding (FSW) machine. The result shows that WAAM is a robustly transferable technique that can be implemented across a variety of different platforms typically available in industry.

For WAAM deposition, a rise in output repeatedly involves high welding travel speed that usually leads to an undesired humping effect. As part of the objectives of this thesis was to study the travel speed limit for humping. The findings from this research show that the travel speed limit falls within a certain region at which humping starts to occur.

One of the objectives of this thesis was to study the effect of lubricants during sequential and non-sequential machining/deposition of the WAAM parts. Conventional fluid lubricants and solid lubricants were used. In addition, the effect of cleaning of deposited wall samples with acetone was also studied. A systematic study shows that a significant amount of solid lubricant contamination can be found in the deposited material. Furthermore, the results indicate that even cleaning of the wire and arc additive manufactured surfaces with acetone prior to the weld deposition can affect the microstructure of the deposited material.

Keywords:

Wire and arc additive manufacturing, additive manufacturing, machining, solid lubricants, microstructure

to the glory of Jesus Christ

for His faithfulness and unconditional mercy

ACKNOWLEDGEMENTS

The support and guidance from Dr Jörn Mehnen and Dr Xavier Tonnellier are greatly acknowledged. Their experience helps in the completion of this research. I also want to acknowledge Professor David Stephenson and Dr Ian Walton for their support during the earlier stage of this project. Acknowledge to the Education Trust Fund (ETF) in Nigeria for the sponsorship of my doctoral studies. My appreciation goes to Ekiti state University, Ado ekiti, Nigeria for graciously releasing me to pursue this PhD research.

Gratitude is extended towards the academic staff of Welding Engineering Research Centre at Cranfield University, in particular Professor Stewart Williams, Dr Fude Wang, Dr Jialou Ding and Dr Pedro Almeida for their assistance. Thanks to the technical staff especially Flemming Nielsen, Brian Brooks of Welding Engineering Research Centre (WERC), Andrew Dyer of microstructural laboratory. I would also like to thank Paul Wakefield and Brian Atkinson over in Building 57 for their advice, contribution, and practical assistant.

I would like to specifically thank all my family members, Mr Gbenga Olaniyan, Mrs Juliet Olaniyan, Gbola Adebayo, Bukkie Adebayo, Tunji Adebayo and my dad, Pa Bisi Adebayo for their unfailing support throughout the duration of this research.

My sincere love to my wife, Bukola and my beautiful children, Inioluwa and Oluwadarasimi, for their love and support. To my late mother, Mrs Grace Ayoola Adebayo, you are appreciated.

Finally, I want to thank God almighty for the courage and the privilege to complete this course.

TABLE OF CONTENTS

LIST OF FIGURES

LIST OF TABLES

LIST OF ABBREVIATIONS

AFM	Abrasive Flow Machining
ANSI	American National Standards Institute
AM	Additive Manufacturing
ALM	Additive Layer Manufacturing
WAAM	Wire and Arc Additive Manufacturing
BCM	Beaded Cylinder Morphology
CAD	Computer Aided Design
CMM	Coordinate Measurement Machine
CMT	Cold Metal Transfer
CNC	Computer Numerical Control
CO_2	Carbon Dioxide
DOE	Design Of Experiment
DMD	Direct Metal Deposition
EBM	Electron Beam Melting
FFF	Free Form Fabrication
FSW	Friction Stir Welding
GMAW	Gas Metal Arc Welding
GTAW	Gas Tungsten Arc Welding
HAZ	Heat Affected Zone
HEDG	High Efficiency Deep Grinding
HLM	Hybrid Layer Manufacturing
LBM	Layer Based Machining
LEM	Laminated Engineering Materials
LM	Laser Melting

LSL	Lower Specification Limit
LW	Laser Welding
MoS_2	Molybdenum Disulphide
MQL	Minimum Quantity Lubrication
MQSL	Minimum Quantity Solid Lubrication
MR	Material Removal
PAW	Plasma Arc Welding
PBAM	Powder Based Additive Manufacturing
PD	Plasma Deposition
RM	Rubber Moulding
RSM	Response Surface Methodology
RUAM	Ready to Use Additive Manufacturing
SAM	Super Abrasive Machining
SAW	Submerged Arc Welding
SDM	Shape Deposition Manufacturing
SEA	Systematic Experimental Approach
SEM	Scanning Electron Microscope
SFF	Solid Freeform Fabrication
SL	Stereo Lithography
SLS/M	Selective Laser Sintering/Melting
SMD	Shaped Metal Deposition
SMS	Selective Metal Sintering
SR	Sculpturing Robot
SW	Surface Waviness
SWIFT	Solvent Welding Freeform Fabrication Techniques
TIG	Tungsten Inert Gas-Welding

UAM	Ultrasonic Additive Manufacturing
USL	Upper Specification Limit
UTM	Untempered Martensite
VH	Vickers Hardness
WAAM	Wire and Arc Additive Manufacturing
WERC	Welding Engineering Research Centre
2D	Two-Dimensional
3D	Three-Dimensional

LIST OF PARAMETERS AND CONSTANTS

AR	Aspect Ratio
Cp	Process Capability
Cpk	Process Capability Index
CTWD	Contact Tip To work Distance (mm)
EWW	Effective Wall Width (mm)
EWH	Effective Wall Height (mm)
H	Bead Height (mm)
HI	Heat Input (J/mm)
I	Current (A)
LSL	Lower Specification Limit
MRH	Material Removal Height (mm)
MRW	Material Removal Width(mm)
Ra	Average Surface Roughness (µm)
Rq	Root Mean Square in Surface Roughness (µm)
Rt	Maximum Profile Height In Surface Roughness (µm)
S1	Wall Side No 1 (mm)
S2	Wall Side No 2 (mm)
S3	Wall Side No 3 (mm)
S4	Wall Side No 4 (mm)
SW	Surface Waviness (µm)
TS	Travel Speed (m/min)
USL	Upper Specification Limit
VI	Volt-Ampere Characteristic
V	Voltage (V)

W	Bead Width (mm)
Wa	Average Waviness (µm)
WD	Wire Diameter (mm)
WFS	Wire Feed Speed (m/min)

Publications

The following documents have been produced from this dissertation:

Adebayo, A., Mehnen, J., and Tonnellier, X. (2012), Limiting Travel Speed in Additive Layer Manufacturing, in: Proceedings of the 9th International conference on Trends in Welding Research, Chicago, Illinois, USA, June 4-8, 2012, pp. 1038-1044. DOI: 10.1177/0954405413502025.

*Adebayo, A., Mehnen, J., and Tonnellier, X., (2013), Effects of solid lubricants on wire and arc additive manufactured structures, Institution of mechanical engineers (IMechE), Part B: Journal of Engineering Manufacture.

*Accepted for publication in the Institution of Mechanical Engineers (IMechE), Part B: Journal of Engineering Manufacture for publication.

1 Introduction

1.1 Research Background

As an economic phenomenon, globalisation has led to intense competition among manufacturing companies. This means that in order to maintain a leading position in the market, the production of components have to be improved in terms of quality and material utilisation. Other manufacturing constraints such as cleaner environment, manufacturing cost implication, legislation and improved material usage have also led to the idea of Additive Manufacturing (AM).

AM can be regarded as a concept for direct production of components in a range of materials such as steel, aluminium, plastic and titanium. This is a process where parts are created from 3D CAD data by adding material layers upon layers. This is opposed to subtractive manufacturing methodologies such as traditional machining. ‘’AM is also known as Additive Layer Manufacturing (ALM), Rapid Prototyping (RP), Direct Material Deposition (DMD), Free Form Fabrication (FFF), Hybrid Layer Manufacturing (HLM)’’ (Kruth et al., 1998).

AM techniques can be classify by the type of the heat sources such as Laser Melting (LM), Ultrasonic Additive Manufacturing (UAM), Electron Beam Melting (EBM), Plasma Deposition (PD), and Gas Metal Arc Welding (GWAM). Powder Based Additive Manufacturing (PBAM) and Wire and Arc Additive Manufacturing (WAAM), which is the Wire Based Additive Manufacturing (Bautfeld and Biest, 2009) are the two main material feeding ways. Collective issues for all the PBAM are that it requires a support structure while the structures that are not vertical are to be build and low deposition rate (Levy et al., 2003). The wire based aims at overcoming these characteristic problems because of its deposition rate which can be far higher and having virtually no restriction concerning the size of the part to be manufactured. This thesis is based on the WAAM technique.

WAAM is an aspect of additive manufacturing in which metallic components are manufactured by welding beads in a layer-by-layer manner (see Figure 1-1).

Figure 1-1: Additive Manufactured part

‘’Typical wire based welding methods such Gas Metal Arc Welding and Gas Tungsten Arc Welding are low-slung cost solutions employed as heat source providing high deposition rate by using high energy response’’ (Ding et al., 2011). The demand for WAAM has been on the increase over the past years. A study in the Wohler’s report 2010 reported that the request for products and services from AM technology has been robust for more than twenty years (Wohlers, 2010). This is because of its innovative, flexibility as this procedure allows the manufacture of large custom-built metal workpiece with high deposition rate, and high quality welds at much faster rate. The technology assists to accomplish enormous savings such as decrease in metal waste, and this reduced the removal of tooling cost (Wohlers, 2010). The complete avoidance of tooling in AM techniques offers design freedom and helps the design process to be further flexible (Karunakaran et al., 2010).

The geometrical independence and greater liberty seems to be the most attractive feature of AM process; undercut, overhangs, free forms, as well as elementary shapes can be easily produced. This high flexibility opens the way to both small lot and in particular mass production (Levy et al., 2003). The combination of geometric freedom and mass customisation give an excellent prospect for medical applications (teeth, bone, supports, implants etc.). However,

the geometrical freedom of some processes is still somewhat restricted by the need to provide and remove support structures underneath the part and within internal cavity. With welding deposition process in which the final net geometry is derived from machining thereby, making the physical geometries of the AM part produced important. Knowledge of this physical geometry is vital to attain a precise and acceptable part. This also contributes to the level of material utilisation achieved during machining. Arriving at the accurate contour profile shape of the coarse slice AM parts is difficult for that, machining operations are required to achieve the desired accuracy (Karunakaran et al., 2010). Studying the effects of machining of this AM structure on the surface integrity and the mechanical properties is of great importance especially for the integration process of sequential and non-sequential deposition and machining using a single optimised system. Sequential deposition and machining being the process by which the material will be machined after few layers of deposition.

Since both AM and machining have their own respective strengths and weaknesses, it is beneficial to achieve the benefits of the two processes in an integrated environment. This could allow complex geometries to be manufactured with improved accuracy and surface finish (Kulkarni. and Dutta, 2000). The deposition and material removal operation on an integrated machine in addition to both sequential and non-sequential deposition during machining could be very beneficial but needs more in depth research and this is one of the objectives of this study.

Many problems caused through machining are due to the generation of heat and subsequent high temperature associated with machining (Wang and Rajurkar, 1999). The high temperature associated with workpiece can also be an advantage and it is discovered that less power is needed to machine metals at high temperature in comparison to that at room temperature (Karunakaran et al., 2010). This is due to the reduced shear strength in the metal caused by the increase in the temperature. The benefits of such a method is anticipated to result

from either two effects: the tempering and weakening of materials at high temperature or evading the change of metastable material such as austenitic manganese steel, wherein transformation is usually induced by the work of machining. It is worth investigating the effects of machining on the sequential and not sequential machining of WAAM parts using dry and solid lubricant to see its viability, which can resolve the issue of machining the inner cavities of parts.

Cutting fluids help to lubricate the machining zone thus reducing the friction between the machining tool and the work piece and decreasing the amount of frictional heat being generated. It also helps to cool the machining zone by removing some of the generated heat. However, cutting fluids also come with several disadvantages. Significant potential health and safety risks and government legislations force companies to reduce the toxicity of all waste including cutting fluids being returned to the environment and to increase the biodegradability of their waste products (Bart, 1998). In addition, cutting fluids make a major portion of total manufacturing cost (see Figure 1-2).

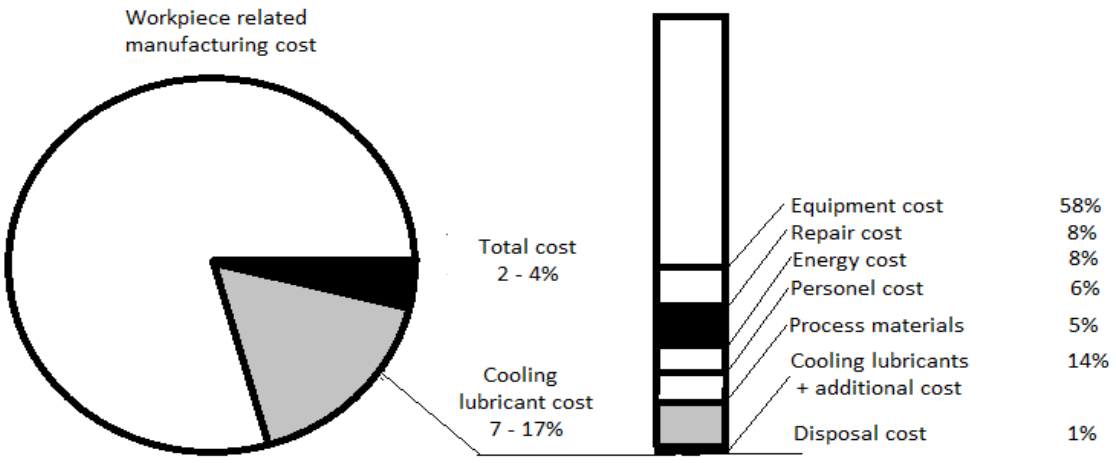

Figure 1-2: Example of total cost of workpiece manufacture (Adopted from Klocke and Eisenblätter, 1997)

The cutting fluid can also result in serious and costly damage (i.e. fire risk) to the machines) as well as posing a serious risk to individuals.

Consequently, there is a real and immediate need to either eliminate or significantly reduce the risk of cutting fluid ignition. The manufacturing sector is confronted with the prospect of monetary punishments and even market marginalisation (Koc, 2007) if it is unsuccessful in meeting the growing eco-friendly standards through a specific attention on controlling of chemical wastes.

Manufacturing Industries have reacted by adapting and developing different manufacturing methods with the aim to be legitimately compliance and economical in the face of growing costs of natural resources and waste management. As an alternative to cutting fluid, solid lubricants such as graphite, molybdenum disulphide are being currently used. These have no pathogenic history and hence do not pose any health hazard to workers (Krishna et al., 2011). The general idea of one of the objectives of this thesis reflects the scope for dry lubrication and minimum quantity solid lubrication (MQSL) in the machining of manufactured parts by means of wider commitment in manufacturing sectors in order to accomplish further justifiable and environmentally accountable manufacturing. The push towards minimum quantity solid lubrication method within industry is continuously progressing in popularity (see Figure 1-3) (Weinert et al., 2004).

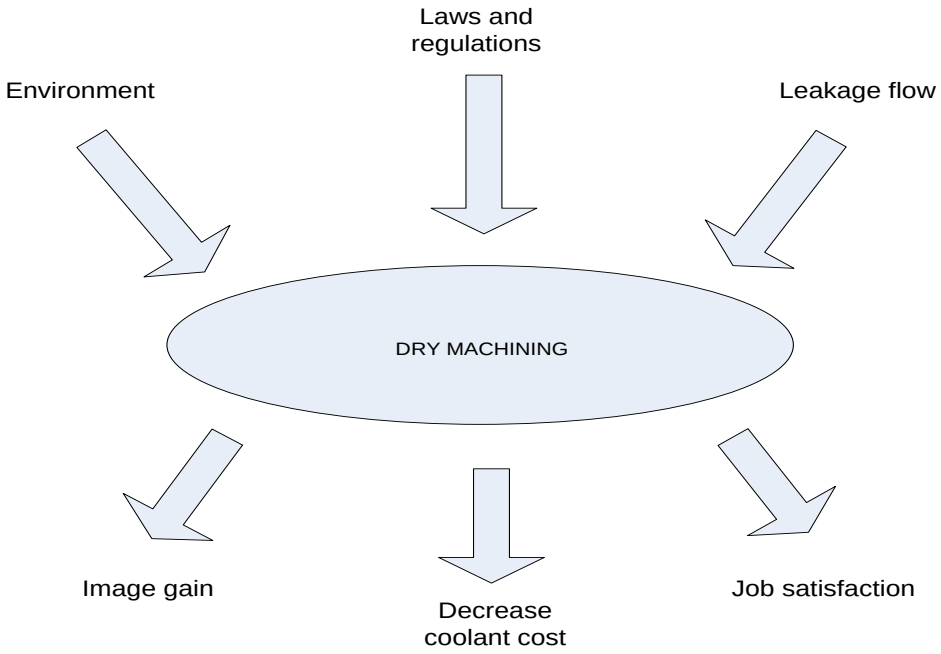

Figure 1-3: Benefits of dry machining (Adopted fromWeinert, 2004)

The benefit of minimum quantity solid lubrication will only be recognised if there are no detrimental effects on the surface. The decrease of considerable exposure to cooling lubricants at the workplace increases job satisfaction and improves the work effect at the same time. Moreover, an enterprise can use economically friendly production procedures for marketing purposes, which will leads to an improved image in the market. Conclusively, it is necessary to explore the possibility of using dry and solid lubricants in machining of WAAM parts, emerging upon the current minimum quantity lubrication philosophies to establish a steady and dependable machining method.

1.2 Thesis Outline

The work carried out during the research project is presented in this thesis in nine chapters. This outline describes a brief idea of each chapter of this thesis.

Chapter 1

This chapter gives an insight into the background and the general introduction to this research.

Chapter 2

This is the literature review, which highlights the main areas of research conducted in AM. Machining of WAAM parts, sequential and non-sequential machining of WAAM part with the various lubricants used in machining was also reviewed.

Chapter 3

Chapter 3 discusses the aim and objectives of the project, research methodology employed with the scope. Also shown in the chapter is the research structure of the study.

Chapter 4

This chapter describes the various machines and the machine set-ups employed to achieve the project objectives. It also includes the metrology and measuring instrument used.

Chapter 5

Chapter 5 introduces a process study of WAAM deposition with comparison of three different WAAM platforms.

Chapter 6

This chapter focuses on deposition process behaviour arising from WAAM depositing which include the study on humping and the WAAM bead geometries.

Chapter 7

This chapter focuses on aspect of the study of sequential and non-sequential machining of WAAM using solid lubricant and convectional fluid lubricant. It also describes the effective wall width during machining.

Chapter 8

Summary of the overall discussion of this study.

Chapter 9

This chapter summarises the important findings of this thesis and identifies some potential areas for further research.

2 Literature Review

2.1 Overview

The purpose of this chapter is to review the existing literature and the understanding of the Additive Manufacturing (AM) processes and machining aspect from both the academia and industrial point of view. The principles of Wire and Arc Additive Manufacture (WAAM) and machining were studied in parallel with the aim of identifying the knowledge gap to control the WAAM and machining processes. Various types of AM deposition processes were also discussed with the fundamental motives for lubricating the machining process. The chapter contains:

- Types of AM processes and techniques
- An insight into the machining of additive manufacturing structures with the function of machining fluids, its merit, demerits, and legislation. The knowledge behind Minimum Quantity Lubrication (MQL), which includes the overview of solid lubricants.

2.2 Additive Manufacturing

AM is the method of manufacturing parts by welding of material layers upon layers instead of the removal of material, as is the case with conventional machining (Levy et al., 2003).

Every layer is deposited to the same geometry via a 3D CAD program. AM permits parts with very intricate geometries to be manufactured without producing any form of tools or fixtures and devoid of producing waste materials. Many advantages such as reduced material waste due to low lead-time can remove numerous intermediate stages of conventional manufacturing (Kruth et al., 1998). More so it gives room to manufacturing heterogeneous structure giving distinctive design benefit (Levy et al., 2003).

Hereafter, selecting an AM technology for manufacture provides unlimited benefits for the whole production value chain. The geometrical sovereignty permits for designing parts as being envisaged without manufacturing constraints. This is due to the extreme lightweight designs and reduced part counts. It is also a fast production route from CAD to physical part with a very high material utilization and without the need to keep expensive casting or forging in stock.

In addition to the cost efficiency, AM provides good material utilization, a very energy-resourceful and environmental approachable manufacturing way and a near net shape after machining. Among the significant use of AM are in the cooling of the wings of the duct of A380, thin walled assemblies in the blades of turbine and lightweight structures in F-1 vehicles (Kruth et al., 1998). Graded structure and microstructures can be got through AM. The AM technique will possibly decrease material anisotropy. Certainly, thick material is frequently anisotropic because of dissimilar microstructures. This is because of dissimilar cooling methods that are ideal with the circumstance that work does not affect uniformly in thick segments (Wohlers, T. 2010).

2.2.1 Powder Based Processes

Many commercial solutions are obtainable for the powder-centered method. For example, the Direct Metal/Material Deposition (DMD), Selective Metal Sintering (SMS), and Stereo-Lithographic sintering (Kruth et al., 1998). These method use laser or electron beam (see Figure 2-1) as a heat source and has an extensive use in aerospace, medical apparatus and automobile industry.

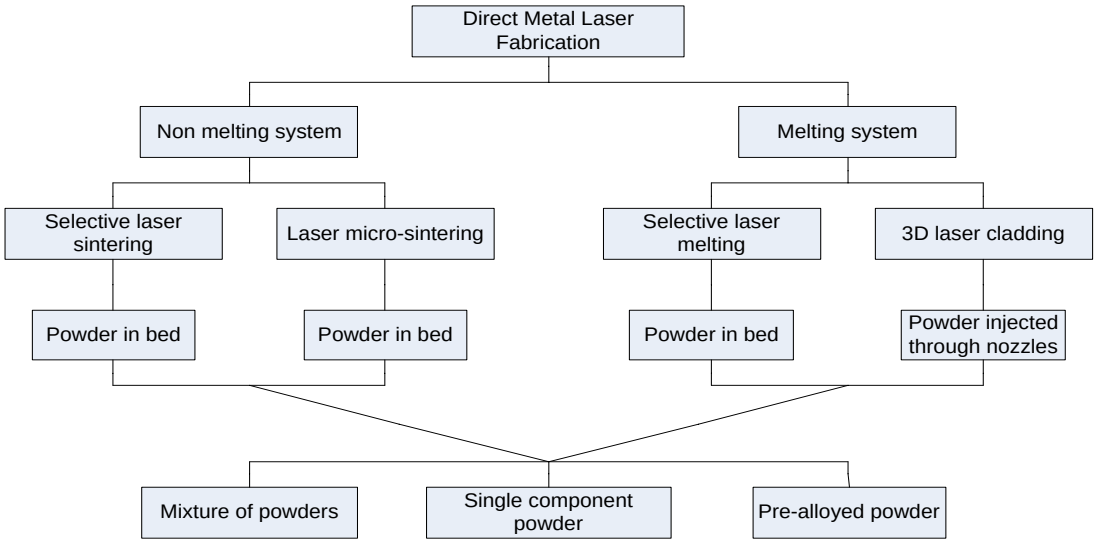

Figure 2-1: Main techniques of Direct Laser Deposition (Adopted from Santos et al., 2006)

The major advantage of the powder based methods are the precision, accuracy and surface finish obtained in some situations are near to machined surfaces (Choi and Chang, 2005). Porosity problems have been stated in Selective Metal Sintering, which is because of the porosity in the powder. However, to improve the density of the product, heat treatment is essential. Lately distinct powders were developed in order to remove the prerequisite of heat treatment, though there have been problems involving mechanical properties of not being consistence in all ways (Rombout et al., 2006).

According to Choi and Chang, (2005) the Direct Metal/Material Deposition process window, for manufacturing components through reliable geometrical stability and mechanical properties, is slim. However, to get improved mechanical properties and reduce the residual stresses, the substrate is preheated. Furthermore, with the increase in the powder feed rate there is likelihood of formation of pores, which restricts the rate of deposition for the process (Choi and Chang, 2005). Further difficulties with this method are that certain amount of powder is squandered per component that also depends on the size, shape and

the process used for the components. Besides, there is a potential risk of inhaling the powder during the process.

2.2.2 Wire Based Processes

Studies and development have been done in Laser based wire feeding method because of the benefits such as high surface finish, precision level, and integrity. Syed et al., (2005) reported that the stability in the method could be further enhanced by means of camera based response controllers and feed forward compensators. Laser wire has a more efficient deposition rate with good surface finish than Laser powder methods when using cladding and the same author reported this. Moreover, it has certain restrictions for example lesser rates of deposition and the variety of wall widths in which they could be utilised in comparison to arc welding methods. Besides, columnar grains were found using the high power lasers in aerospace materials, and it affects undesirably the consistency in the mechanical properties (Baufeld and Biest, 2009).

To increase the deposition rate and mechanical properties other welding processes such as Gas Tungsten Arc Welding (GTAW), Plasma Arc Welding (PAW), and Tungsten Inert Gas Welding (TIG) have been studied. It was established that Tungsten Inert Gas Welding resulted in improved deposition rates and broader wall thicknesses varieties when compared to Laser is detriment to surface finish and distortion (Baufeld and Biest, 2009). Gas Tungsten Arc Welding has showed to be a superior possibility in relation to deposition rate and thickness range, besides with lesser distortion level as compared to TIG Welding (Cao et al., 2009). Though the surface waviness are greater than Laser and other arc welding processes stated, hereafter machining operations for instance milling and grinding are necessary on the deposited bead. Restriction of surface waviness is reduced by means of Cold Metal Transfer method and rolling. Cold Metal Transfer is a cutting-edge dip transfer method wherein metals are deposited in the molten pool owing to surface tension. An even bead profile is produced causing less surface waviness, fewer heat input resulting in low

distortion and improved mechanical properties (Cao et al., 2009). Table 2-1 illustrates the benefits and disadvantages of various AM processes.

Table 2-1: Benefits and disadvantages of AM processes Adopted from (Lorant, 2010)

	ADVANTAGES	DISADVANTAGES
Direct Laser Deposition	- Good surface finish	- Depends on the quality of powder - Positioning of the part in the bed has an impact - The bed dimensions limit the part size - The rate of production is low: 50g/hour - Great investments
Electron Beam Freeform Fabrication	- Can be used for conductive metals and reflective alloys - Good mechanical properties	- Poorer surface finish than parts built by Direct Laser Deposition - High investments
TIG based Additive Layer Manufacturing	- Possibility to weld super alloys - Making large components possible - Fast Additive Manufacturing process	- Not as accurate as Electron Beam Freeform Fabrication and Direct Laser Deposition

Over the past years, a number of studies have investigated the utilisation of arc welding methods, *i.e.* GTAW and GMAW, which is aimed at the near net shape processing of 2-Dimentional and 3-Dimensional metal parts in addition to good material properties. In view of this, WAAM has received distinctive consideration since it has an advantage over the traditional manufacturing techniques (Lorant, 2010). WAAM methods have the potential for unswervingly manufacturing of

huge volume manufacturing chunks with high structural integrity at high production rate, and at a greatly reduce cost.

2.3 WAAM bead geometries

The important role played by the welding parameters and the weld bead dimensions in determine the weld wall thickness and its influence on the Effective Wall Width (EWW) (which the amount of material that will be left after machining) during machining was highlighted by Dickens *et al.* (1992). The also discusse the effects on the surface quality of the part manufactured and conducted a variety of single beads with one variable at a time experimental method. However, the main aim of this study stood to create an experimental and efficient knowledge base aimed at the connection in-between weld bead geometries and the key welding parameters. Selected parameters used in the investigation were the travel speed (TS), wire diameter (WD), wire feed speed (WFS), contact tip to work distance (CTWD) and voltage, the outputs measured were bead width (W) and bead height (H). The result of this study showed WD and WFS have encouraging outcome on the W and H though higher TS had a negative impact. Dickens *et al.* (1992) recommended that more studies be required to evaluate the impact of the relationship among geometric features and process variables in a multi-layered part.

The feature of a weld is influenced by the weld input parameters throughout the welding process consequently welding can be well-thought-out as a multi-input multi-output process. Unfortunately, a major setback encountered by industrialists is to find a control of the process inputs to get a good weld deposition with necessary bead geometries and weld superiority with slight damaging residual stresses and distortion (Farad and Mehdi, 2011).

Bead geometries are important characteristics of AM part. According to Bradstreet (1989),the cooling rate of a weld can be predicted from the weld cross sectional area and the arc-travel rate. The bead cross sectional area with its

height and width affects the shrinkage, which controls mostly the residual stresses and the distortion (Shumovsky, 1952).

Moreover, the weld bead consequences from the solidification of liquid metal, surface tensions play a significant role in defining the ultimate bead geometry. App et al., (1963) reported from their studies on submerged arc welding that several welding parameters such as travel speed and current influence the bead shape and size. Gurev and Stout, (1993) observed in metal inert gas welding that the bead width increases with increasing heat input into the work i.e with either decreasing arc-travel rate or with increasing current. It was also shown that under-cutting of weld bead was associated with high arc-travel rate. He also studied the effect of metal transfer characteristics on bead geometry. Under conditions of spray transfer, an increase of voltage produces increased bead width but a significant decreases in bead height, penetration and reinforcement area.

Oshima et al., (2004) stated that the weld bead quality is governed by the arc process and parameters. These factors have a vital consequence on arc welding stability and control that determines the overall end quality of the weld bead with the occurrence or non-appearance of welding imperfections and defect. Investigations have been done on the effects of arc voltage, travel speed, wire diameter, and arc current on the quality and bead geometries shape, predominantly with respect to the deposition rate and penetration. In a study by Kim et al., (2003), it established both modelling and investigational analysis on impact of voltage, travel speed and welding angle on bead on plate (GMAW), wherever the effect on bead penetration has been shown. In another study, Suben and Tusek (2002) described the effect using shielding gas combination on the quality and weld bead geometry. He also examined the imperfections in welding in relation to arc instability in short circuiting GMAW. Conclusion from this study showed that it is potentially possible to identify imperfections linked to gas shielding. Productivity controls the cost and all this depend on the travel speed,

electrode wire diameter and the welding current. However, increasing the travel speed makes the weld bead susceptible to defects and this could cause a restriction in welding processes (Mendez and Eagar 2000).

In an investigation by Almeida and Williams (2010), the influence of interaction between welding parameter with the weld bead features was evaluated by the use of both 3D and contour graph (see Figure 2.2). However, the objective of the study was to look in larger depth the impacts of the main welding deposition factors, such as TS, WFS, WD and WFS/TS on the development of bead physical characteristics.

The effects of interactions of factors such as WFS, WFS/TS and WD, on the weld bead and plate fusion characteristics of single and multi-layer deposition responses were examined using the response surface methodology (RSM). The functional relationships between parameters and weld bead characteristics were determined by the response surface models that were fitted to experimental data provided by the response surface design. The developed models were checked for their adequacy and significance, and used for simultaneous process optimisation of several responses. Authors concluded that the influence of WFS on W seems less profound when compare to the WFS/TS particularly when the values of WFS is low, as revealed in the process model chart.

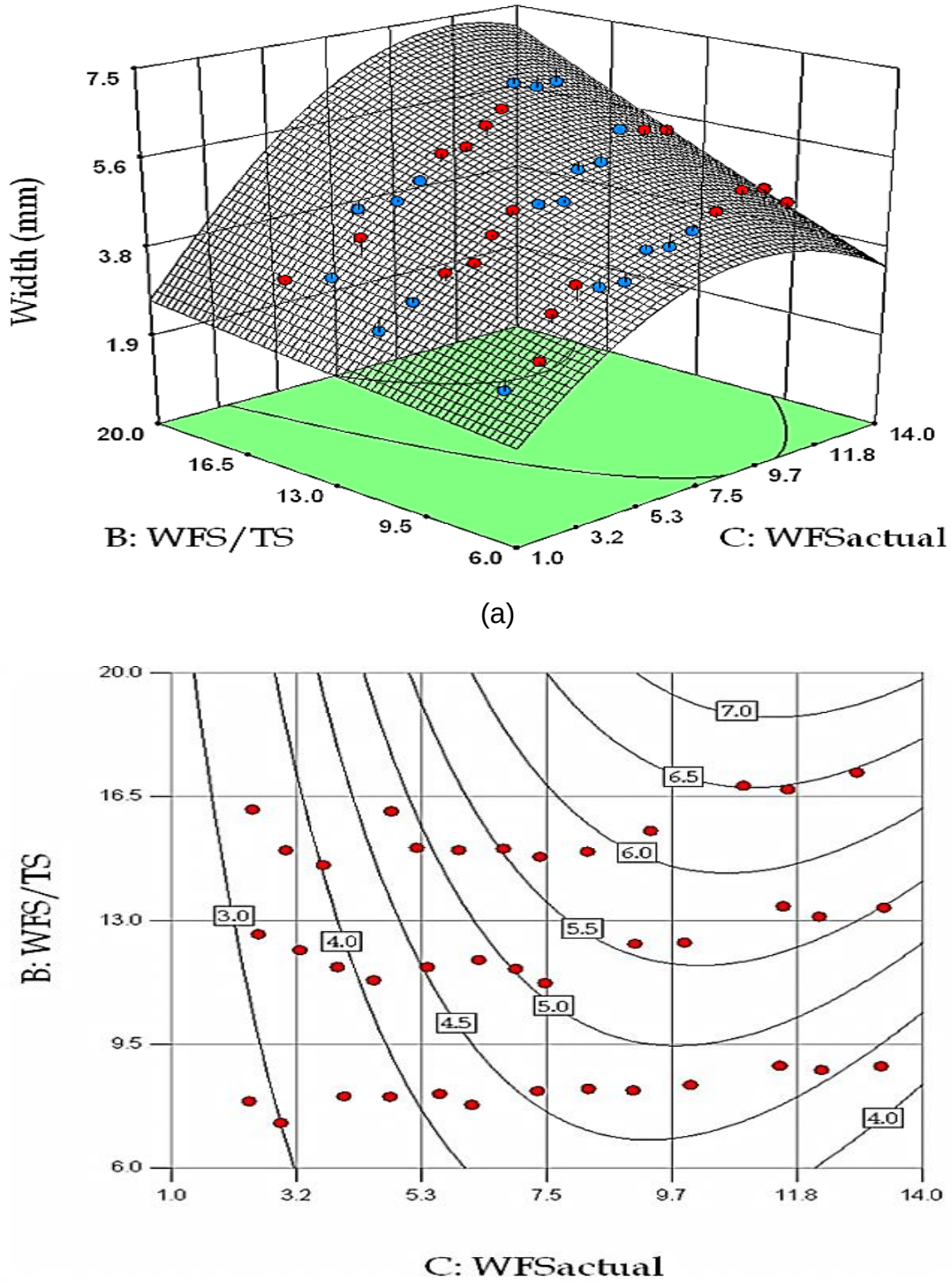

Figure 2-2: Process model Optimization chart (a) 3D response surface (left) with contour graph (b) presenting the interactions of process factors on response when using 0.8mm wire (Almeida and Williams, 2010).

2.3.1 Weld imperfections and defects

Welding processes are liable to imperfections and defects. If the quality of the weld bead is in contradiction of the structural integrity, it is considered a defect, otherwise it is an imperfection. Mendez and Eagar, (2000) identify cracking, porosity, inclusions, excessive convexity, and humping, undercutting and uncompleted fusion as the key imperfections in arc welding. The genesis of these imperfections is largely reliant on welding methods and the welding parameters; however, it can be related with the composition of the shielding gas and material selection as discussed in section 2.3.

The most important imperfections and defects related with arc welding will be discussed in the subsections.

2.3.1.1 Porosity

Porosity is generally linked with the effect of gas for the period of the solidification process of a weld bead and generally categorised as a cavity-type discontinuity. The key sources of this defect are (Hobart Institute of Welding Technology 1997):

- Insufficient flow rate of shielding gas;
- Existence of oxides with or other contaminants;
- Inappropriate parameters;
- Too much welding speed, resulting in weld pool freezing already before gases go away;
- Some presence of impurities such as phosphorus or sulphur on weld parent material.

2.3.1.2 Undercutting

The undercutting defect is generally detected in arc welding. This is characterised via a deep depression in the weld manufactured in the molten interface. Gratzket, et al., (1992), Mendez and Eagar, (2003) concluded in their studies that the undercut defects are owing to one or some of the following key reasons:

- Extreme arc voltage and welding current.
- Too much travel speed.
- Travel speed with comparatively small currents (100-250A).
- Inappropriate angles of the electrode, particularly on vertical and horizontal welds.
- The material chemical composition, specifically the materials which have sulphur contents.
- Insufficient wire feed speed.

However, there is little corrective way that is normally suggested:

- Utilisation of slower travel speed;
- Decrease in wire feed speed;
- Increase in the arc pressure effect.

The forces acting at the rearmost of the weld pool produce a thin molten layer, which gets solidified prematurely. Moreover, it will further stop the wetting features in the area affected and hence the formation of undercutting. However, decrease of travel speed would lessen recirculation flow impact in the weld pool and reduce the undercutting formation as reported by the same author.

2.3.2 Weld bead humping

Humping is a defect caused by high travel speed; it is however, the occurrence of developments of a hump on a weld bead at consistent deposition. This can

also be defined as a periodic undulation of the weld bead, with a typical sequence of undulation comprising of hump and a valley as shown in Figure 2-3. It happen due to the momentum of the back flow of the molten pool (Soderstorm and Mendez, 2006) and high welding travel speed (Nguyen et al., 2005) which can lead to an undesired humping effect.

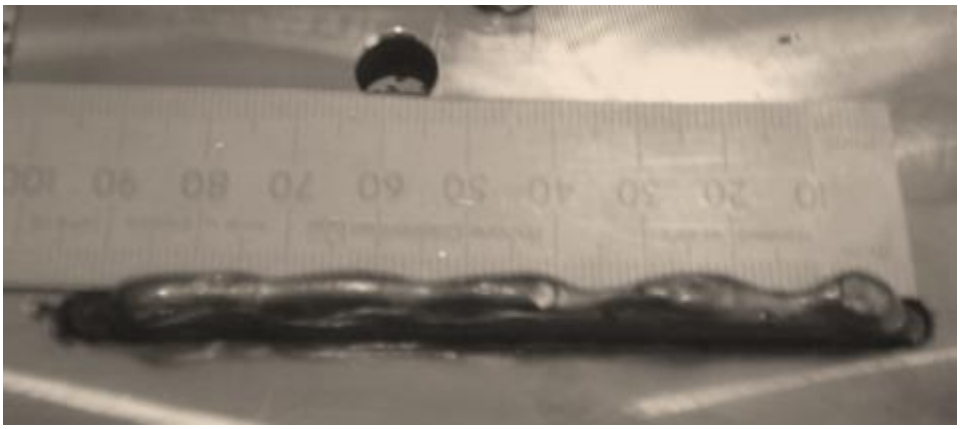

Figure 2-3: Bead humping

Some analysis of the high speed welding defects has been done from different authors with different experimentations. The first identified report was Bradstreet (1968), on humping with tunnelling. In addition, Nguyen et al., (2005) made available his study on humping process during GWAM. Many researchers have described humping as it happens. Bradstreet (1968) also observes humping when using laser welding and Nguyen (2005) reported that it has been prominent in electron beam welding.

The existence of humping restricts the choice of working welding speeds in many fusion-welding processes and stops further increase in productivity in a welding operation. At present, the physical mechanisms responsible for humping are not well understood. Thus, it is problematic to understand how to reduce humping in order to attain higher welding speed (Nguyen et al., 2005).

There are two types of Humping namely: Gouging Region Morphology (GRM) and Beaded Cylinder Morphology (BCM).

For GRM, morphology is characterised by open, unfilled dry spot in between the humped beads. Besides, the front of the weld pool exhibits a very large depression known as the gouging region. The bulk of the molten metal, which is called trailing region reside in the back of the weld pool. In some cases, two small channels appear at the walls of the gouging region. Other defects that share similarity with this humping mechanism are tunnel porosities, in which the gouging region extends under the surface of the weld and the split bead weld where the gouging region splits the weld bead longitudinally (Soderstorm and Mendez, 2006). In GRM, gouging is a result of arc forces that drives the molten pool to the tail of the arc. However, it is more frequent in GTAW because of the high-pressure arc. To minimise GRM, Soderstorm and Mendez, 2006 suggested the use of a hollow electrode tip which can lessen the arc pressure. Besides, shielding gas mixture and welding position has revealed their effects on humping. Using a downhill welding method, it could be reduced since the rear flow momentums in the molten pool are decreased through the use of gravitational force. This is however seen that reactive shielding gases resulted in considerably fewer humping when relate to the inert gases. The reason being to evade humping it is required to have a wider weld pool aimed at the same deposition, which is obtained by reactive gas mixtures (Soderstorm and Mendez, 2006).

BCM is noticeably different from GRM. Not only are the characteristics dry spot missing but also the welds show no evidence of depressions below the workpiece. The weld bead in this case has a continuous undulating aspect. In BCM, the motivating force is the decrease in the surface energy through producing a sphere formed intermittent deposition as an alternative to an uninterrupted cylindrical bead. In order to minimise this category of humping, methods similar to GRM could use. Furthermore, it was shown that increasing thermal conductivity give rise to the travel speed required to cause humping. This is as a result of preheating decreasing the molten metal tail, therefore reduction in the welding deposition(Soderstorm and Mendez, 2006).

In the study conducted by Cho and Farson (2007), it was shown the existence of two conditions responsible for humps. The earlier one is the motion brought through surface tension pinching force with the later being the untimely solidification of the molten pool which split up the molten pool in front and rear portions. This hump phenomenon is however, a defect caused by high speed welding which happens owing to backflow momentum of the molten pool. Methods to reduce the effect of hump is by utilising a downhill welding, using hollow electrodes preheating, and reactive shielding gases,(Soderstorm and Mendez, 2006).

Bradstreet (1968) reported a reliance on the arc current, voltage, travel speed shielding gas, and electrode conditions. With the parameter range investigated, undercut was mostly associated with humping. The rate of this undercut was discovered to be quite stable all along with the weld length and unchanged by the occurrence of a hump. Savage (1979) studied in detail the dependence of humping on this parameter in Gas Tungsten Arc Welding of a hardened steel of 20mm width. The important characteristic is that, for a fixed rate of the arc current, there exist a crucial travel speed over which the humping phenomenon starts. However, this literature was unable to come out with the exact travel speed limit.

In the identified literature, none discusses humping in the WAAM sector of welding and the exact travel speed limit. This establish the purpose of this study which is to study the bead geometry within the framework of establishing the travel speed limit for a good WAAM so as to control the process of achieving a good multi-layer parts.

2.4 Machining of AM Structures

The increasing awareness in additive and subtractive shaping theory which are synthesized to combine the layer manufacturing processes and material removal processes. Recently, layer based machining has emerged as a promising way of integrating additive and subtractive shaping theories.

AM has the ability to manufacture any complicated 3D physical model devoid of geometric restrictions by welding 2D layers in a specific way. Nevertheless, the surface of the AM parts is extremely rough in contrast with the general Numerical Control (NC) machined part owing to the AM process itself. This is due to the stair effect from stacking layers with various level of thickness. However, in order to improve the surface quality, more post machining like grinding or milling is necessary.

Furthermore, in considering the improvement of the surface quality of the AM part, several researchers have made some studies. Conventional finishing like the hand grinding has mostly been used for the reason that it is simple and fast. Moreover, Cobb et al., (1993) suggested using additional capable finishing methods like abrasive blasting, barrel tumbling and vibration finishing. Also, Williams and Melton (1998) established a finishing method for stereo-lithography manufactured products by means of Abrasive Flow Machining (AFM) which remove little volume of materials via flowing a semi solid abrasive-laden media through or across the workpiece. Meanwhile, in determining the special effects of Abrasive Flow Machining finishing in accordance with media grit size, media pressure, build orientation and other variables, statistical analysis was used. The outcome exhibited the key improvements remained realized through one or more Abrasive Flow Machining cycles. In other words, these machining methodologies are certainly damaging to the original part limitations and unreasonably time consuming.

Yang et al., (2002) discussed the machining-based rapid prototyping process in which the geometry of manufactured part surface is determined with machining (shaping, grinding). Other examples of machined-based rapid prototyping includes the following: Deskproto (www.deskproto.com) and this is a commercially accessible computer software developed for the use of concept modeller by CNC milling, step milling by which a model is made into thick layers which are machined independently, then contructed to form assembly. The

properties of the above machining based rapid prototyping system, with the layer machining (LBM) system are summerised in Table 2-2 [where SR is sculpturing robot, SDM is shape manufacturing, computer-aided manufacturing of laminated engineering materials (CAM of LEMs), solvent welding freeform fabrication techniques (SWIFT)].

Table 2-2: Machining based RP processes (Adopted from Yang et al., 2002a).

	Stock layer		NC machining		Stacking operation				
Process	Number	Thickness	End Effector	Degree of freedom	Cutter	Bonding method	Post assembling	Input layout	Raw material
SR	Single	NA	Robot	6	Ball-end milling	NA	NA	NURBS	Foam
SDM	Multiple	Adaptive	CNC	5	Milling cutter	Deposition	NA	ACIS	Specific material
CAM of LEMs	Multiple	Variable	CNC	5	Laser cutter	Adhesive and sintering	Registration system	STL,DXF,IGES	Metal, ceramic
SWIFT	Multiple	Uniform	CNC	3 or 5	Flat-end milling cutter	Solvent welding	NA	STL	Thermoplastic
Millit	Multiple	Uniform	CNC	3	Milling cutter	Adhesive	Registration system	STL/ DXF	Unknown
TLOM	Multiple	Adaptive	Robot	6	Flexible blade	Adhesive	Manually	NURBS	Foam
Desk Proto	Single	NA	CNC	6	Milling cutter	NA	NA	NURBS	Any milliable
Step milling	Multiple	Unknown	CNC	3	Milling cutter	Adhesive	Registration system	Unknown	Unknown
LBM	Multiple	Adaptive	Robot/ CNC	7/5	Ball-end milling cutter	Adhesive	NA	STL/ SLC	Any milliable

Yang et al., (2002) concluded that owing to the dynamic effect, Layer Based Machining (LBM) can be better used in huge objects devoid of thin wall and the investigative assesment regarding whatever models that could be manufactured with LBM is desirable.

Wall et al., (1992) evaluated computer numerically controlled (CNC) machining, stereo lithography (SL), computer aided design (CAD) modelling, and rubber moulding (RM). After comparing many aspects of model making, the authors concluded that computer numerically controlled machining was still the preferred choice for many prototyping applications. More recently, the advantage of computer numerically controlled machining compared with other prototype

making technologies were summarised by Tangelder and Vergeest, (1994) as the following:

1. Computer Numerically Controlled machining is fast, especially for large part dimensions and /or large part quantities. Relatively light, cheap and easy to cut material can be used in many cases.
2. A wide range of materials, with varying strength properties, could in practice be applied (although this may be at the expense of speed)
3. High accuracy could be obtained (at the expense of time)
4. There are in, principle, no limit on the dimensions of a part. Computer numerically controlled machining in multiple stages with different part placements is feasible.
5. Cost can be low compared with other physical prototyping technologies since many companies already have Computer Numerically Controlled devices.

Song and Chen (2001) reported that robot machining has its special properties that are not the same as traditional Computer Numerically Controlled machining:

1. Robot machining has a greater working envelop compared with traditional Computer Numerically Controlled machining.
2. Robotic machining is very reasonably affordable compare with Computer Numerically Controlled machining.
3. Robotic machining is primarily a tool positioning system. Owning to the flexible kinematic of robot arms, they are often capable of machining parts with intricate details and complex shapes.
4. The accuracy of robot machining is lower than that of traditional Computer Numerically Controlled machining. Most articulated robots have an accuracy ranging from ±0.05 to ±0.1mm. Though much lower than Computer Numerically Controlled machines, its superior to other rapid prototyping technology such as SLA, and Selective Laser Sintering (SLS) which have an accuracy of no better than ±0.1 to ±0.2mm.

5. A robot can withstand a smaller machining force than traditional computer numerically controlled machining. Therefore, due to the limited stiffness only wood, wax, foam or other similar light materials are usually processed using robot machining. Metal can be machine at low speed and with very large robots. However, the choice of material is much wider than for other Rapid prototyping (RP) technologies.

Wohler (2010) listed the common limitations for current rapid manufacturing processes to include the material variability and features, processing rate, accuracy in terms of dimension, surface finish, and geometry capability and cost effectiveness. In order to counter these limitations, more studies have been conducted into the use of Computer Numerically Controlled machines for Rapid prototyping (RP). For example, Hassold (1995) presents the prospect of using Computer Numerically Controlled machines as a rapid prototyping method. The author describes the possible benefits and limitations that researchers may come across through the application, as well as problems like cost. Chen et al., (2001) described layer based machining for RP on which they analyse a process by the means of laminated slabs of plastic, milled as separate layer and bonded to the earlier layer. Additional methodology is to utilise Computer Numerically Controlled machining for prototyping die. Nevertheless, these methods do not offer flexibility of manufacturing several parts, but they provide short run production promising with the aids of Computer Numerically Controlled machining and this have come to be part of the basics of Computer Numerically Controlled - Rapid Prototyping.

2.4.1 Deposition and machining integration

The main benefit of manufacturing a part by AM process is that the geometric complexity of the part manufactured has considerably low effect on the manufacturing method than the instance of traditional material removal (MR) processes. Furthermore, many viable additive manufacturing processes need less human involvement and setup time.

The principal disadvantage of AM with respect to MR is that the accuracy and surface finish of AM parts are not as good because of its stairways effects. In addition, current drawbacks of AM include a limited choice of material and unsuitability of the process for mass production of components (Kulkarni and Dutta, 2000).

Since both AM and MR have their own respective strengths and weaknesses, achieving the benefits of the two processes through an integrated system will be beneficial. This could allow intricate geometries to be processed with improved accuracy and surface finish with less necessity for intricate setup with fixturing arrangements.

The major advantage of integrating AM and MR for manufacturing is that the accuracy of the part can be improved**.** If the time required to deposit a layer is presumed as independent of the layer thickness, and the speed of machining is assumed greater than the speed of the deposition process, then the overall speed of the integrated AM and MR is faster than the AM process alone (Kulkarni and Dutta, 2000)

There have been few initiatives for sculpting the exterior boundary of layers to improve the surface finish of the AM part. Hope et al., (1997) consider the decomposition of the part (and its associated support structure) into manufacturable ‘compacts’. These compacts can then be fabricated using a combination of additive manufacturing and milling on a five-axis CNC machine. Their approach however does not include tool-path generation algorithms that would facilitate the path planning of this procedure.

Hope et al., (1997) also discuss the ideal of increasing part accuracy, without affecting the cutting or assembly time, by cutting layer with sloping edge that match the surface contour. They propose a system using a five-axis water jet cutter that would be able to generate slope layers, which would be layer assembled on a separate platform. Their future work include a reference to

generating not just sloped layer but curved layer by using a hot wire or thin laminate to cut the layers to match the surface curvature.

However, a new integrated method is planned that will bring together the advantage of the setup of AM with great accuracy of CNC. The process makes use of structural material in order to manufacture parts by carrying out both welding and machining on a single hybrid system. It integrates both material deposited in form of layers upon layer with material removal to arrive at the necessary surface finish. Therefore, the novel integrated method can intensely decrease the total time for the deposition and improve shape accuracy in comparison with convectional AM process. Above all, it brings to one system the ideas of AM and CNC (Hope et al., 1997).

Though robot machining is with its special properties, the problems associated with CNC machining cannot be over emphasised. One of the most noticeable limitations is that parts with hollow shapes cannot be machined (Chen and Song, 2001).

In Figure 2-4(a), as the tool attempt to mill the lowest point within the hollow, there is collision in between the wall surface and the tool holder. According to Chen and Song, (2001) in order to resolve this issue, the author presented a layer machining process in which the entire deposited part is cut up into layers (see Figure 2-4b). The lower part is milled as in Figure 2.4(c). Meanwhile the hollow on the lower is lower than that of the original deposited part, there is no collision occurring between the tool holder and the deposited wall surface. After machining of the lower layer, more layers are glued on it with the aids of homogenous glue. At that time, the machining of fresh layer can be continual with no collision as in Figure 2-4(d).

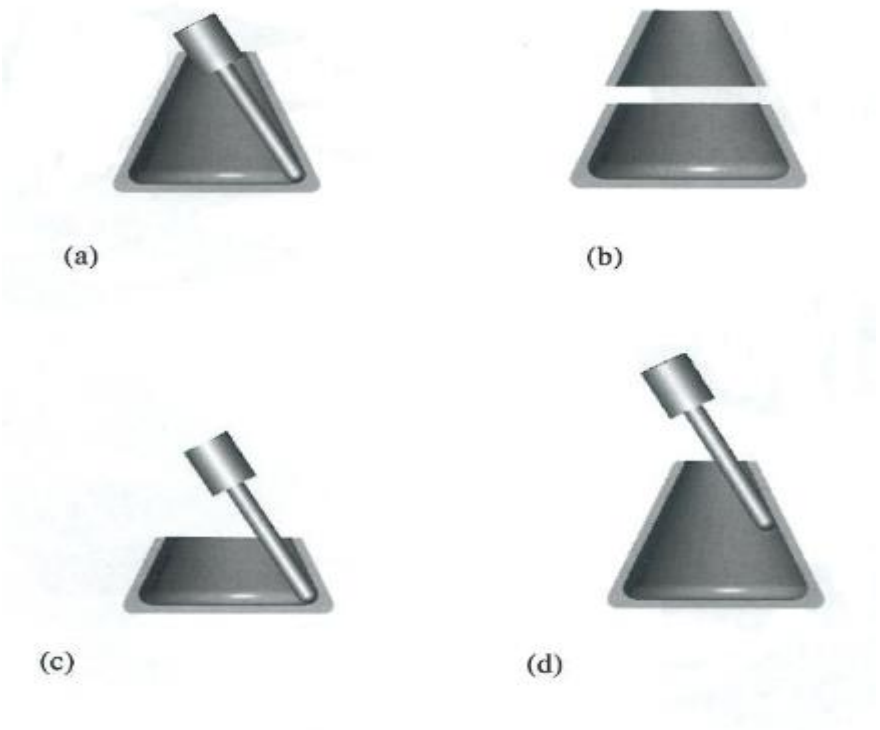

Figure 2-4: Process of deposition and layer based machining (a) tool unable to machine the inner part (b) the part was cut into two to be able to machine it (c) the inner part was machines after cutting it into two and (d) parts using glue to combine the layers (Adopted from Chen and Song, 2001).

Contrary to this idea of layer based machining, one of the aims of this research is to introduce the sequential machining and deposition in the building of parts using AM process. This involves no adhesive as done by the previous researcher. Instead of adhesive, deposition operation will be continued after machining in order not to give room for material failure due to the use of adhesive. Sequential machining of AM can also be done when cold or hot with the process of this research.

2.5 Surface Integrity

As a result of the removal mechanism, the machining operation due to the mechanical stress influences the subsurface of the machined work piece. Residual stresses develop depending on the specification of the machined work

piece material. These stresses can have positive effects on the component characteristics; hence, structural/phase changes may occur at the subsurface that have a negative effect on the component characteristic.

This shows the complexity of the mechanism of the surface formation during machining. The better the surface formation is known, the more the specifically and accurately the process parameters to the tool specification and the choice of an eligible cooling lubricant can be optimized.

The condition of the surface which is the outcome arising from manufacturing processes has been known with taking a major effect on the manufactured goods performance. Surface integrity, which was first used by Field and Kahles, (1964) is well defined as the improved condition of a surface manufactured through machining or additional surface generating process. Surface alteration could comprise metallurgical, mechanical, chemical, and further changes. This change although limited to a small surface layer could limit part quality or could in many situations makes the surface of no use.

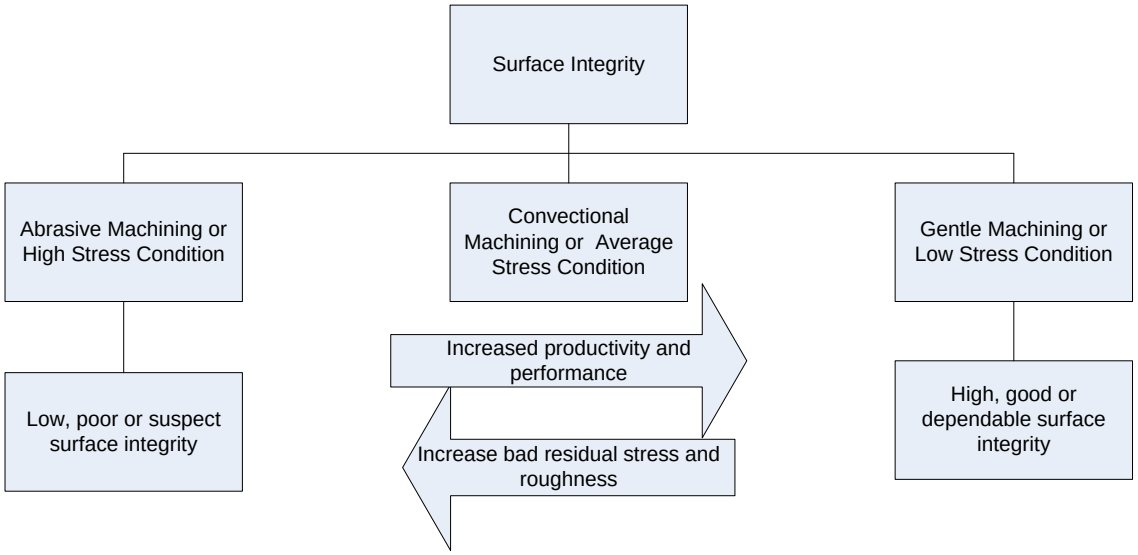

Figure 2-5: Schematic description of Surface Integrity (Adopted from Griffiths et al., 2001)

In order to attain additional product improvement, elementary knowledge of the variations in the condition of surface is necessary (Lucca et al 1998).
Within the machining region, a surface could be defined as a margin in between a machined part with its environment. Surface integrity defines the qualities of a surface that has been machined in addition to its connection to practical performance. In machining, surface integrity defines the rudiments and current developments in the study conducted into the surface integrity in machining processes.

Altogether, surface integrity can be divided into two [Field and Kahles, 1964]:

- The external topography of surfaces (surface finish); and
- The mechanical properties, microstructure, and residual stress arising from inner subsurface layers.

Performance features that are normally sensitive to surface integrity may comprise; corrosion rate, fracture strength, fatigue strength, and tribological performance (like wear, friction with lubrication, and dimensional accuracy. Surface integrity resulting from the machining process is recognized as having significant impacts on the components performance
It is greatly recognized that the performance of a parts is greatly affected by the feature with the reliability of the surface manufactured in respect of the topography in addition to mechanical and metallurgical conditions of the inner layers (Field and Kahles, 1964). In the past, several researchers have made efforts to explore the interaction amongst the machining method parameters, the nature of the surface changes manufactured with their consequence on manufactured goods efficiency performance. Persistence need to attend to the increasing need on the parts performance, dependability, and robustness has been the main driving force behind this, thereby stimulating the improvement of the material with improved opposition to severe loading settings and aggressive environment, in cooperation with the development of high-performance manufacturing methods.

Surface integrity resulting from the machining process is acknowledged with having a substantial influence on the component performance. Shaw (1996) described the three areas that relate to the surface integrity namely surface finish, metallurgical damage, and residual stress.

2.5.1 Surface Roughness

Surface geometry is made up of three components namely form, waviness, and roughness. The combination of the latter of these is accepted to be the surface texture. Figure 2-6 below show a diagrammatic representation. Separation of these components for quantitative analysis is achieved by filtering of the surface profile measured. (I.e. roughness-high frequency, form- low frequency)

Surface roughness is generally based on statistical measurements. For example, Ra is known as average of the roughness, Rq is the root mean square value, and Rt is the maximum profile height.

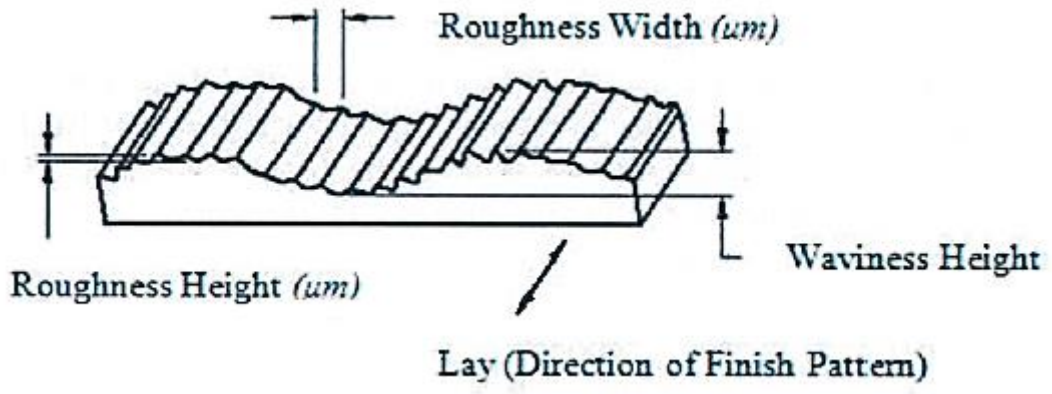

Figure 2-6: Surface roughness and waviness (Comley 2005).

The surface texture is representative of the machining performance, the two main aspects of interest are surface roughness, and machining lay. The latter is commonly referred to as directional (Comley, 2005). Standardization enables accepted surface roughness terms to be used to qualify surfaces and correlate

them with accepted production techniques. Table 2-3 from Shaw, 1996. shows published value for Ra-Centre Line Average used as a guide to production capability.

Table 2-3: Process Capabilities for Surface Roughness (Shaw 1996)

Process	Roughness-Ra (μm)	
	Average	Special
Grinding	0.1 - 1.6	0.025 - 6.3
Honing	0.1 - 0.8	0.025 - 6.0
Polishing	0.1 - 0.4	0.0125 - 0.8
Lapping	0.05 - 0.4	0.0125 - 0.8
Super finishing	0.05 - 0.2	0.0125 - 0.8

2.5.2 Residual Stress

Understanding the actions of residual stresses is important to the assessment of part lifespan (Williams, 2005). Working surfaces continuously stressed under operational conditions such as bearings, cams, gears etc. are greatly influenced by the residual stresses.

A study in Society of Manufacturing Engineers (1983) indicated that machining processes bring together compressive and tensile stresses to recently developed surfaces. If the surface is pushed outside its plastic limit, however, induced stresses persist as residual stresses, penetrating into several depths. Usual residual stresses triggered through the choice of manufacturing techniques are presented in Figure 2-7. The type and magnitude are related with machining forces, the forming temperatures and process time. For example, tensile residual stresses, which is often a product of abusive and abrasive manufacturing techniques, normally points toward poor component performance, because the surface is likely to fail through micro cracking.

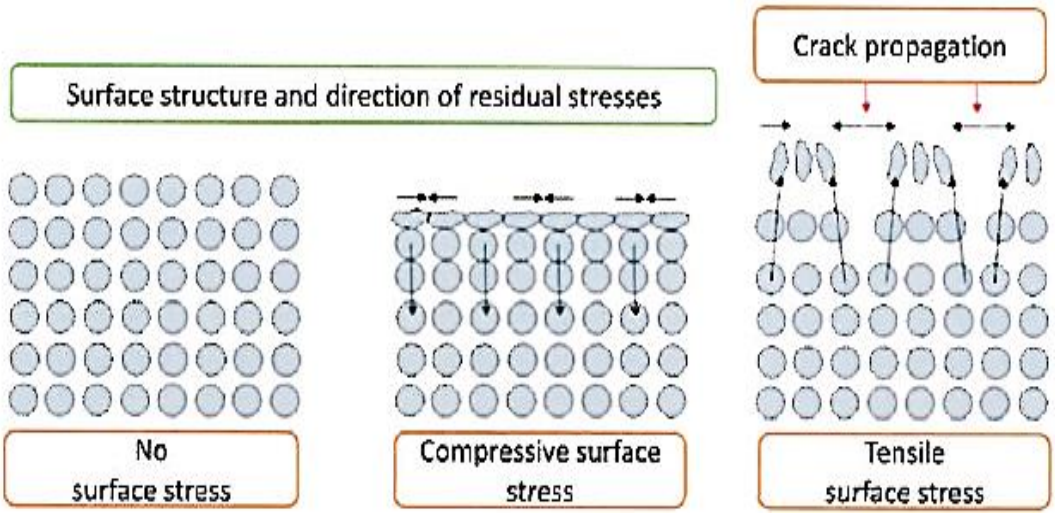

Figure 2-7: Configuration lattice in a number of stress states (Morris T, 2011).

Tensile residual stresses are related to irregular plastic deformation of the surface and high temperature gradients (Malkin and Guo, 2007). However, with the optimisation of machining factors with effective cooling, these stresses can be greatly reduced.

Many undesirable changes are taking place in the work piece (such as cracks, residual stresses, burning, softening, re hardening and phase transformation) are as a result of thermal damage. Heat treatments of metals are a perfect instance of how temperature influences material properties through the production of carbides, martensite and conditioning of the size of grains etc.

The detection of residual stresses can be done with various means i.e. neutron diffraction, ultrasonic, electron diffraction and x-ray diffraction (using Bragg's Law). The indication of the type of stress and the strength is done through magnetic detection. Stress relieve through annealing is possible but this depends on the depth and the type of the residual stresses.

Metals are held at raised temperatures for duration of time to improve and reduce the size of the grains; hence, this result in a uniform distribution and an

equalisation of the stresses. It directly relates to the effect of temperature on microstructure.

2.5.3 Microstructure and Hardness

The greater the percentage of machining energy directed into, or absorbed by the work piece the greater the probability of microstructure transformation. Dangerous circumstances of temperature contact could lead to burn, as well as permanent physical destruction of the material. Moreover, this is worth noting that the unaided eye may not automatically see this damage.

Iron-carbon (Fe-C) phase transformations shows that time is an issue in the carbon steel phase transitions, principally owing to the carbon atoms diffusion through the solid solution. However, machining can encourage phase transformation within a short space of time, flash temperatures. The correlation of this could be shown with sugar and coffee (Shaw, 1996), by addition of sugar, which resulted in the diffusion of the solution being slow; when adding some physical movement such as stirring with a spoon, the rate of diffusion is significantly reduced.

Phase transformation diagram of Fe-C cooling time and hardness of Fe-C alloy is shown in Figure. 2-8. The machined surface of steel can be raised higher than the Eutectoid and Ac3, by localised flash surface temperatures, at which point the formation of the microstructure morphs into body centred γ austenite. Under precarious machining parameters this austenitic microstructure will be effectively frozen in, trapping carbon in a solid solution, known as Untempered Martensite (UTM, α'). The rapid cooling is due to energy dispersion between the heat partitioning components. Micro and Macro cracks are common in areas of UTM, with UTM visible as a white layer when the surface is etched with a dilate solution.

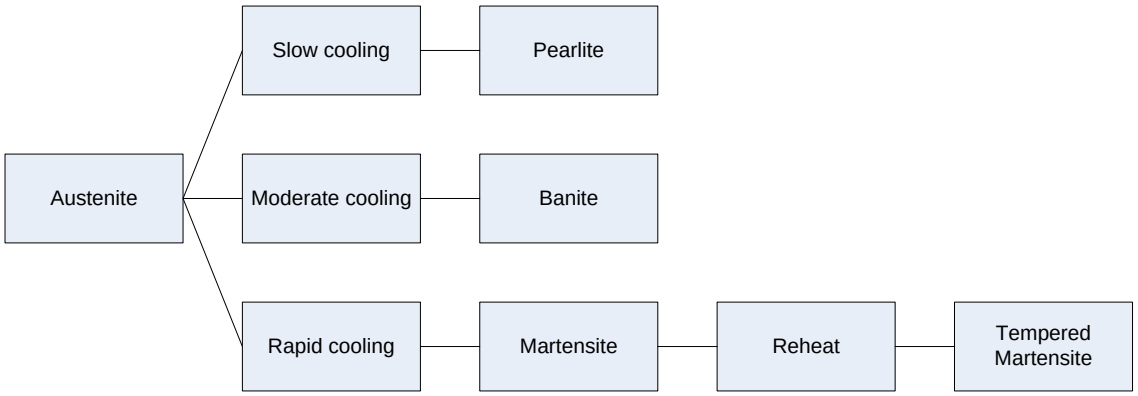

Figure 2-8: Possible transformation involving the decomposition of austenite (Adopted from Morris, 2011).

2.6 Machining Lubrication

2.6.1 Cutting Fluids

Cutting fluids are the convectional alternative to be used as both lubricant and coolant. However, its use has many adverse impacts i.e. environmental, dermatitis to the machinists, toxic waste in form of pollution and soil adulteration through dumping and consequent agricultural product and food contamination (Byrne and Scholta, 1993). Despite their wide spread use, they are a substantial health and environmental threat during their operation. In a study, it is affirmed that around 80 per cent of entirely occupational ailments of the machinist were as a result of skin contact with the machining fluid (Krishna et al., 2011). Krishna et al., (2011) also reported that in the USA only nearly 0.7 to 1 million machinists are open to metal working fluid.

In material removal, the use of cutting fluid can pose significant health and safety risks. Any cutting fluid that generates a mist, whether it be water or oil based, may cause respiratory ailments such as loss of lung function and occupational asthma (Sutherland and Kulur, 2000). Prolonged exposure may cause cancer to the oesophagus, colon stomach, pancreas, rectum, and larynx (Gunter and

Sutherland, 1991). It is for this reason that there are strict limits on the amount of mist a machine operator can be exposed to. There is also a serious hazard of skin dermatitis when water based fluid systems are used (Howes and Tonshoff, 1991) and they are always susceptible to bacteriological activity that can be potentially damaging to health. Water based fluid systems therefore require the use of anti-bacterial agents that require frequent checks a possible replenishment, with the subsequent impact on full life cycle costs.

Cutting fluids symbolises a significant proportion of the overall manufacturing costs, with surveys showing that between 7%-17% of the total production costs are attributed to the usage of cutting fluids when the cost of purchase, maintenance, and waste disposal are taken into consideration. Some suggest that the cost is even higher, nearly 20% (Brinksmeier and Brockhoff, 1997) and whilst these figures. It is clear there are significant costs associated with the use of cutting fluids and this is the main reason of using MQL and solid lubricants.

The environmental impact of all lubricants, which obviously includes cutting fluids, has led to a draft of legislation being introduced aimed at minimizing any potential ecological damage. For instance, European legislation has forced the removal of nitrite from cutting fluids as well as short chain chlorinated paraffin, which were used as extreme pressure additives (Bart, 1999).

Government legislation also tends to force companies to reduce the toxicity of all wastes including cutting fluids being returned to the environment and to increase the biodegradability of their waste products (Bart, 1999). In recent years, a number of environmentally friendly biodegradable cutting fluids have been introduced into the market. A biodegradable cutting fluid is one where microorganisms can ingest and metabolise the fluid and essentially return it to nature.

However, for total biodegradability to be achieved all the components of the fluid need to be completely broken down. If one or more components of the fluid

cannot be broken down, then it is considered only partially biodegradable (Bart, 1999).

The biodegradability of a cutting fluid can be measured, but unfortunately, several different standards and testing methods exist to generate the required data. This can lead to some confusion over what “biodegradability” (Battersby, 2004) actually means. However, an International Standard – ISO 15380 does exist, and this standard stipulates that at least 60% of the major components of the cutting fluid, for example the base fluid used to manufacture the cutting fluid have biodegraded after 28 days (Battersby, 2004).

2.6.2 Minimum Quantity Lubrication

An alternative approach to high-pressure coolant and traditional flooding is the Minimum Quantity Lubrication (MQL), which is a development in the direction of dry machining. Comprehensive investigation carries on progressing the idea in metal-working, described by Weinert et al., (2004) which involves the emphasis to decrease the costs. Furthermore, utilising minimum quantity lubrication likewise targets to sustain if at all it does not improve the surface integrity in the produced parts.

In order to resolve a number of issues arising from cutting fluid as discussed in section 2.6.1, clean machining with Minimum Quantity Lubrication is proposing as the alternative. The notion of Minimum Quantity Lubrication is described as machining using a very little quantity of coolant. This method comprises of the usage of slight quantity of water with soluble oil, 6-100ml/h^{-1}, conveyed in a compressed air stream, focused at the instrument cutting edge

2.6.3 Cryogenic Cooling

This involves applying super cooled nitrogen to the grinding zone to control the workpiece temperature but unfortunately, this technique can adversely affect the accuracy of the grinding machine. The super cooled nitrogen being applied to the

workpiece can set up large thermal gradients with the machine structure and consequently seriously impair the dimensional accuracy and stability of the machine tool (Massam, 2008). The cost of liquid nitrogen also makes the process uneconomical for normal grinding processes (Paul and Chattopadhyay, 1995) and there are problems associated with grinding wheel wear and the subsequent reduction in wheel life due to the low lubrication properties of liquid nitrogen.

2.6.4 Dry Machining

Dry machining have for some time been seen as potential ecologically friendly and economical manufacturing processes where cutting fluids are not used. Future environmental and occupation health and safety legislation coupled with the increasing costs of waste disposal makes dry machining an attractive proposition, and in time, industry may be compelled to implement dry processes. Dry machining or cutting processes is the most common, often using special self-lubricating coatings applied to the cutting tools (Byrne et al., 2003) to minimise friction and thus heat generation. Salmon, 2000 refers to the example of Daimler Benz where a 16% cost saving was achieved by dry machining. Whilst this may have been a conventional metalworking process, it still generated considerable excitement within the industry and the cost saving is often quoted.

There are however significant disadvantages with dry grinding such as the higher contact temperatures, higher grinding forces and lower wheel life attributable to the lack of lubricant and the resultant increase in thermal wear, dust generation and a lack of corrosion protection for both machined ferrous surfaces and possibly even the machine structure (Salmon, 2000).

2.6.5 Solid Lubricants

Solid lubricants are materials that utilise powders or thin films in order to offer shield against damage through movement stuck between surfaces in order to lessen friction in addition wear. Many other nomenclatures usually used in place of solid lubrication consist of dry-film lubrication, dry lubrication and solid film

lubrication. Even though the same nomenclatures suggest that solid lubrication occurs under dry condition but fluids are often utilised as a lubricant with solid additive or medium.

Solid lubricants are frequently used in systems as soon as conventional lubricants are not suitable i.e. in situations of:

- Dangerous pressures and temperatures
- Unreachable places
- Avoidance of contamination
- Environmental and atmospheric protection

Morris T, (2011) highlighted the main merits and demerits of solid lubrication being:

- It is recognised to be better effective than fluid lubricants with high loads and speeds
- Solid lubricant does not deteriorate easily.
- Highly stable in extreme temperatures and pressure.

While the foremost demerits are:

- Reduced self-healing properties of film structure when compared to fluids
- Heat dissipation is poor

The advancement of up-to-date tribology has identified several solid lubricants which can withstand and offer lubricity over a wide spread choice of temperatures. If solid lubricants could be effectively useful to the machining region in a suitable fashion as a way of reducing the heat produced owing to friction, improved process results could be obtained.

Few studies have been carried out on the feasibility of using solid lubricants. Li and Liang, (2006) considered the effects of cutting parameters on the cutting temperature in near dry machining for sharp and worn out tools. Through strict industrial guidelines with the environmental features all over the world,

researchers have been at work to realize economically friendly justifiable manufacturing. It is predominantly gotten by means of clean machining method making use of Minimum Quantity Lubricant such as MoS_2 powder, grease based graphite mixed with water and SAE 20 oil in several extents in its place of flooding coolants. The results was encouraging and it is involve a substantial decrease in tool wear rate, dimensional inaccuracy and surface roughness by minimum quantity lubrication mostly through decrease in the cutting region temperature.

Venugopal and Rao, (2004) examined the usage of graphite as a lubricating medium in grinding process to decrease heat generated at the grinding region. The operational role of graphite as a solid lubricant is obvious from whole improvement in the process. Different process parameters like specific energy, cutting force, temperature, and surface roughness were detected and described to be decreased while likened to those in grinding with convectional coolant.

In a research conducted by Suresh and Venkateswara, (2006) graphite and molybdenum disulphide, assisted end milling method has been described to offer significant progress in the process performance when related to that of machining using cutting fluid in relations to specific energy cutting force, and surface quality. Solid lubricants like MoS_2, MoS_2 based grease, graphite based grease, and silicon compound mixed with SAE 20 oil have been shown to improve surface quality at different amount while machining with aluminium and brass.

Machining parameters has an effect on the solid lubricant particle size. Improved performance with respect to cutting force, surface finish, and tool wear in turning of EN8 steel with boric acid and graphite is noticed for particle size of 50μm amid the alternatives put into consideration in the research by Rao and Krishna, (2006).

Shaji and Radhakrishnan, (2002) discovered the likelihood of usage of solid lubricants in grinding as a method to lessen the heat produced owing to friction, to finding a substitute for the convectional fluid coolant. He used high temperature solid lubricants that are obtainable in powder state e.g. calcium fluoride (CaF_2),

barium fluoride (BAF_2), graphite, and molybdenum trioxide for the experiment. The paper reported that the wheel loading with lack of appropriate flushing system was discovered to be the main limitation in attaining perfect result. It concluded that the use of solid lubricants in grinding could materialize as an operational substitute to the convectional coolant, if it could be used in a suitable approach with means to eliminate swarf and wheel cleaning.

Solid lubricants were also suggested as possible alternatives to cutting fluids as a way of providing lubricant to the machining zone. Shaji and Radhakrishnan., (2002, 2003) also attempted to use graphite as a lubricant and whilst finding that this offered good lubrication properties there were problems associated with wheel loading, as there was no mechanism for flushing away debris. In an attempt to overcome these problems, Radhakrishnan and Shaji, 2005 conducted an investigation into the use of molybdenum disulphide solid lubricant in conjunction with conventional cutting fluids (neat oil and a water based cutting fluids) applied purely for the purposes of cleaning the wheels. Whilst Radhakrishnan and Shaji, 2005 did conclude that solid lubricants were preferable to water based cutting fluids for both the shallow cut and high efficiency deep grinding regimes, their use resulted in a reduction in the specific grinding energy as well as a reduction in the grinding power. He found their use was more problematic in the creep feed regime as there was a significant rise in the workpiece temperature. This may have been attributable to the fact the both the grinding power and the specific grinding energy increased when solid lubricants were used in the creep feed regime. However since over 90% of the thermal energy is removed by the fluid in creep feed grinding, the fact that solid lubricants offer little or no cooling probably explains the significant rise in the workpiece temperature and frictional heating. Teer et al., (2001) showed the effects of graphite and molybdenum disulphide coating on the wear resistance of the wheel and measurements were done to look at the variation of the friction coefficient and the surface finish. Graphite and MoS_2 were chosen for the experiment because of its tribological properties. The solid lubricants were deposited on the wheel mixed to a titanium composite

known as M_oST (15% of titanium) developed for cutting tools and the layer was about 1µm thick. Graphite because of its poor adhesion ability was deposited on a base layer of chromium. The combination of graphite and chromium is known as Graphit-Ic. This gave a coating thickness of 2.5µm. The wear testing was based on reciprocating grinding in dry and wet conditions. The result showed the benefit of solid lubricants on the wear of the wheel and on surface finish. However, under wet condition, this type of coating seems to be inefficient. The most interesting result was the good characteristics of the molybdenum coating at high speed and under dry condition.

There are some important properties in defining the appropriateness of a material for use as a solid lubricant (Teer et al., 2001):

- Thermal structure: One of the important characteristics of solid lubricants is in the high temperature application that is not allowed by other lubricants. Solid lubricant will not experience undesirable phase or structural change with high or too low a temperature range because of the good thermal stability.
- Volatility: Lubricants will have a small vapour pressure for the anticipated usage at extreme temperature and in low-pressure condition.
- Melting point: Melting point should not be exceeded because the atomic bonds which preserve the molecular structure are ruined, making the lubrication not effective.
- Electrical conductivity: solid lubricants should be a very poor conductor of electricity or preferably should be an insulator.
- Chemical reactivity: the lubricants should be able to form a durable, adherent film on the base material.
- Chrystal structure: Solid lubricants such enjoy a lamellar crystal arrangement with inherent low shear strength. However, the lamellar structure is favourable for materials as lubricants, non-lamellar materials also offers acceptable lubrication.

- Oxidation stability: lubricants should not experience unwanted oxidation alterations when used inside the appropriate temperature range.

There are several properties to put into consideration when chosing for optimum performance. The manufacturing of lubricant is a separate with dedicated research laboratory working towards unceasingly strict necessities arising from customers and governmental organisations (Fuchs, 2007). However, Table 2-4 describe series of features mainly significant before bring together solid lubrications into a system.

Table 2-4: A range of materials used as solid lubricants and their most significant characteristics (Adopted from Radhakrishnan and Shaji, 2005).

Lamellar solids		
	Tmax (°C)	**Special features**
MoS_2	350	Stable to >1150°C in vacuum
WS_2	400	Oxidative stability >MoS_2
Graphite	500	Ineffective in vacuum/dry gases
TaS_2	550	Low electrical resistivity
CaF_2/BaF_2	1000	Ineffective below 300°C
Polymers		
UHMWPE	100	Exceptionally low wear
FEP	210	Chemically inert; useful at cryogenic temperature
PTFE	275	
Polyamides	300	Friction > PTFE
Polyurethanes	100	Useful for abrasive resistant but friction relatively high
Nylon 11	150	
Soft metals		
Pb, AU, Ag, Sn, In		**Useful in vacuum**
Oxides		
PbO/SiO_2, B_2O_3/PbS		**Effective only at high temperature**
Miscellaneous		
$AuSbS_3$, $Sb(SbS_3)_2$, $Ca_2(MoS_2)$		**Oil and grease additives.**
$Zn_2P_2O_2/Ca(OH)_2$		**White lubricants additive**
Plasma-spray coatings		
Ag/Ni-Cr/CaF_2/Glass		**Wide temperature range lubricant formulation 20 - 1000°C**
Ag/Cr_3C_2/Ni-Al/BaF_2-CaF_2		

2.6.5.1 Methods of applying solid lubricants

Particular reference needs to be made to instances of solid lubricants in machining. Under a certain situations along with the evolution of a appropriate

application technique in which the layers of solid lubricant been introduced to the machining region, Shaji and Radharkrishnan, (2002) conducted a study on surface grinding with the use of graphite as a solid lubricant. He designed the experimental set up and built it, a relative performance study of graphite assisted grinding with dry, and convectional-flooded coolant grinding was made. He concluded that active part of graphite as lubricant was obvious from the progress of production parameters associated to the frictional factor and that the lubrication is effectively dealt within the anticipated method an effective way for replacing flushing feats with the wheel cleaning met in the coolant grinding, must be considered.

It is important that the solid lubricant be applied efficiently to the machining region in order to accomplish improved result. In view of this condition, Suresh et al., (2010) design and developed an electrostatic solid lubrication system (Figure 2-9) with the main aim of reducing or eradicating the usefulness of the cutting fluid when applying solid lubricants as a high velocity jet in machining at a tremendously low flow rate.

The author did a relative evaluation analysis of wet machining and dry machining environments with the proposed method. An outstanding result obtained from the study is that solid lubricant machining used with his developed experimental set up resulted in numerous improvement in tool life. Tool life improves intensely owing to the ability of the solid lubricant to be able to be delivered appropriately into the chip-tool boundary region and achieve both lubrication and cooling tasks adequately.

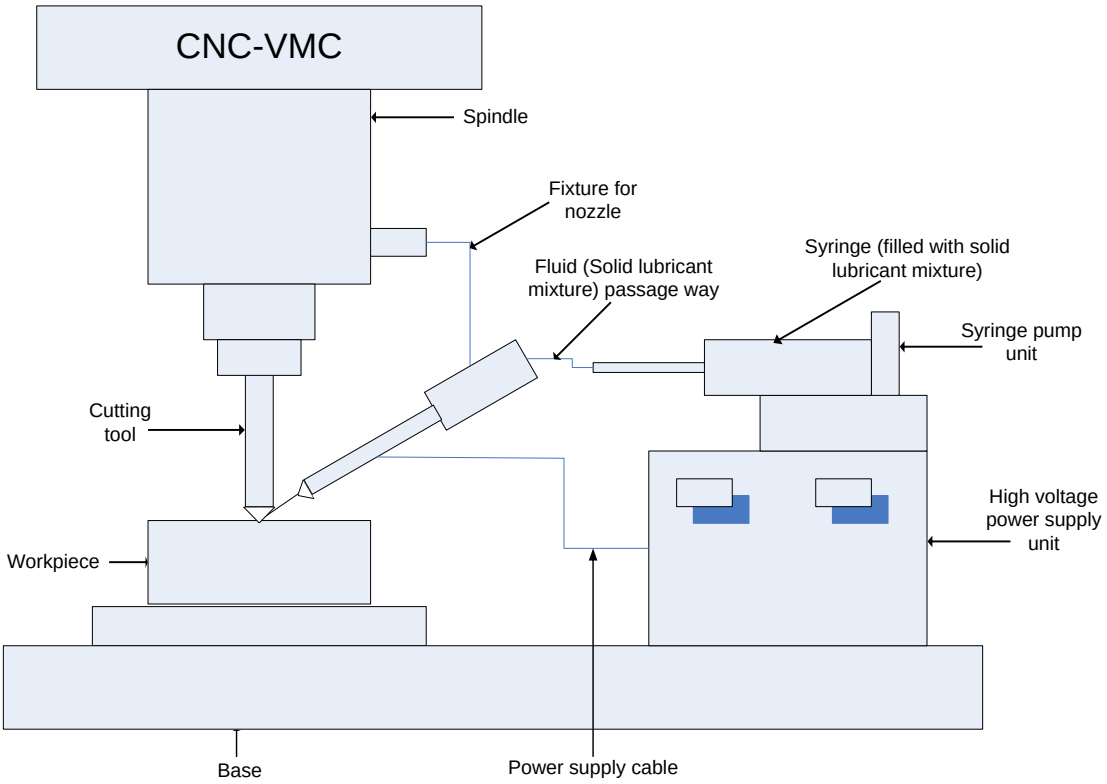

Figure 2-9: Electrostatic solid lubricant setup (Adopted from Suresh et al., 2010).

Suresh and Venkateswara, 2006 perform an experimental study on the consequence of solid lubricants on cutting forces and surface quality in end milling. Rambaudi CNC milling machine' was used in the experiment. The set up for solid lubricant power assisted machining was developed for the study and this is shown in Figure 2-10.

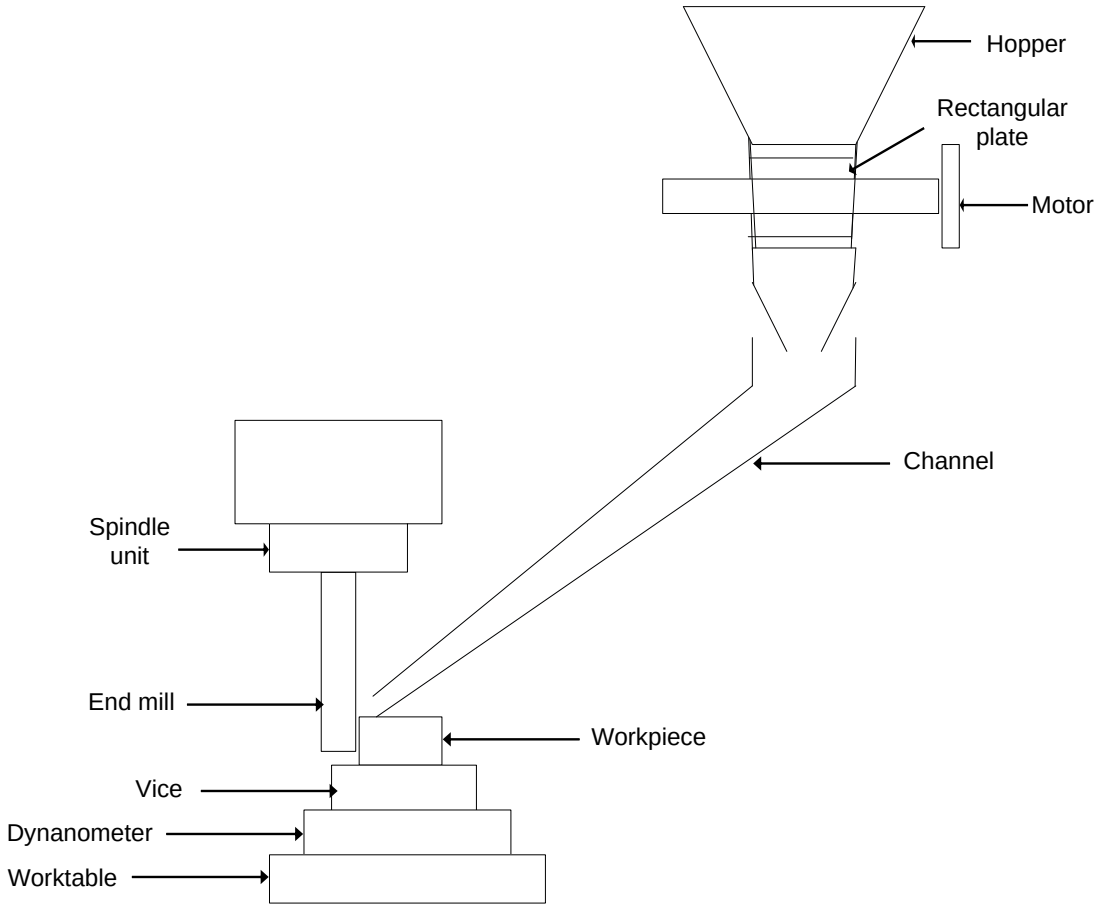

Figure 2-10: Experimental setup with the graphite feeder (Adopted from Suresh and Venkateswara, 2006).

With the end milling of AISI 1045 steel, cutting force and surface roughness were noted and the conditions considered for the experiment were radial rake angle, cutting speed, radius nose, and federate. Using this method, results shown that the friction produced in between the tool and workpiece has been greatly reduced.

Other ways used in the application of solid lubricants includes:

- Powdered Solids: This is the oldest and the simplest way of applying solid lubricants.

  There are various ways of applying powder as discussed below:

1. Burnishing: This is the rubbing method in order to apply a small film of powdered solid lubricants like, M_oS_2 graphite etc. to a metal surface to give a 0.1-10µm burning film. This process resulted in an extremely polished surface, which is useful where lubrication requirement with wear life are not severe, that is clearance condition has to be sustained and where wear debris, which arises from the lubricant, has to be reduced. In ensuring a better application, the particle size of the powder and surface roughness of the metal substrate are critical to ensure better application.
2. Hand rubbing is a method used for roughly spread over a thin coating of solid lubricant.
3. Dusting: Powder is applied without any thought for smooth application of the lubricant, which results in a loose and uneven application.
4. Dispersion: These are solid lubricants mixtures in neither fluid nor grease. The utmost common solid usually used are M_oS_2, graphite PTFE and Teflon. The grease or fluid provides normal lubrication whereas the solid lubricant increases lubricity and provides extreme pressure protection.

- Bonded coating: A bonded coating provides superior film thickness with improved wear life and they are the best in reliability and durability ways of applying solid lubricant (Suresh and Venkateswara, 2006). With careful condition, coating comprises of a solid lubricant with binding resin agents that are applied to the material to form a protective layer by brushing, dipping or spraying. Air-curled coatings are usually restricted to the working temperature less than 260^oC whereas the heat-cured coatings are generally used to 370^oC. The frequently used lubricants are MoS_2, PTFE and graphite. Furthermore, the binders comprise metal salts, ceramics, and organic resins. Organic resins are typically stable under 300^oC. Inorganic binders like the metal salts and ceramics allows bonded films to be used in temperature greater than 650^oC. Type of the binder to be used

is influenced by facility processing, environmental compatibility and mechanical properties.

With the views of various authors in the above-mentioned studies, using solid lubricants in machining is viable as a substitute to the cutting fluid.

2.7 Statistical Analysis through the Process Capability Studies

For the machine or the process to generate products of minimum cost, without incurring losses due to rejects, rework and or scrap, its process capability must be able to match the product specification (Kane, 1986). The primary reason for quantifying a machine or process capability is to determine what product tolerance a machine can meet or hold. Capability study is an example of the use of statistics in quality control. This is one of the terms of reference, which demands attention during the drawing up of any well-formulated quality program.

The concept of capability stems from the fact that no two objects are alike and a small variation always exists between any two apparently similar objects, which will be revealed by sufficient sensitive measurement.

Considering a production process, the capability is defined as the “natural tolerance “of the machine, equipment, or process (Deleryd, 1999). In other words, the calculated capability is a measure of accuracy of the machine or process in the form of minimum variation in the measured feature of the output product. The feature may be a size, geometric feature or even a material property, as long as it is measured in discrete units.

It should be recognized that little could be done about chance variations other than to revise the process. This chance variation is the sum of the effects of a whole complex of chance caused. In this complex of causes, the effect of each cause is slight and no major part of the total variation can be traced to a single cause.

The variation cited above may be caused by:

a) Variation due to the machine itself
b) Variation in the raw material submitted for operation
c) Operator's influence, if any.

It is considered necessary to differentiate between process and machine capabilities. A "Process Capability" is a measure of the variation caused by all the three reasons stated above whereas "Machine Capability" is a measure of the machine variation alone after eliminating the other two sources of variation as far as its practicable.

The distinction would immediately make it obvious that the process capability is of greater practical importance as it evaluates the process performance under production conditions

2.7.1 Benefits of capability studies

Process capability studies are conducted with the use of control charts and statistical methods to define the ability of a process to conform to specification. The results from a capability study provide the process engineer with more knowledge of their process. The acquired information is used in process improvement investigation and may lead to upgrading a process or change in production specification. Losses attributed to inadequate processes, poor maintenance and the like, can be minimized through process capability study.

Process capability studies have a large number of applications and Kane (1986) provided some of these applications to include:

- Predicting how well the process will hold the tolerances.
- Assisting produce manufacturer in choosing or adapting a process
- Stipulating performance requirements for new equipment.
- Selection of workers/operators
- Specifying requirement of new or reconditioned manufacturing equipment.
- Scheduling work on different machines.

2.7.2 Capability determination and indices

It order that a machine or process can generate products at minimum cost, that is without incurring losses due to rejects, reworks, and or scrap. Its capability must be able to match the product specifications. The performance of a process is usually measured by its capability to match specification limits.

Kane, (1986) advocated that the performance of a process can be measured by means of process capability indices. Moreover, the performance indices can be used to monitor and evaluate process trend and be used as a measure for process improvement. The Cp and Cpk, reflects how well a process can match specification limits.

Cpk assesses process viability by comparing the spread and centring the process. The extent to which the expected values fall within these limit determines how capable the process is meeting its requirement. Capability increases as the process becomes narrower and as the process is centred closer to the target. The goal is Cpk≥1.33. Table 5-4 show the various quality conditions as described by Pearn, 1997).

Table 2-5: Quality conditions of Cpk (Pearn, 1997).

Quality condition	Values of Cpk
Insufficient	Cpk< 1.00
Acceptable	1.00 ≤ Cpk< 1.33
Satisfactory	1.33 ≤ Cpk< 1.50
Excellent	1.50 ≤ Cpk< 2.00
Super	2.00 ≤ Cpk

Higher process capability index suggests the greater process yield. However, higher capability index likewise point toward the lower process anticipated loss (Chen et al; 2001). Consequently, the process capability index may be regarded as an effective and outstanding ways to measure manufactured excellence with

performance. Several engineering designers and shop floor controller made use of process capability indices by way of communication indicator in order estimate and improve the manufacturing process (Chen et al; 2001).

LEFT BLANK INTENTIONALLY

3 Research Aim and Objectives

3.1 Introduction

Currently, advanced manufacturing industries, for instance automotive and aerospace encounter pronounced challenges owing to increasing service demand in addition to general usage, motivating for high quality of product requirements and maintainable processes. (Sequeira-Almeida, 2012)

Many researches have tried in order to ascertain the overall necessities of next generation industries in the competitive economy and the continuously growing industrial environment through identifying changes, which will help in their survival. This initiative should be capable of reacting to changes in addition to cost effectiveness (Koren *et al.*, 1999). In order to react to these changes, there is a clear need to examine the process of Additive Manufacturing (AM) and the related issues of shape measurement with the machining of manufactured parts. Literature has helped to identify the core areas, which contribute to the improvement of AM process. Figure 2-17 shows the various aspects that have been identified as important to improve the usage and manufacturing of AM parts.

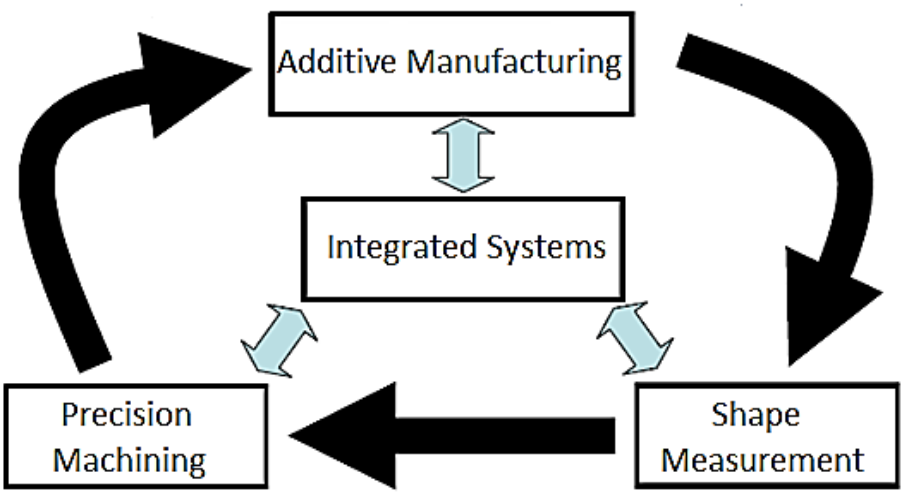

Figure 3-1: Next generation additive manufacturing

The process involves deposition of materials, measurements and machining through and new integrated finishing. The demand for WAAM parts in commercial application are increasing as complexity of manufacturing is decreasing through WAAM. A performance comparison of WAAM systems would help in specifying the best machine suited for WAAM deposition .The traditional method for the WAAM involves a number of different stages resulting in high cost and long lead-time. The typical process route requires deposition through integrating robot with a welding power system. Industries invest on robots while the use of precision CNC machine i.e. SAM Edgetek machine may be capable of deposition of WAAM parts better because of its repeatability and accuracy. It will also be of help with the inclusion of Friction Stir Welding machine, which is used to manufacture large objects. Comparison of these integrated systems with different properties with the aim of specifying the best system could reduce the cost and lead-time for WAAM.

However, significant amount of literature has been in the print in relation to the effect of processing conditions on laser deposition, but these investigations were majorly on metal deposition using powder (Kelly and Kamper, 2004, Kobryn *and* Semiatin, 2000). Comparatively less studies have been dedicated to the deposition through wire feeding. Furthermore, there are still insufficient studies on the defects arising from AM and its machinability from the experimental and industrial point of view. It is important to note that all the studies (Nguyen et al., 2005; Soderstorm and Mendez, 2006 and Bradstreet, 1968) reviewed so far in the field of humping in welding has been limited to the convectional welding method i.e. bead on plate rather than metal AM.

Despite an increase in the advancement of AM, there are inadequate studies on the machining of AM structures. Few studies has been done on the data relating the manufactured sample with the level of the effective wall width that could be attained after machining i.e. the control of machining process so that minimum material is removed during machining cannot be over emphasised. This study tends to bridge the gap which controls the WAAM deposition process influence

on the deposited geometries prior to and post machining by evaluating material removal requirements to completely remove the surface defects due to the following bead profile, variation in geometry with respect to height and length and post machining distortion. Understanding this deposited geometry and the geometry tolerance to nominal parts allows for definition of machining strategy. However, the use of MQL and solid lubricant in the machining will be an advantage with the view of reducing or minimising the use of liquid lubricants which has a potential hazard implication.

3.2 Research Aim

WAAM processes have induced flexibility into the manufacturing of 3D metallic components, in as such; there has been a variety of academic work using various type of AM process. However, very little work has been published on the complete process, which integrates manufacturing and machining of deposited part. The lack of published material and the inherent difficulty in the machining of WAAM parts, especially parts with hollow shapes and materials with thin walls made it a challenge for this research.

However, this research work focuses on characterisation of integrated WAAM and machining processes. This is a collaborative research project under the Ready to Use Additive Manufacturing (RUAM) program (RUAM is an IMRC/EPSRC sponsored project that ran from October 2007 until December 2010).

3.3 Research Objectives

The literature review in chapter 2 enabled to establish the basis for this study by capturing the current developments and the research gaps. However, the findings and the challenges arising from the manufacturing industries also supported in defining the scope of this research. In order to accomplish the aim of this study, a number of objectives have been defined. This PhD is undertaken to realize the following objectives:

- Characterise and analyse individual aspect of WAAM wall geometries on three different WAAM platforms namely Super Abrasive Edgetek Machine (SAM) platform, ABB Robot platform and the Friction Stir Welding (FSW) machine platform.
- Analyse and identify the WAAM process behaviour on part structures.
- Study the sequential deposition/machining using Minimum Quantity Lubrication (MQL) and solid lubricants and study into the limitation of WAAM in material removal during machining.

3.4 Research Scope

This research will investigate the deposition process of WAAM wall structures under different platform and its effects on machining. The investigations will involve the deposition and machining of thin WAAM wall structures. The surface and the subsurface integrity investigation of the components will enable characterization and interrelationship analysis to be carried out.

Experimental work will be predominantly undertaken on the Edgetek Super Abrasive Machining (SAM) platform, ABB robot platform, and Friction Stir welding (FSW) machine platform integrated with a Power Wave welding machine and Cold Metal Transfer welding machine.

This research will not involve the design of WAAM part, cost implication, cost analysis, and manufacturing of large WAAM components.

3.5 Research Methodology

Investigation of WAAM and machining would be performed on a SAM Egdetek machining centre, ABB robot and a large friction stir welding machine. The WAAM deposition experiments would be also compared with existing or new experiments from a robotic deposition system. Experiments are to be performed using a set of industry relevant materials such as steel.

Simple test geometry (i.e. wall width, wall height and the perpendicularity of the walls) will be chosen which includes representative typical WAAM product features. Tactile as well as optical measurement will be used. Exact measurement will be performed to analyse WAAM part and machining quality with view on a potential automated integration into a single WAAM machine.
Systematic experiments will be performed for each research objective, i.e. for individual aspects of manufacturing and machining as well as for the integrated machine.

Validation of machine setup and parameter recommendations will be performed using extensive literature survey which is the backbone of this PhD research project as well as expert judgement (e.g. systematic surveys). All aspects of this research will be supported by literature.

Literature review was undertaken as part of the research. It covers the area of WAAM process, solid lubricants, minimum quantity lubrication and machining of WAAM part etc. However, the underlisted steps were taken to broaden this review:

- Identification of keywords: the main keywords on the subject of WAAM and welding processes were sought.
- The use of database search: With the help of the database provided by the Cranfield University library, more than 200 research articles, books and thesis were sought.
- Filtering of papers: Papers filtered were built on the areas of this research.
- Analysis of the key papers: This was done in order to identify the research and analysed.
- Research gap: the research gap was identified at this stage.

3.6 Research Structure

The study has been thoroughly planned to follow through the three research objectives (see figure 3-2). However, the flow diagram classifies the separate research objectives sideways with their connected decisions. The systematic methodology permits important decisions to be carried forwards from the conclusion of the objectives, thereby establishing the foundation of better understanding until the overall aim objective of the study was realised.

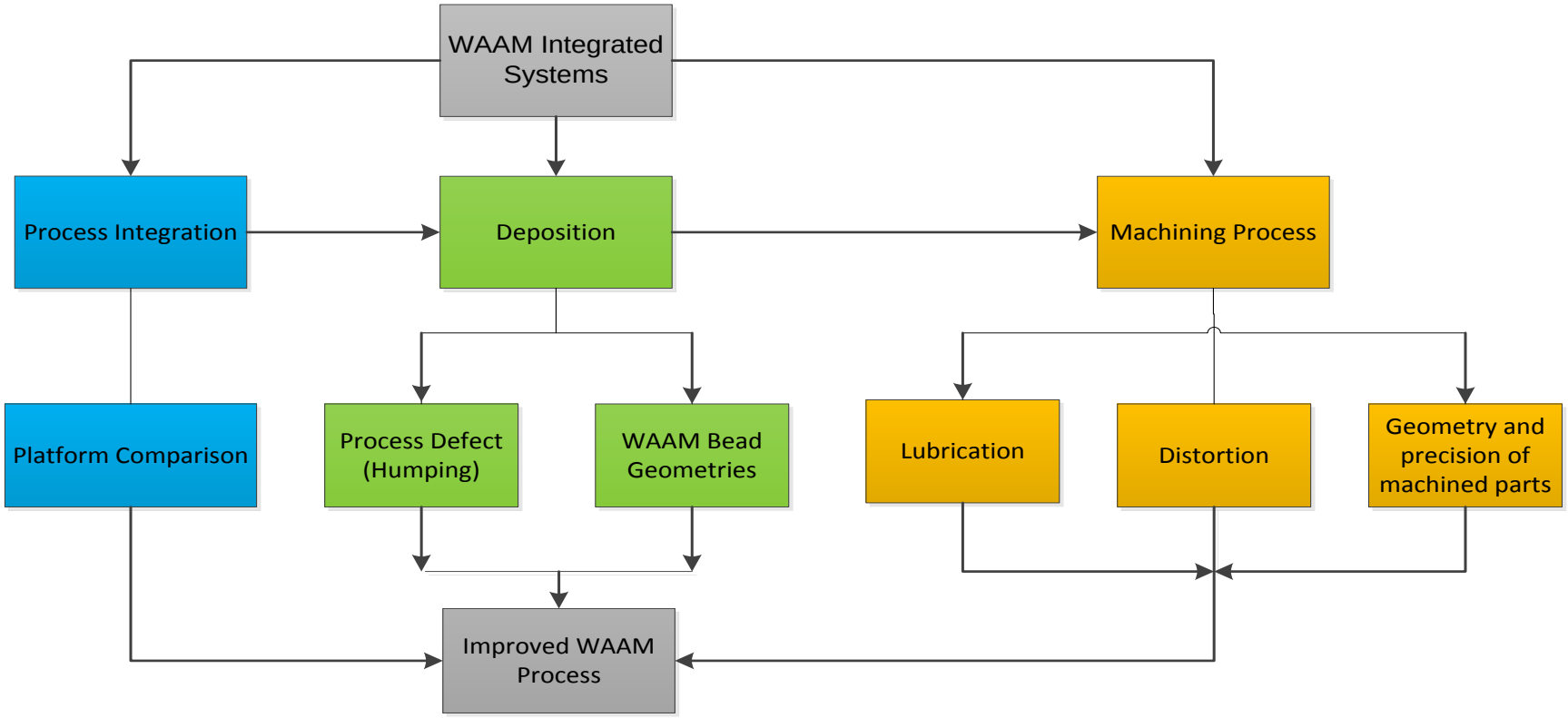

Figure 3-2: Flow chart illustrating the route to achieve the project

LEFT BLANK INTENTIONALLY

4 Machine and Experimental Set-up

4.1 Overview

This chapter describes the general machine set up and the main equipment used for achieving the aim of this research. This includes the SAM Edgetek machine, ABB Robot, Friction Stir Welding machine and the power sources used as well as equipment to characterise the trial samples. The procedure for samples preparation was also highlighted. Additional specific descriptions and the parameters used are stated in methodology sections in each corresponding chapter.

4.2 Metrology Techniques

4.2.1 Surface Profile

The surface roughness measurements were done with Taylor Hobson Talysurf profilometer using a 2-micron radius ruby-tip probe. Profilometer operation includes linearly probing along the length of a surface in order to acquire the nature of the topography. The equipment is illustrated in Figure 4-1. The specification is shown in Table 4-1.

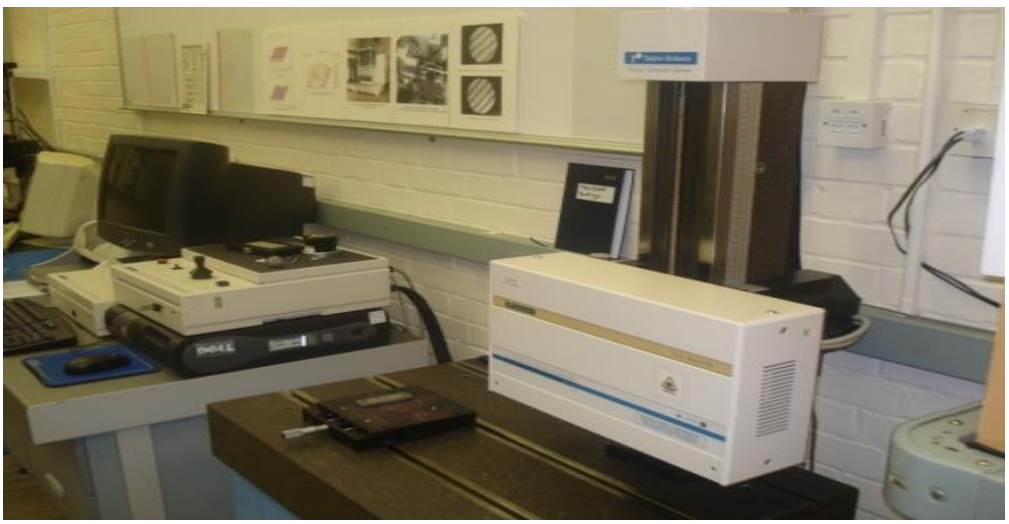

Figure 4-1: Taylor Hobson Talysurf 120L

Standard values of “cut-off” filtering and the frequencies of surface irregularity components were 8mm and 0.125mm^{-1}. A "Gaussian" filter, which is recommended in ASME and ISO standards was used.

Table 4-1: Talysurf 120L Specifications

Traverse Length	120mm
Traverse Speed	10mm/sec maximum
Measuring Speeds	1mm and 0.5mm/sec ±5%
Gauge Type	Phase Grating Interferometer 1mN force nominal
Measuring Range	10mm
Resolution	12.8nm @ 10mm range
Straightness	0.5µm over 120mm traverse
Accuracy	0.2µm over any 20mm traverse

The samples were positioned on a granite table while the ruby tipped probe is directed to locate a datum height on the y-axis. Slowly, the probe is gradually retracting over the surface. The probe uses a laser interferometer that is aimed at the rear of the probe carriage assembly. This is designed to detect variations in the surface height as the probe follows the surface contours. This profilometer Talysurf was used for the measurement of the WAAM sample surface roughness.

4.2.2 Coordinate Measurement Machine

TESA V300DC Coordinate Measuring Machine (CMM) is used to assess the physical geometrical characteristics (i.e. accuracy, repeatability) of the sample. It is usually used in the inspection process of manufacturing a product. This is a Computer Numerical Controlled machine system in which measurements are defined by a probe attached to the moving axis of this machine. Probes can be laser, optical, and mechanical.

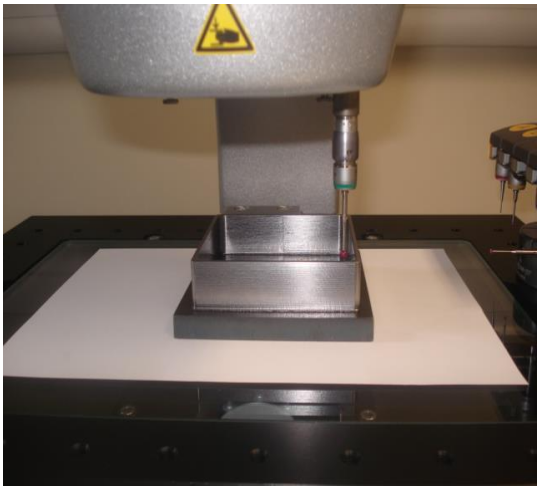

Figure 4-2: TESA V300DC Coordinate Measuring Machine (CMM)

TESA V300DC CMM is comprised of three axes, an X, Y and Z. They are orthogonal to one another in a characteristic three-dimensional coordinate system. For each axis, a scale system specifies the position of that axis. The touch probe transfers the reading, as directed by the programmer. The X, Y, Z coordinates of each of these points is then used by the machine to fix size and position with micrometre precision.

4.2.3 Hardness Testing

Hardness testing was conducted on the Zwick Vickers micro-hardness tester (see Figure 4-3). The regime involves applying a force of 200gf for 10s. This is used since the material used for the trials is mild steel. Nine measurements of the micro-hardness indention were done at 25µ intervals. The instrument is automated and it is indicated as accounting for a 3% error. The process was repeated more than three times on each of the sample in order to offer an acceptable resolution in the results.

Figure 4-3: Zwick Vickers Micro Hardness tester

The Zwick/ZHV executes micro Vickers hardness test to ISO 6508, ASTM E92 standard and certified to UKAS (a United Kingdom Accreditation System). The specification of the equipment is show in Table 4-2.

Table 4-2: Zwick Vickers micro-hardness specifications

Automatic turret for one-button control of lens/indenter exchange	Indentec C.A.M.S Testing system software by Newage TI Inc.
Newage Testing Instruments Controller Driver	Automatic conversion to other scale-no conversion table required
Test Scale shown in display	Manual test weight change
Entirely automatic test arrangement to predetermined time frame eradicates operator impact during hold time	VMH/HK Knoops hardness

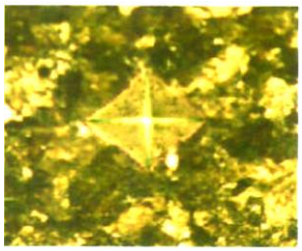

Figure 4-4: Vickers micro hardness testing pattern

4.3 Machines

4.3.1 SAM Edgetek Machine

Several of the trials were done on a Holroyd Edgetek Super Abrasive Machine (SAM). The SAM Edgetek machine is as shown in Figure 4-5 in addition to the specifications listed in Table 4-3. The machine was designed for high stock removal machining. This machine has three linear motion and two rotary motions.

Table 4-3: SAM Edgetek Machine specification

37kW grinding spindle
9,000 rpm spindle speed
Cutting speeds up to 203 m/s
Wheel speed up to 200m/s
Wheel diameter 0.350m
Feed rate up to 0.125 m/s
High pressure coolant delivery up to 83 bars
3 axis indexer work head
Force and power monitoring

Figure 4-5: SAM Edgetek Machine

The Edgetek machine utilises linear roller bearing methods. The linear systems with its corresponding resolution accuracies, repeatability and positioning is as described in Table 4-4. The machine is also equiped with a CNC FANUC controller.

Table 4-4: SAM Edgetek - Linear axes (X, Y, and Z) specification

		Slide Ways Accuracy		
Way System	Position feedback	Positioning	Repeatability	Resolution
Schneeberger Hi-precision linear roller bearing	Heidenhain Linear scale with X,Y,Z axes	±0.005mm/ 300mm	0.005mm/ 300mm	0.01mm

The SAM Edgetek machine is used with a welding machine (See Figure 4-6) to form a hybrid system in which can perform both welding and machining operation on the same system in order to achieve the advantage of both additive manufacturing and material removal.

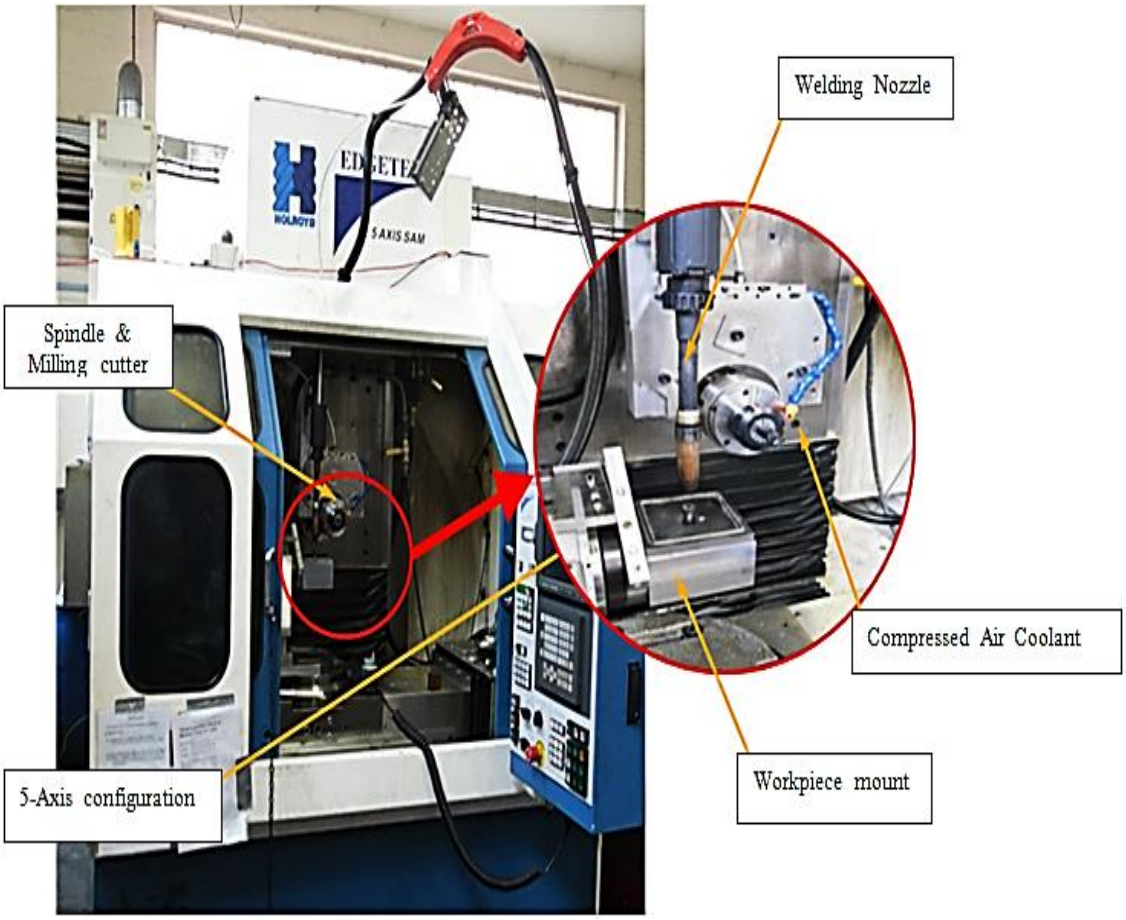

Figure 4-6: Integrated SAM Edgetek machine

4.3.2 Friction Stir Welding Machine (FSW)

Friction Stir Welding is defined as a solid-phase joining technique. TWI Ltd (Thomas, 1995) developed this method in 1991. The technology originates in the rotary friction welding process, which utilises a lathe to hold one component stationary with the other being held in a rotary chuck. Rubbing the two parts together generates heat, which plasticises the two materials, whilst extruding

contaminants away from the join face. This results in an anatomically cleaned friction joint, which exhibits an intermetallic bond (Mathers, 2002).

It is an uninterrupted process, which comprises plunging a part of a specially shaped moving tool between the abutting faces of the joint. The relative motion between the tool and the substrate produce frictional heat that creates a plasticised 'third party' region around the immersed portion of the tool. The contacts of the shouldered region of the tool with the workpiece also produce significant frictional heat as well as preventing plasticised material from being expelled.

The parent name of the FSW machine is Crawford Swift Powerstir 360 Stir weld machine (see Figure 4-7). It consists of vertical spindle, travelling table and a Fanuc 18i MA CNC controls the machine. Details of the machine plan is shown in Figure 4-7b and the machine specification shown in Table 4-5.

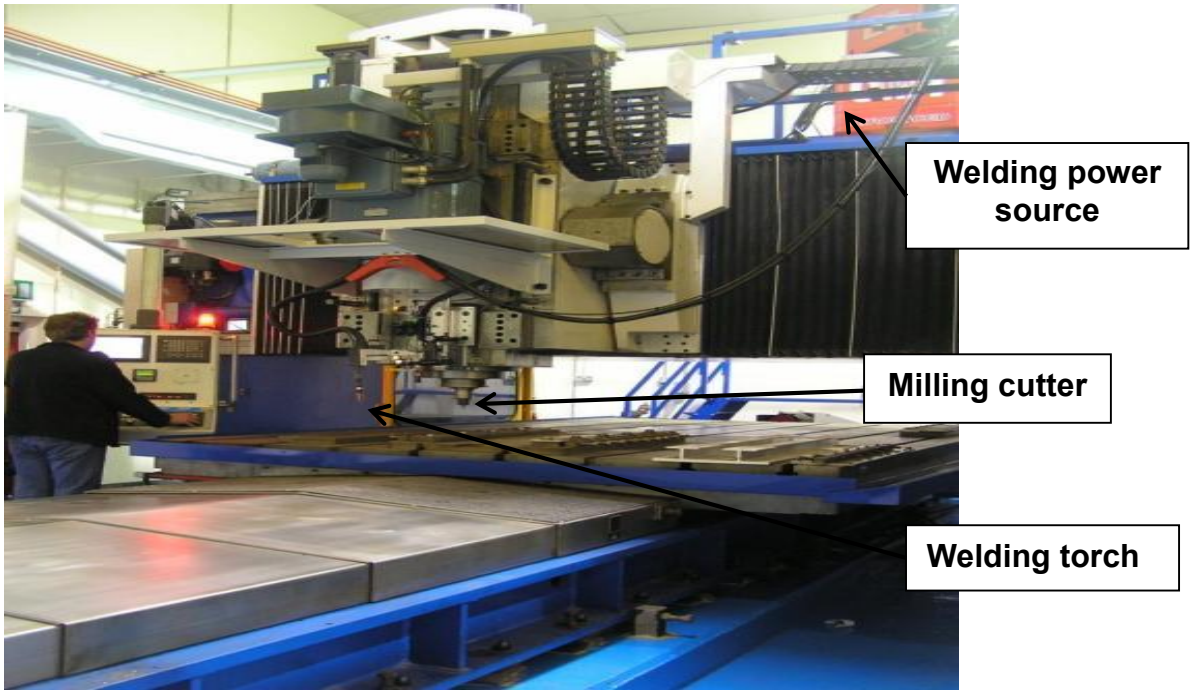

Figure 4-7: Large Friction Stir Welding

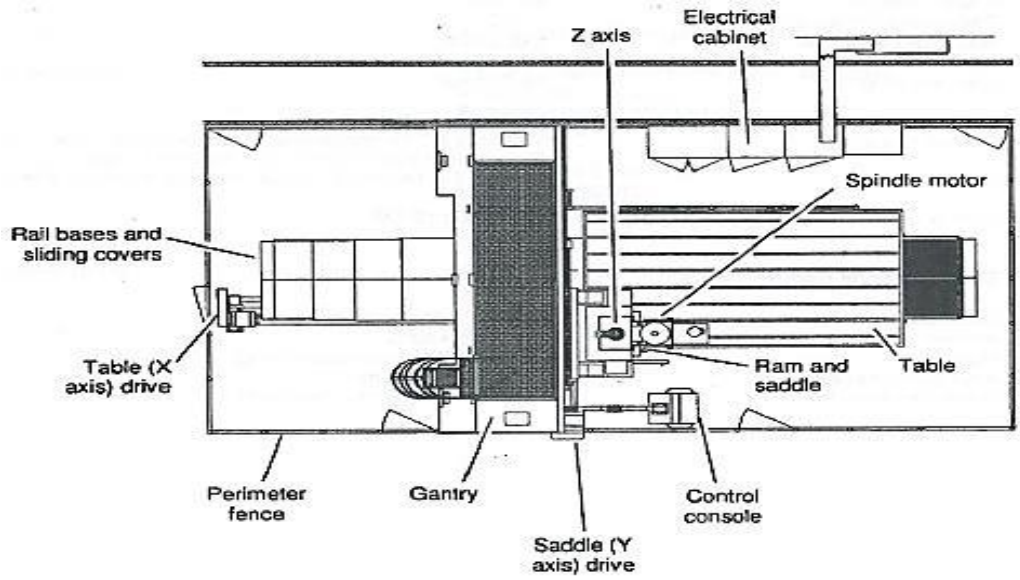

Figure 4-8: Plan view of the FSW machine

Table 4-5: FSW specifications

Maximum Component height	500mm
Y axis traverse	3500mm
X axis traverse	2000mm (2500mm when disconnected from ball srew)
Z axis traverse	400
Ram swivel (manual)	+/-5°
Maximum spindle speed	1000rpm
Machine weight	33000kg
Control system	GE Fanuc 18i MA

4.3.3 Welding Equipment

Welding trials were conducted using a Fronious TPS 5000 Cold Metal Transfer (CMT) power source. This is highly flexible machine which had the capability to weld in further MIG transfer modes i.e. spray, pulse etc. up to a maximum of 500A using a variety of filler wire diameters with a duty cycle of 40% at 500 A . The machine is fitted with a remote programming interface (RCU5000i) which allowed storage of a range of synergic tandem welding programs (for a variety of fillers and base materials) and had the functionality to allow modification of welding

parameters during welding and programming of tailored synergic parameters. The machine has the capacity to operate in different transfer mode (i.e. pulse, spray, or dip). The technology had previously been employed on dual tandem pipe welding, utilising steel filler wires with good stability and functionality of the process realised. The power source and programming interface is shown in Figure 4-9 mounted on an articulated six-axis robot arm (ABB IRB 2400) for torch manipulation.

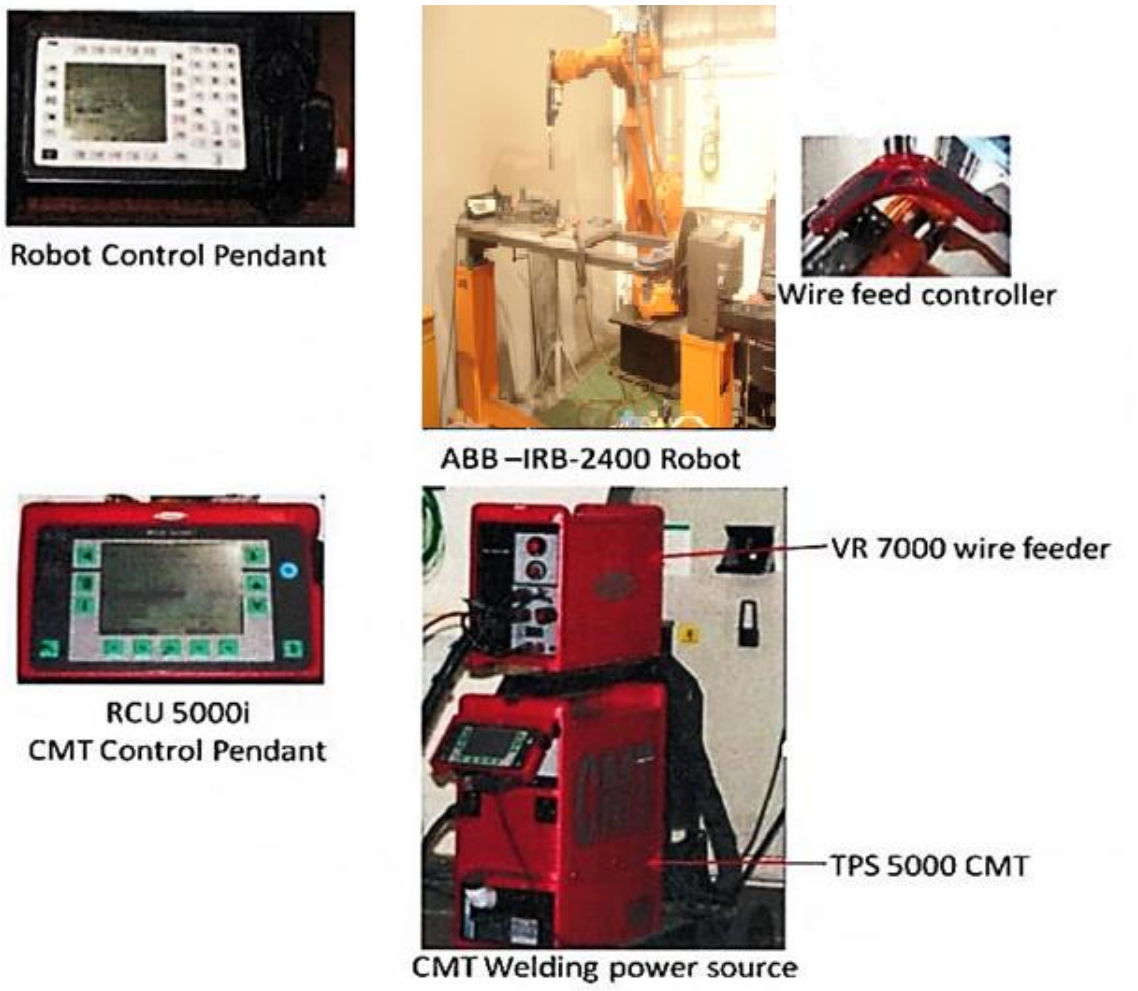

Figure 4-9:Fronious TPS 5000 Cold Metal Transfer (CMT) with an articulated six-axis robot arm (ABB IRB 2400)

The feed unit was fitted with uncalibrated dial for setting the wire feed rate. Consequently, prior to each weld, the system had to be set to the required value to ensure accurate and repeatable feeding. A calibrated mechanical tachometer was employed whereby cold wire was adjusted until the required wire feed rate was realised.

The ABB robot machine specification is as shown in Table 4-6 and the performance specification illustrated in Table 4.7.

Table 4-6: ABB Robot machine specification

		Supplementary loads (Upper arm)		
Payload	No of axis	Wrist end	Rear end	Base unit
20kg	6	2kg	10kg	35kg

Table 4-7: ABB Robot performance specification

Position repeatability	Path repeatability	Linear path accuracy	Resolution
0.03mm	0.11 – 0.15mm	2.5 – 3.0mm	0.01° in each axis

Light shield Argon/Carbon Dioxide (Ar/CO_2 (20%)) shielding gas produced by Brin's Oxygen Company, Ltd (BOC) was used in all the experiments with the flow rates of 15 L / min. However, the Contact To Work Distance (CTWD) was also retained at 13mm for the entire experimentations. The choice of shielding gas mixture and the Contact To Work Distance were selected according to the welding program requirements.

4.4 Material preparation

4.4.1 Before welding

In order to minimise the occurrence of porosity, the base materials were prepared prior to welding by subjecting them to grinding in order to remove the oxides layers and with a fine grade abrasive in order to make the surfaces horizontal.

This is devoid of needless polishing, followed by mechanical brushing using a circular wire brush until all surface contamination was visually removed. Plates were then cleaned with acetone to remove any particle matters.

4.4.2 Micrographic preparation

All welds to be examined were sectioned and attached in a special mould utilising an epoxy resin to allow them into grinder and polisher (see Figure 4.9). The samples were mechanically ground using a Buehler Meta Serve grinder-polisher as shown in Figure 4-10 in three steps, employing the typical grit sizes ranging from #120 to #2400 (American National Standards Institute (ANSI) grit). Wear rates were maximised by replacing the worn abrasives with newer ones. In the polishing stage, a polishing disc was concealed with a cloth and impregnated with 5µm diamond paste, in addition to 1µm silica suspension in water to create a polished surface. The sample was the rinsed with tap water and dried with ethanol (C_2H_5OH). In revealing the microstructure, the samples were etched using nital solution 2 % of nitric acid (HNO_3) in alcohol in order to attain a good contrast. However, the macrostructures were examined and pictures were taken using the Nikon Optiphot-66 optical microscope (see Figure 4-12).

Figure 4-10: Cross section of sample embedded in resin body

Figure 4-11: Buehler MetaServe automatic grinder - polisher

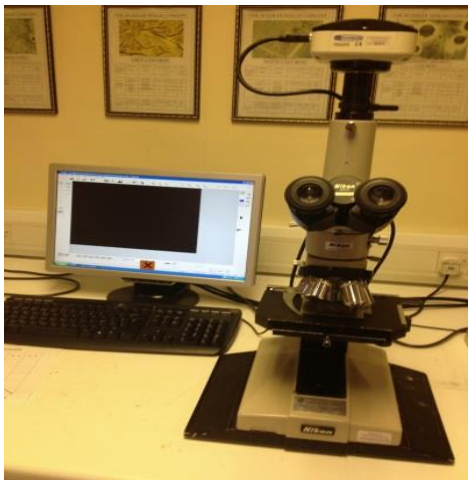

Figure 4-12: Nikon Optiphot-66 optical microscope

4.4.3 Scanning Electron Microscope (SEM)

A Scanning Electron Microscope (SEM) is designed to be able to examine microstructural and ultra-structural details of samples, within an SEM chamber, in their uncoated natural state. An SEM is able to examine wet, oily and outgassing samples, without any form of preparation, and is able to maintain specimens within their natural state for prolonged periods within the SEM viewing chamber. The SEM offers high resolution secondary electron imaging in a gaseous environment of practically any composition at pressures as high as 50 Torr, and temperatures as high as 1500^{o}C.

An SEM is specifically suited to dynamic experimentation at the micron to nanometre scale. SEM technology allows for dynamic experiments involving fluids and the possibility of imaging samples undergoing compression and tension. SEM can therefore be regarded as a micro dynamic experimentation chamber where materials can be examined at a range of mechanical loads and temperatures under a variety of gases/fluids.

The SEM comprises an electron column, which generates a stream of electrons, a compartment where the electron beams intermingle with the illustration sample, the detector, which monitors a variability of signals resulting from the beam sample interaction and a viewing system, which makes an image from the signal.

The electron column accelerates and focuses a beam of electrons onto the sample surface. The interaction between the sample surface and the beam electrons causes a variety of signals emission. These signals are detected and reconstructed into a virtual image displayed on the monitor (see Figure 4-14).

An XL30 Scanning electron microscope (shown in Figure 4-13) was utilised in analysing the effects of lubricant in the sequential deposition and machining of

Figure 4-13: Scanning electron microscope

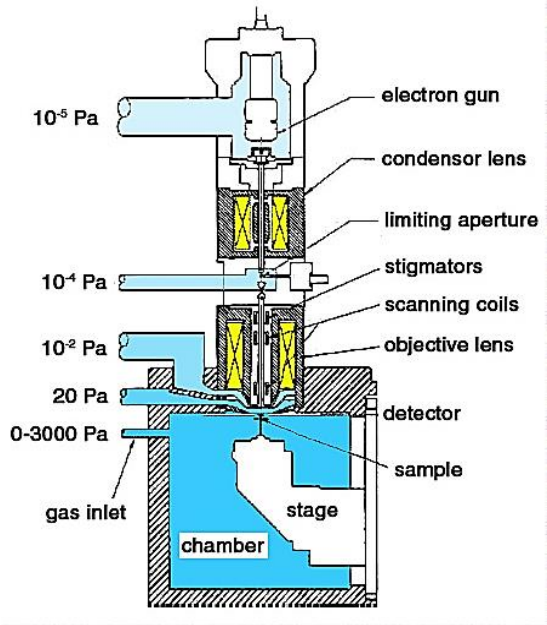

Figure 4-14: Schematic representation of scanning electron microscope (Morris, 2011)

WAAM samples. Because of the fine detail revealed by the electron microscope, as compared to the optical microscope, far more careful attention is given to the specimen preparation by giving the final polishing using fine diamond paste as the abrasive after first repeatedly polishing and etching, as for the optical microscope. The final etch is much lighter than that given to a normal metallographic specimen, in order to give topography contrast that is not stained.

5 Wire and Arc Additive Manufacture (WAAM) Deposition

5.1 WAAM Platform Comparison

5.1.1 Overview

This chapter describes the platform comparison of the AM deposition aspect of the study using the WAAM process. The comparison involves the deposition of WAAM square samples using three different WAAM platforms. The platforms compared are the WAAM platforms available in Cranfield University; the Integrated SAM Edgetek machine in the mechanical workshop and the ABB robot platform and Friction Stair Welding (FSW) platform, both at the Welding Engineering Research Centre (WERC). The various platforms were selected because of their characteristics; i.e. the SAM Edgetek is a precision machine with good accuracy and repeatability. It makes use of a linear bearing, while the ABB robot is very flexible and is widely used in industry. The latter makes use of the articulated arms in the deposition of WAAM parts. The FSW machine is used for the manufacturing of large WAAM objects. The process of comparison involves deposition of WAAM square samples and comparisons are made with respect to the physical weld bead geometrical output accuracy of the sample.

The weld characteristics are affected by the weld input parameters throughout the welding process. Consequently, welding may be well thought of as a numerous input numerious-output process. Moreover, (Farad and Mehdi, 2011) reported that a common difficulty faced by the manufacturer is the way in which process input is controlled in order to achieve an improved weld deposition with the necessary bead characteristics and weld quality resulting in negligible damaging residual stresses and distortion. As a result of this, the weld depostion parameters were kept constant but at an optimal setting following the recommendations of Sequeira-Almeida (2012) on all the platforms compared.

Bead geometries such as bead height, bead width and bead walls perpendicularity are important physical characteristics of WAAM manufactured

walls. The bead cross-sectional area, together with its height and width, affects the total shrinkage, which controls the residual stresses and therefore the distortion (Ding, et al., 2011).

The weld bead outcomes from the solidification of fluid metal in defining the eventual bead characteristics and the interfacial tensions play an important role. Geldart et al., (2003) reported in their studies on submerged arc welding that several welding conditions such as travel speed influence the bead shape and size. Gurev et al., (1993) and Geldart et al., (2003) identify the bead height and bead width as the most important output resulting from a welding deposition and this has motivated the determination of the output parameters used in comparing the platfoms in order to assess the relative performance of the machines.

Process capability was used in analysing the results of this section. Considering the advantages of the process capability as presented by Deleryd (1998), it is obvious that by using this method, knowledge about the process can be gathered. Areas for improvement can be identified, resulting in a better product. However, there are four important steps involved in conducting the process capability study in this research. The steps are as shown in Figure 5-1 and the detailed description is found below.

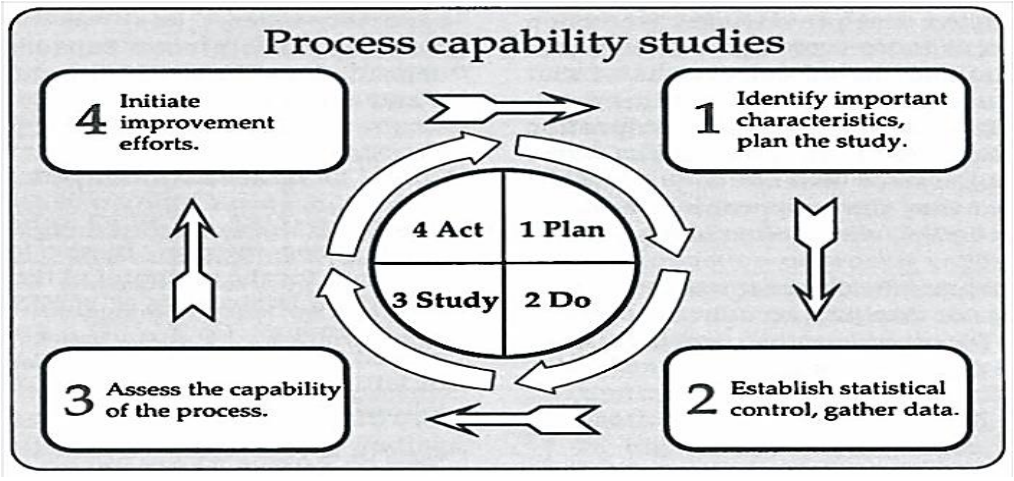

Figure 5-1: Steps in process capability studies (Adopted from Deleryd, 1997)

- Identify the essential characteristics

  This is to identify the important geometric characteristics that affect the overall output of the manufactured sample. It is not possible for the producer to monitor every characteristic, therefore the most important geometrical characteristics must be selected. In the case of this research, the important characteristics selected were the wall height, wall width and the perpendicularity of the wall. These are important characteristics when dealing with WAAM deposited thin walls (Sequeira Almeida, 2012).

- Establishing statistical control and gathering data

  Stability is paramount to attaining a good result from the process. The process must show a reasonable degree of statistical control. With the establishment of the statistical control of the process, the data was collected over a period so that the anticipated components of variation are shown in the data. In estimating the machine capability, a homogeneous set of data was obtained; i.e. the data was taken from the same material, in the same set up and using the same process.

- Assessing the process capability of the system

  In assessing the capability of the process, a histogram of the individual characteristic values was plotted. The Minitab software was used in analysing the capability of the process. The advancement of process capability index initiated the introduction of Cp, through Juran, (1974). He defined the process capability index, Cp as

$$Cp = \frac{USL - LSL}{6\sigma} \qquad 5\text{-}1$$

  where USL represents the upper specification limit, LSL is the lower specification limit and σ represents the standard deviation.

  However, the motivation of Juran (1974) is on the scattering of the studied process and this does not take into consideration the centring of the

process. To overcome this issue, Kane (1986) introduces Cpk, which can be defined as:

$$Cpk = \frac{Min(USL-\mu,\ \mu-LSL)}{3\sigma} \quad 5\text{-}2$$

where USL represents the upper specification limit, LSL is the lower specification limit, σ represents the standard deviation, and μ is the expected value of the study characteristic. The Cpk processes the distance concerning μ and the nearest specification limit, and relates this distance to half the natural process spread, 3σ. To justify the use of 3σ limits, Shewhart (1980) motivated the use of 3σ limits because they work well in practice as well as scientifically and provide effective action limits.

- Initiate improvement effort driven goals
  The improvement possibilities recognised from the process capability index are initiated. This provides suggestions on how to improve the process.

5.2 Materials and Experimental setup

This investigation is aimed at characterising the important geometries of WAAM manufactured structures from three different platforms with the view of comparing the platforms. The electrode used throughout the investigation is mild steel wire consumable electrode G3Si1 with diameters of 0.8mm and 1.2mm. The size of the wire was choosen because of its wide use in WAAM deposition and also because it has an excellent feedability and consistent welding performance, with extremely little spatters and improved bead profile and physical appearance. The chemical and mechanical properties are shown in Table 5-1 and 5.2.

Table 5-1: Mild steel electrode wire chemical composition (www.lincolnelectric.com)

Chemical composition typical wire (W%)								
C	Si	Mn	P	S	Ni	M_O	Al	Fe
0.06-0.14	0.7-1.00	1.30-1.60	0.025	0.025	0.15	0.15	0.02	Balance

Table 5-2: Mild steel electrode wire mechanical properties (www.lincolnelectric.com)

Mechanical properties			
	Yield strength (N/mm^2)	Tensile strength (N/mm^2)	Elongation (%)
Typical values	490	590	27

The base plate used in all the trials is rolled S355J2+N grade structural steel which was supplied with the specifications ASTM A1011/1011M and BS EN 10025:2004. The composition of the base plate in wt% is summarised in Table 5-3.

Table 5-3: Chemical composition of the base plate (www.lincolnelectric.com)

Chemical composition typical base plate (W%)								
C	Si	Mn	P	S	N	Cu	Ni	Fe
0.20	0.55	1.60	0.025	0.025	0.012	0.55	0.05	97.02

In selecting the base plate, consideration was taken into making sure that it conformed to the minimum chemical and mechanical requisite of the electrode wire (i.e. G3Si1), especially the minimum ultimate and yield strength. Furthermore, the base plate was chosen because of low cost and extensive

application in most structural manufacturing. Figure 5-2 shows the schematic diagram of the base plate.

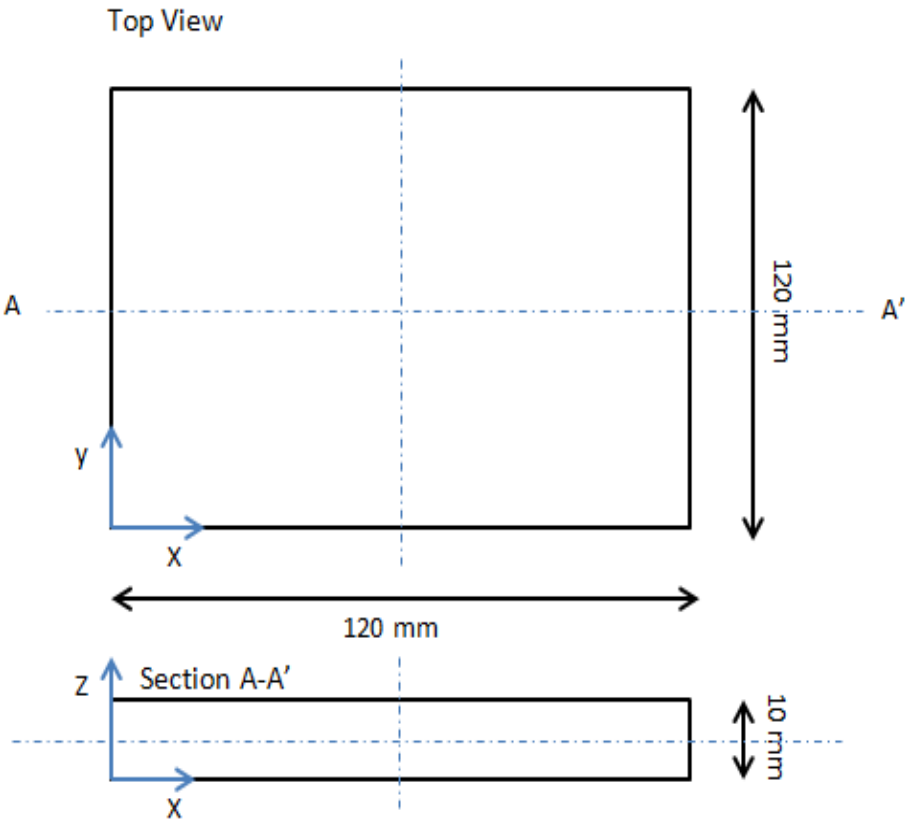

Figure 5-2: Schematic diagram of the base plate

The experimental parameters used for the trials are the same on all the platforms and are shown in Table 5-4. The difference in the parameters is the travel speed, which is a fuction of the platform and this was chosen in order to deposit WAAM walls of different widths. Screening experiment was done to arrive at the deposition parameters.

Table 5-4: Experimental parameters

Parameters	Trial 1	Trial 2
Travel Speed (TS) m/min	**0.2**	**0.3**
Wire Feed Speed (WFS) m/min	6.0	6.0
Electrode wire diameter (mm)	0.8	0.8

Operation mode (program)	Pulse soft (P19)	Pulse soft (P19)
Shielding gas	Argon Shield light CO_2	Argon Shield light CO_2
Flow rate (l/min)	15	15
Contact tip to work distance CTWD (mm)	13	13

The shielding gas used, argon shield light carbon monoxide, was carefully chosen according to the welding program with the welding power source in order to have a good WAAM deposition.

The illustration of the experimental set up on various platforms is shown in Figure 5.3. The individual machines have been described in detail in Chapter 4 of this thesis.

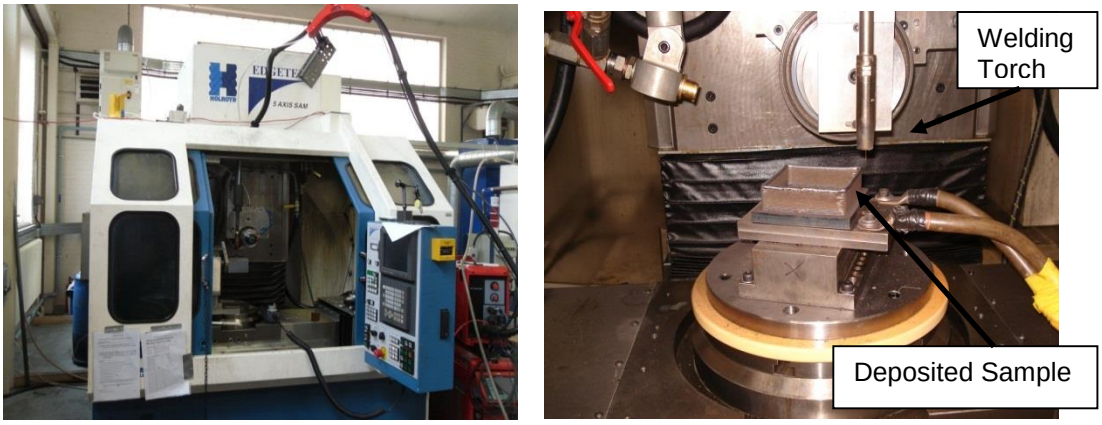

(a)

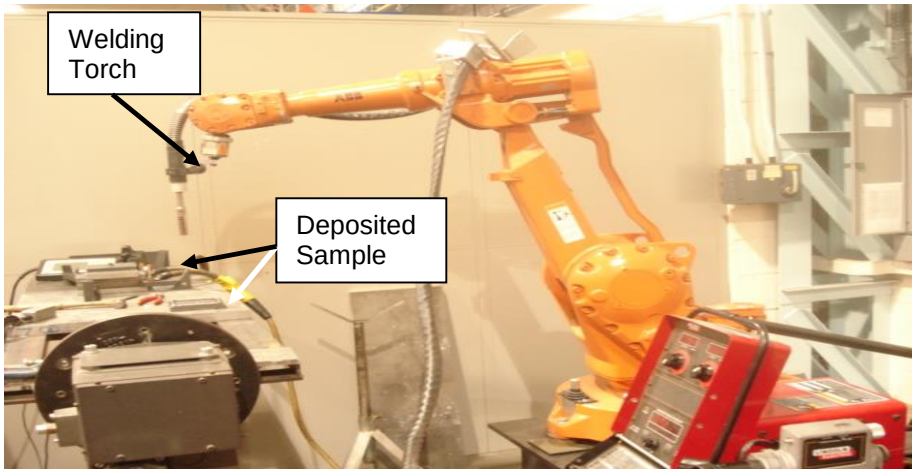

(b)

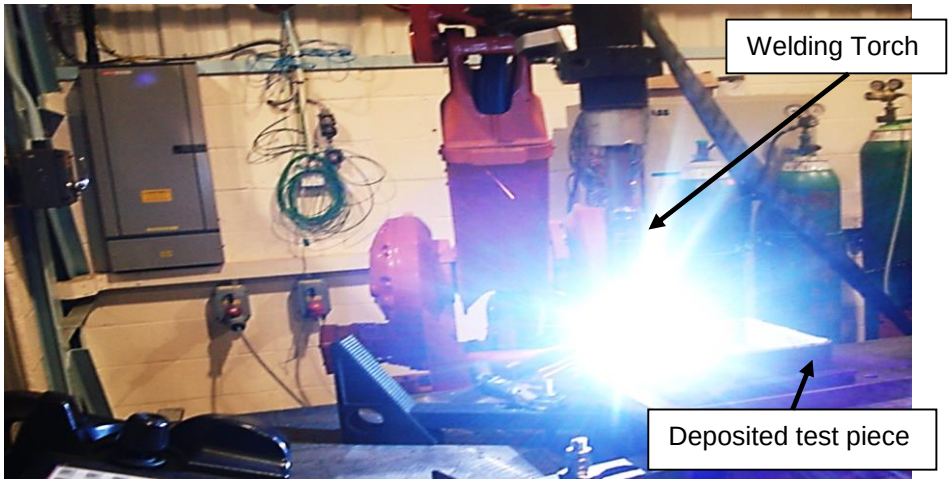

(c)

Figure 5-3: Machine experimental set up for (a) SAM Edgetek machine (b) ABB robot (c) Friction stir welding machine.

5.3 Methodology

The direct comparison of machines is a challenging task, particularly when the machines' structures are different, as is the case here. However, the comparison method was motivated by Geldart et al., (2003), who recommended that benefits could be achieved by using the machines to manufacture parts and then compare their performance using standardised criteria. The criteria used were the physical geometrical accuracy in the wall height, wall width, the wall perpendicularity and the surface finish. These were carefully chosen since they were acknowledged as the main process performance requirements for the production of WAAM products.

The use of all possible parameters would be difficult, time consuming and possibly inconclusive as the benefits of separate parameters and their interdependence is frequently application sensitive (Geldart et al., 2003). In choosing the parameters, Wire Feed Speed (WFS) and Travel Speed (TS) were acknowledged by Dickens et al., (1992) as the key parameters in determining a desired bead physical geometry and surface quality of the part produced. TS was varied from trial 1 to trial 2, from 0.2m/min to 0.3m/min, to change the wall thickness and to study the effect of this change on the various machines. Another reason for changing to TS instead of WFS is that it is governed by the comparing machines, while WFS is a function of the welding machine.

In conducting the comparison, a measurable test component, square samples measuring 100mm x 100mm x 10mm (see Figure 5-4) were selected. The square box test piece was chosen, since four walls per sample can be analysed, which will increase the accuracy of the results.

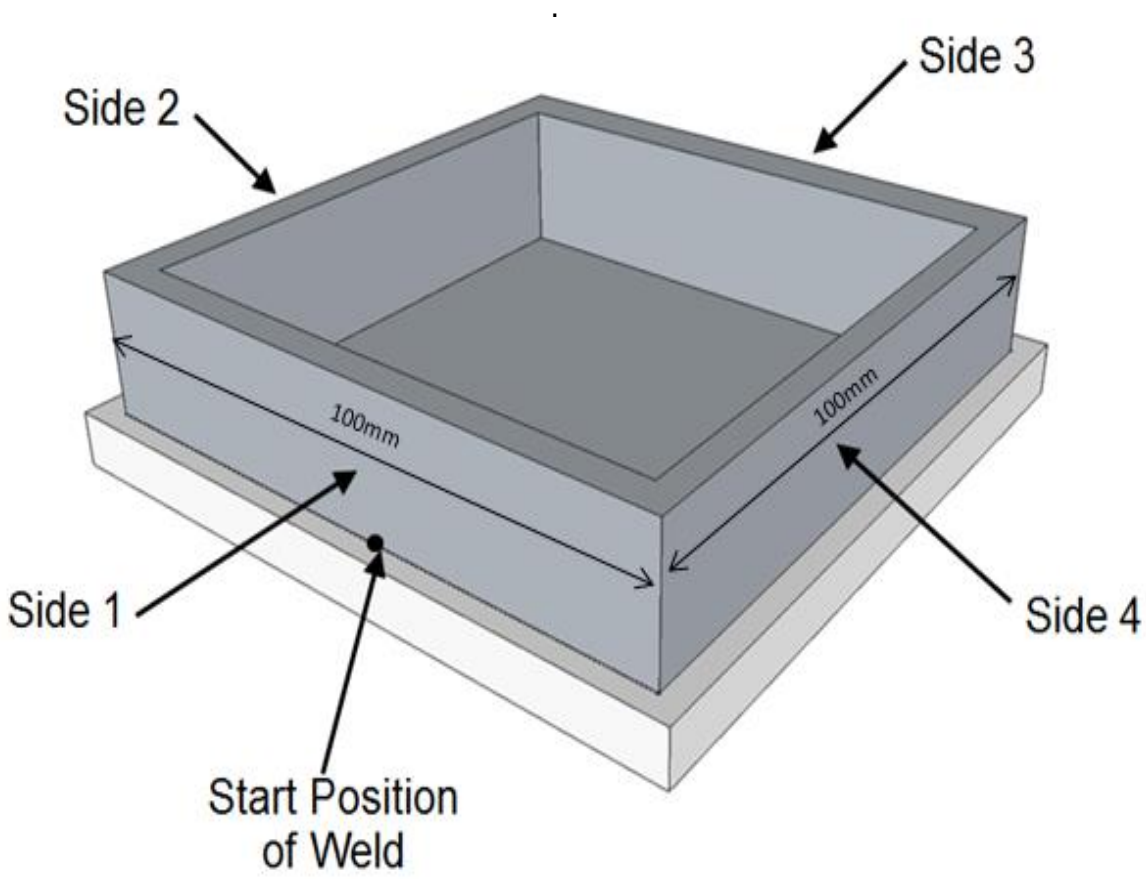

Figure 5-4: Test piece

The test piece consisted of a box with straight walls built on a substrate intended to check the performance of the WAAM platforms under the same trial conditions on the three platforms. The conditions at which the study took place consisted of manufacturing WAAM square samples on all the three WAAM platforms using the same parameters.

The trials consisted of manufacturing twelve (12) test samples each with four (4) sides using a TS of 0.2m/min and another set of twelve (12) test samples with four (4) sides using a TS of 0.3m/min on each of the three machines, producing a total of twenty-four (24) individual test samples per machine with (forty-eight) 48 sides to analyse. The welding parameters for the trials were kept constant for all the three machines and are described in detail in Table 5.4.

After the welding depositions were completed, the test samples were characterised using the TESA V300DC CMM machine (See Figure 5-5) and the results of the comparison were given in graphical form for each platform. Thereafter, surface profile data was recorded using the Talysurf 120L machine and the average value was obtained for the surface waviness (Wa) and Peak to Valley height (Rt).

Figure 5-5: Measurement of trial samples on TESA V300DC CMM machine.

5.4 Results

The results of the comparison trials are presented in charts. Each of the charts displays the range of measurements generated for each of the features giving an overall comparison of the geometrical accuracy of the test piece. After dimensional measurement, surface waviness for each of the test sample was measured and the average value was obtained. However, process capability was utilised in assessing the capability of each of the WAAM platforms using the results generated from the dimensional measurement.

5.4.1 Sample Width

Figure 5-6, Figure 5-7 and Figure 5-8 show the width of the samples for the SAM Edgetek, ABB Robot and the FSW machines respectively obtained using a TS of

0.2m/min with all other constant parameters, as shown in Table 5-4. S1, S2, S3 and S4 represent side 1 to side 4 of the sample as shown in Figure 5.4.

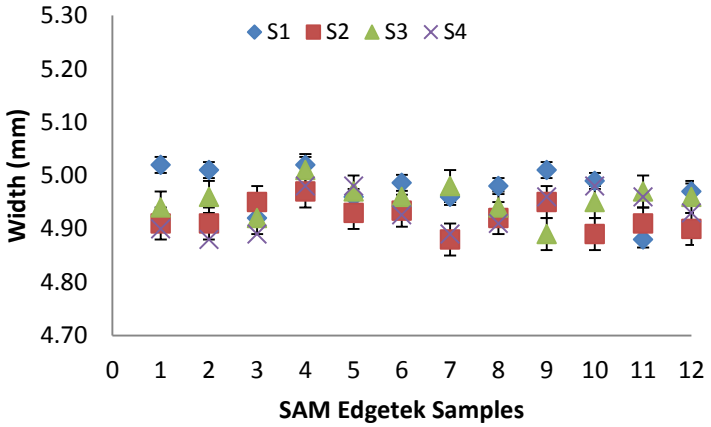

Figure 5-6: Variations in the width of the samples in the SAM Edgetek for trial 1

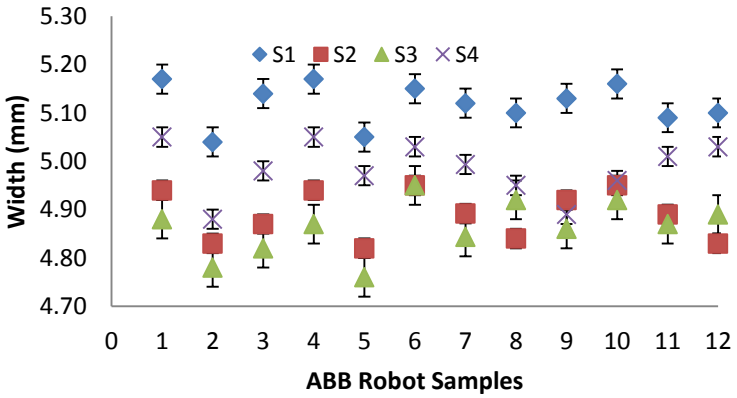

Figure 5-7: Variations in the width of the samples in the ABB Robot for trial 1

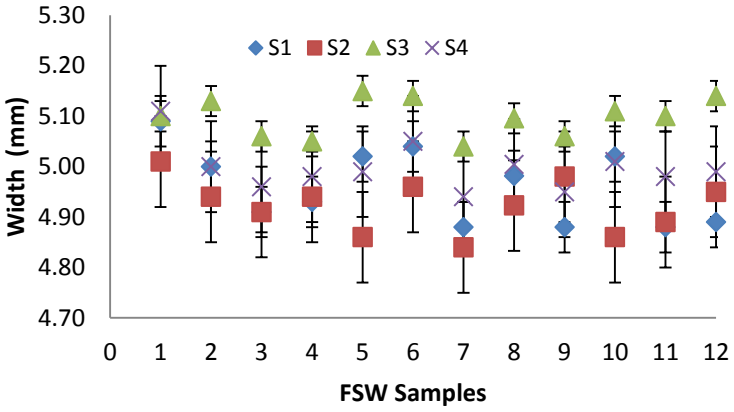

Figure 5-8: Variations in the width of the samples in the FSW for trial 1

The results obtained regarding the width showed that the SAM Edgetek samples are very consistent and close to another, with an average of 4.95mm with an average standard deviation of 0.14mm. In the ABB Robot sample, the width has an average of 4.96mm with a standard deviation of 0.20mm, while in FSW the average width is 5.01mm with a standard deviation of 0.27mm.

Figure 5-9, Figure 5-10, and Figure 5-11 show the variations in the width through an increase in the TS from 0.2m/min to 0.3m/min, with all other parameters remaining constant. The average width for the SAM Edgetek sample in this case is 3.92mm with a standard deviation of 0.27mm. However, the ABB Robot samples have an average width of 3.96mm and standard deviation of 0.31mm, and FSW has an average of 4.16mm with standard deviation of 0.29mm. The drop in the width obtained in trial 2 was as a result of highest travel speed used.

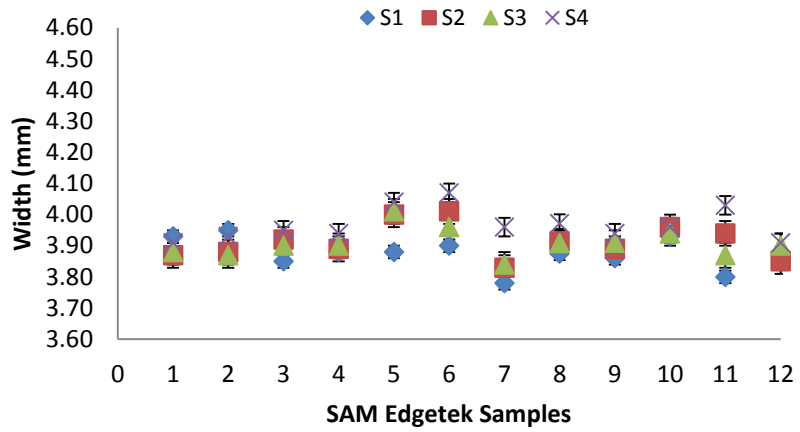

Figure 5-9: Variations in the width of the samples in the SAM Edgetek for trial 2

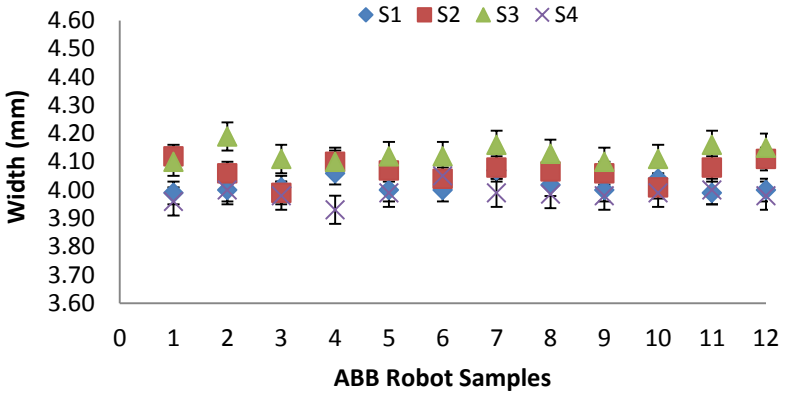

Figure 5-10: Variations in the width of the samples in the ABB Robot for trial 2

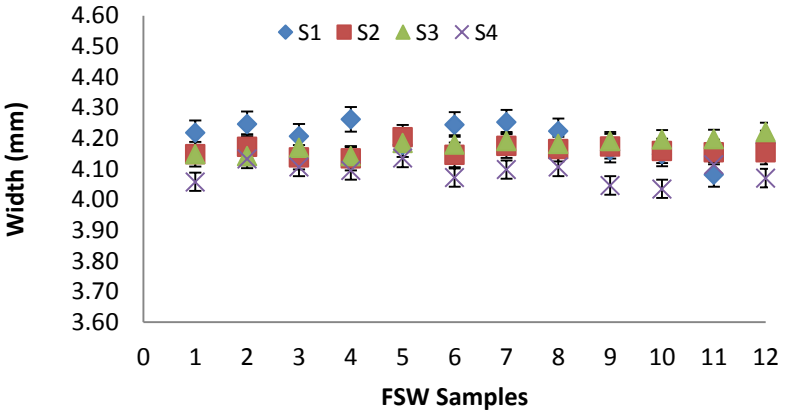

Figure 5-11: Variations in the width of the samples in the FSW for trial 2

5.4.2 Sample height

The final height obtained is another important geometry in the platform comparison. All parameters being the same, it is anticipated that the final height should be the same, irrespective of the platform or process.

Figure 5-11, Figure 5-12 and Figure 5-13 show the final height obtained on each platform with a TS of 0.2m/min. On the SAM Edgetek platform, the average height obtained is 34.3mm with a standard deviation of 0.4mm, while the ABB Robot has an average of 32.8mm with a standard deviation of 0.64mm. However, in FSW, the average height is 32.2mm with a standard deviation of 0.68mm. It is noted that the heights are not closely spread in the FSW.

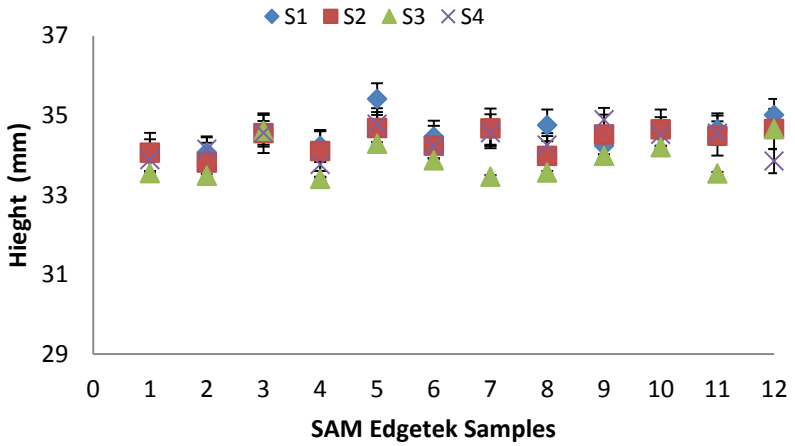

Figure 5-12: Variations in the height of the samples in the SAM Edgetek for trial 1

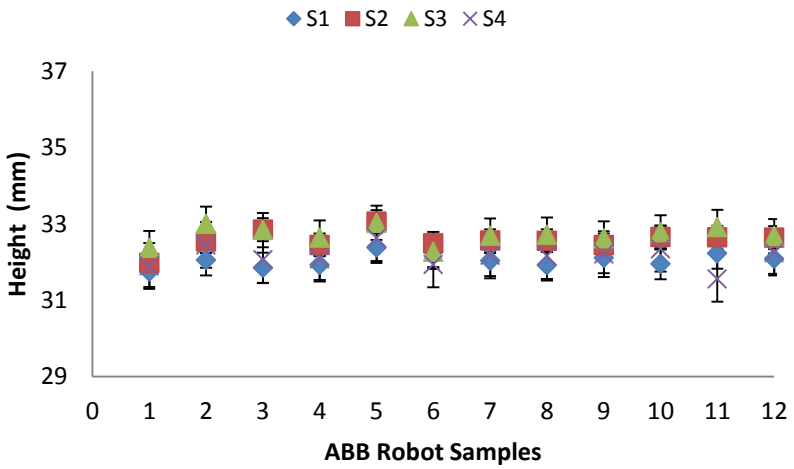

Figure 5-13: Variations in the height of the samples in the ABB Robot for trial 1

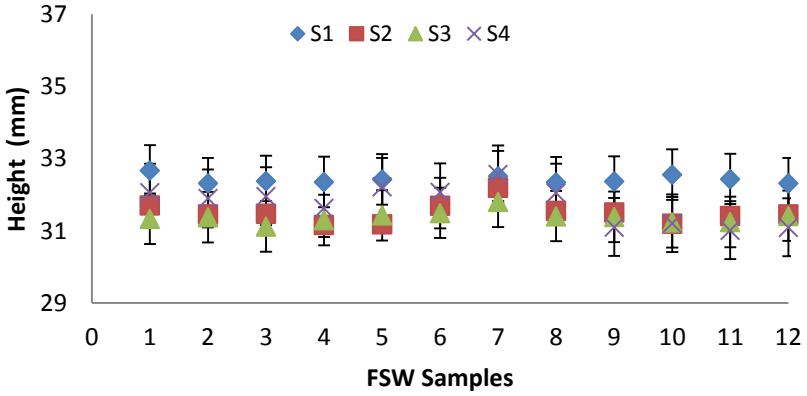

Figure 5-14: Variations in the height of the samples in the FSW for trial 1

There is a reduction in the final height with an increase in TS as seen in Figure 5-15, Figure 5-16, and Figure 5-17. The final height in SAM Edgetek samples decreased to an average of 27.9mm with a standard deviation of 0.60mm, while the ABB Robot samples have an average of 26.5mm and a standard deviation of 0.26mm. FSW has an average of 26.3mm and a standard deviation of 0.35mm.

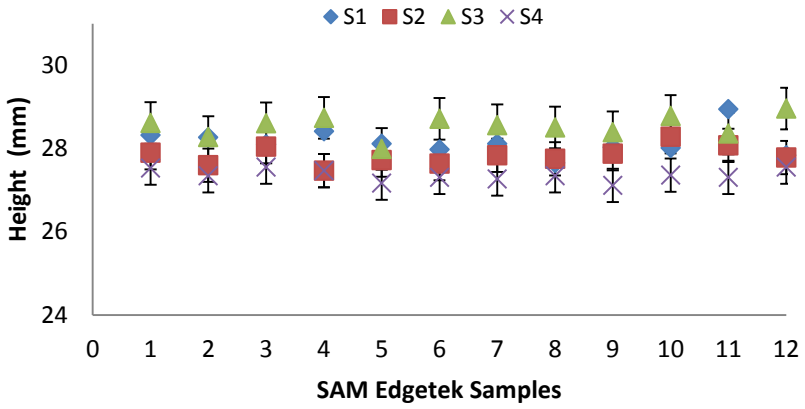

Figure 5-15: Height of the samples in the SAM Edgetek in trial 2

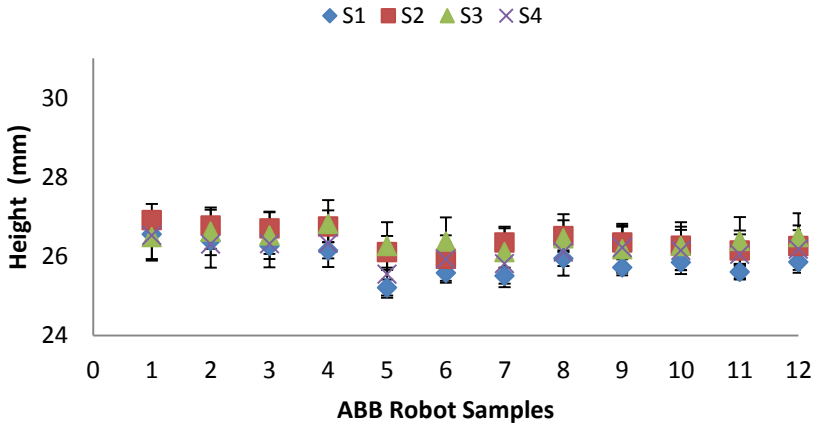

Figure 5-16: Height of the samples in the ABB Robot in trial 2

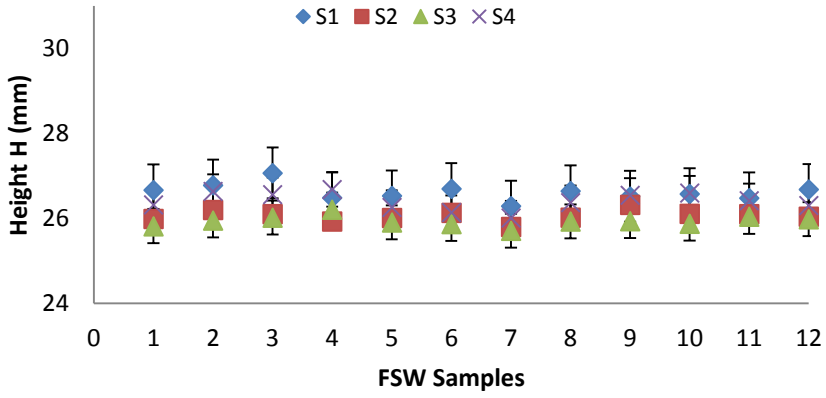

Figure 5-17: Height of the samples in the FSW in trial 2

From trial 1 and 2, it is shown that the SAM Edgetek platform produces a higher wall than the ABB Robot and the FSW platform. However, when comparing the consistency of this value, both the ABB Robot and the SAM Edgetek machine have a higher consistency, whereas the FSW platform showed a larger variation in the height of the wall produced.

5.4.3 Perpendicularity

The perpendicularity of the wall was measured on the TESA V300DC CMM machine. In measuring the perpendicularity of the two-sided walls, the outer wall (S-OUT) and the inner walls (S-IN) is as shown in Figure 5-18. The measurements were taken on both the outer walls and the inner walls with 40 points taken on each wall side.

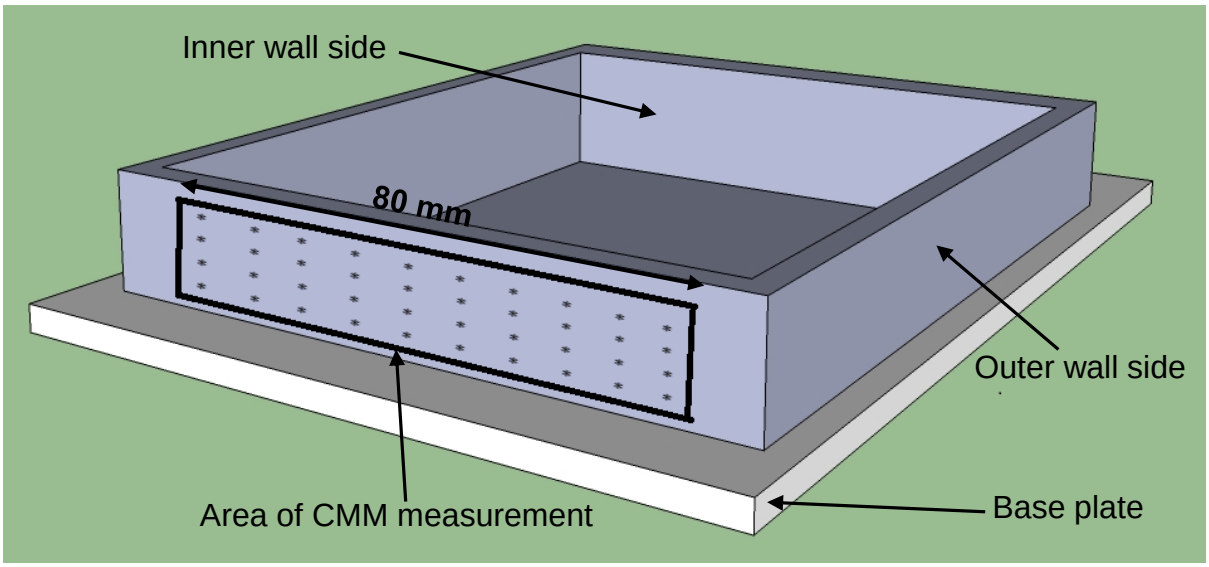

Figure 5-18: Illustration of deposited wall sides with the area of CMM measurements

The first three layers were not considered due to the results from the previous trials which showed that these layers are usually thinner than the previous layers

and errors might be introduced in trying to use the CMM probe to measure those regions.

Figure 5-19, Figure 5-20 and Figure 5-21 show the perpendicularity of the deposited walls on the three platforms using a TS of 0.2m/min. The deposited walls from the SAM Edgetek samples (see Figure 5-19) and the ABB Robot samples (see figure 5-20) produced better walls in terms of the straightness with an average of 89.9° with a standard deviation of 0.52° for the SAM Edgetek samples. The sample deposited from the ABB Robot had an average of 89.8° with a standard deviation of 0.54°, while the deposited sample on the FSW (see Figure 5-21) has an average of 89.5° with a standard deviation of 0.68°.

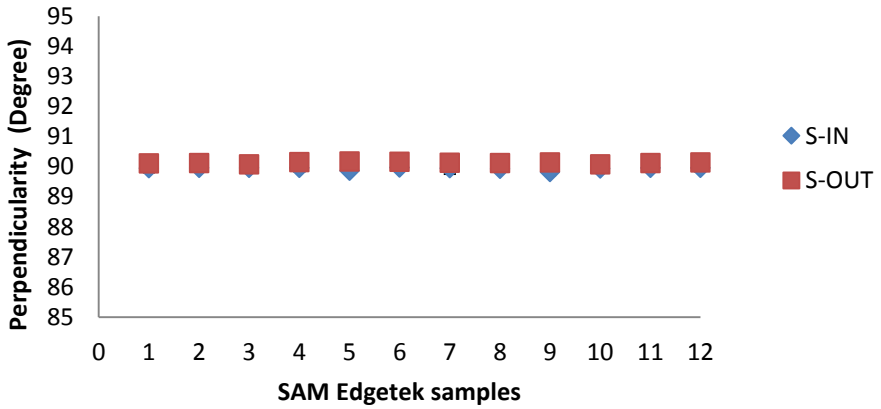

Figure 5-19: Perpendicularity of the SAM Edgetek deposited walls for trial 1 (Average value and standard deviation)

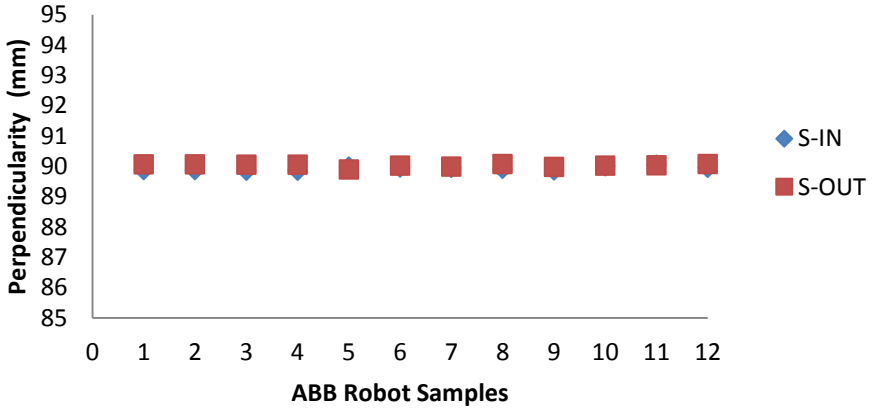

Figure 5-20: Perpendicularity of the Robot deposited walls for trial 1(Average value and standard deviation)

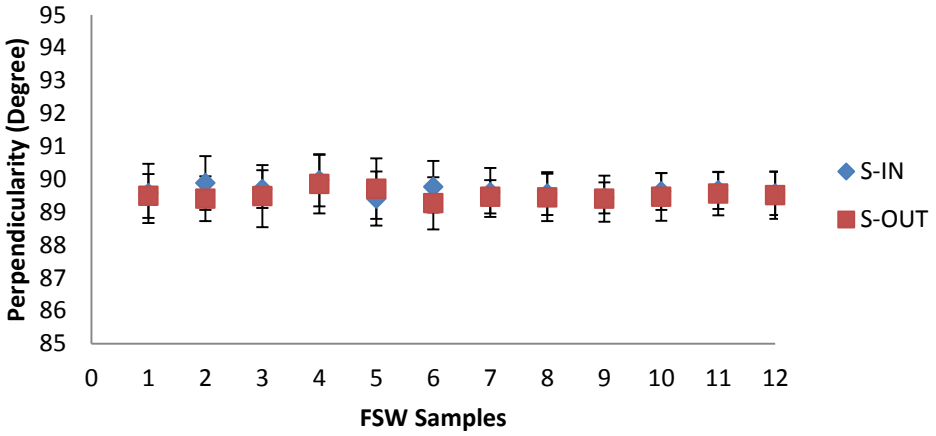

Figure 5-21: Perpendicularity of the FSW deposited walls for trial 1(Average value and standard deviation)

However, the walls (as shown in Figure 5-20) are not straight, as both walls tend to point toward the same direction.

The same procedure was repeated with an increase in TS to 0.3m/min. Figure 5-22, Figure 5-23 and Figure 5-24 also show the variation in the perpendicularity for the three platforms. The SAM Edgetek samples (see figure 5-22) showed a straight wall with an average of 89.9˚ with a standard deviation of 1.46˚, while the ABB Robot (see figure 5-23) showed walls with an average of 90.1˚ with standard deviation of 1.03˚. The wall samples manufactured from the FSW (see Figure 5-24) have an average of 89.5˚ with a standard deviation of 0.46˚.

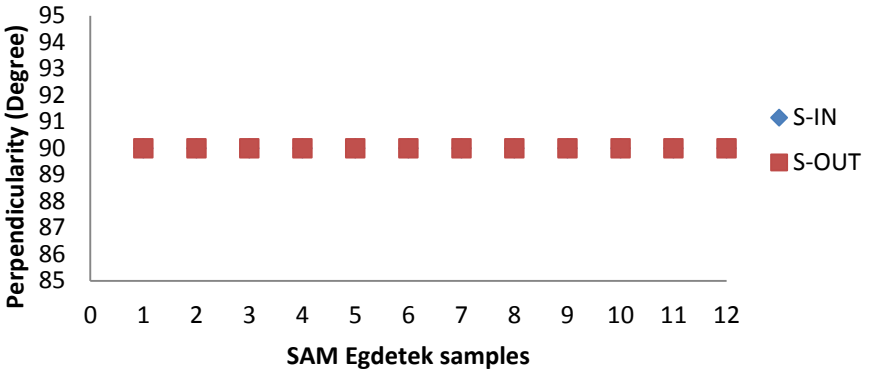

Figure 5-22: Perpendicularity of the Edgetek deposited walls for trial 2(Average value and standard deviation)

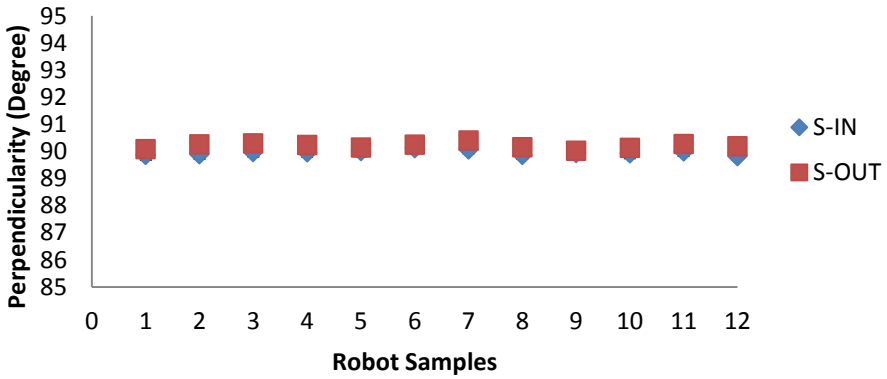

Figure 5-23: Perpendicularity of the ABB Robot deposited walls for trial 2(Average value and standard deviation)

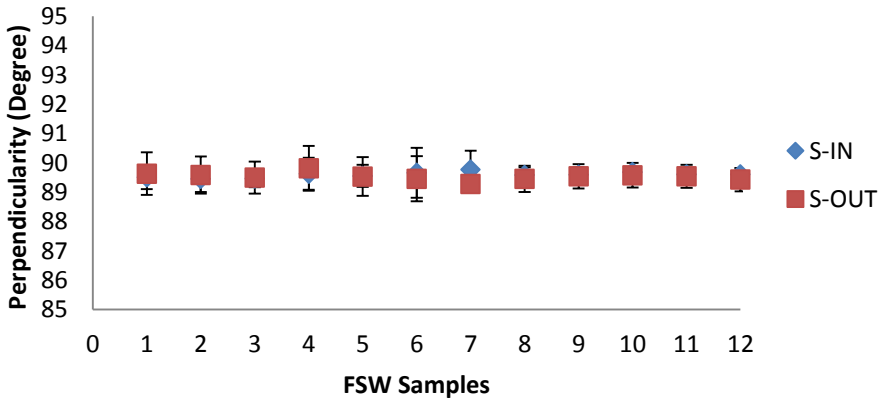

Figure 5-24: Perpendicularity of the FSW deposited walls for trial 2(Average value and standard deviation)

5.4.4 Surface topography

The properties of surface topography are critical to the functionality of the WAAM wall. Machining is required to give a good finishing operation. The geometrical quality of the surface topography of the walls was characterised by the amplitude parameters: average surface waviness (Wa) and the total waviness (Wt) parameters, which is the peak–valley measurement. Figure 5-25a and Figure 5-25b illustrate the surface waviness values as an average over the repeated trials for the samples from the three platforms.

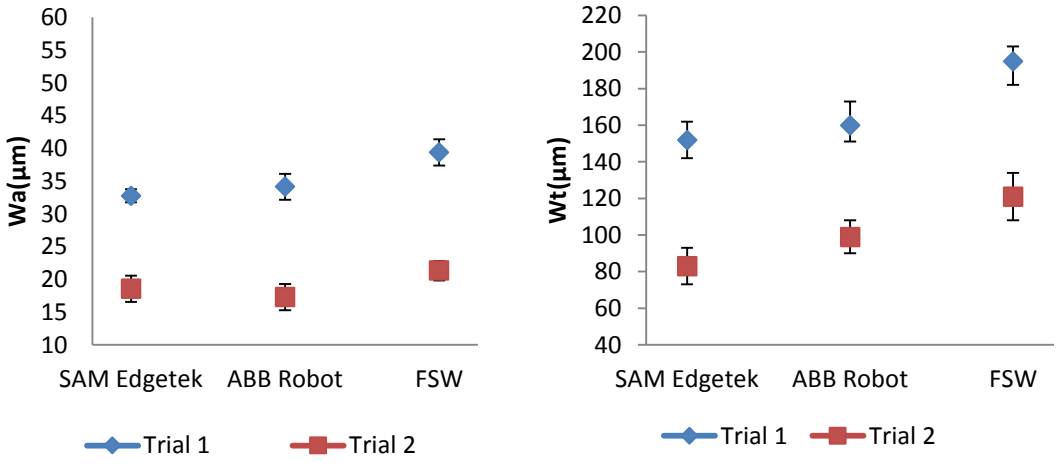

(a) (b)

Figure 5-25: Effects of platforms on surface waviness of the deposited walls with (5-25a) showing surface waviness (Wa) and (5-25b) showing peak-valley values Wt. (Average value and standard deviation)

The results show a better surface waviness when using the SAM Edgetek platform, compared to the ABB Robot and the FSW especially in trial 1, however the ABB robot produces walls with an improved surface waviness in trial 2. SAM Edgetek samples achieved the lowest Wa and Wt. The effect of the TS on both Wa and Wt for constant WFS indicated that both the Wa and Wt reduce as the TS increases. It also shows that Wa and Wt depend significantly on TS. This is not necessarily evidence that the SAM Edgetek machine is significantly better than the ABB robot because the difference in waviness may be as a result of the welding process.

5.4.5 Process capability Analysis

In analysing the performance of the various platforms, Minitab software was used to calculate the Cpk for the processes. Table 5-5 to Table 5.10 show the Cpk values for the selected geometries.

Table 5-5: Result of the Cpk analysis for the width of the sample trial 1

Platform	*Cpk*	*Sample mean (mm)*	*SD (mm)*	*P-Normalty*
SAM Edgetek	1.34	4.95	0.037	0.056
Robot	0.48	4.96	0.129	0.063
FSW	0.49	5.00	0.093	0.439

Table 5-6: Result of the Cpk analysis for the width of the sample trial 2

Platform	*Cpk*	*Sample mean (mm)*	*SD (mm)*	*P-Normalty*
SAM Edgetek	1.16	3.92	0.053	0.324
Robot	0.48	3.96	0.100	0.051
FSW	0.30	4.16	0.056	0.333

Table 5-7: Result of the Cpk analysis for the height of the sample trial 1

Platform	*Cpk*	*Sample mean (mm)*	*SD (mm)*	*P-Normalty*
SAM Edgetek	1.44	34.3	0.397	0.056
ABB Robot	0.41	32.8	0.677	0.055
FSW	0.11	32.2	0.641	0.051

Table 5-8: Result of the Cpk analysis for the height of the sample trial 2

Platform	*Cpk*	*Sample mean (mm)*	*SD (mm)*	*P-Normalty*
SAM Edgetek	1.09	27.9	0.602	0.502
ABB Robot	0.70	26.5	0.262	0.054
FSW	0.24	26.3	0.352	0.053

Table 5-9: Result of the Cpk analysis for the perpendicularity for sample trial 1

Platform	*Cpk*	*Sample mean (°)*	*SD (°)*	*P-Normalty*
SAM Edgetek	1.00	89.97	0.324	0.393
ABB Robot	0.62	89.99	0.537	0.064
FSW	0.56	89.99	0.509	0.219

Table 5-10: Result of the Cpk analysis for the perpendicularity for sample trial 2

Platform	*Cpk*	*Sample mean (°)*	*SD (°)*	*P-Normalty*
SAM Edgetek	1.39	89.99	0.146	0.053
ABB Robot	0.56	89.99	0.588	0.164
FSW	0.42	89.56	0.452	0.061

Cpk studies can be viewed as a statistical method. This means that data is gathered, transformed and presented, and actions are taken based upon the results. In order to explain the results, Cpk was presented in a series of charts (Figure 5-26 to Figure 5-31). Each chart displays the Cpk values and the WAAM platforms for each of the features, giving the overall comparison of the geometrical accuracy of the test piece.

Figure 5-26 shows the Cpk of the widths of the test piece from all three platforms for trial 1. The summary of the Cpk results indicates that the SAM Edgetek machine platform is more capable of producing a better test sample in terms of the width because high Cpk is more desirable. However, the results revealed that the other platforms show less capability when considering the width of the test sample manufactured. Trial 2 also produced the Cpk (Figure 5-27) which followed the same trend as in Figure 5-26. Irrespective of the TS, the SAM Edgetek platform has a better capability, compared to other platforms.

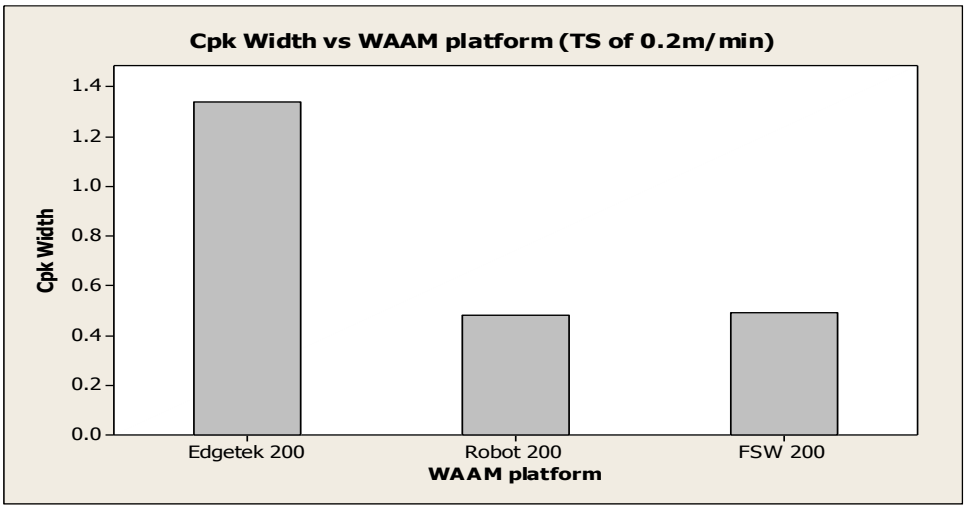

Figure 5-26: Summary of the Cpk for the width of the samples from all the platforms for trial 1

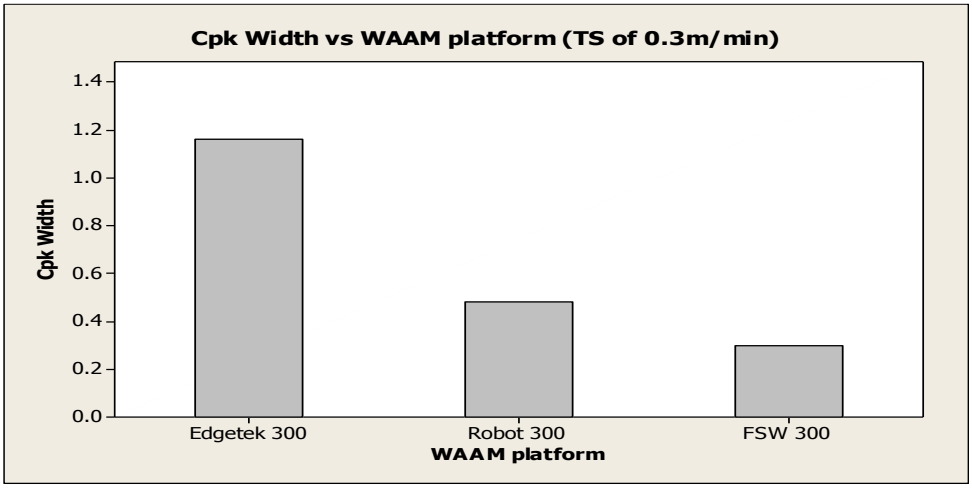

Figure 5-27: Summary of the Cpk for the width of the samples from all the platforms for trial 2

The SAM Edgetek has a better platform because of its Cpk values. Hence, the platforms are capable of manufacturing good parts with fewer defects when width is of great importance.

Another physical geometry analysed with Cpk is the height of the test sample produced. Figure 5-28 and Figure 5-29 illustrate the Cpk obtained with the height

of the test sample from all the platforms. It is shown that not all the processes meet the target. The summary of the Cpk for the height of the test sample from all the platforms for trial 1 and trial 2 follows the same trend as shown in Figure 5-28 and Figure 5-29.

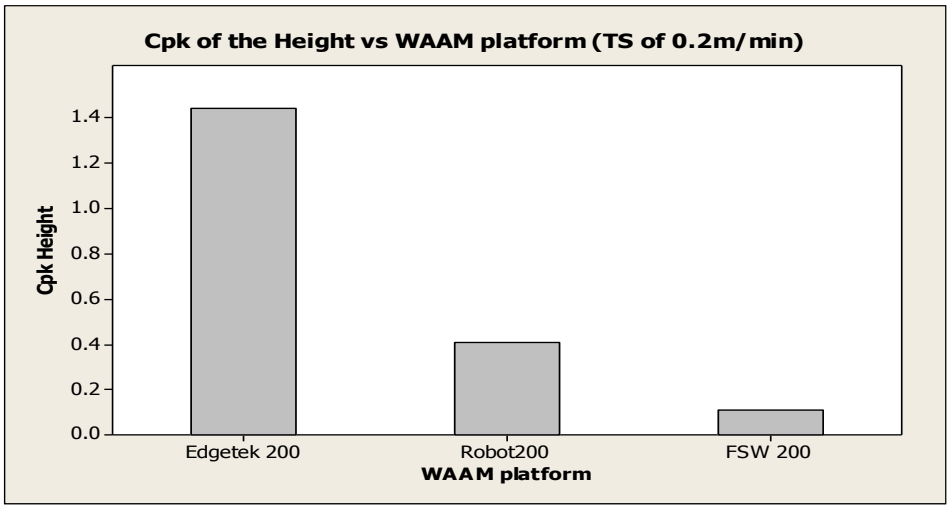

Figure 5-28: Summary of the Cpk for the height of the samples from all the platforms for trial 1

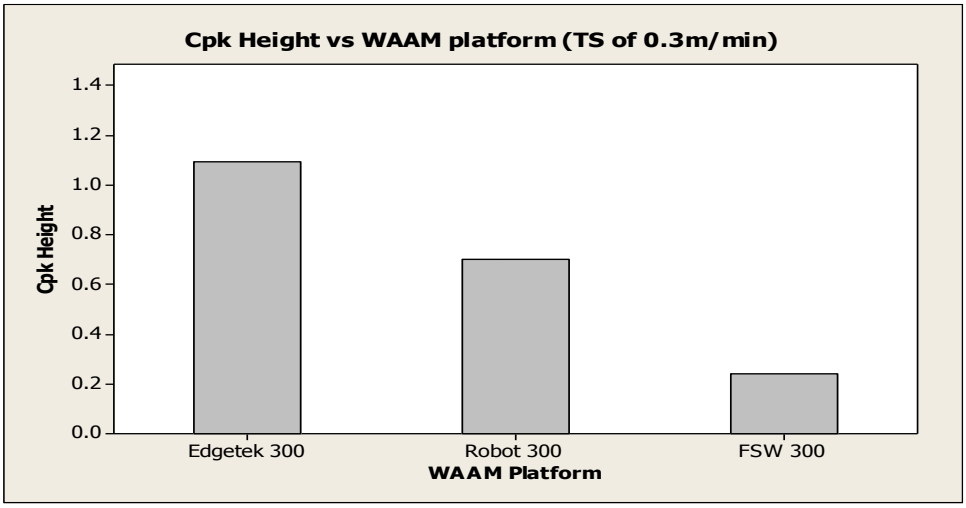

Figure 5-29: Summary of the Cpk for the height of the samples from all the platforms trial 2

Figure 5-30 and Figure 5-31 highlight the Cpk of the perpendicularity of the test sample for trial 1 and trial 2 respectively. With the deposition of the test samples using the SAM Edgetek platform, it has a Cpk of 1.00, which is about meeting the test sample specification.

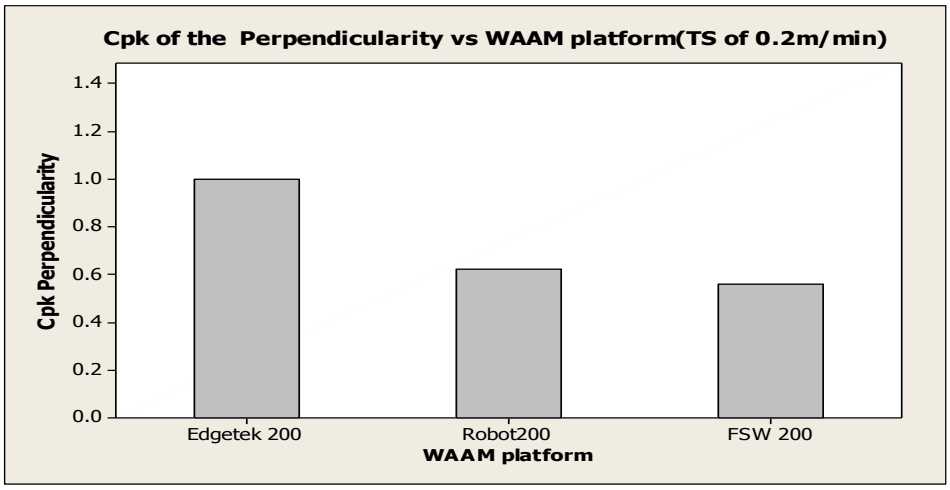

Figure 5-30: The Cpk of the perpendicularity of the test sample from all the platforms for trial 1

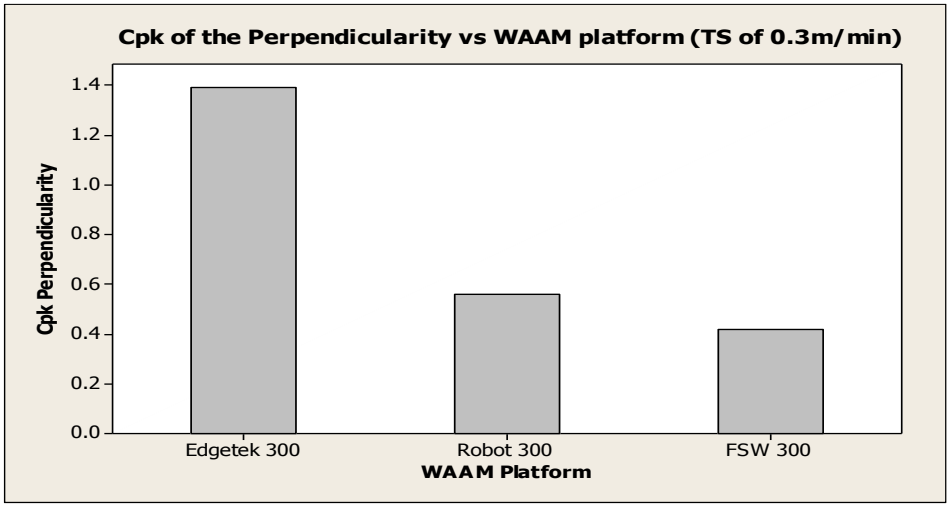

Figure 5-31: Cpk comparison of the perpendicularity of the samples walls from all the platforms for trial 2

However, the Cpk values of the perpendicularity of the ABB Robot and FSW platforms is less than 1, which is an indication that some test samples fall outside the specification limit, making the test sample less reliable.

5.5 Discussion

This chapter concentrates on the comparison of three different WAAM platforms in terms of the physical geometrical accuracy (such as the wall width, wall height and the wall perpendicularity) in the manufacture of WAAM parts. A square test sample (as shown in Figure 5-2) was selected because of the ability to measure and analyse each deposited wall of the square sample separately, giving an in depth knowledge of the deposited part. The manufacture of parts with lower minimum feature dimensions leads to a substantial decrease in the deposition efficiency because of the huge amount of material that will be machined off before achieving the necessary dimensions in the preferred tolerance. For this reason, the quality of the deposited parts is affected as a consequence of the restricted control over the dimension of the flowing pool size.

The quality of WAAM parts can normally be characterised on the features; for instance, geometrical accuracy and the metallurgical aspects in the manufactured parts (Zhan et al., 2003). However, these geometrical features are intensely characterised by the profile or the shape and the dimension of the manufactured bead walls.

The physical dimensions and the bead shapes are important characteristics in determining a precise wall width being manufactured. The shapes of the wall also determine the effective wall width (EWW) during machining, especially when dealing with thin walls with a good buy to fly ratio.

5.5.1.1 Bead width

In the present study, it was found that the bead width obtained from all the three WAAM platforms in trial 1 were within close range. The difference between all the platforms is insignificant, although the SAM Edgetek platform has a lower

standard deviation compared to the ABB Robot and FSW platforms. The trend was also similar in trial 2 except for the ABB Robot platform. In comparing the width obtained in all the platforms, Figure 5-28 showed that more accurate and close width ranges were obtained in trial 2, compared to the other deposited sample. Figure 5-32 illustrates the width comparison of all three platforms analysed. It can be seen in trial 1 (see Figure 5-32a) that the width from all the platforms were close to one another, however when considering the errors, which is an indication of how close the values were, it is evident that the SAM Edgetek machine produced a high level of consistency both in trial 1 and trial 2.

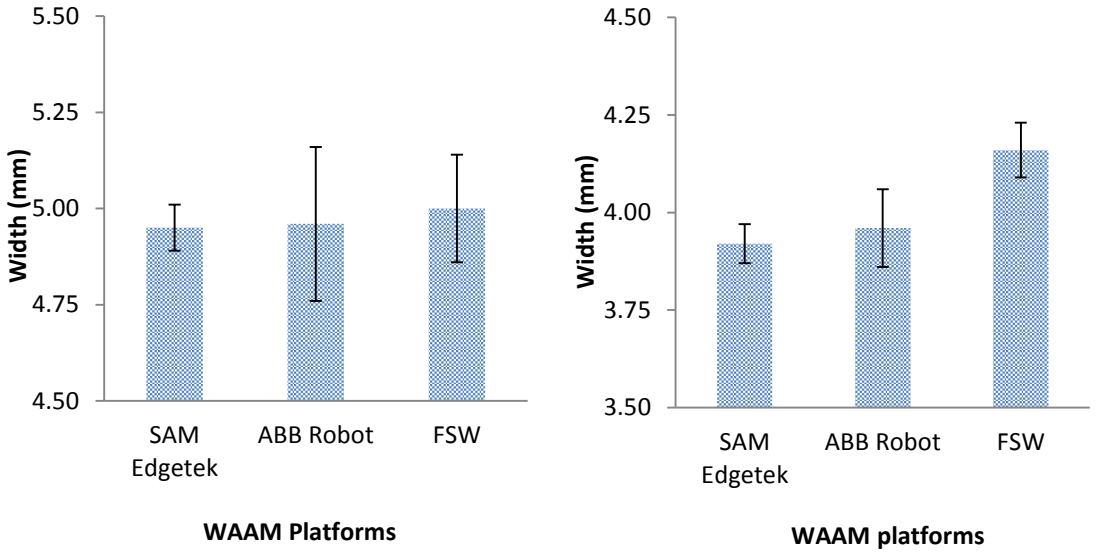

(a) (b)

Figure 5-32: Comparison of the width of samples from various WAAM platforms (a) for trial 1 and (b) trial 2.

5.5.1.2 Bead height

It is interesting to observe that there is some variation in the height from the entire platform in all the platforms. As expected, using different TS brought about differences in the bead height since this affects the amount of materials deposited per unit time. Moreover, in comparing the platform at the same TS and parameters, there are variations in the bead heights from all the platforms (see

Figure 5-29). The reason attributed for this is the variation in welding power (V or I), since the SAM Edgetek platform was carried out in a different workshop to the ABB Robot and the FSW. In all, the sample deposited by the SAM Edgetek platform has a greater wall height when compared with the two other platforms. Another reason that may be attributed to the variation in the wall height was the machine accuracy, which, as expected, affected the output and the parameter setting. Nevertheless, during the experiment the same parameter setting was used, eliminating this source as the cause of the variation in the obtained wall height.

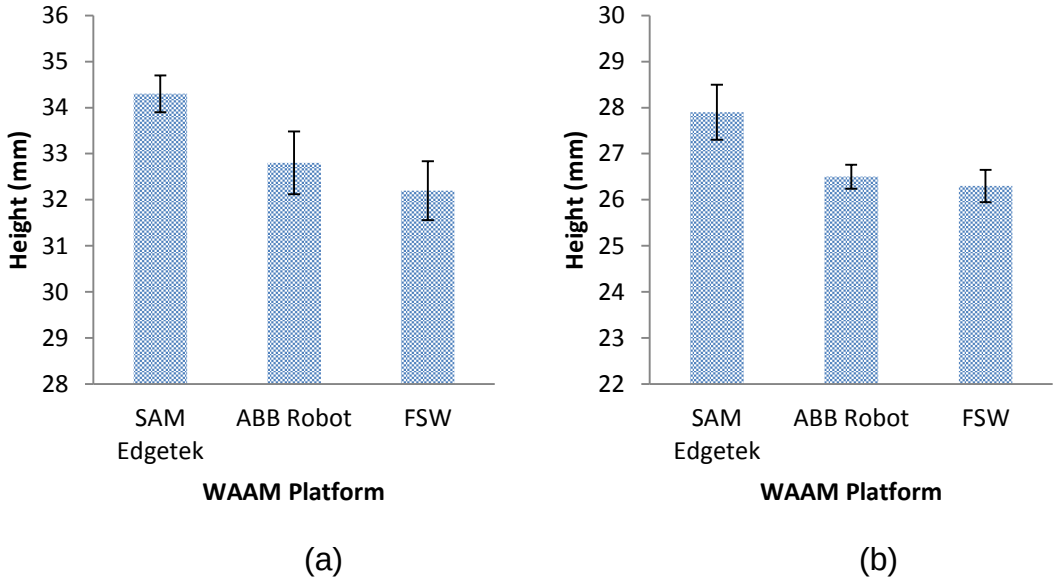

Figure 5-33: Comparison of sample height from various platforms (a) for trial 1 and (b) trial 2.

5.5.1.3 Wall perpendicularity

The effects of the wall perpendicularity of thin walls requiring machining may be undesirable if not properly addressed. The application of machining to thin manufactured WAAM parts is critical considering the effective wall width, since not much material could be machined away. This study identifies the various shapes of deposited multi-layer walls in WAAM if not straight and that all the

various shapes have their own effect on the machining of these samples. The possible shape of the wall is as shown in Figure 5-34.

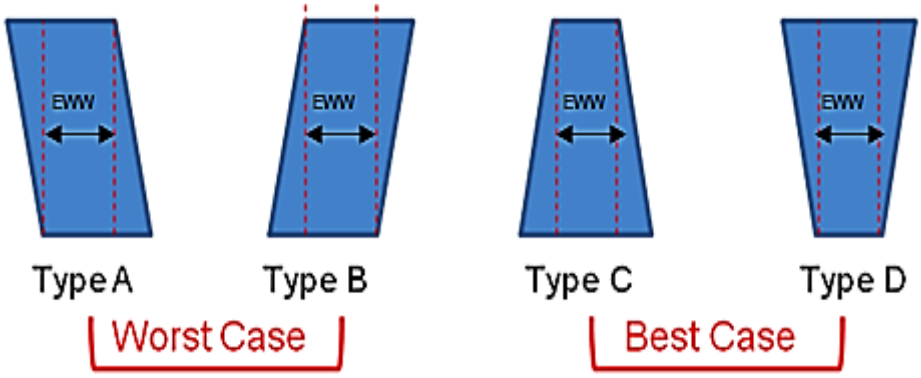

Figure 5-34: Deposited wall shapes

The worst case are types A and B, since more material will be machined off and with the wall build up continuing, there is a low possibility of attaining a straight wall after machining due to the wall deviation. However, with types C and D, thin straight walls can be obtained after machining.

Wall perpendicularity is, however, important when machining the WAAM thin wall samples. In a welding sense, it is of little or no effect when deposition parts might be 3^{o} off being perpendicular. Nevertheless, when machining is needed, coupled with the width requirement; i.e. the effective wall width, the shape of the wall is as low as 1^{o} off from being perpendicular, determining the amount of material that will be removed. Moreover, when building higher thin WAAM walls; i.e. 100mm, the deficiency in the wall perpendicularity was physically shown, which could not be noticeable in short walls such as 20mm.

5.5.1.4 Surface Waviness

The property of welded wall waviness is critical to the functionality of WAAM components. The surface waviness of the samples from the SAM Edgetek and ABB Robot platforms is better compared to the samples from the FSW. Variations in the welding parameters were kept constant during the experiment and as such,

the high surface waviness obtained in FSW can be isolated from the welding parameters. The surface waviness was found to depend on TS as shown in Figure 5-25. However, there is no significant difference in the values of surface waviness obtained in the SAM Edgetek and ABB Robot platforms when compared with the surface waviness of the test sample using the FSW platform. This could be as a result of the TS, which is a function of the machine.

5.5.1.5 Cpk

The overall Cpk values were arrived at by averaging the Cpk values for all the geometries used in this study. Using an average of the various Cpk could be justified by Kane (1986), who advocated that the performance of a process could be measured by means of process capability indices. However, in order that a machine or process can generate products at minimum cost, that is without incurring losses due to rejects, reworks and or scrap, its capability must be able to match the product specifications (Chen et al.,2001). In arriving at the average Cpk, Cpk assesses process viability by comparing the spread and centring the process. The extent to which the expected values fall within these limits determines how capable the process is of meeting its requirement.

Figure 5-35 illustrates the average of all the Cpk for the various geometries from all three platforms. The SAM Edgetek platform has an average Cpk of 1.24 which is near to the goal, i.e. Cpk≥1.33 (Pearn 1997)[1].

[1] See Table 2-5 in chapter 2 for the details of the quality condition using Cpk.

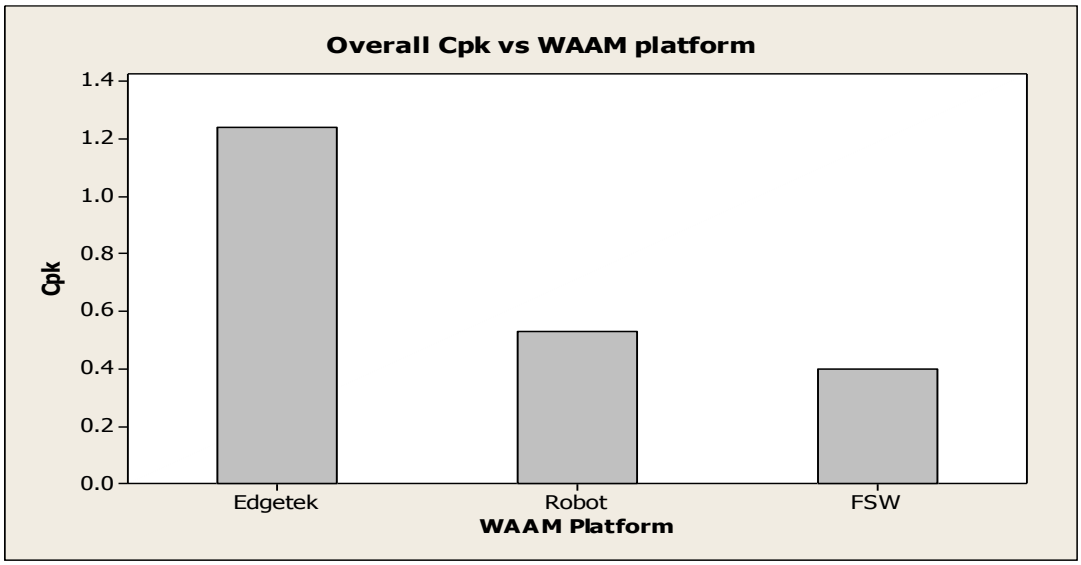

Figure 5-35: Average of all the Cpk for the various platform aspect

However, the Cpk of the ABB Robot and the FSW platforms fall below a mandatory Cpk value of 1; i.e Cpk < 1.00, which shows that these platforms are insufficient. According to Chen et al., (2001), a higher process capability index suggests the greater process yield. However, a higher capability index likewise points toward the lower process anticipated loss (Chen et al; 2001). Moreover, the lower Cpk of the robot and the FSW platforms does not suggest that they cannot manufacture good parts however, due to the spread and centring of the process, since it is expected that the value falls within this limit to determine how capable the process is of meeting the specification.

Overall, the SAM Edgetek platform was shown to have a better level of accuracy when compared to the ABB Robot and FSW machine platforms and the results are broadly in line with the expectation because of the level of accuracy of the SAM Edgetek machine. The physical geometries of the test sample chosen were, by the nature of the comparison, well within the capability of all three platforms.

The results are also valid for the geometries chosen but are not exhaustive, as very different results may have been obtained if different geometries had been

chosen however, in all, the chosen geometries produce an accurate representation of the various platforms chosen.

6 WAAM humping and weld wall beads characteristics

This section investigates the issues arising from Wire and Arc Additive Manufacture (WAAM) deposition. These issues involve weld bead humping and the physical distortion of WAAM walls.

In WAAM, an increase in productivity can be achieved through the use of high weld travel speeds. However, this can be overshadowed by the so-called humping effect. Humping is a defect in welding which expresses itself by the formation of humps and valleys that prevent further welding deposition operation. The generation of these defects is studied by critically examining the various weld travel speeds from different weld parameters.

The economic gains and environmental impact of WAAM solutions over traditional manufacturing technologies for large-scale manufacture is directly dependent on the processing speed, and therefore on the deposition rate capability (Sequeira-Almeida, 2012). This gives the torch Travel Speed (TS) and other welding parameters in WAAM a significant role in defining the quality of parts produced. As further advancement was discovered in welding control, weld quality would be expected to be improving. Moreover, increase in TS beyond a certain limit creates a weld defect generally called humping.

This study primarily deals with the effects of machining of WAAM walls putting into consideration the machining of such WAAM walls.

6.1 Weld Bead Humping

6.1.1 Materials and Machine-Set-Up

The materials used for the experiment are shown in Table 5-2, Table 5-3 and Table 5-4 in Chapter 5. In this case, the trials were conducted with wire diameters of 0.8mm and 1.2mm respectively. The wire was sourced from Lincoln Electricity Company (See Appendix A).

All weld depositions were undertaken on a SAM Edgetek machine integrated with the Cold Metal Transfer (CMT) welding machine (See Fig. 4-6 in Chapter 4) and with (Ar/CO2) 20% as the inert shielding gas. The SAM Edgetek machine was designed for high stock removal grinding to rival traditional hard turning methods. The substrate used is mild steel with a length of 100mm, breadth of 100mm and thickness of 20mm (see Figure 5-2 in Chapter 5).

6.1.2 Methodology

This experiment was conducted using a systematic experimental approach. These experiments were conducted using the parameters from a Cold Metal Transfer process model optimisation chart for structural mild steel (see Figure 2.2 in Chapter 2). The chart gives the optimum operating conditions to achieve target bead characteristics. The models were developed for predicting weld bead characteristics using various wire diameters. Some control variables such as Wire Feed Speed/Travel Speed, Wire Feed Speed, and Wire diameter were used to produce an output similar to bead geometry characteristics, resulting wall width and resulting wall height.

The welding parameters for the experiment were selected based on the process optimisation chart earlier stated and this serves as the working envelope for the experiments. Different walls were built with different travel speed and wire feed speed combinations. The trial was initially carried out with a 0.8mm wire with an observation of the travel speed limit at which humps begin to appear. Subsequently, a higher wire diameter of 1.2 mm was used to confirm the travel speed limit for humps that begin to appear and to isolate wire thickness from the causes of the humping. This was carried out by working around the TS limit observed using 0.8mm wire as shown in Table 6-1(b). In addition, WFS/TS was used in order to get a constant cross section area and to keep a constant heat input.

Table 6-1: Experimental welding conditions for (a) 0.8mm and (b) 1.2mm electrode wire respectively

Trials	WFS(m/min)	WFS/TS	*TS(m/min*
1	4.5	8	*0.563*
2	4.8	8	*0.600*
3	5.0	8	*0.625*
4	7.0	8	*0.875*
5	8.0	8	*1.000*
6	9.0	8	*1.125*
7	5.0	10	*0.500*
8	6.0	10	*0.600*
9	7.0	10	*0.700*
10	6.0	12	*0.500*
11	7.0	12	*0.583*
12	7.2	12	*0.600*
13	7.5	12	*0.625*
14	8.0	12	*0.667*
15	7.0	14	*0.500*
16	8.4	14	*0.600*
17	9.8	14	*0.700*
18	5.0	15	*0.333*
19	6.0	15	*0.400*
20	6.8	15	*0.453*
21	8.0	15	*0.533*
22	9.0	15	*0.600*
23	10.0	15	*0.666*
24	7.0	15	*0.467*
25	9.0	18	*0.500*
26	10.8	18	*0.600*
27	12.6	18	*0.700*

(a)

Trials	WFS(m/min)	WFS/TS	*TS(m/min*
1	1.0	2	*0.500*
2	1.2	2	*0.600*
3	1.4	2	*0.700*
4	1.6	2	*0.800*
5	2.0	4	*0.500*
6	2.4	4	*0.600*
7	2.8	4	*0.700*
8	3.2	4	*0.800*
9	3.0	6	*0.500*
10	3.6	6	*0.600*
11	4.2	6	*0.700*
12	4.8	6	*0.800*
13	4.0	8	*0.500*
14	4.8	8	*0.600*
15	5.2	8	*0.650*
16	5.5	8	*0.690*

(b)

6.1.3 Results

During the deposition of the WAAM wall samples, it was observed that many of the wall build-ups deposited above certain travel speed experience hump defects and as such, the wall build-ups could not be continued. Table 6-2 and 6-3 illustrate the summary of the results for both 0.8 mm and 1.2 mm wires. The deposited walls with the hump defects were classified as unstable and those without humping were classified as stable. In the stable process, the walls were manufactured successfully to up to 12 layers. However, in the case of unsuccessful build up, humping appeared as early as the second layer in some cases and this did not allow more layers to be built upon it. Hence the wall build-up could not be continued.

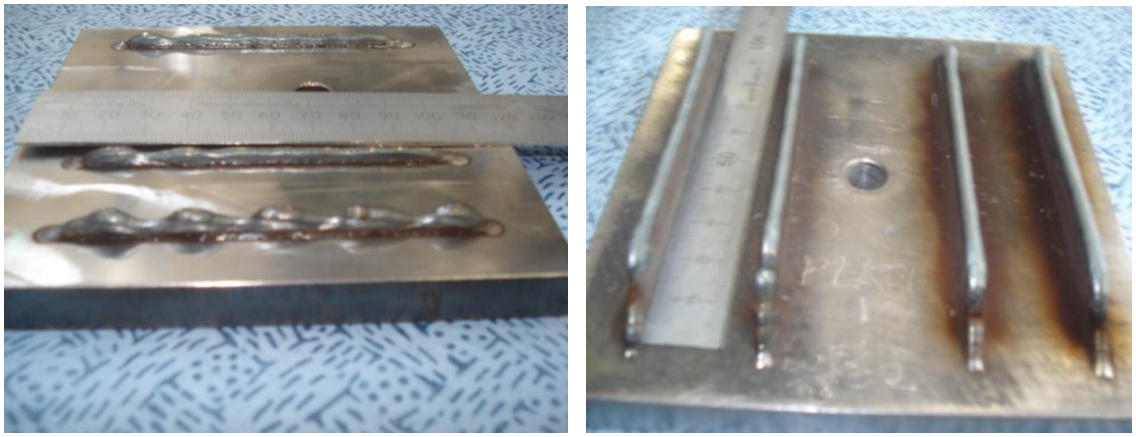

(a) (b)

Figure 6-1: Deposited weld sample: (a) with humps (b) without humps

Table 6-2: Trial result summary for CMT trials 0.8mm wire

Trials	WFS (m/min)	WFS/TS	TS (m/min)	Stability process
1	4.5	8	*0.563*	Stable process
2	4.8	8	*0.600*	Unstable from 3rd layer
3	5.0	8	*0.625*	Unstable from 3rd layer
4	7.0	8	*0.875*	Unstable from 2nd layer
5	8.0	8	*1.000*	Unstable from 2nd layer
6	9.0	8	*1.125*	Unstable from 2nd layer
7	5.0	10	*0.500*	Stable process
8	6.0	10	*0.600*	Stable process
9	7.0	10	*0.700*	Unstable from 2nd layer
10	6.0	12	*0.500*	Stable process
11	7.0	12	*0.583*	Stable process
12	7.2	12	*0.600*	Unstable from 5th layer
13	7.5	12	*0.625*	Unstable from 3rd layer
14	8.0	12	*0.667*	Unstable from 3rd layers
15	7.0	14	*0.500*	Stable process
16	8.4	14	*0.600*	Unstable from 3rd layer
17	9.8	14	*0.700*	Unstable from 2nd layer
18	5.0	15	*0.333*	Stable process
19	6.0	15	*0.400*	Stable process
20	6.8	15	*0.453*	Stable process
21	8.0	15	*0.533*	Stable process
22	9.0	15	*0.600*	Unstable from 6th layer
23	10.0	15	*0.666*	Unstable from 3rd layer
24	7.0	15	*0.467*	Stable process
25	9.0	18	*0.500*	Stable process
26	10.8	18	*0.600*	Stable process
27	12.6	18	*0.700*	Stable with poor surface waviness

Table 6-3: Trial result summary for CMT trials 1.2mm wire

Trial	WFS (m/min)	WFS/TS	TS (m/min)	Stability process
1	1.0	2	*0.500*	Stable process
2	1.2	2	*0.600*	Stable process
3	1.4	2	*0.700*	Stable process
4	1.6	2	*0.800*	Unstable from 9th layers
5	2.0	4	*0.500*	Stable process
6	2.4	4	*0.600*	Stable process
7	2.8	4	*0.700*	Unstable from 9th layers
8	3.2	4	*0.800*	Unstable 6th layers
9	3.0	6	*0.500*	Stable process
10	3.6	6	*0.600*	Stable process
11	4.2	6	*0.700*	Unstable from 9th layers
12	4.8	6	*0.800*	Unstable from 4th layers
13	4.0	8	*0.500*	Stable process
14	4.8	8	*0.600*	Stable process
15	5.2	8	*0.650*	Unstable from 9th layers
16	5.5	8	*0.690*	Unstable from 4th layers

The detailed results showed that with the 0.8mm wire, thirteen out of twenty-seven samples had a successful build-up without humping, while the remaining fourteen were unstable due to humping. In the case of the 1.2mm wire, nine successful build-ups were achieved, while seven were unsuccessful. The travel speed at which the humping starts to occur in the unsuccessful wall build-up was apparent.

6.1.4 Discussion

6.1.4.1 Effect of travel speed on weld bead humps

Theoretically, greater weld speeds can be obtained by optimising numerous process parameters while maintaining the same heat input per unit distance (Carry, 2002). Nevertheless, it will offer the necessary productivity improvement even though it is maintaining the same weld dimension. However, despite having the same amount of heat input per unit distance, continued increases in the weld travel speed are limited in practice by the deterioration of the quality of weld bead (Nguyen, 2005).

Figure 6-3 and 6-4 are two-parameter maps show the experiment parametric plot highlighting the regions where process parameters produced good weld beads or generated humps and other welding defects.

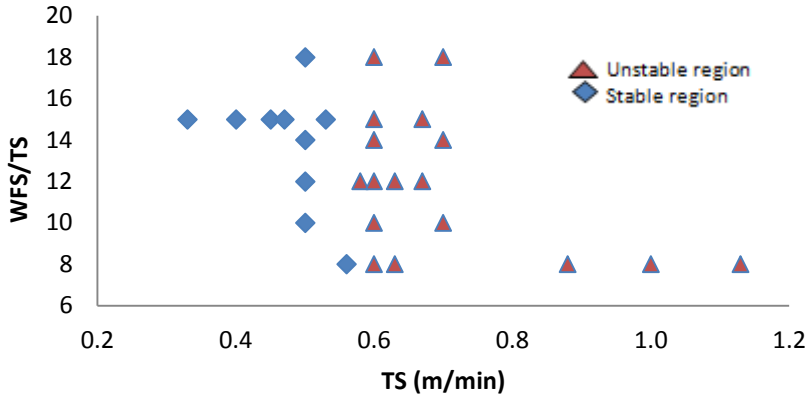

Figure 6-2: Parametric plot showing the travel speed limit (0.8 mm electrode wire)

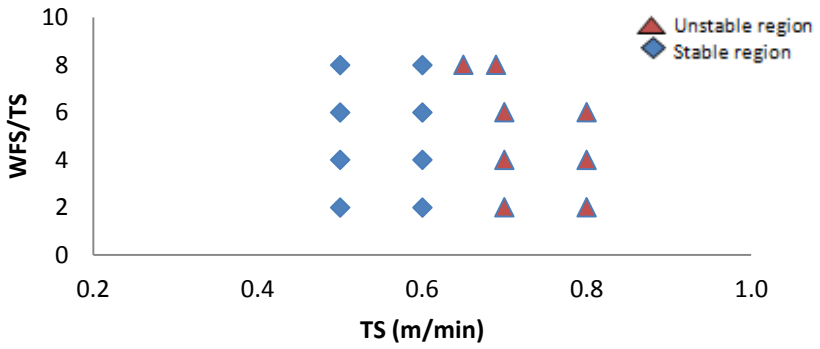

Figure 6-3: Parametric plot showing the travel speed limit (1.2 mm electrode wire)

However, from these results, it was shown that for a travel speed of 0.6m/min and below, the deposited walls showed no significant variation in terms of dimension or shape along their length. Such processes were classified as stable. Moreover, any attempt to go above a travel speed of 0.6m/min was hindered due to the development of humps which exhibited intermediate swellings that are separated by valleys and, as the travel speed increases, the consistency of humps increases. The occurrence of humps can be seen by the significant variations in the weld bead's deposit dimension and shapes that occur alongside the length of the hump and valley.

Figure 6-3 and 6-4 show that, around the TS of 0.6m/min, the humping started to appear. Below this TS of 0.6m/min, the WAAM depositions produced were classified as stable process since the WAAM deposited beads show no significant variation in the WAAM bead deposited along the length. On the other hand, above this critical TS, the WAAM beads deposited begin to show a recurrent swelling that is characterised by valleys. This becomes consistent as the TS increases. Consequently, the dissimilarity between the stable-deposited WAAM beads and beads with humps can be evidently identified with the significant occurrence of humps and valleys.

An experiment conducted by Sequeira- Almeida (2012) (See Appendix E) used for modelling surface waviness, effective wall width and metal deposition efficiency of multi-layer welds in steel of 0.8 mm wire diameter (10 layers high) also noticed humping in his set of experiments with no certain value at which the humping starts was recorded.

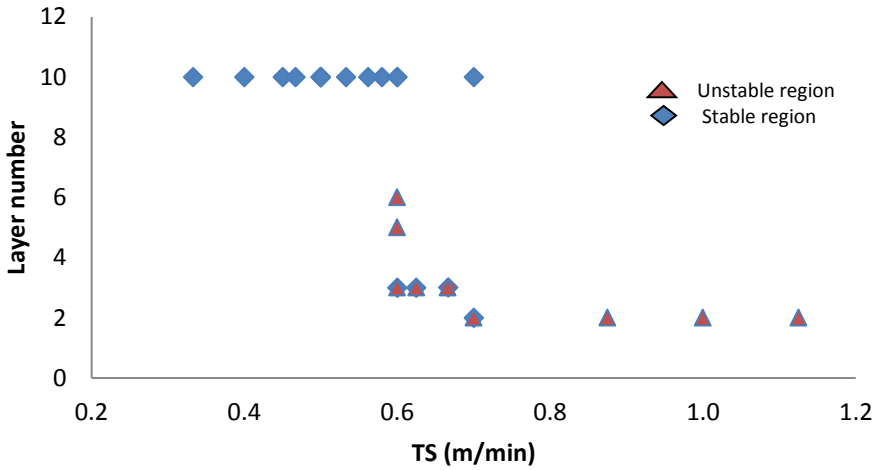

Figure 6-4: Travel speed limit and the number of build-up layers attained (0.8mm electrode wire)

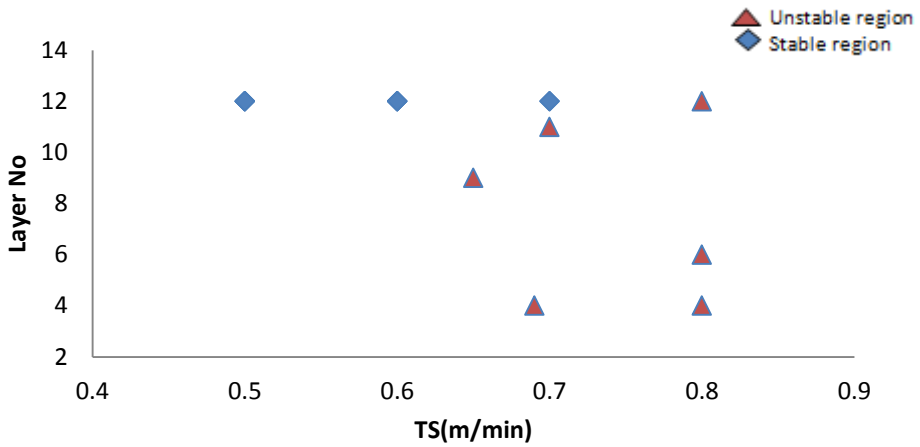

Figure 6-5: Travel speed limit and the number of build-up layers attained (1.2mm electrode wire)

The occurrence of this humping at high speeds can also be attributed to the activities taking place along the flow channel of the deposited molten metal. As WAAM deposition took place, a new bulge was subsequently formed because of the flow strait of the molten WAAM metal to the earlier swelling/bulge having been made impassable by the solidification of the molten metal. In spite of the circumstance that the welding torch was moving forward with a high travel speed, the swelling continued to increase in dimension, since it was receiving more WAAM molten metal deposition. With this observation, the flow of the molten fluid inside the deposited bead must be mainly in the direction of the rear of the deposited WAAM weld pool, through high momentum and velocity. This backwards direction of molten metal flows with high velocity within the weld pool and remains consistent with observation by Beck et al. 1990 using numerical simulation.

However, with a low surface tension, the WAAM molten metal will run off the sides of the WAAM weld walls or base plate (in case it is the first layer) and thus, flattens out into the surface of the previous bead. Consequently, there will be no humping or bulging/swelling formed because the swelling is controlled by means of the high surface tension, hence continually upsurged in size of the rear flow of WAAM molten metal and this is required to have high momentum and velocity. Therefore, the thrust in the rear flow of the WAAM molten metal is in control, not

simply for the early occurrence of hump, but also for the increase in the swelling (Nguyen, 2006).

The increase in the sizes of the swelling is through upward bulging and this is static with regard to the base plate or the subsequent deposited weld bead. As the swelling is static with a strong rear flow in the WAAM molten metal along the direction of the deposition, the frontward recirculation in the deposited molten pool does not take place (Bradstreet 1968). Consequently, rear filling of the front portion in the WAAM weld pool is impossible. Non-existence of this real filling allows the elongation and eventually the solidification of the WAAM molten metal, resulting in the formation of valleys shown in the humped weld bead (see Figure 6.2). Moreover, solidification in addition to blockage of the flow in the deposited molten welds will result in the occurrence of fresh build-up or fresh bulging. Therefore, the high momentum as well as the high velocity of the rear engages the flow of WAAM molten metal from the WAAM weld pool and stops rear filling of the front portion.

In summary, the humping phenomenon in WAAM has been investigated from the point of understanding the appropriate working travel speed limit using a Cold Metal Transfer welding machine. It is clear from the study that a limiting speed of 0.6m/min exists, at which humping starts to take place. As the travel speed increases above this limit, the formation of this discontinuous weld bead defect begins to worsen until the process cannot be continued.

However, Figure 6.6 describes the effect of travel speed on deposited width. The result shows that TS plays an important role in determining the width of a deposited sample. It is absolutely not the only parameter that determines the width but is more pronounced when combined with other parameters such as WFS, WFS/TS, and wire diameter.

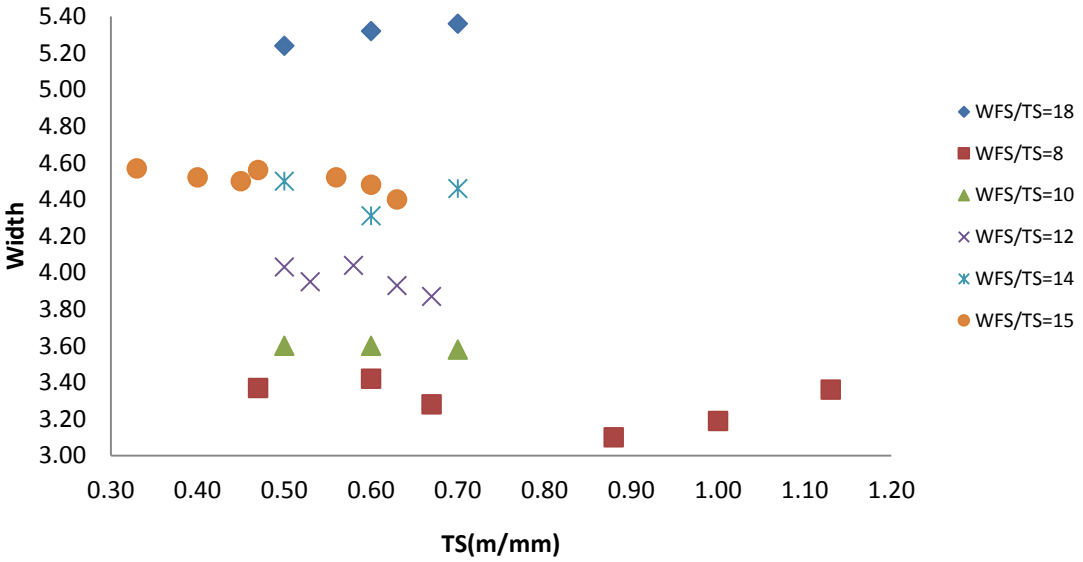

Figure 6-6: Effect of TS on deposited width

6.2 WAAM wall bead characteristics

6.2.1 Materials

This study looks into understanding the influence of welding parameters such as TS, WFS and WD on the physical bead geometries characteristics. The welding operation mode used in this study is the Lincoln Power wave 455/STT integrated with the Edgetek machine (as show in Figure 4-6). The wire diameters used were 0.8mm and 1.2mm. The welding settings used in this study are shown in Table 6-4.

Table 6-4:Pre-welding conditions

Welding Process	Power source	Shielding gas	Flow rate (l/min)	Program mode	CTWD (mm)	WD (mm)
WAAM	Lincoln power wave 455/STT	Ar/CO_2 (20%)	15	Pulse soft (P19)	13	0.8/1.2

6.2.2 Methodology

This study involves the build-up of single and multi-layer walls by making use of the same approach to a single layer. The base plates were prepared before the weld build-up as described in Section 4.4. Steady and reproducible welding settings were guaranteed by a constant CTWD at 13mm. Uninterrupted weld beads of around 100 mm [2] were gradually put down on the base plate in a WAAM technique one layer at a time in the same trend only. A maximum of seven straight walls per base plate were deposited next to one another parallel to the deposition direction (see Figure 6-7). The distance between the walls was 15mm, apart from the fourth and the fifth walls which had a distance of 25mm because of the clamping hole between them. The first single layer was deposited for all the seven walls as shown in the illustration of the deposit strategy. The height and the width were measured after allowing it to cool down to room temperature. Subsequently, the next layer deposit was carried out starting from the second deposited wall leaving out the first single bead. This was done until the last bead deposit was carried out for the seventh wall.

Meanwhile, the detailed plan of experiment is described in Table 6-5. In this investigation, the welding parameters chosen were the most important with respect to weld deposition producing recognisable differences in the beads' geometries. The trials were repeated at least twice to increase the accuracy and the repeatability of the results.

[2] +/- 1 mm max. due to imprecision of the welding process itself.

Table 6-5: Experiment welding parameters and respective bead profile measurement[1]

Sample No	WD (mm)	TS (m/min)	WFS (m/min)	V (V)	I (A)	Power (W)	W (mm)	H (mm)
1	0.8	0.2	5	9.9	56.9	563	2.75	2.51
2	0.8	0.3	7	11.21	68.2	765	3.68	2.15
3	0.8	0.4	9	12.95	89.6	1160	4.55	1.98
4	0.8	0.4	7	11.54	58.5	675	3.54	2.11
5	0.8	0.2	9	12.08	72.6	877	3.88	2.31
6	0.8	0.3	5	10.06	49.9	502	3.45	2.24
7	0.8	0.3	9	12.68	78.5	995	4.34	2.22
8	1.2	0.2	5	17.23	88.2	1520	4.25	2.85
9	1.2	0.3	7	19.11	90.5	1729	4.88	3.33
10	1.2	0.4	9	20.65	94.6	1953	5.32	3.46
11	1.2	0.4	7	18.95	86.1	1632	4.98	3.41
12	1.2	0.2	9	21.89	91.5	2003	5.56	3.51
13	1.2	0.3	5	18.54	88.3	1637	4.32	3.35
14	1.2	0.3	9	20.41	92.6	1890	5.84	3.58

[1] WD, wire diameter; WFS, wire feed speed; TS, travel speed; Volt, voltage; I, current; W, deposited bead width; H, deposited bead height.

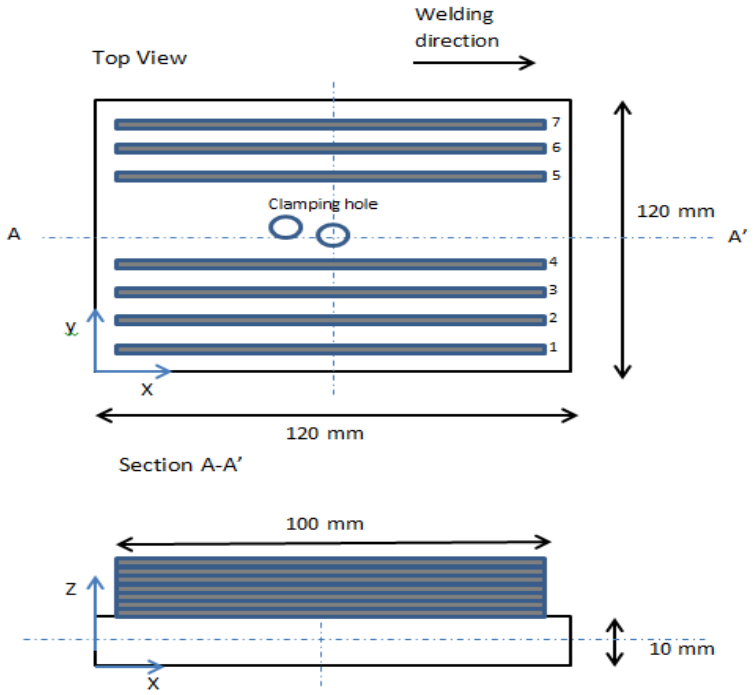

Figure 6-7: Illustration of wall deposits strategy on the base plate

Measurements of the height and the width of each layer were taken using a digital calliper and were taken at every 20 mm length across the weld deposited bead. All five measurements were taken for each single bead laid down and this was repeated three times to improve the accuracy. The important parameters of the deposited single bead profile, the bead height (H), bead width (W) and the aspect ratio (AR), were measured for all the deposited beads as shown in Figure 6-8.

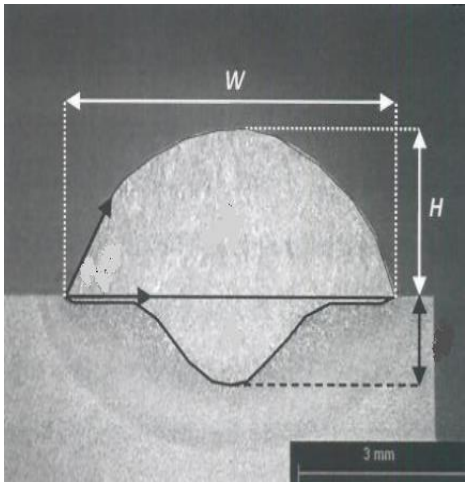

H: Height of the bead in mm

W: Width of the bead in mm

Aspect ratio: H/W

Figure 6-8: Single bead showing the measured output

The measurement of the succesive multi-layer profile such as the increase in height (delta H) and increase in width (delta W) was, however, carried out in relation to the number of layers as indicated in Figure 6-9.

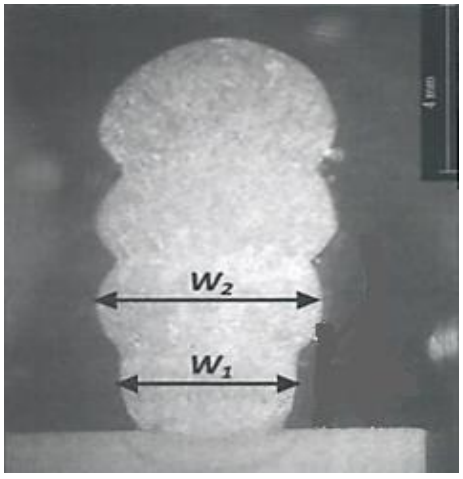

Wn: Bead width for n^{th} layer (mm)

Figure 6-9: Multi-layer bead showing the measured output

6.2.3 Results

The investigation reported in this section was carried out with the machine set up shown in Figure 4-6. Figure 6-10 shows one of the manufactured walls produced during the investigation

Figure 6-10: Sample A1 from one of the trials.

Figure 6-11 illustrates the change in wall width per layer obtained during the trial. The results show that the widths obtained in the first three layers of the deposition are rather narrower than the subsequent layers deposited after the third layer of deposition. The width increases as the number of layers deposited increases. Moreover, this increase continues until the third layer is reached, and thereafter the width becomes the same. The widths of the deposited layers after the third layer (i.e. from the fourth layer to the tenth layer) were very close. In constant WFS/TS, there is a reduction in the width of the deposited weld bead when increasing travel speed. This is triggered by the reduction in the material as it is being deposited per unit time with a smaller amount of heat input from the arc to the weld pool, and this decreases the weld pool temperature. Moreover, the decreased temperature gives rise to the viscosity of the weld pool, increasing the constricting weld pool surface energy, thereby reducing the impact of the arc pressure and aerodynamic forces on the molten metal. Hence, the entire impact of this resulted in a narrower weld.

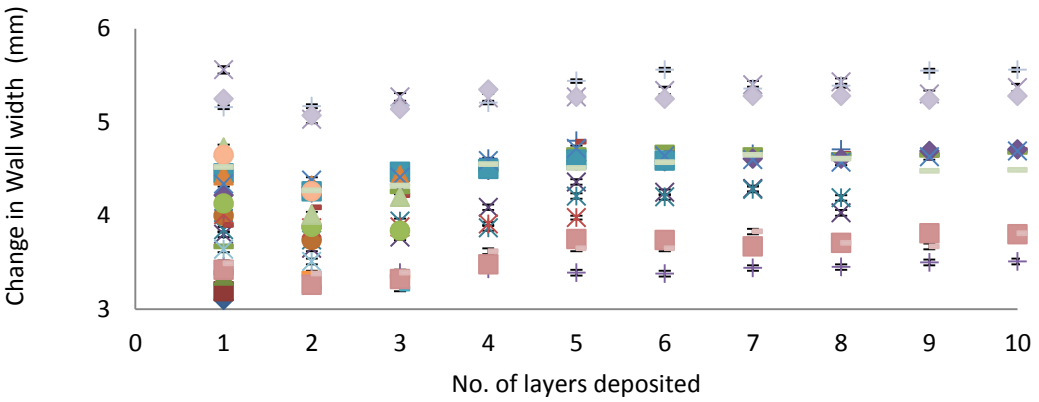

(a)

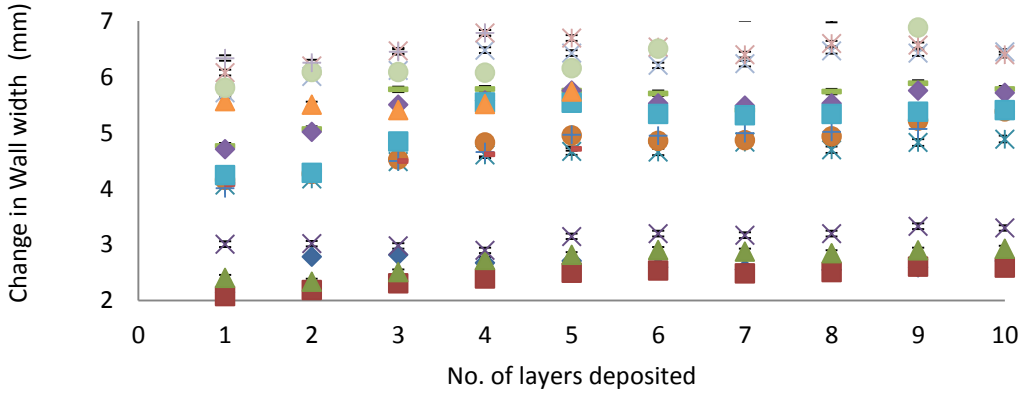

(b)

Figure 6-11: The relation between bead width per layer for the wall build up using (a) 0.8mm and (b) 1.2mm electrode wire process parameters.

This observation is noticeable using both the 0.8 mm (as in Figure 6-11a) and 1.2 mm (as in Figure 6-11b) wires. However, the width obtained using the two wires are different because the amount of wire deposited with 1.2mm is higher than that of 0.8mm wire.

Figure 6-12 described the effects of the deposition on the bead height for the study. It is also noticeable that the first layer of all the deposition is the highest for all the trials conducted. It is observed that the height per layer decreases as the number of deposited layers increases until the third layer. Interestingly, the height

per layer becomes nearly the same as from the third layer to the last layer deposited. However, this special effect might be triggered by the circumstance of the first deposited layer being built upon a uniform plan base plate and the fact that rapid cooling effects can occur in the first three layers.

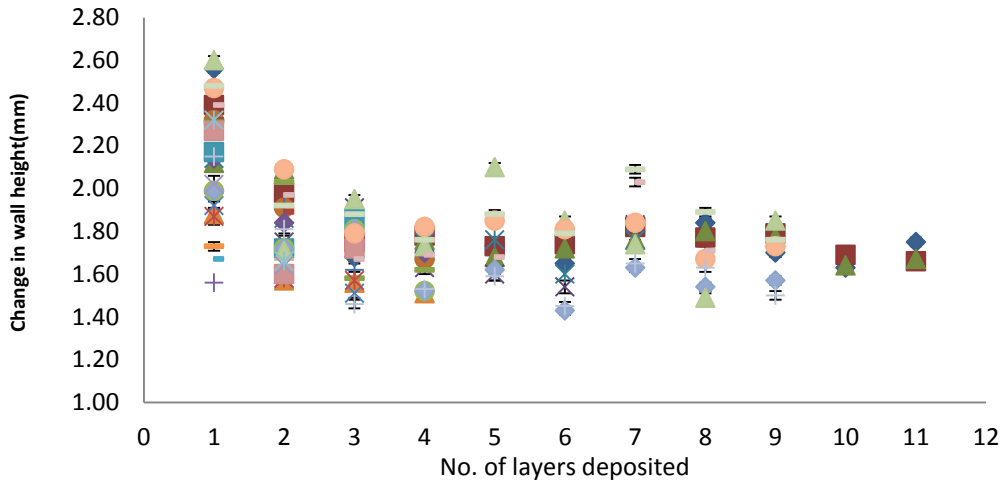

(a)

(b)

Figure 6-12: Increments per layer for the wall height build up (a) 0.8mm and (b) 1.2mm electrode wires process parameters)

The heat affects the process as the number of layers deposited increases because of the volume of heat sink in the deposition.

The dependence of the relative deposited bead height and the deposited bead width (i.e. deposited bead height per layer/ bead width per layer) is illustrated in Figure 6-13. The aspect ratio is higher (i.e. 0.55) in the first layer and gets smaller until the fourth deposited layer where the value tends to drift towards a constant value (i.e. 0.40) as the number of layers increases. The noticeable difference is in the first three layers deposited. This is noticeable in all the trials.

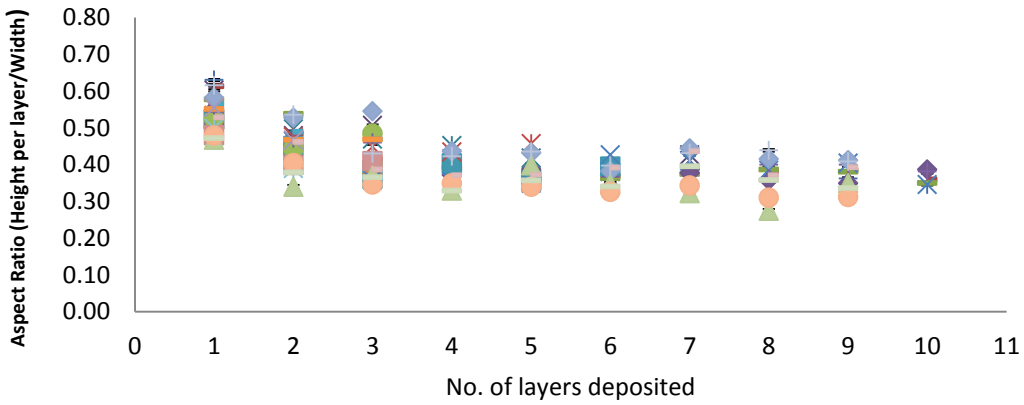

(a)

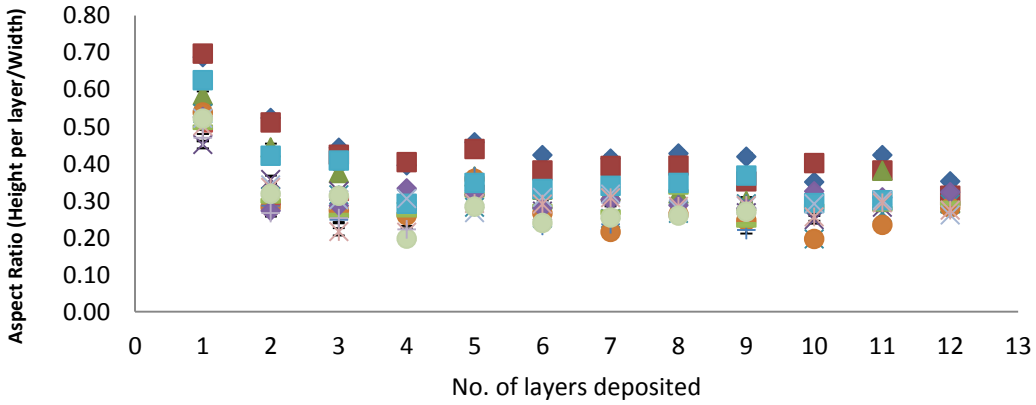

(b)

Figure 6-13: The dependence of the aspect ratio (height/width) and the layer number for (a) 0.8mm and (b) 1.2mm electrode wire diameter trials

Figure 6-14 also shows the dependence of the aspect ratio in terms of cumulative bead height/cumulative bead width. This is the effect of multiple layers on the bead height and width relative to the number of layers deposited. The relationship can be described as linear; i.e. as the layer number increases, the aspect ratio increases.

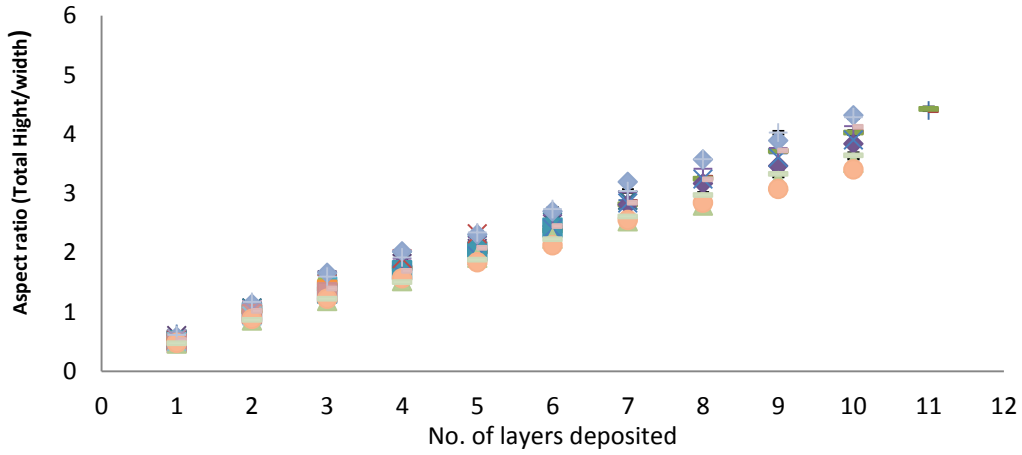

(a)

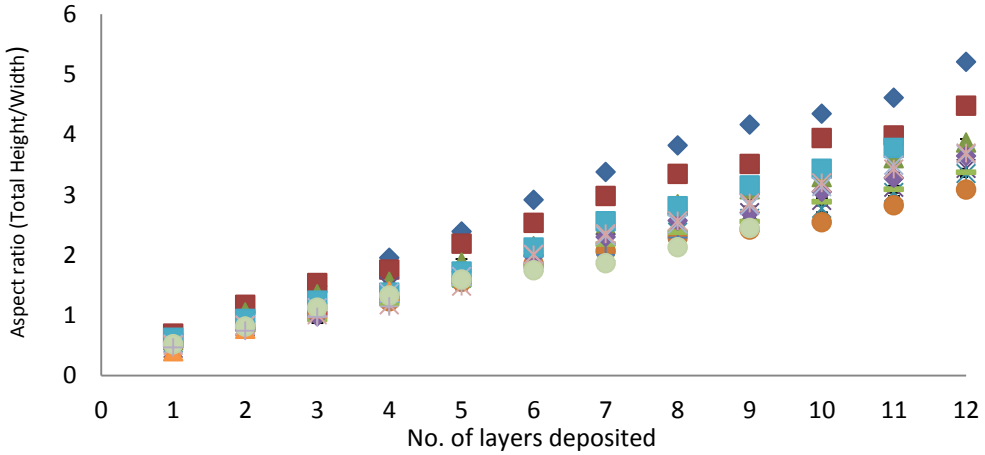

(b)

Figure 6-14: The dependence of the aspect ratio(total height/width) and the layer number for (a) 0.8mm and (b) 1.2mm electrode wire diameter trials

Figure 6.15 shows the effect of TS on the width of the deposited wall at constant WFS/TS. The results indicate that the width is reliant on the WFS/TS ratio. Even

with an increase in the TS and with WFS/TS ratio kept constant, there are little or no effects of the TS on the process. It is believed that when the WFS/TS are not kept constant, there is a huge variation in the width of the welding process.

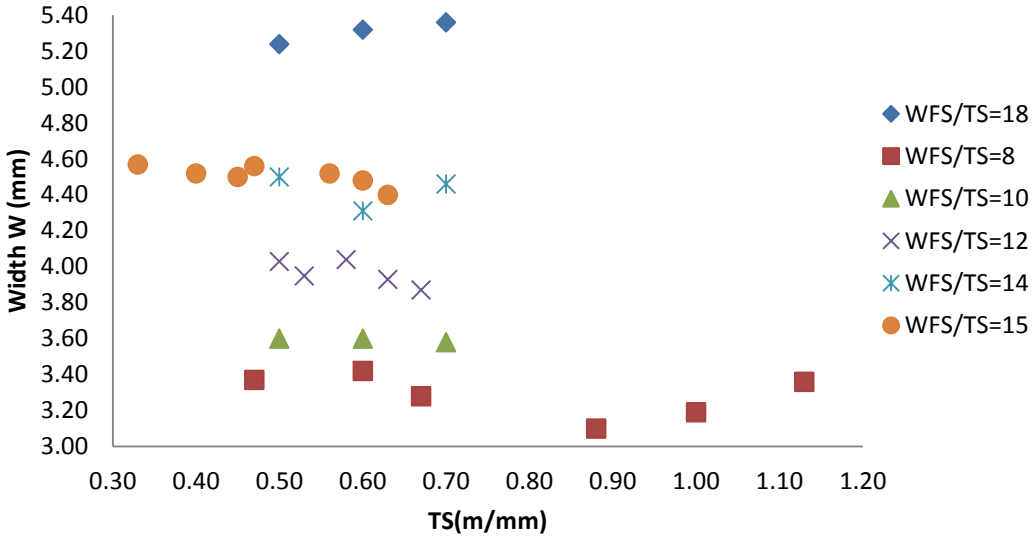

(a)

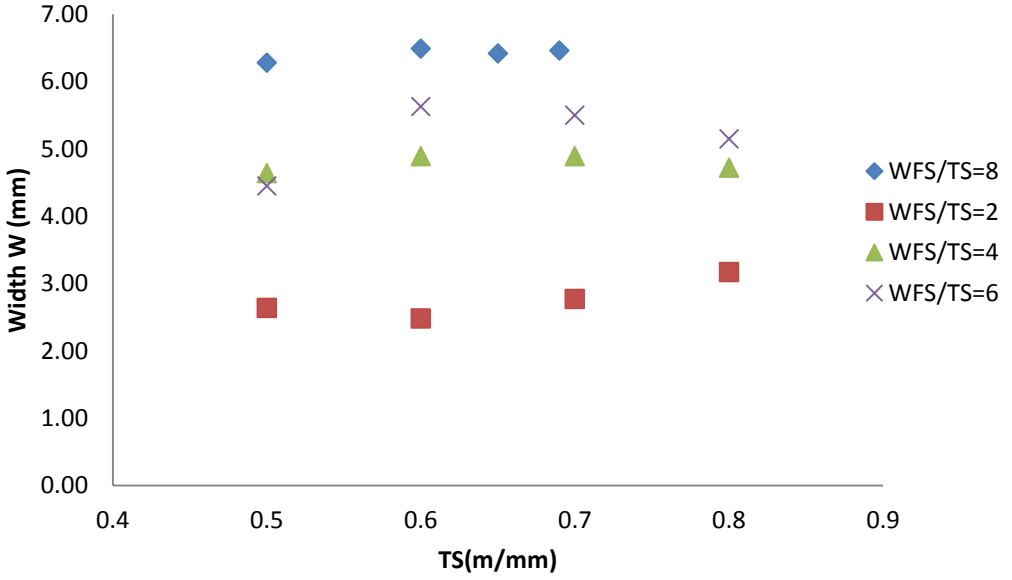

(b)

Figure 6-15: Average width in relation to WFS/TS ratio obtained during the study for (a) 0.8mm and (b) 1.2mm wire electrode diameter trials

6.2.4 Discussion

For a constant WFS and TS, there is a big difference in the first layer of the entire wall built up compared to the subsequent layers. This first layer is constantly narrower in width and greater in height. The ratio of height/width is very significant, unlike the other layers, which tend towards a constant. It is quite important to take into consideration the usefulness of the first three layers when building a WAAM part. This is important when dealing with thin walls, taking into consideration the effective wall width to be obtained during the machining of the part since a great amount of material in the wall will be machined off in order to achieve the vital effective wall width.

However, selecting the appropriate combination of process parameters is important to improve the quality and accuracy of parts manufactured through the WAAM process. The results indicate that selecting the appropriate process parameters is significant in determining the deposited bead characteristics. Inappropriate assessment of the comparative bead height in a multi-layer WAAM deposition can affect the position of the welding torch to be too distant or to near to the previous deposited layer. This can lead to insufficient shielding. The variation in CTWD will affect the overall bead geometry and the shape of the part produced.

A significant outcome of narrower beads with significantly higher beads was produced for the whole WFS/TS range. The main motive behind the adoption of WFS/TS approach in place of TS was to be sure that better and identical bead welds were obtained in all of the experimentations in order to avoid an unbalanced combination of the parameters; for example, disproportionately high WFS and a low TS. However, holding the WFS/TS relationship constant, the heat input that will be delivered to the weld is kept in a region of a constant level. This is noticeable in the micrographic cross section as shown in Figure 6-9 and in the charts as shown in Figure 6-11 and 6-12.

Moreover, as the TS increases, the WFS also increases. It is also evidently clear that the dependence of width and height of a weld bead on the WFS/TS ratio is very significant and does not really depend on the WFS, which makes the TS

important in controlling the width and the height of weld beads. Higher and wider weld beads are manufactured with higher WFS/TS at constant WFS. This consequence is predominantly noticable in the sample manufactured with both higher WFS and TS ratios (see Figure 6-15). This observation is anticipated because of the large volume per unit length of materials being deposited with higher WFS/TS.

7 Machining of WAAM parts

7.1 Lubricants in machining of WAAM parts

Several researches (i.e Levy et al., 2003, Kruth et al., 1996, Baufield and Biest, 2009 etc) have been carried out into the various aspects of manufacturing using AM. However, fewer studies (i.e Chen and Song, 2001, Yang et al., 2002) have been carried out on the machining aspect of AM materials. Various AM parts of intricate sizes have been produced with less concern for the machining of this part, especially when the surface finish is paramount to the requirements.

Although machining of additive manufactured walls has its unique features, it has some inherent problems of CNC machining methods. The most obvious problem is that models with hollow features or deep cavities cannot be machined (Chen and Song, 2001). When tooling attempts to machine a bottom point inside a cavity, a collision occurs between the tool holder and the model surface. To solve this problem, a layer based AM deposition with machining is being proposed. Sequential welding deposition and machining operation on a single system is being studied as a viable way of overcoming the constraints of machining hollow parts using the AM method.

In a study conducted by Chen and Song, (2001) a deposited AM sample with a hollow shape was cut mid-way to allow the hollow parts to be machined. After the machining, the parts were glued together with the aid of an adhesive but the method being introduced in this research will not involve the use of adhesive as this involves the sequential welding deposition and machining on the same system, which eradicates the use of adhesive that might affect the overall quality of the part manufactured.

This study was also carried out to understand the feasibility of sequential deposition with machining with various lubricants; i.e. solid lubricants and convectional liquid lubricants. A thorough knowledge of the effects of AM structure on the surface integrity and the mechanical properties of WAAM deposited materials is of great importance, especially for the integration process

of sequential deposition and machining. However, the interaction of the solid lubricant on the microstructure is of great interest. In order for the use of a solid lubricant to be acceptable, it must not contaminate the material or have any undesirable effect on the microstructure. The results of the study are expected to guide on the viability of sequential welding deposition with machining.

7.1.1 Materials and Machine set-up

The investigation was conducted using the pre-set operating parameters shown in Table 7-1. The material used is mild steel (details of this materials has been described in section 6.3.1 in Chapter 6) with the Fronius Trans Pulse Synergic 5000 cold metal transfer welding machine as the deposition process.

Table 7-1: Deposition parameters

Welding parameters	
Wire diameter	0.8mm
Travel speed	0.3m/min
Wire feed speed	8m/min
Contact Tip to Work Distance (CTWD)	11.5mm
Shielding gas	Argon shield light CO_2

The program used in the CMT machine was CMT 875. Details of the equipment are shown in Figure 7-1 below, with the ABB IRB 2400 Robot connected to the CMT machine for the motion of the arc. ABB IRB 2400 Robot was used in this case because the accuracy is not of importance, as the effect of lubrication on WAAM is being analysed.

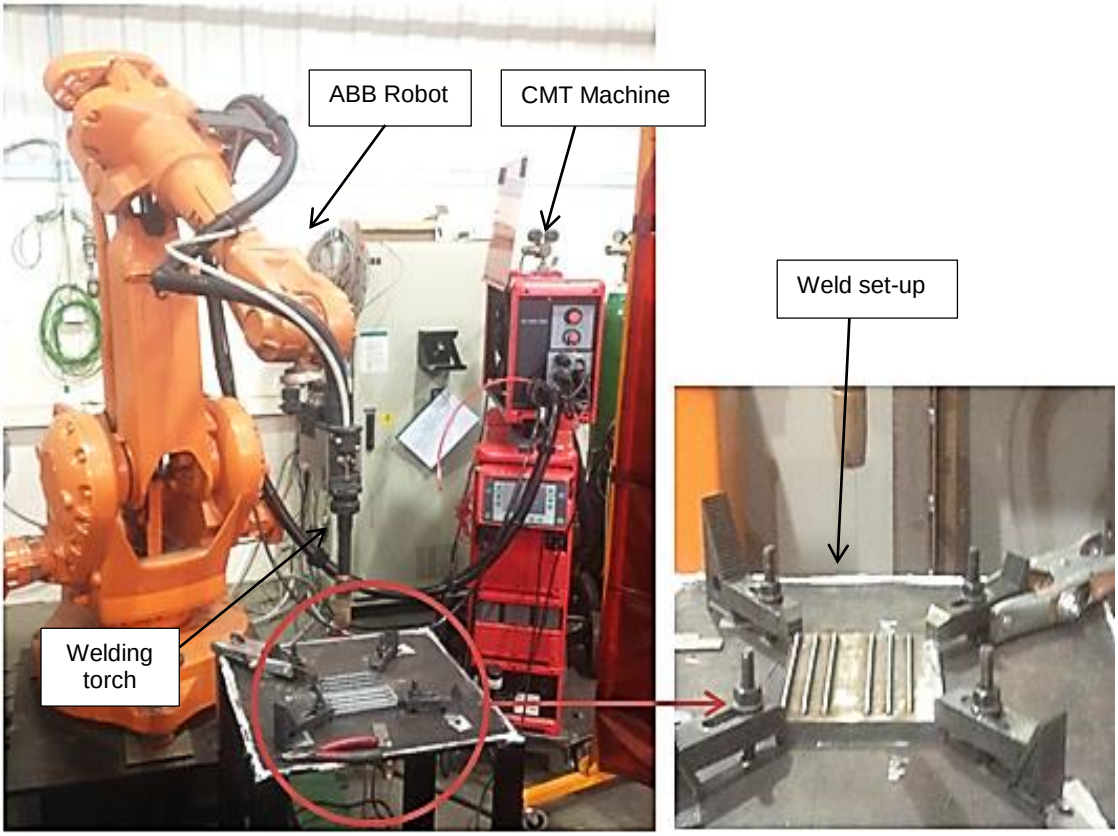

Figure 7-1: Experiment set up

7.1.2 Methodology

One of the aims of the investigation is to study the possibility of using a solid lubricant in the sequential machining and deposition of the AM part. In view of this, graphite powder and molybdenum disulphate powder were utilised in the trials. They were selected due to their wide usage as solid lubricants and their ability to maintain their properties at high temperature. Widely used convectional oil based liquid lubricant was also used, EcoCool machining fluid, which is an industrially available working liquid in machining that does not have other extracts that are possibly detrimental to the environment.

A systematic experimental approach was used [see Table 7.2]. Stage 1 involves sequential deposition of walls with or without the application of lubricants. This is without any form of cleaning operation performed on the walls before or after each layer of deposition. Stage 2 involves the sequential deposition of walls with

and without the application of lubricants as in stage 1, however, with cleaning of the lubricant after each layer of deposition. The cleaning operation involves thorough manual cleaning of the top surface of the deposited WAAM beads with the use of cotton wool and 99% acetone. Acetone is used widely in industry to remove the traces of lubricants after the machining operation to avoid any contamination of the material surfaces.

Trial 1.1 consists of wall build-up without cleaning after each layer of deposition, while the Trial 1.2 consists of wall build-up with cleaning after each layer of deposition. Trial 1 is the only trial that does not involve any form of lubricants, either solid or liquid. This experiment serves as the control. Trial 2 involves the application of MoS_2 on the surface of every single layer deposited. In trial 3, graphite powder was applied and trial 4 involves the application of machining fluid. Each time, 4 ml of solid lubricants was applied over a deposited single bead of 80mm. For all the trials, the materials were allowed to cool down to room temperature

Table 7-2: Trials procedure

Trial	Stage 1 - Sequential deposition without cleaning after each layer of deposition	Trial	Stage 2- Sequential deposition with cleaning after each layer of deposition
1.1	No lubricant used	1.2	With cleaning (no lubricants)
2.1	Application of MoS_2 used as lubricant	2.2	Application of MoS_2 used as lubricant, cleaned after each deposition
3.1	Application of graphite powder as lubricant	3.2	Application of graphite powder as lubricant, cleaned after each deposition
4.1	Application of oil based lubricant	4.2	Application of oil based lubricant, cleaned after each deposition

The layout of the base plate and the deposited walls is shown in Figure 7-2. For each trial, stage 1 always coresponds to the first three walls (Walls 1, 2 and 3) while in stage 2 (Walls 4, 5 and 6), a cleaning operation was performed using acetone on each deposited single bead that makes up the walls.

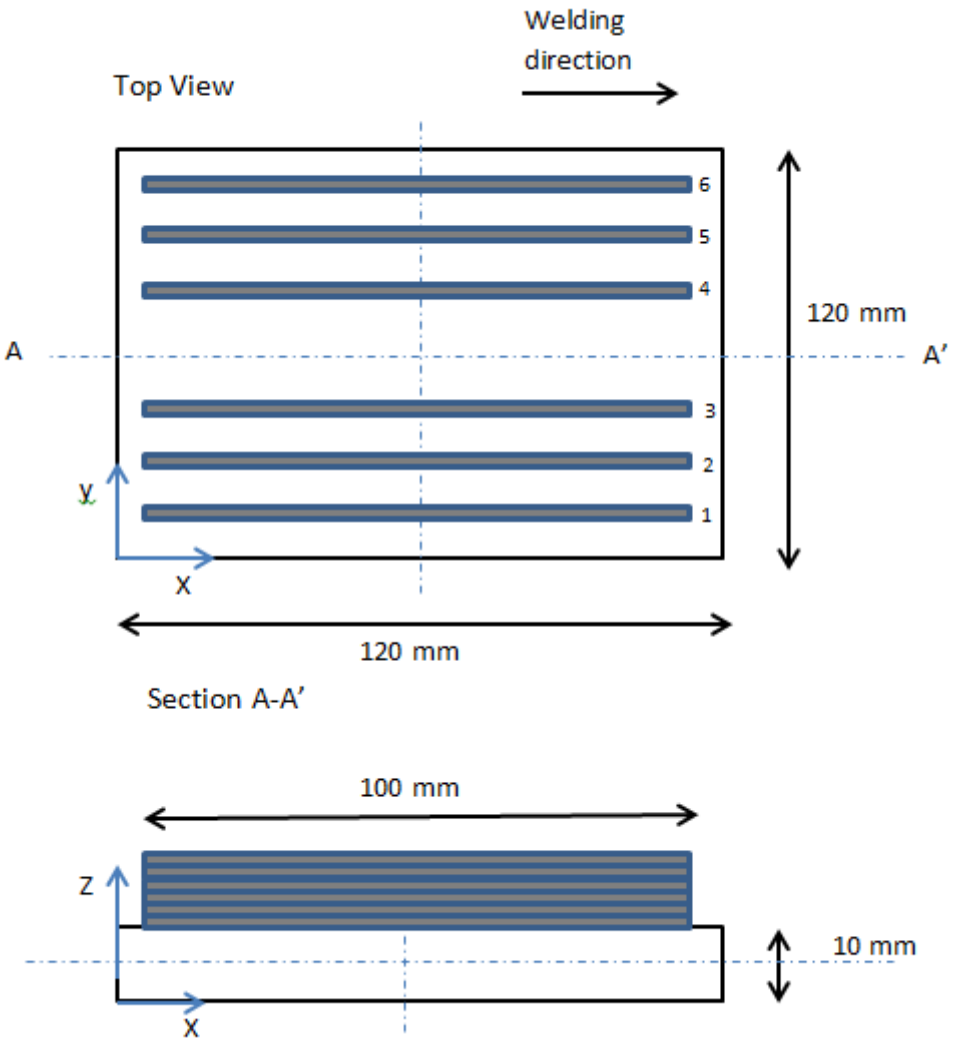

Figure 7-2: Illustration of the base plate with the wall build up

After the deposition, the walls were sectioned (section A - A in Figure 7-2 and photo Figure 7-3) to show the microstructure of the samples. The subsurface layer preparation was carried out before imaging the microstructure of the material. This process involves setting the samples on the resin and allowing to cure (Figure 7-4). Other microstructural preparation includes grinding using

different grades of abrasive grinding paper, a 6µm diamond paste for polishing and then etching with a 2% Nital solution for 20 seconds. This exposes the grain structure to identify the microstructure. All the processes were followed precisely because of the importance of obtaining thorough images of any change in the microstructure of the material, in order to assess the suitability of sequential deposition and machining.

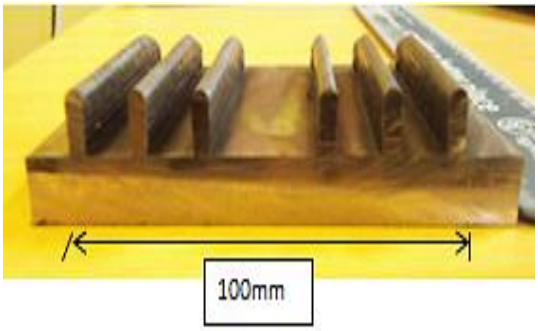

Figure 7-3: Sectioned wall sample

Figure 7-4: Some of the finished samples, embedded in resins

Figure 7-5a shows the region of the application of lubricants. The region is the point of the application of lubricants as well as the layer of interface between each layers of deposition (Position L, M and R in Figure 7-5b). The measurements were taken at this point of interest and Figure 7-5b illustrates the actual point of measurements. Some measurements (Position U and D in Figure 7-5b) were taken from the point of interest in order to be able to compare the results. The microstructures were taken at the interface of the weld (section A – A in Figure 7-5a) which is also the area of the application of the lubricants.

The micro hardness of the structures was examined on a Zwick micro Vickers hardness-testing machine using a load of 200g, which was applied for a duration of 20 seconds. The micro hardness test was conducted three times and measurements taken across the weld interface at points Upper (U), Down (D), Left (L), Middle (M), and Right (R) (see Figure 7-5b) and measured at regular intervals. For the study, an XL 30 Scanning Electron Microscope (SEM) was employed for detecting any form of lubricants embedded in the material. The samples were scanned and analysed using the image processing software INCA®. All the trials was repeated three times to improve the accuracy of the results.

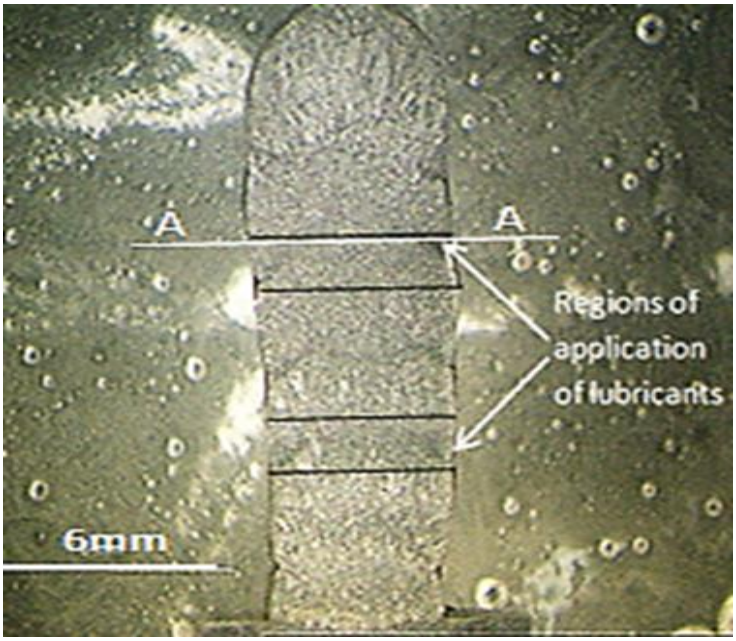

(a)

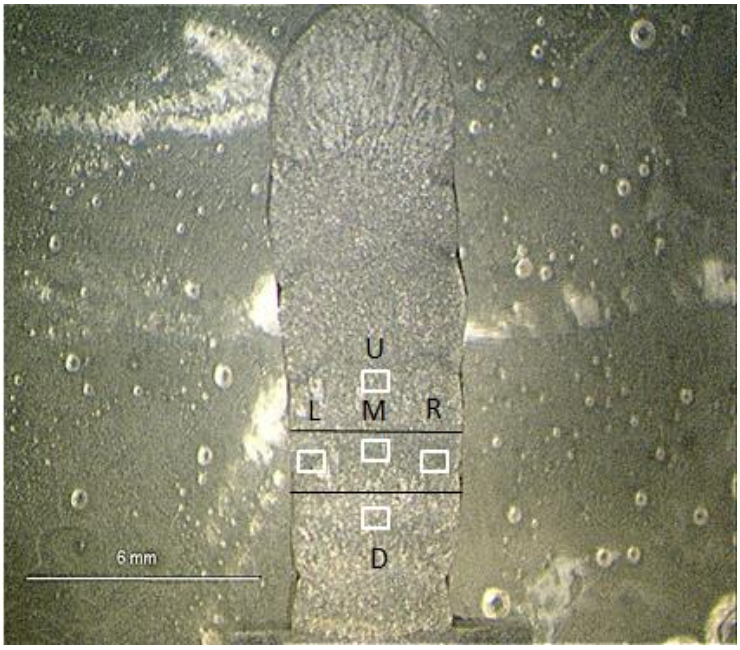

(b)

Figure 7-5: (a) Regions of the application of lubricants (b) Positions of U, L, M, R, and D described in the text

7.1.3 Results

7.1.3.1 Microstructure

This section describes the differences in the microstructure of the various trials. Figure 7-6 illustrates the microstructure of the deposited materials at the weld interface with no form of lubricant applied.

The microstructure in Figure 7-6(a) shows the microstructure of the weld sample at the interface with sequential deposition of the wall without cleaning after each deposition (no lubricant). It shows that the structure is composed of columnar proeutectoid ferrite and fine acicular pearlites intermixed with a small quantity of fine acicular pearlite between the columnar dendrites which is similar to the result obtained from a study conducted by Ohashi et al., 2009. However, Figure 7-6b shows the microstructure obtained when the sample was cleaned with acetone prior to each layer deposition (Trial 1.1). The micrograph shows an anequiaxed grain and mainly consists of ferrite with a large grain structure. This could be attributed to the cleaning of the deposited surfaces. No other form of contamination is expected from the process. Although the acetone was allowed to dry off before depositing the next layer, it brought about an increase in the grain size of the sample.

The microstructure of the sample during sequential deposition with MoS_2 as lubricants is shown in Figure 7-7a and b (Trial 2.1 and 2.2). Figure 7-7a illustrates the microstructure of the sample when the sample weld bead was not cleaned after each layer of deposition but MoS_2 was used as lubricant. The microstructure here is predominantly bainite with islands of ferrite. It is known that the rate of formation of bainite in the process of the intermediate transformation is determined by the rate of removal of carbon from the front of the growing crystallite due to the diffusion redistribution and by the number of emerging crystallisation centres. The carbon redistribution during this process was affected by the inclusion of MoS_2, which was used as a lubricant and thus finds its way into the molten metal during the WAAM deposition. This addition of MoS_2 promotes the formation of the bainite structure.

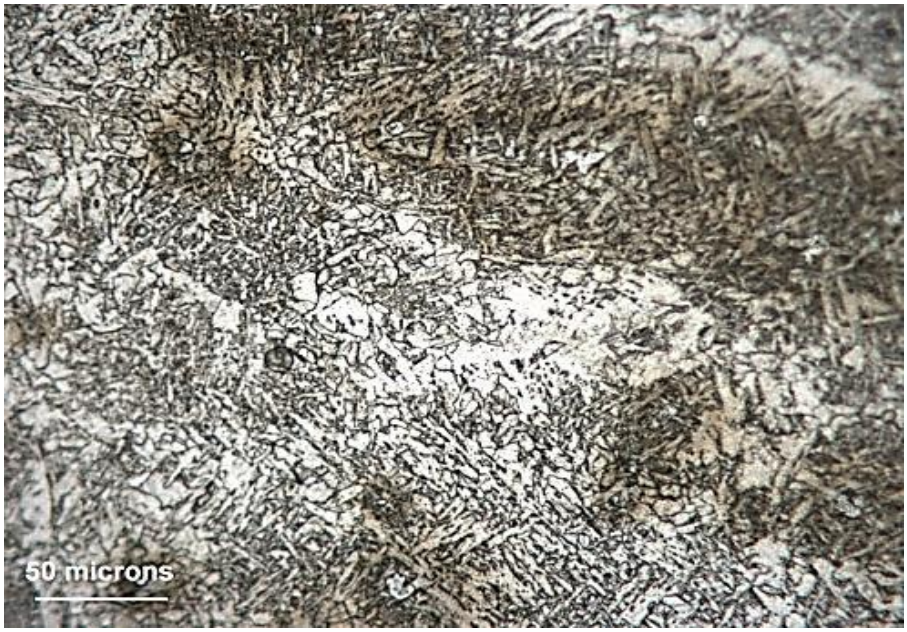

50 microns

(a)

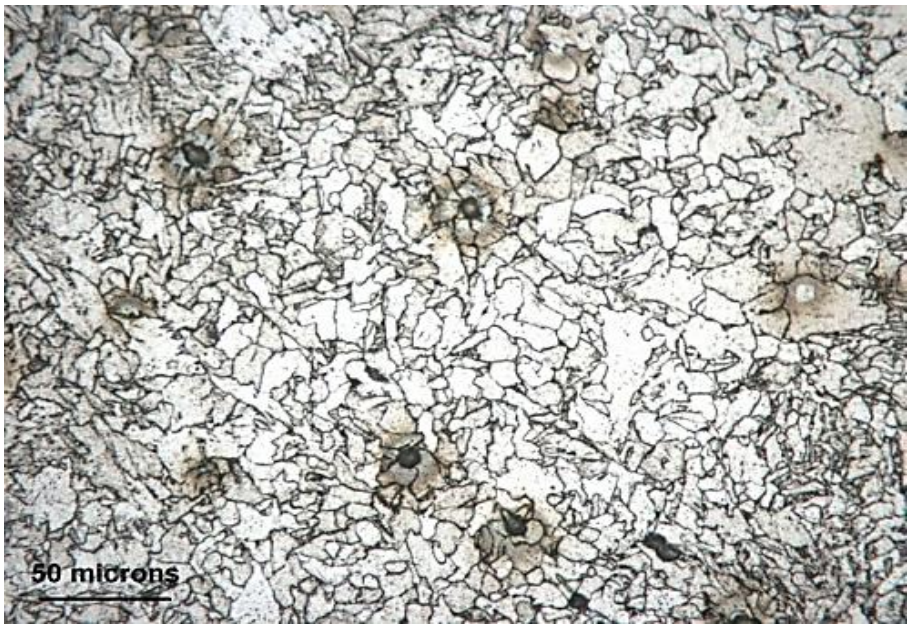

50 microns

(b)

Figure 7-6 Cross section of the microstructure of the sample during deposition without lubricants. Sample (a) not cleaned after deposition (Trial 1.1) and Sample (b) cleaned after deposition (Trial 1.2).

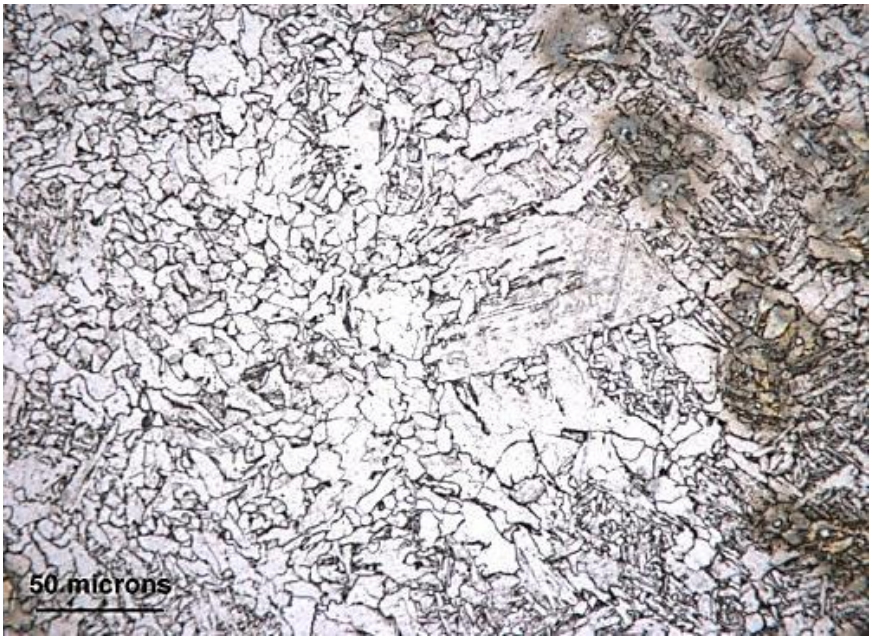

50 microns

(a)

50 microns

(b)

Figure 7-7: Cross section of the microstructure of the sample during deposition with MoS_2 as lubricants. Sample (a) not cleaned after deposition (Trial 2.1) and Sample (b) cleaned after deposition (Trial 2.2).

There are some patches of large ferrite grains, which can be attributed to the contamination of the weld surface by the MoS_2. However, Figure 7-7b, which is Trial 2.2, shows the microstructure with cleaning of the surface of the deposited layer after the application of MoS_2. The microstructure comprises of mixed coarse grains and some amount of long-grained ferrite. Some large grain structures are also noticed in this sample.

Microstructures in Figure 7-8a and b (Trial 3.1 and 3.2) show the structure of the samples when graphite was used as the lubricant. Graphite being an allotrope of carbon can combine easily with the molten mild steel materials used in this trial. However, in Figure 7-8a, which is the microstructure of the sample during sequential deposition with graphite as a lubricant, the graphite remains on the surface of the weld bead without cleaning. The microstructure here is characterised by the presence of ferrite with aligned and non-aligned second phases, grains boundary ferrite and a ferrite/carbide aggregate that appears to be fine pearlite. The fine pearlite occurs as a result of the mixture of carbon with the weld pool during deposition. Moreover, when the graphite was cleaned, the microstructure (see Figure 7-8b) exhibited equated ferrite grain and a larger grain of fine pearlite and the weld has been re-austenite by subsequent weld deposit. This has the effect of refining the grain structures by eliminating the columnar grains and replacing them with relatively fine polygonal ferrite surrounded by acicular ferrite.

50 microns

(a)

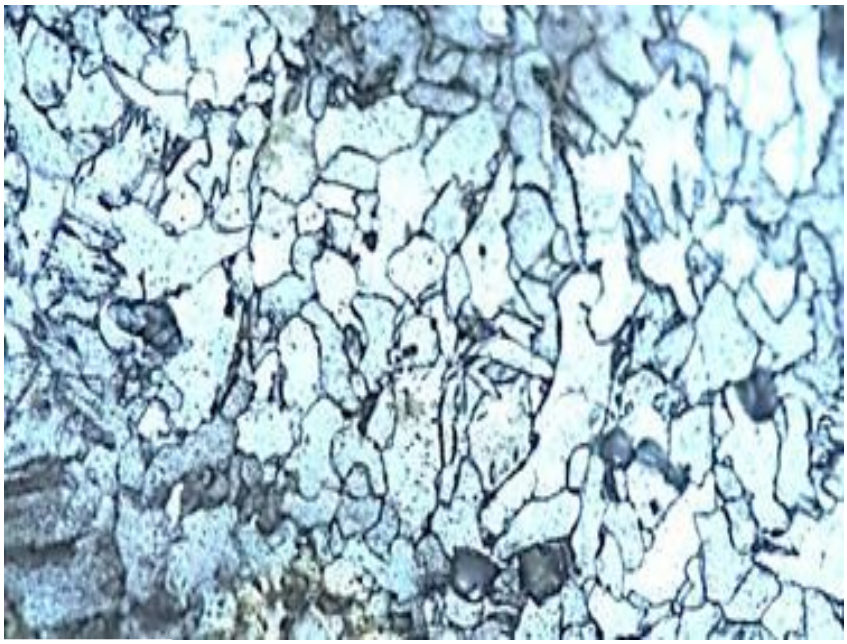

50 microns

(b)

Figure 7-8: Cross section of the microstructure of the sample during deposition with graphite as lubricants. Sample (a) not cleaned after deposition (Trial 3.1) and Sample (b) cleaned after deposition (Trial 3.2).

With the sequential deposition of layers with an oil-based lubricant without cleaning after each deposition (see Figure 7-9a - Trial 4.1), the structure shows a tempered martensite which reduces the hardness but tends to increase the ductility of the material. It also has pashes of the mixture of ferrite and pearlite grains. When the fluid lubricant was cleaned (see Figure 7-9b - Trial 4.2), the microstructure exhibited fine grains of acicular ferrite formation with some pashes of coarse pearlite.

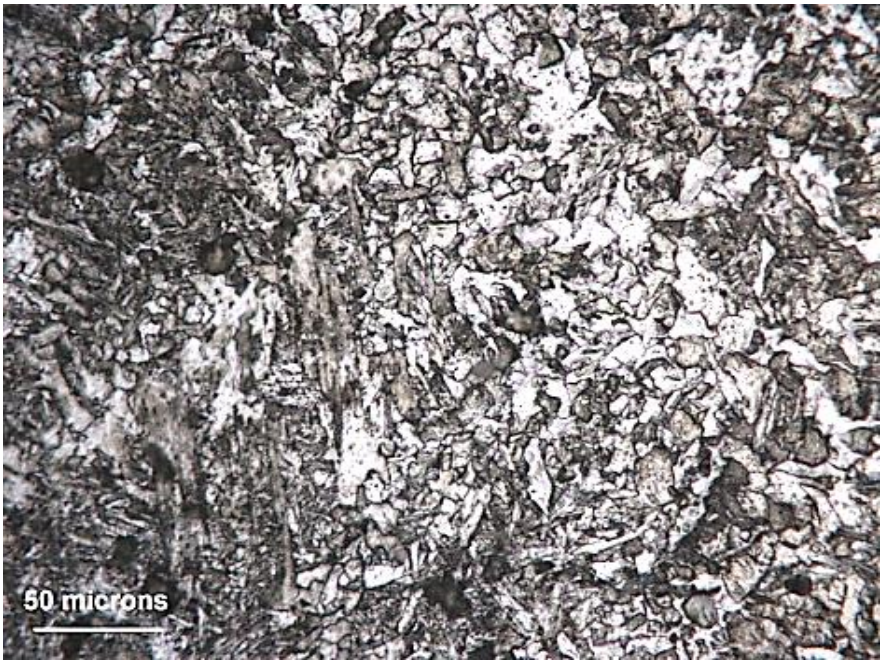

50 microns

(a)

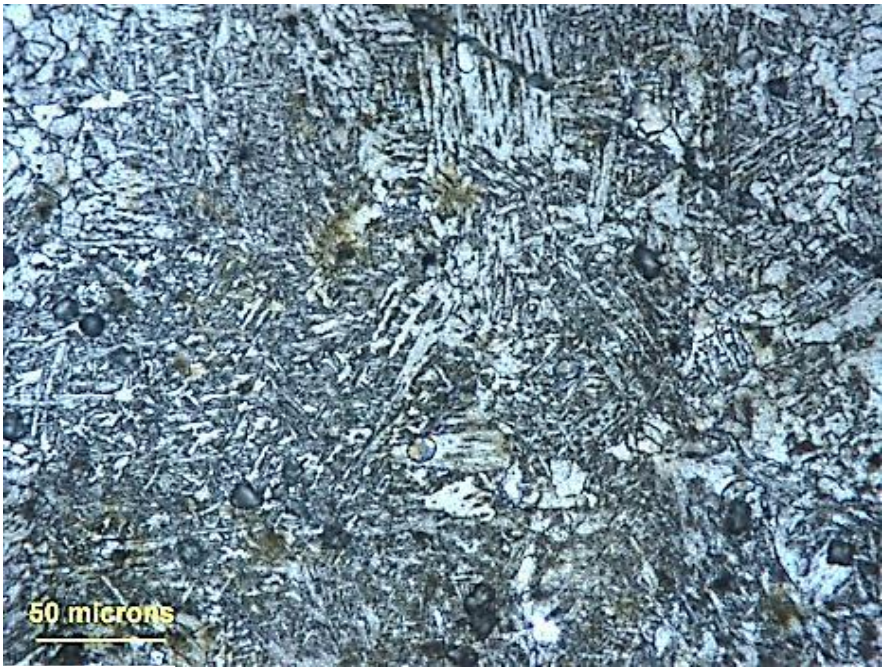

50 microns

(b)

Figure 7-9: Deposition with liquid lubricant (Eco Cool oil emulsified mixed with local main water supply 1:10) as the lubricant. Sample (a) not cleaned after deposition (Trial 4.1) and Sample (b) cleaned after deposition (Trial 4.2).

7.1.3.2 Micro hardness of the weld

Figure 7-10 shows the comparative hardness profile for the samples. One can see through the solidification of the deposited weld zone, that the parent material commonly lost its unique strength induced through strain hardening (Yang et al., 2002). Generally, in the event of carbon and low alloy steel, the development of bainite or martensitic stages in the deposited weld region encourages an upsurge of hardness. The macro hardness chart in Figure 7-10a showed the hardness of the deposited material with and without cleaning when no lubricant was applied in the interface of the layer. It has an average hardness of 219VH and the micro hardness outside the deposited layer interfaces have an average of 258VH when no cleaning took place.

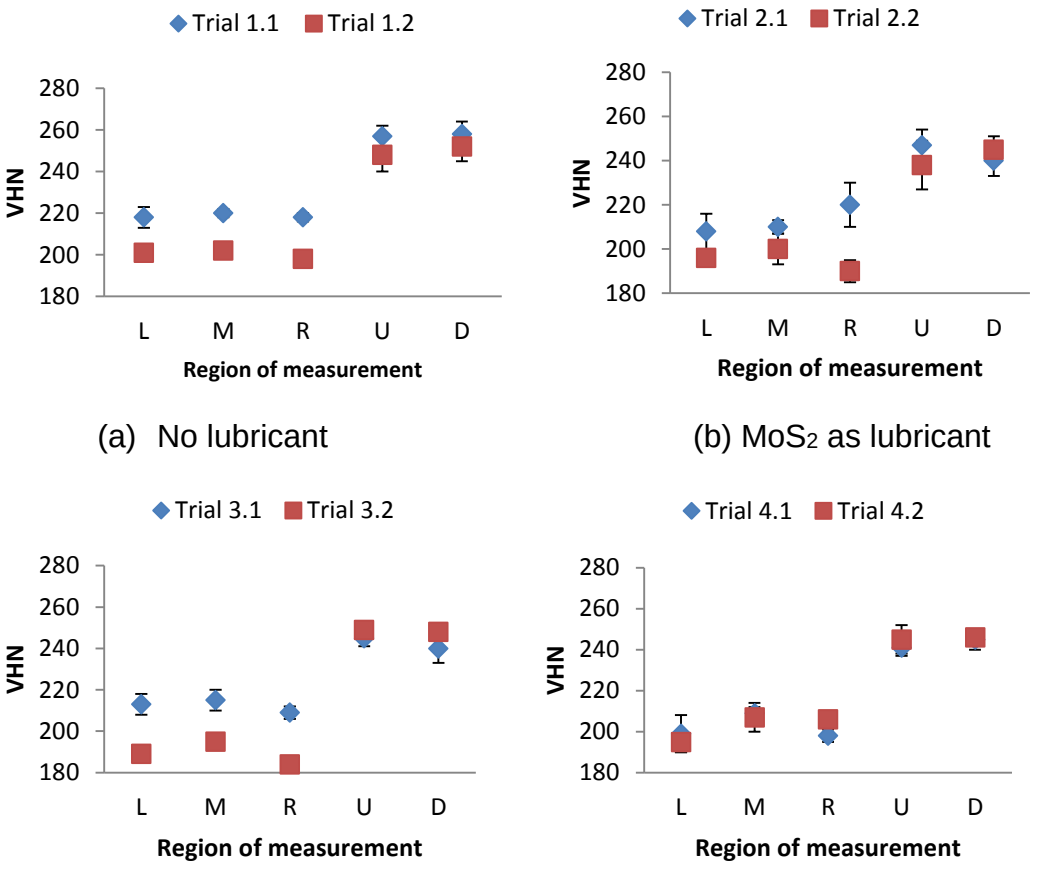

(a) No lubricant

(b) MoS_2 as lubricant

(c) Graphite as lubricant

(d) MQL

Figure 7-10: Effects of the application of lubricants of the micro-hardness.

With the cleaning, the average hardness at the interface of the layers dropped to 200VH and a micro hardness outside the deposited interface of 250VH. However, Figure 7-10b shows the micro hardness profile with the application of MoS_2 as a lubricant. In this case, MoS_2 was applied to the interface of the layers deposited and subsequent layers deposited without cleaning as shown in Trial 2 stage 1 and with cleaning as shown in Trial 2 stage 2. The average micro hardness without cleaning at the weld interface is 213VH and for the micro hardness taken outside the weld interface, an average of 244VH. When the cleaning operation was carried out, the average micro hardness at the interface falls to 196VH and outside the region of interface, the average micro hardness of 242VH.

Furthermore, when the same process was repeated with the use of graphite as a lubricant, Figure 7-10c shows the outcome of the results of the micro hardness with the average micro hardness of 212VH when the graphite was used without cleaning and outside the weld interface there is an average micro hardness of 243VH. However, when the graphite was cleaned, the average micro hardness at the weld interface also dropped to 190VH and outside this region, an average of 249VH was attained. Figure 7-10d shows the micro hardness profile with the use of an oil-based lubricant to the interface. This is with no cleaning. The average micro hardness for the material is 202VH as compared to the region outside the weld interface with an average micro hardness of 243VH.

With cleaning of this lubricant with acetone and allowing it to dry off, the micro hardness remains virtually at the same level as with no cleaning operation. It has an average micro hardness of 203VH and outside the weld region, it has an average of 245VH.

7.1.3.3 Temperature around the welding region

In order to be mindful of the temperature around the welding zone during deposition, a temperature-modelling plot was produced with mild steel as the material (see Figure 7-11) using a three-dimensional transient thermal model, and the software used was the Abaqus 6.9-3. During the WAAM deposition, the

heat generated includes that generated through the welding arc, the heat conduction arising from the deposited sample and heat loss from the surface and the cooling system underneath the base plate. Radiation and convection heat losses were modelled and the heat loss through the backing bar was also modelled. The welding arc was simulated as a volumetric heat source with a power density moving along with the torch. The Goldak double ellipsoidal heat source was used to apply the heat to the WAAM deposits (Ding, 2012). The power density of the region in front of the arc centre and the region behind the arc centre was defined separately using the equation 7-1 and equation 7-2.

$$q_f = \frac{6\sqrt{3}Qf_f}{\pi\sqrt{\pi}a_f bc} e^{\left[-3\left(\frac{x^2}{a_f^2}+\frac{y^2}{b^2}+\frac{z^2}{c^2}\right)\right]} \tag{7-1}$$

$$q_r = \frac{6\sqrt{3}Qf_r}{\pi\sqrt{\pi}a_r bc} e^{\left[-3\left(\frac{x^2}{a_r^2}+\frac{y^2}{b^2}+\frac{z^2}{c^2}\right)\right]} \tag{7-2}$$

Where qf is the power density distribution in the front quadrant and qr is the power density distribution for the rear quadrant. The parameters b, and c, which describe the weld pool width and depth, were measured from cross-section metallographic profile. The values for a_f and a_r are estimated from weld pool surface ripple markings. Q is the energy input considering the factor of efficiency; f_f and f_r are the factors for distributing the power to the front and rear of the rear source, and they have the relation that $f_f + f_r = 2$ and x, y and x being the directional distribution of the heat source.

In order to simulate the deposition process, the filler material was simulated using the “element birth technique” (Ding, 2012). Using the change option in ABAQUS, entire elements of the deposited WAAM wall were deactivated at the initial step of the analysis, and then sections of elements are activated in successive steps to simulate the metal deposition as the weld torch travels along the base plate. A pre-processing program was developed in Matlab to help efficiently generating the element sets and the input file for Abaqus. Automatic time incrementation was

used in the simulation with the allowed maximum time increment of 0.1 s for the heating steps and the allowed maximum time increment of 15 s for the cooling steps. The steps in the thermal analysis are as follows:

Step 1 (1 x 10^{-10} s): All of the elements of the deposited wall are deactivated.

Step 2 (1 x 10^{-10} s): The first section of the deposited wall elements is activated.

Step 3 (0 – 1.2 s): Heat source moves, continuously applying heat flux.

Step 4 (1.2 s – 60 s): Steps 2 – 3 are repeated activating new element sections of the deposited wall and applying the heat flux.

Step 102 (60 s – 460 s): Torch removed and the component cools down to room temperature.

From Step 103 (from 460 s): Steps 2 – 102 were repeated to simulate the thermal performance of the material adding process from the second layer.

The plot shows the temperature of the weld pool. This helps to understand what happened to the lubricants during and after the WAAM deposition. The plot shows the temperature of the weld pool during deposition to be almost 2800ºC and every other region around the welding pool lies between the 1500ºC and 30ºC. A review on the study of the melting point of graphite between the year 1963 to 2003 concluded that graphite melts at 4527ºC ± 200ºC (Savvatimskiy, 2005).

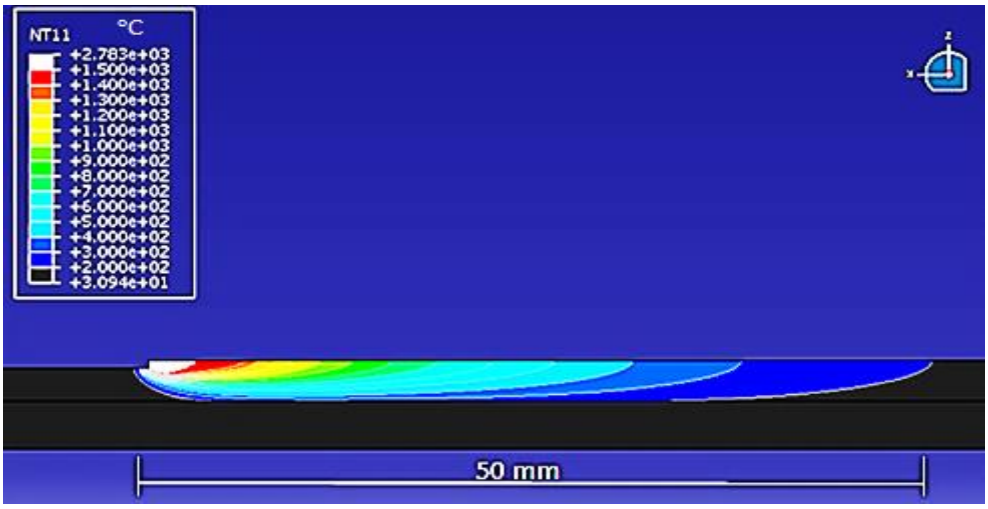

Figure 7-11: Temperature plot during the welding operation

With this data, the graphite used in the trial will not melt or sublime since this is above the highest temperature of the welding pool. Moreover, the graphite might have mixed with the molten material during the welding deposition. Contrary to the high melting point of graphite, the MoS_2 has a much lower melting point of 1185^{o}C. MoS_2 sublimes above this melting point and they are moderately unreactive chemically unless physically and mechanically activated (Farr, 1975).

At a temperature of above 700^{o}C, MoS_2 may react with steel at the weld pool:

$$MoS_2 + 2Fe + Heat = 2FeS + Mo$$

The molybdenum that resulted from this reaction can diffuse into the weld pool. Moreover, at room temperature, chemical reactions could be expected and in fact were sometimes noticed between disulphide, metal surfaces, and mist air (Far, 1975). In practice, such activity is not deleterious, although it may be a factor in the eventual consumption of lubricants.

7.1.3.4 SEM Analysis

The major objective of this investigation is to study the effects of using lubricants in a hybrid system of sequential welding and machining. An XL 30 Scanning Electron Microscope (SEM) was used in detecting any form of lubricant embedment at different stages of the experiment. The samples were sectioned and scanned with the help of the image processing software INCA. The percentage of lubricant embedment for a certain section, which is the interface between the weld at the point of the application of the lubricants, was analysed. The region of the SEM analysis of the sample is shown in Figure 7-13.

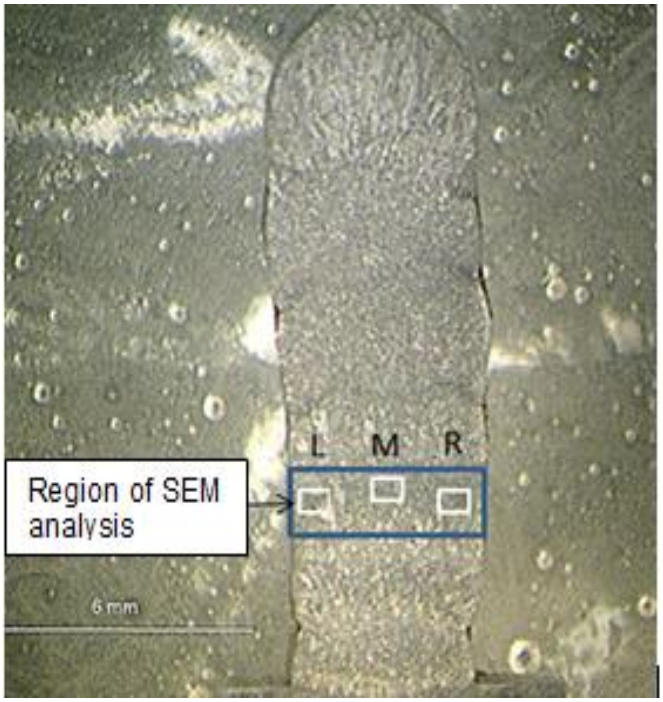

Figure 7-12: Illustration of the region of SEM analysis

However, in the analysis, SEM estimated the chemical composition using the image processing software (see Figure 7-12 and Figure 7-13). This software indicates the concentration of most elements present for a certain scanned area.

The percentage of lubricants at the interface between the deposited weld; i.e. the point of the application of the lubricants, was analysed. In the analysis, SEM was used to estimate the chemical composition (see Figure 7-13 and 7-14). This indicates the elements present for the certain scanned area. Figure 7-13 shows the elements present in the Trial 1a sample with sequential deposition of the wall without cleaning after each deposition when no lubricant was applied. The elemental composition of the samples is also shown in Table 7-3. The analysis shows the presence of carbon (C), potassium (K), aluminium (Al), and oxygen (O). Other elements present include magnesium (Mn) and iron (Fe).

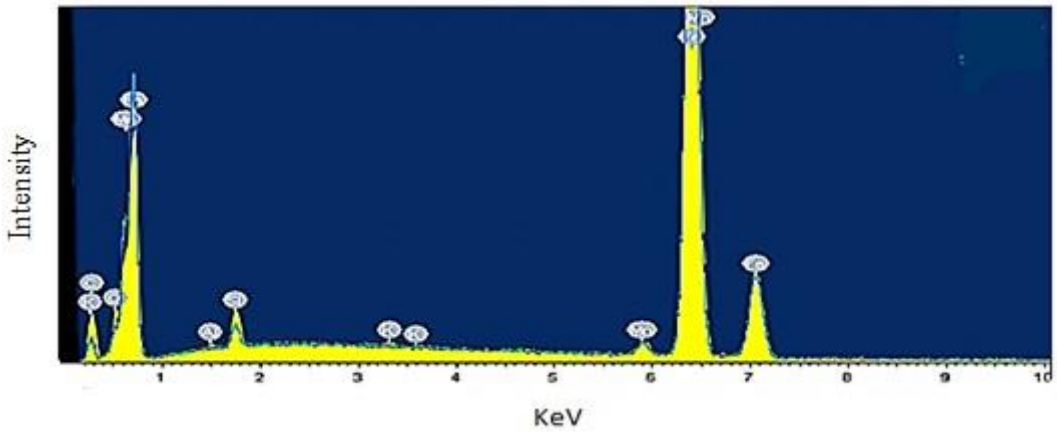

Figure 7-13: Spectroscopy diagram for sequential deposition of wall without cleaning after each deposition with no lubricant.

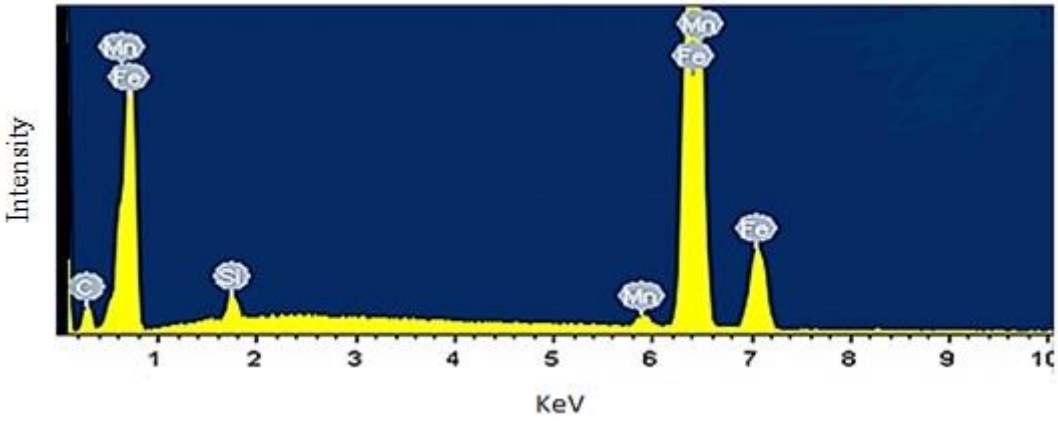

Figure 7-14: Spectroscopy diagram for sequential deposition of wall with cleaning after each deposition with no lubricants.

Table 7-3: Elements composition of the samples

No of exp.	C (%)	O (%)	Al (%)	Si (%)	K (%)	Mn (%)	Fe (%)
1-1	10.99	3.31	0.18	1.58	0.15	1.28	82.50
1-2	12.20	-	-	1.13	-	1.28	85.38
2-1	8.28	3.33	-	1.36	-	1.22	85.80
2-2	6.57	-	-	1.21	-	1.32	90.90
3-1	8.41	-	-	1.29	-	1.33	88.96
3-2	6.21	-	-	1.11	-	1.31	91.37
4-1	4.64	-	-	0.96	-	1.31	93.09
4-2	4.85	-	-	1.08	-	1.51	92.56

All these elements are in the composition of the sample without any form of treatment or additive. It is observed that the elements present in the sample with sequential deposition of the wall without cleaning after each deposition (when no lubricant was applied) were as shown in the material specifications, but not all of the elements from the material specification were present in the other trials.

Moreover, the composition by percentage of each element differs, despite the fact that they were from the same material. The only different condition in all the trials is the application of lubricants and cleaning operation that took place. In the Trial 1a and 1b, the percentage of carbon present is at a high level when compared with other trials. Trial 1a has a carbon content of 10.99% by weight and Trial 1b has an elemental content of carbon of 12.20% by weight. Moreover, Figure 7-13 shows the elements present in the sample with sequential deposition of the wall with cleaning after each deposition. The rest of the results from this trial, apart from Trial 1 stage 1 and Trial 2 stage 1, show that the presence of oxygen follows the same pattern as shown in Figure 7-14. Other elements might be present in the analysis but could be insignificant.

7.1.4 Discussion

The objective of this research is to focus on ascertaining the viability of sequential deposition and machining with the view of understanding the influence of a solid lubricant in the process. This investigation has shown the effects of using acetone to clean WAAM samples on the microstructure. Without the application of lubricants, the grain size of the microstructure tends to become larger than when cleaned with acetone (see Figure 7-6b). However when lubricants were applied, there are pashes of large grain sizes. The large grain size appears in all the microstructures that were cleaned with acetone and this may be as a result of the reaction of acetone with the surface of the weld samples. The micro hardness at these regions is lower because of the increase in the grain size and this affects the material ductility, which makes the material more brittle.

Hardness is another critical property investigated. The hardness of the samples where no lubricant was applied recorded the highest VH, but with a reduction in

the VH value when cleaning was applied due to the increase in the grain size. However, with the application of both graphite and molybdenum disulphide on the sample, a reduction in the VH also existed and this can also be attributed to the increase in the grain size and the effects of contamination that took place through the application of the solid lubricants. There are pashes of long grains, which are because of contamination of the microstructure, and this is shown clearly in Figure 7-7a and b. Moreover, with the application of Ecocool fluid as the lubricant, the variation in the VH is not significant between the samples with cleaning and without cleaning. This can be attributed to the Ecocool fluid lubricant having no significant effect on the microstructure and the mechanical properties.

Generally, it was found that in the welding zone where no lubricant was applied, a higher micro hardness can be observed than when cleaning took place. Also the micro- hardness outside the weld deposition zone at the surroundings has pronounced higher micro-hardness values. These phenomena occur as a result of the grain size. A previous study (Liu et al., 2003) indicated that, in general, the Hall-Petch type of linear relationship was followed between micro hardness and the grain size.

$$\mathrm{HV} = \mathrm{a} + \mathrm{b}d^{-1/2}$$

Where HV is the micro hardness, d is the grain size, a and b are the parameters related to phases in materials and in one weld, they are constant. It can be seen that the smaller the grain size, the higher the degree of micro-hardness. The grain boundaries, thus, become the main obstacle to the slip of dislocations and the zone with a smaller grain size would have higher micro hardness as more grain boundaries would impose more restrictions to the dislocation movement.

This investigation has shown the effects of using acetone to clean WAAM samples on the microstructure. Without the application of lubricants, the grain size of the microstructure tends to become larger when cleaned with acetone. When a lubricant was applied, there were pashes of large grain sizes. The large grain size appears in all the microstructures that were cleaned with acetone and this can be attributed to the reaction of acetone with the weld samples. Although

the acetone was allowed to dry before depositing the next layer, it caused an increase in the grain size of the sample. The pashes of large grain sizes exhibited in Figure 7-7a, Figure 7-7b and Figure 7-8b occured as a consequence of using solid lubricants. The solid lubricants contaminated the material microstructure.

7.2 Material removal in WAAM

In any additive manufacturing process, apart from obtaining the accurate dimensions, attaining a good surface quality through machining and maximised material removal are of utmost importance. It is generally known that the deposition parameters used in the course of a welding deposition process has a great effect on the geometry of the resulting weld beads, and in turn influences the properties of the deposited part. However, the significance of the deposited weld bead geometries is well thought to be vital during additive manufacturing procedures where the deposited beads combine to form a final near net-shape.

This study was designed to establish a comprehensive understanding of the interaction between key process parameters; i.e. TS and WFS in the deposition of WAAM structures and the Effective Wall Width (EWW) of multi-layer deposition parts. The EWW is paramount during manufacturing and machining of WAAM structures. This was carried out through experimentation with the effect of various input parameters on the deposited geometry observed and quantified. Machining was used in determining the material removal (maximum thickness of material required to be removed by a machining process),

7.2.1 Materials

A mild steel wire electrode of 1.2 mm in diameter was used throughout this trial. The shielding gas used was Ar/CO2 (20%). The pre-set operating conditions are summarised in Table 7-4. The experimental design describing the output of welding settings, in addition to the bead profile measurements is shown in Table 7-5.

Table 7-4: Welding conditions

Welding Process	Power source	Shielding gas	Flow rate (*l*/min)	Program mode	CTWD (mm)	WD (mm)
CMT	Fronius CMT	Ar/CO_2 (20%)	15	Pure CMT	13	1.2

7.2.2 Methodology

A systematic experimental design was used in the deposition of the WAAM wall structure as shown in Table 7-5. The experiments were carried out in a random order to minimise the effects of some variables that are uncontrollable, consequently reducing the incidence of methodical errors. Steady environments were maintained during these trials for manufacturing a uniform weld quality.

Table 7-5: Experiment welding parameters and profile outputs[3]

Trial	*Trial order*	*WD (mm)*	*WFS/TS*	*TS (m/min)*	*W (mm)*	*EWW (mm)*	*MRW (mm)*	*H (mm)*	*EWH (mm)*	*MRH (mm)*
1	2	1.2	2	0.4	2.77	2.12	0.65	13.91	13.6	0.31
2	5	1.2	2	0.5	2.64	2.02	0.62	12.14	11.85	0.29
3	10	1.2	2	0.6	2.48	1.96	0.52	11.68	11.32	0.36
4	11	1.2	4	0.4	4.89	4.15	0.74	16.49	15.63	0.86
5	8	1.2	4	0.5	4.72	4.07	0.65	16.18	15.36	0.82
6	9	1.2	4	0.6	4.64	4.06	0.58	15.35	14.79	0.74
7	3	1.2	6	0.4	5.63	4.72	0.91	20.19	19.08	1.11
8	7	1.2	6	0.5	5.25	4.57	0.68	19.88	18.81	1.07
9	6	1.2	6	0.6	5.15	4.41	0.74	19.52	18.44	1.08
10	4	1.2	8	0.4	6.49	5.38	1.11	24.22	23.01	1.21
11	12	1.2	8	0.5	6.42	5.33	1.09	23.83	22.66	1.17
12	1	1.2	8	0.6	6.28	5.23	1.05	23.12	21.94	1.18

[3] WD, wire diameter; WFS, wire feed speed; TS, travel speed; W, deposited bead width; EWW, effective wall width; MRW, amount of materials removed from the width; H, deposited bead height; EWH, effective wall height; MRH, amount of materials removed from the top layer

The trial samples were deposited on the SAM Edgetek machine integrated with a Fronius CMT welding machine. Twelve WAAM walls of varying experimental parameters were deposited on a base plate and a total of up 12 layers were deposited. The length of the walls was 100mm. The height and the width of each of the walls deposited were measured using a digital vernier calliper and the measurements were taken at four different locations, 20mm apart, and this was repeated five times to improve the accuracy of the measurements. The average was then found and used as a representative of the expected precision of the measurement.

The samples were milled on the same Edgetek machine with a depth of cut of 0.1mm and feed rate of 0.6m/min. This was in order to gain the actual EWW and EWH. The milled sample was subsequently measured on the TESA CMM machine (described in Section 4.2.2 in Chapter 4 of this thesis) to gain the EWW and EWH. This was in order to know the amount of material left after machining the walls to remove the step effect of the WAAM deposition.

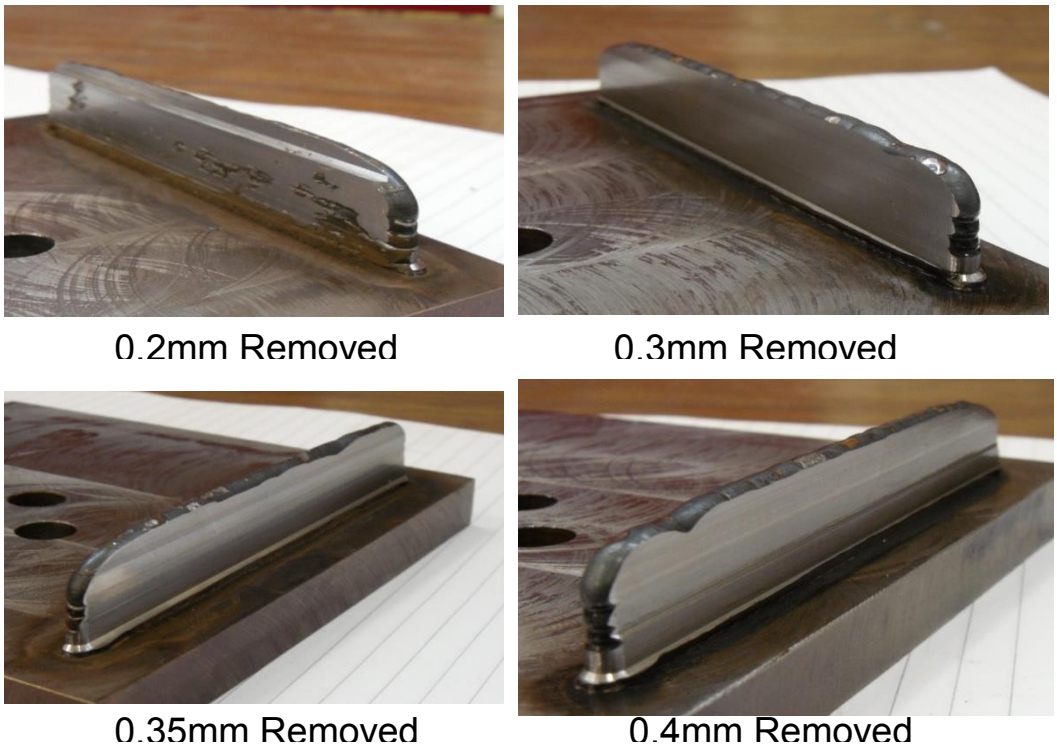

Figure 7-15: Milled deposited sample

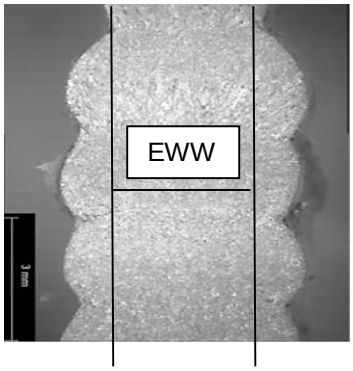

Figure 7-16: Micrograph showing the EWW of a sample

7.2.3 Results

Figure 7.17 describes the influence of the WFS/TS combination on the wall width W, EWW and the amount of materials that would be cleaned off during machining. As expected, with the increase in the ratio of WFS/TS, the material width also increases and this has a residual effect on the amount of materials that would be cleaned during machining. The study shows an increase in the materials removed. However, the distance between the EWW and the wall width W of the wall start to increase as the WFS/TS increases. Increase in the wall width W can be attributed to more material deposited per time especially with increase in WFS/TS ratio.

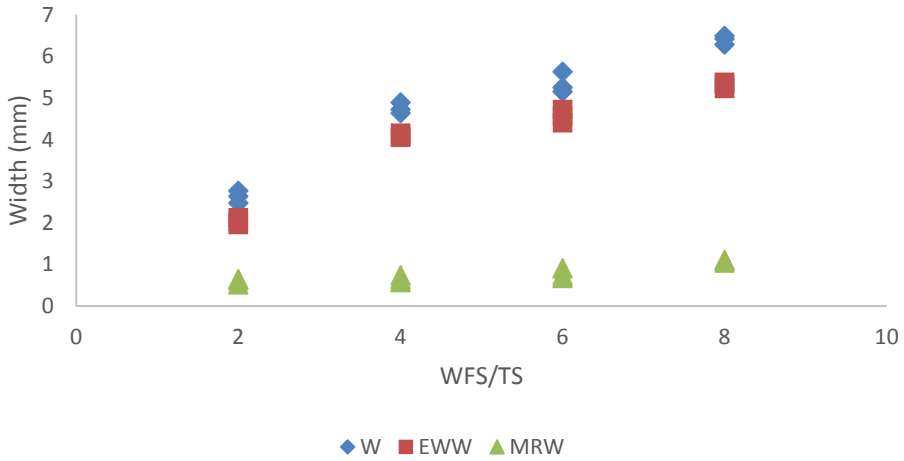

Figure 7-17: Effects of WFS/TS on wall W, EWW and MRW

Figure 7-18 demonstrations the dependence of the wall height H, on the WFS/TS combination. The H and WFS/TS are directly proportional to each other and the relationship is linear.

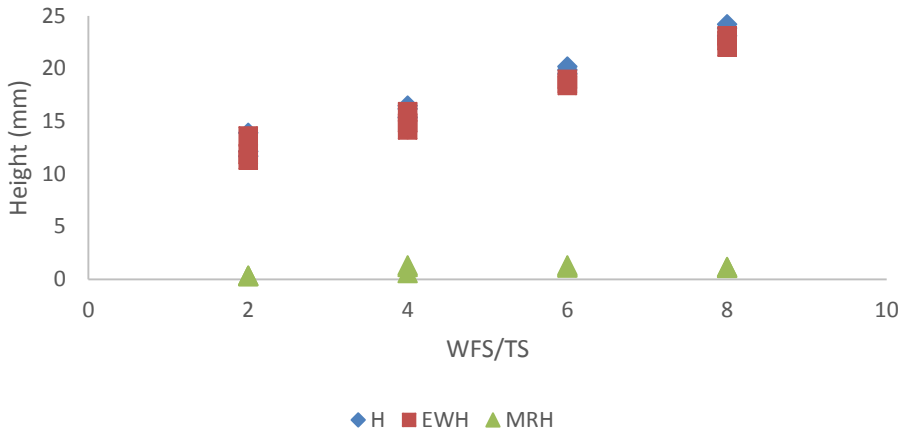

Figure 7-18: Effects of WFS/TS on wall H, EWH and MRH

The chart shows a non-significant difference in the materials removed from the height of the wall samples and is not significant on the overall height of the sample.

Figure 7-19 illustrates the effects of the TS on the wall W, EWW and MRW. The results indicate that W depends strongly on the TS and WFS/TS ratio. However, increases in the value of TS result in reduced wall W and subsequently the reduction in the EWW and MRW. This makes the impact of TS less evident in the MRW as the TS is increased. However, the ratio of WFS/TS also played an important role as an increase in the ratio resulted in an increase in the wall W.

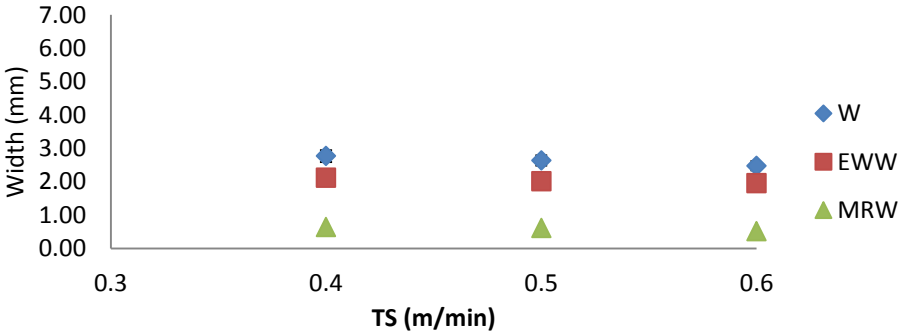

a) WFS/TS = 2

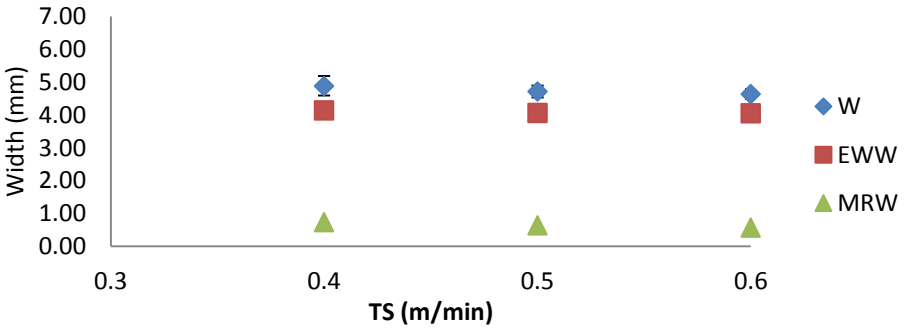

b) WFS/TS = 4

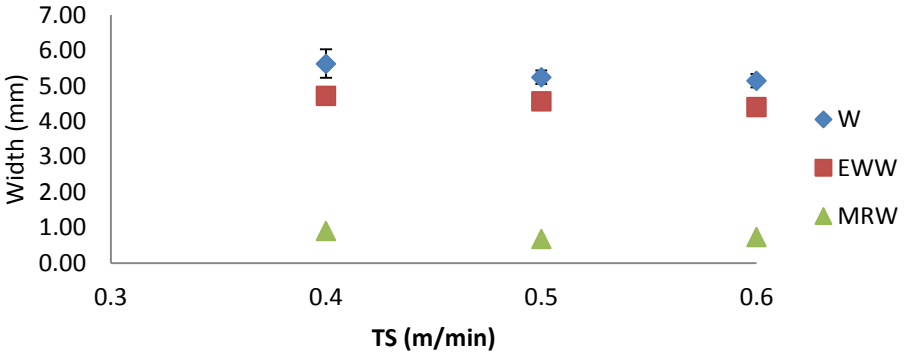

c) WFS/TS = 6

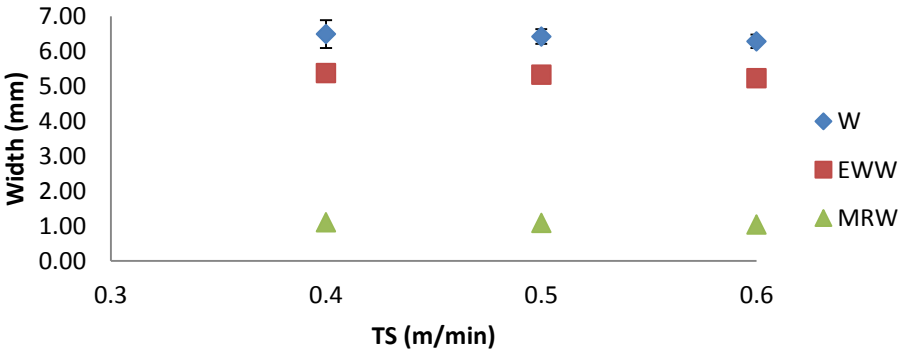

d) WFS/TS = 8

Figure 7-19: Effect of TS on wall W, EWW and MRW for the various WFS/TS.

The amount of materials to be removed during machining, if the rough surface of the deposited wall is to be machined away, is demonstrated in Figure 7-20. It was noted that as the TS is increased, the amount of material to be removed also decreases. This correlates with the fact that the amount of materials deposited as the TS increases is reduced per unit length. Nevertheless, the higher the WFS/TS ratio, the greater the material to be machined away from the wall surfaces.

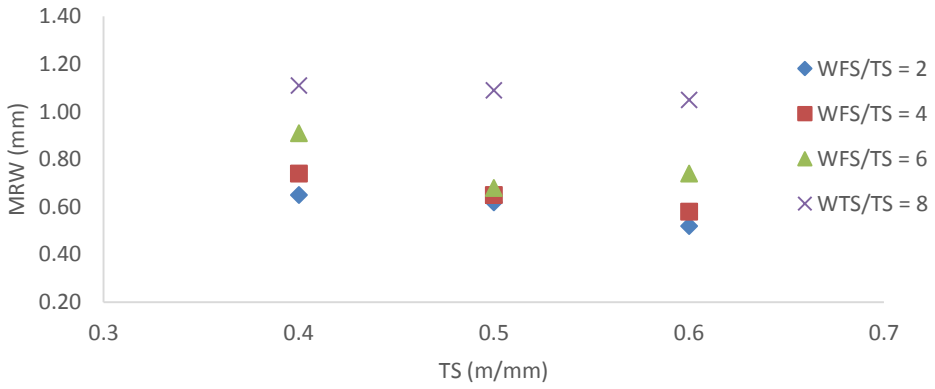

Figure 7-20: Effect of TS on MRW

As shown in Figure 7-21, there is no significant difference in the material removed from the height of the samples especially when using a lower WFS/TS. As the WFS/TS increases, the material removed also increases.

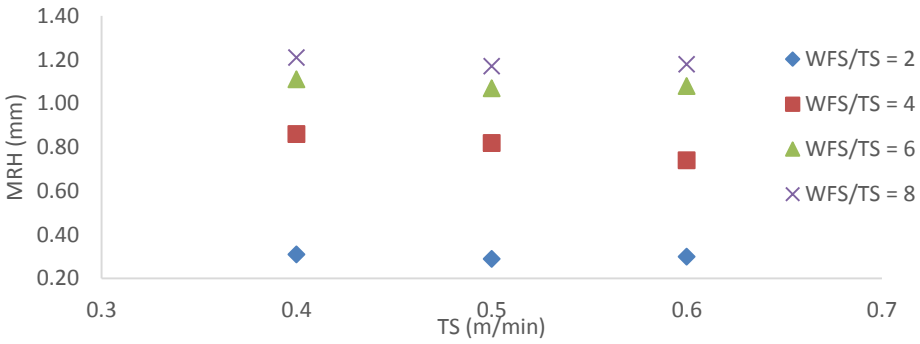

Figure 7-21: Effect of TS on MRH

Moreover, an increase in the TS brings about a small increase the material removed. This is insignificant when compared to the material removed with an increase in the WFS/TS ratio as shown in Figure 7-22.

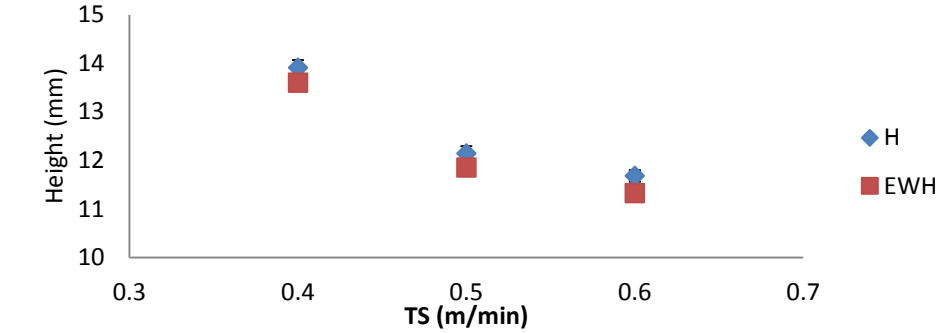

(a) WFS/TS = 2

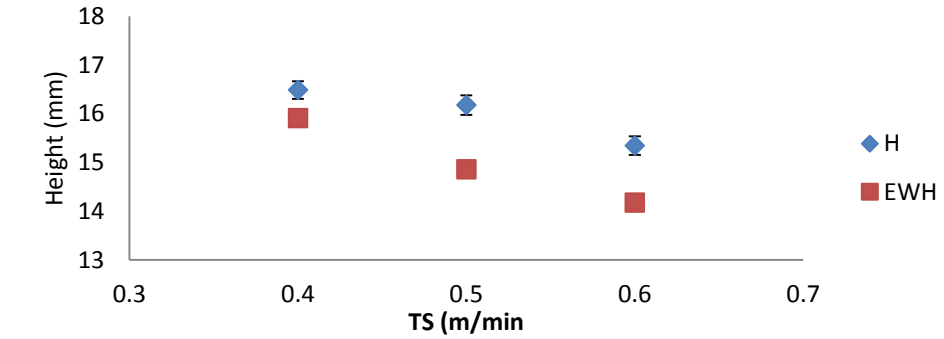

(b) WFS/TS = 4

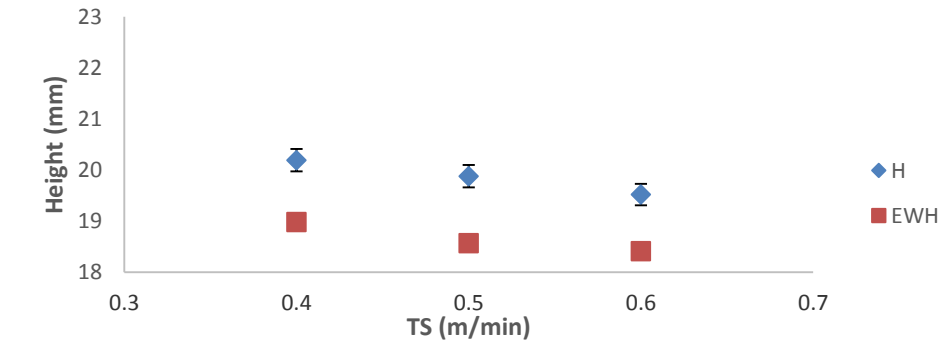

(c) WFS/TS = 6

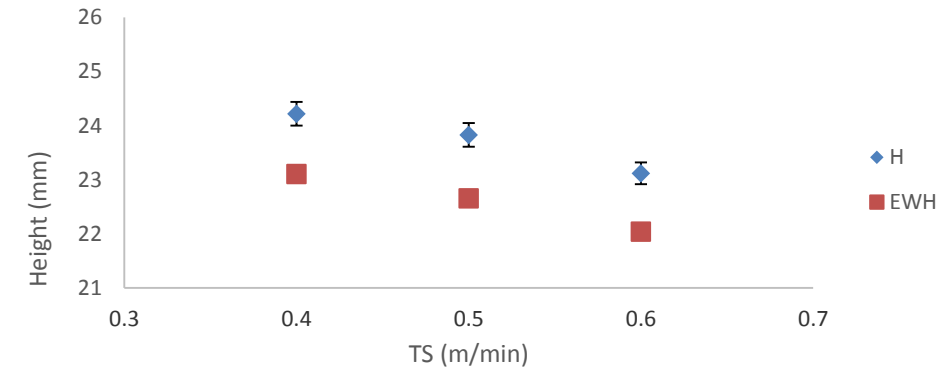

(d) WFS/TS = 8

Figure 7-22: Effect of TS on wall H, EWH and MRH for the various WFS/TS.

7.2.4 Discussion

This study investigates the influence of WAAM deposition on the WAAM output geometry prior to machining and post machining operation; i.e. control of the WAAM process so that the minimum material is removed in order to achieve a good machining quality with less material wastage. It is also a study into the practical depth of the integration interaction of the WAAM deposition primary parameters.

The elements of attention in terms of weld bead wall geometry were the average wall thickness and the build-up height, in addition to the surface waviness, which was characterised in terms of the machining removal thickness (MRW and MRH). It was defined as the maximum thickness of material required to be removed by a machining process to bring the deposited back to a solid vertical surface. This method is preferred to other measures; i.e. Surface roughness (Ra), because this relates directly to the amount of tool engagement necessary during machining. It also serves as the representative of potential material wastage.

In the current study, it was discovered that the effect of the WFS/TS ratio on deposited wall characteristics (such as H and W) has a greater impact on the W and H of the wall samples as well as the EWW. This brought an increase in the wall width and wall height, as seen in Figure 7-17 and Figure 7-18. This is because larger constant cross section areas were deposited as the ratio of WFS/TS increases. It is not surprising to note that the range of EWW increases with a higher WFS/TS ratio. The amount of materials that need to be cleaned during machining also increases as the WFS/TS is increased. This is significant in the W of the wall (see Figure 7.20). However, the amount of materials that will be removed from the height of the wall is not so significant, even with an increase in the WFS/TS ratio because of the cross sectional area (see Figure 7.21).

The WFS/TS is the utmost important parameter responsible for determination of the W and H, predominantly at low WFS. On the other hand, this does not translate to less material being removed during machining. When varying the

WFS/TS, there was a large difference in the H (see Figure 7-22) and W (see Figure 7-19) of the deposited wall samples.

In order to achieve a desired wall deposition with a mind-set of an EWW, it is imperative to deposit a wall W of greater than the width required in order to be able to machine it. The key to this is the control of the WAAM deposition parameter in order to achieve the required EWW, as any significant deviation from the shape and profile of the deposited wall may be considered as an inefficiency in the process and this will increase the material removal and wastage, which would contribute to unnecessary costs.

7.3 Distortions in machining of WAAM wall structure

Distortion of materials is one of the foremost issues associated with the welding process. Contraction during the cooling of materials after deposition causes a tensile residual stress, predominantly in the longitudinal direction [Colegrove et al., 2009]. Any welding process induces changes in the base material and generates unwanted stress and deformation due to heat input. These stresses remain in the material after welding deposition and result in an unwanted distortion. To counterbalance some of these stresses triggered by the welding process, the structure deforms, creating distortion. Loss of dimensional control with structural integrity and an upsurge of fabrication costs owing to poor fit-up between manufacture parts are both consequences of distortion. This has a huge effect when machining a deformed WAAM thin wall, especially when dealing in microns as against the welding world, which is usually in 0.1mm scale. Although thick-deposited walls also deform, it is much more crucial with thin WAAM walls because less materials could be machined away from it.

The study is aimed at reviewing the effects of distortion in machining of WAAM wall structures. Building WAAM parts requires a supporting structure; i.e. base plate, which might be removed after depositing the necessary part. This study intends to analyse the effect of removing this base plate in the form of distortion on the WAAM wall build-up. The result is intended to give an idea of distortion in the sample, which, if not accounted for, might affect the effective wall width of the

sample. It also gives the best method to cut off the base plate before or after machining to be able to get a reasonable and accurate result in the subsequent wall width.

In the actual sense, effective wall width is the material that will be left after machining both surfaces of the deposited walls. It is the final product after machining and understanding the capabilities and limitations of distortion is critical to the control of deposition of materials during welding. Hence, knowledge of weld deposition distortion is critical in order to improve the wasted quality of additive layer manufactured structures.

7.3.1 Material

In conducting this experiment, the pre-set conditions used in conducting the experiment are shown in Table 7-6.

Table 7-6:Pre-experiment conditions

Power source	Shielding gas	Flow rate (l min^{-1})	Program mode	CTWD (mm)	WD (mm)	Effic (ɳ)
Lincoln power wave 455/STT	Ar/CO_2 (20%)	16	Mode 40	13	1.2	0.8

In order to obtain an insight into the effects of distortion, two sets of WAAM square samples (see Figure 7.23) were deposited using the integrated SAM Edgetek machine using the conditions in Table 7-6.

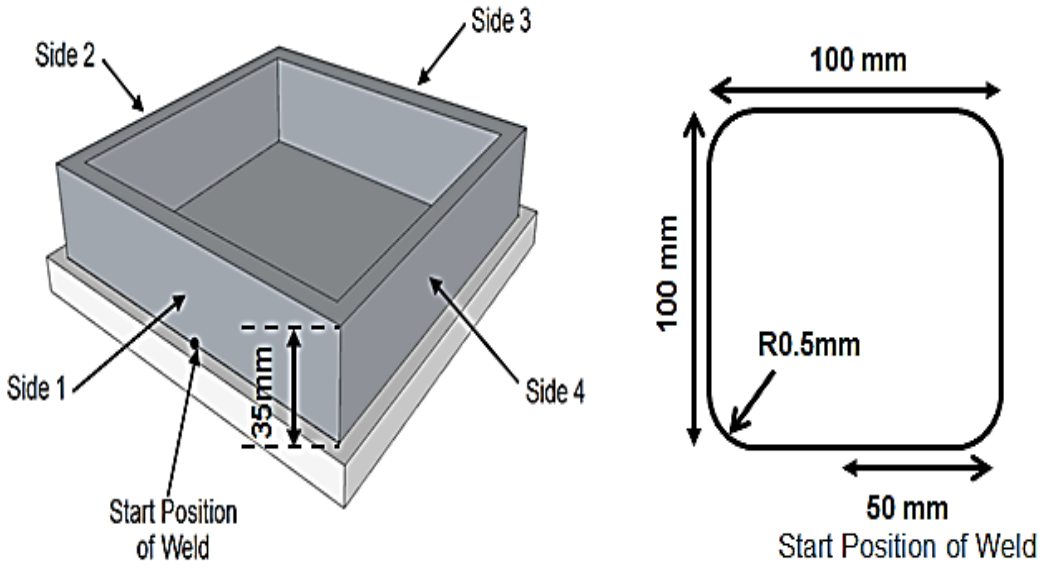

Figure 7-23: The Nominal WAAM CAD model and centreline tool path for the square sample

7.3.2 Methodology

The welding parameters used in the deposition are shown below in Tables 7-8 and 7-9. In the two sets of deposited samples, the WFS was kept constant at 1.2 m/min but the TS was varied. TS was set for 0.2 m/min for the first trial and 0.4 m/min for the second trial.

Table 7-7: Summary WAAM deposition parameters utilised in the trial using TS of 0.2m/min.

Trial no	TS (m/min)	WFS (m/min)	H (mm)	W (mm)	EWW (mm)	V (volt)	I (A)	HI (J/mm)
GEB2	0.2	1.2	34.89	4.94	3.58	18.87	73.01	330.60
GEB4	0.2	1.2	34.22	5.01	3.77	19.56	77.25	362.64
GEB5	0.2	1.2	34.72	4.96	3.56	20.01	78.02	374.68

Table 7-8: Summary WAAM deposition parameters utilised in the trial using TS of 0.3m/min.

Trial no	TS (m/min)	WFS (m/min)	H (mm)	W (mm)	EWW	V (Volt)	I (A)	HI (J/mm)
GE3	0.4	1.2	32.51	4.15	2.67	18.23	73.52	160.83
GE9	0.4	1.2	33.21	4.14	2.57	19.22	75.94	175.15
GE10	0.4	1.2	32.28	4.15	2.32	19.56	74.25	174.28

The variation in the TS was applied in order to manufacture samples with different widths.

A systematic experimental approach was used and this involved two stages. Stage 1 involved deposition of the sample on a base plate (120mm x 120mm x 10mm), measuring the wall perpendicularity on the CMM machine. The base plate was subsequently removed using band saw leaving the manufactured part without the base plate and the wall perpendicularity was measured again in order to see the effects of removing the base plate on the wall structure.

Stage 2 of the experiment also involved the deposition of the square sample on the base plate, measured the perpendicularity of the deposited WAAM wall and subsequently machined the wall surfaces and measured the perpendicularity of the machined wall again. Thereafter, removing the base plate and re-measuring again using the same process as in stage 1. The measurement of the cut samples were carried out immediately after removing the base plate and repeated again after 10 days. This was carried out in order to verify whether there were still stresses in the material, which might be further relieved after removing the base plate.

The measurements were taken on the Coordinate Measurement Machine (CMM) as shown in Figure 7.24. The CMM measures the perpendicularity of the wall by using its probe to take thirty six points on each of the four walls on the outside

and inside of the structure (see Figure 7.24 for illustrations of sides 1, 2, 3 and 4) of the sample and calculate the perpendicularity.

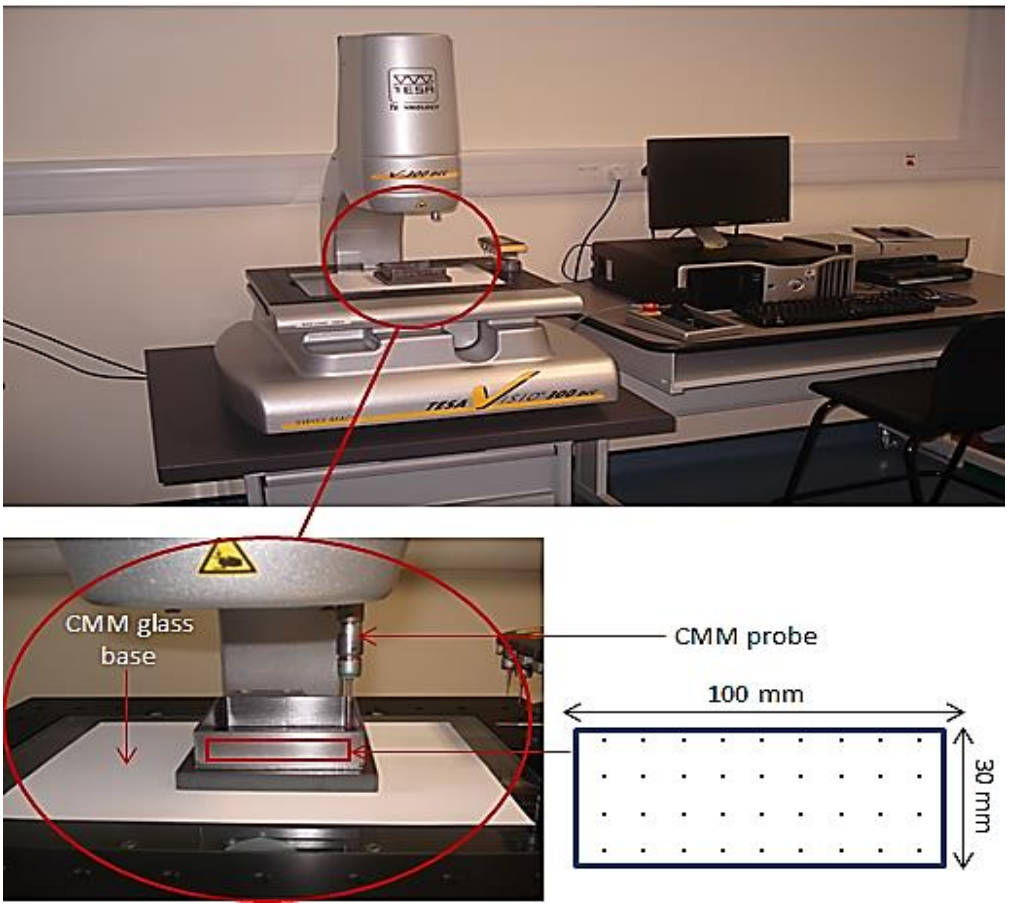

Figure 7-24: CMM machine setup for distortion experiment

After the deposition of the WAAM sample, the width and the height were measured with the aid of both the CMM machine and a digital venire calliper and the results compared. The experiments were repeated five times to improve the overall accuracy of the result.

(a)

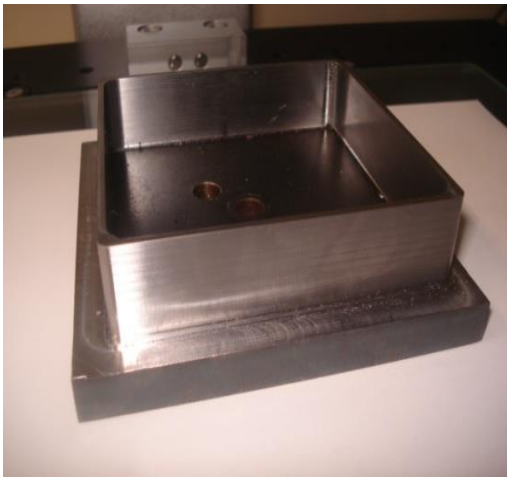

(b) **(c)**

Figure 7-25: Test samples (a) Deposited sample with the base plate without machining (b) Deposited machined sample with the base plate (c) Deposited machined sample without the base plate.

7.3.3 Results

Figure 7-26 shows the result of the trials when the sample was not machined nor was its base plate removed. This is the deposited sample on the base plate (see Figure 7-25a) and this is the level of perpendicularity of the deposited wall prior to removing the base plate and prior to machining. It can be seen from Figure 7-26 that the deposited walls were not actually perpendicular to the base plate, but

the graph shows the actual perpendicularity of each of the four walls deposited which can be compared to when the base plate is removed or the surface of the wall machined.

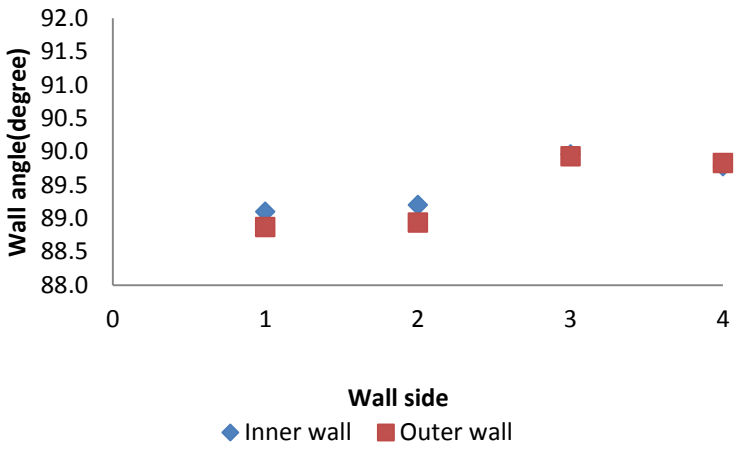

Figure 7-26: Position of the walls of the deposited sample with the base plate (without machining the surface of the sample).

The position of the same sample just after removing the base plate is shown in Figure 7-27. It is, however, noticable that there were changes in the position of the perpendicularity of the sample when compared to the condition shown in Figure 7-26. These changes were noticed, but in the welding point of view, looked so insignificant. However, when considering the machinability of the sample coupled with the consideration of the effective wall, it is important to take this into consideration when building WAAM parts that require machining.

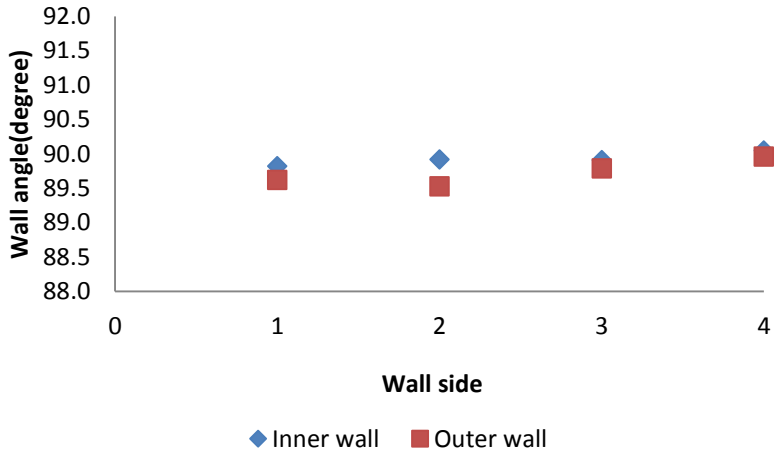

Figure 7-27: Position of the walls of the deposited sample after removing the base plate (without machining the surface of the sample)

Figure 7-28 describes the position of the deposited sample when it is left for 10 days after removing the base plate. The sample did not show any significant changes from what was observed in Figure 7-27. Small changes were, however, noticed in wall side 3 of the sample.

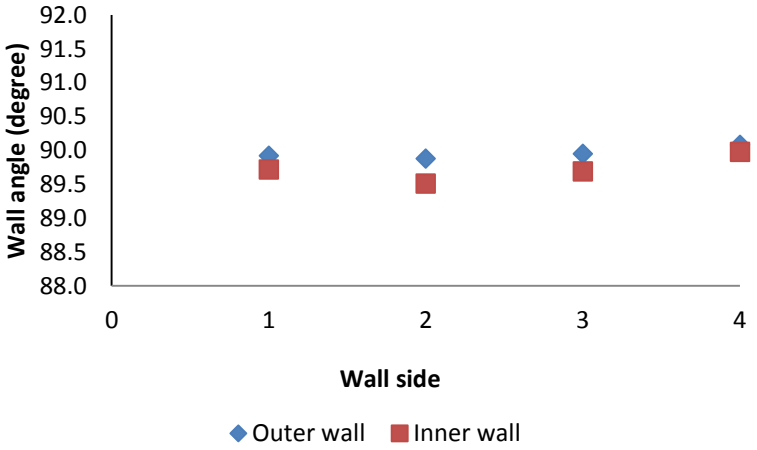

Figure 7-28: Position of the walls of the deposited sample after removing the base plate and left for 10 days (without machining the surface of the sample).

Figure 7-29, Figure 7-30 and Figure 7-31 highlight the position of the sample when the surfaces of the sample were machined. Figure 7-29 shows the position of the sample with the base plate after machining.

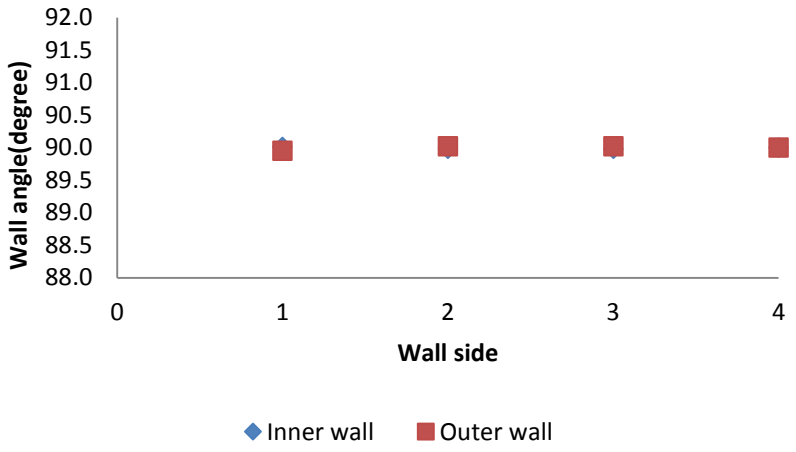

Figure 7-29: Position of the walls of the deposited sample before removing the base plate after machining the surface of the sample.

It can be seen from the graph that the walls of the deposited samples were straight due to the machining of both the inner and the outer surfaces. The base plate of this sample has, however, not been removed.

Moreover, the sample was left for a further 10 days and re-measured again and the result is shown in Figure 7-30. The result shows no indication of further movement or distortion of the wall after 10 days. There were no major differences in the position of the wall as shown earlier in Figure 7-29.

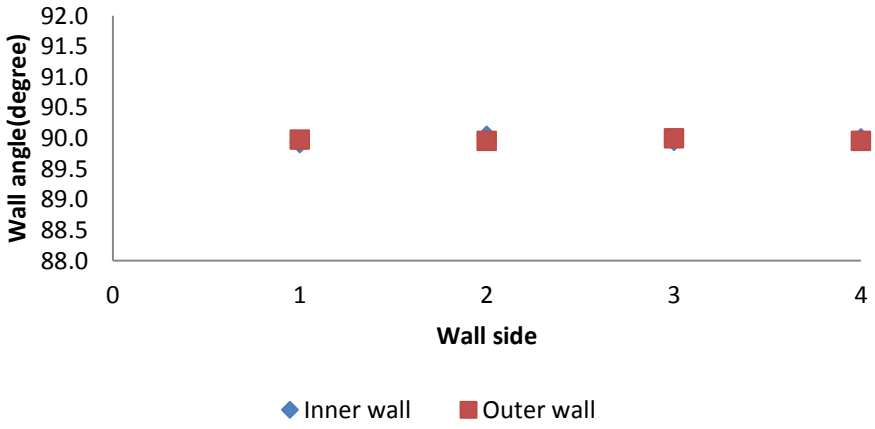

Figure 7-30: Position of the walls of the deposited sample before removing the base plate and re-measuring 10 days after machining the surface of the sample

Figure 7-31 shows the position of the walls of the deposited sample after removing the base plate, after machining the surfaces. The result shows a significant change in the position of the walls. This is an indication of some stresses being relieved in the material after removing the base plate. The same sample was left for 10 days and the sample re-measured; Figure 7-32 shows the result, which indicates that there were no significant changes in the position of the samples.

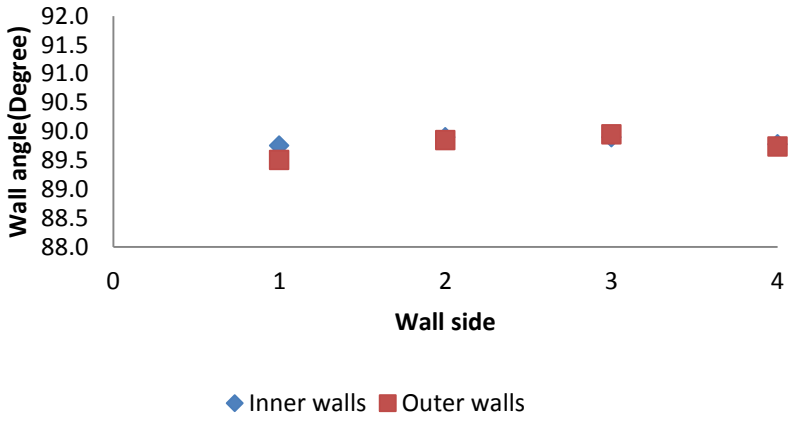

Figure 7-31: Position of the walls of the deposited sample after removing the base plate after machining the surface of the sample.

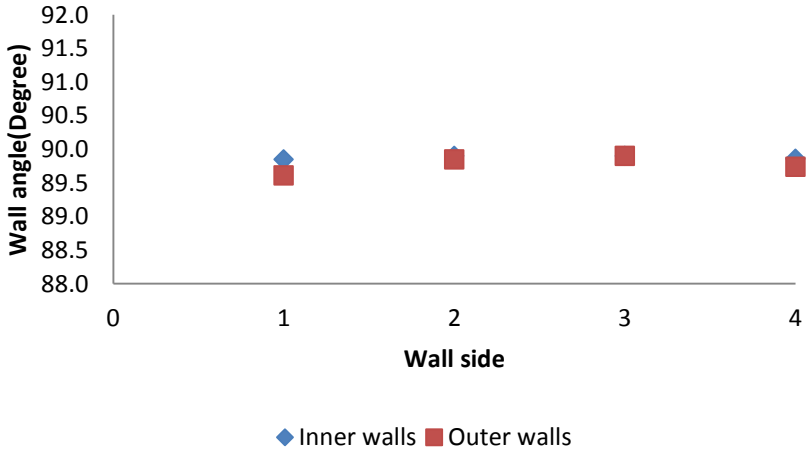

Figure 7-32: Position of the walls of the deposited sample after removing the base plate and re-measured 10 day after machining the surface of the sample

7.3.4 Discussion

A key element to a fully successful application of WAAM is the ability to understand the impact of machining and the usage of a base plate as a support during the manufacture of a WAAM part. This section of the thesis focuses on the effects of removing the base plate on the deposited WAAM samples. This was carried out with the aim of identifying the best way to remove the base plate in order to counter the problem created by stresses induced and other dimensional inaccuracy during the process of base plate removal or machining.

The result of this study shows that the stresses on the deposited walls were relieved during the process of removing the base plate, which led to the wall being moved away from its original position. However, there was no further distortion of the wall when left for 10 days after removing the base plate.

The distortion in the wall can be attributed to some of the stresses being relieved, which is due to the non-uniform shrinkage over structural thickness that produced the angular distortion due to the welding temperature distribution, as the built in stress could not be relieved. The process of cutting the base plates could also have contributed to the redistribution of the stresses in the wall. Leggatt (2008) noted that the residual stresses may have been affected by operations other than welding occurring during material manufacture, or service life. There may be no record of some of these operations, even for components with demanding quality control requirements.

The final shape of the wall accounts for useful parts; the aim of any good production process is to reduce the material wastage and improve the buy to fly ratio. The shape of the deposited thin wall affects the effective wall width and, if not properly controlled, could cause huge material wastage. Conclusively, from the result obtained in the above experimental results, it can be seen that removing the base plate shows a significant effect on the wall position and the geometrical accuracy, and once the base plate is removed, the structure remains stable. However, machining deposited structures shows no significant distortion after 10

days due to the residual stress effect and removing the base plate of the machined structure shows a significant effect on the structure.

8 Overall discussion

This thesis investigates some of the common concerns arising from Wire and Arc Additive Manufacturing (WAAM). These issues take into account of the following:

- WAAM platform comparison
- WAAM defects
- Machining of WAAM parts

8.1 Platforms comparison

The first objective of this thesis was to compare the different platforms (namely the SAM Edgetek machine, ABB robot platform, and Friction Stair Welding platforms) used in the integration and deposition of WAAM parts, in order to evaluate the effectiveness and the process capability of each platform.

The results from this study were tailored to offer a general guide to the accuracy and repeatability of the various platforms. Though this process cannot be used to enumerate the differences between the various platforms, a number of conclusions can be drawn from the studies. The superiority of WAAM metal parts can be commonly characterised on various aspects; i.e. achievable range and geometric accuracy, and metallurgical properties of the as-deposited parts (Zhang et al., 2003). The geometric properties are, therefore, strongly characterised by the shape and dimensions of the deposited weld beads. The shape and dimensions of the weld beads are important criteria in determining the range of target widths which can be produced, influencing at the same time the surface finish of the component produced.

The results of this study are presented and discussed in Sections 5.4 and 5.5. It is evident in the results that the performance of the SAM Edgetek machine platform is more pronounced than the other two platforms considered.

Further evidence from the geometrical accuracy of the part produced showed that the parts manufactured from the SAM Edgetek machine are very close and consistent with the targeted specification when compared with other platforms

(see Figures 5.5, 5.6 and 5.7). The perpendicularity results (see Figure 5.118 to Figure 5.23) show the particular suitability of both the SAM Edgetek machine and the ABB Robot. The analysis of the results from the process capability (Cpk) show that the parts from the SAM Edgetek machine were produced to a greater level of accuracy and repeatability than the other platforms. The high accuracy of the SAM Edgetek machine was to be expected, as it has higher degrees of accuracy and repeatability. Integration of this machine with WAAM improves the time used in manufacturing parts with a good surface finish. The ABB Robot, which is widely used in WAAM, produces parts with a good level of accuracy. The Friction Stir Welding machine produces parts with a lower accuracy than the other two platforms and is used to manufacture large parts.

However, all the platforms have shown variations in their performances and it is paramount to consider the level of error generated during the process. This was measured in terms of the error bars and, in general, the errors generated were lowest in the SAM Edgetek machine platform.

Overall, it was found that for the majority of the features, the SAM Edgetek machine and ABB Robot machine platforms provided a higher accuracy than the Friction Stir Welding machine platform. The accuracy of all the platforms was within what would be considered industrially acceptable high accuracy tolerance. For convectional industrial applications, all the platforms can be considered to produce a high accuracy of WAAM deposition. However, the choice of platform depends on the application to be performed, i.e. deposition or machining.

8.2 WAAM defects

8.2.1 Humping

The results of this study indicate the existence of limiting travel speed for humping to occur in WAAM. Some studies have been carried out previously on humping, but all were carried out on bead on plate welds unlike the present study, which was carried out using WAAM. However, economic gains and environmental impact of WAAM solutions over traditional manufacturing technologies for large-

scale manufacture is directly dependent on the processing speed and, therefore, on the deposition rate capability (Sequeira, 2012). The processing speed and the deposition rate can be improved with the increase of the welding torch Travel Speed. Increasing Travel Speed has been hindered with humping which is a weld defect. However, it was noted that as the Travel Speed increases above a critical value, the humping starts to occur and increasing it above this value increases the frequency of humping. Figure 6.2 and Figure 6.3 show the critical travel speed (TS) limit of 0.6m/min above which humping commences irrespective of the electrode wire diameter.

As indicated in the study conducted by Mendez and Eagar (2003), high arc pressure and momentum of the molten metal droplet depressed the surface of the weld pool directly under the arc, generating a gouge weld pool. The molten metal and the previous layer deposit flows in two channels, which surround the welding arc, along with a very thin layer located underneath the arc welding. Directly at the rear of the welding arc, these separated flows come together resulting in a combined stream of molten weld metal. This continues to move in the direction of the tail of the weld pool. The molten metal with the previous deposited layer was displaced away from the front in the direction of the tail of the weld pool, subsequently producing a swelling and thereafter solidifying. This, nevertheless, stops the recirculation of the deposited molten metal headed for the front of the pool as explained in the study conducted by Ding (2011). As a result, the back filling of the front portion did not take place. With reference to what was observed in the welding pool, the deposited molten metal is mainly moving towards the tail of the weld pool through a higher momentum and velocity. The high velocity and the rearward flow of deposited molten metal in the weld pool are consistent with the numerical simulations carried out by Beck et al., (1990).

8.2.2 WAAM wall bead characteristics

This study was carried out to understand the influence of welding parameters; i.e. TS, WFS and WD, on the physical bead geometry characteristics (i.e. bead H

and W in vertical multilayer) and the effects when machining WAAM wall parts. However, the choice of an appropriate combination of deposition parameters is key to improve the features of the WAAM parts produced.

The result of this work provides an insight into the effects of the first three layers of a multilayer deposition of WAAM walls on the effective wall width during machining. In the study, it was established that the weld bead geometrical characteristics such as bead H and bead W are much affected in the deposition of a multi-layer weld when the first three layers are deposited (see Figure 6.11 and Figure 6.12). As stated in the results, the first three layers are constantly narrower in width and higher in height. Subsequently, the width and the height after the third layer become constant. The height reduces whereas the widths grow larger. The overall effect on the machinability of such walls is the significant reduction in the effective wall width as a result of the first three layers. Hence, the first three layers of any multi-weld wall have to be taken into consideration when the machining of such walls is required. The possible reasons attributed to this result are:

1. The heat sink when the material is being deposited on a cool flat surface of the base plate is at a fast rate; i.e. it cools faster in the first three deposited layers due to a large volume of heat sink taking place.
2. The first layer of any multi-layer weld deposition is usually deposited on a flat surface of the base plate while the subsequent deposited layers were on a near curvilinear profile. This contributes to the reason why the first layer of any deposited bead is higher in height.

8.3 Machining

8.3.1 Lubricants in machine and deposition of WAAM parts

As part of the objectives of this study, an investigation was also carried out to understand the sequential deposition and machining with various lubricants; i.e. solid lubricants and convectional liquid lubricant. A thorough knowledge of the effects of a WAAM structure on the surface integrity and the mechanical

properties of WAAM deposited materials are of great importance, especially for the integration process of sequential deposition and machining.

This study examined the use of solid lubricants such as graphite and Molybdenum disulphide, and Minimum Quantity Lubrication in the sequential deposition and machining of WAAM parts and characterises the effects of solid lubricants on the microstructure. The outcomes of this study provide an insight into the use of solid lubricants in sequential machining and deposition of WAAM structures. It also provides beneficial information on using sequential machining and deposition in the machining of WAAM structures with hollow shapes. It was shown from the study that introducing solid lubricants during sequential deposition and machining of WAAM structures could contaminate the microstructure and alter the chemical composition of such material. During the hot deposition of the part, the solid lubricants can dissolve or mix into the welding pool, thereby contaminating the material. However, cleaning of deposited wall samples with acetone during welding was also discovered to have an effect on the microstructure and hardness during sequential deposition of samples. There is an increase in the grain size of the microstructure when cleaned, resulting in a reduction in the material hardness. Nevertheless, the result from the Scanning Electron Microscope analysis was used to determine the presence of traces of foreign elements in the samples due to the cleaning of the samples. The Scanning Electron Microscope analysis shows the existence of contaminating elements in the parent material but absence after the cleaning of the sample.

Furthermore, the FEM temperature modelling of the welding pool shows that solid lubricants could have reacted with molten metal during the sequential deposition and machining. Knowing the temperature distribution and the melting point of the lubricants is important for selecting the appropriate solid lubricant if there is an important need to use solid lubricant.

8.3.2 Effects of distortion of WAAM sample on machining

The main drawback associated with WAAM systems using a high deposition rate is the tolerance loss observed in the as welded near net shape parts (Pedro

2012). The tolerance loss eventually led to poor accuracy during the machining of WAAM thin walls. The aim of this section is to study into the limitation of WAAM base plate during material removal (i.e. milling and grinding) of WAAM structures. The distortion due to the base plate during deposition can lead to a significant reduction in the effective wall width. This is because the large volumes of material will be machined away in order to achieve the required dimensions within the desired tolerances. With this, the quality of the manufactured component is for that reason unfavourably affected as a result of a more limited control over the base plate.

The result of this study indicated that removing base plate has an effect on the wall position and this has a significant effect of the Effective Wall width obtained during machining. However, the position of the wall sample shows no desirable effect when machined with the base plate. The cause of the changes in the wall width can be attributed to the stress being relieved from the walls when the base plate has been removed.

As identified in Section 5.5.1.3, the shape of the deposited walls can be either type A or B (see Figure 5.33). Either of the shapes reduce the Effective Wall Width and eventually led to material wastage. In order to avoid this type of wall shape, the study recommended machining the wall surfaces (if need be) before removing the base plate. This will give room to attain a better Effective Wall Width. Moreover, with the mind-set of the Effective Wall Width, it is paramount to build walls of greater than the width required to be able to machine, but this will result in material wastage.

LEFT BLANK INTENTIONALLY

9 Conclusions

This research was conducted to contribute to the knowledge of the manufacturing and machining of Wire and Arc Additive Manufactured (WAAM) structures on an integrated WAAM on integrated WAAM platforms. In the following, the most significant contributions shall be highlighted:

9.1 Machine comparison

The comparison results are for the criteria chosen but are not exhaustive. Different results might have been obtained if different performance criteria had been chosen. However, in industrial environments the comparison will valid for the set of components and allow decisions to be made according to which type of machine was proved most suitable. The studies on the machine comparison show that:

- There is a variation in the width of the test sample obtained in the SAM Edgetek machine platform compared to the ABB robot and friction stir welding machine platforms. This is due to the difference in accuracy of each machine and this has affected the width of the sample produced.
- The SAM Edgetek machine platform is able to manufacture the test sample to the specification in terms of the height obtained, whereas test samples manufactured on the ABB robot platform and the friction stir welding machine platform were below the target specification. The SAM Edgetek machine is more precise than the other machines due to its linear path accuracy.
- The test samples produced from the SAM Edgetek machine platform satisfy the geometrical perpendicularity of the parts to a higher degree than other platforms.
- The weld bead surface qualities are significantly influenced by the different platforms. The SAM Edgetek machine platform has shown to be superior when considering the surface profile.

- Cpk analysis showed that the SAM Edgetek platform is a more capable process in manufacturing WAAM wall parts than the ABB robot platform and the friction stir welding machine platform.
- WAAM, despite of some issues pointed out, is indeed a quite robustly transferable technique, which allows industry to apply it on a variety of very different platforms without sacrificing quality too much. The thesis has highlighted some pros and cons of the different platforms and at what to look first when implementing a WAAM process on a similar platform.

9.2 Deposition

By investigating the deposition of WAAM parts, the following are considered the output of the study:

- Investigation of the humping process in WAAM has shown the existence of a limiting speed of 0.6m/min at which humping starts to take place. As the travel speed increases above this limit, the formation of this discontinous weld bead defect starts to worsen, until the process cannot be continued. This humping can also be attributed to the activities taking place along the flow channel of the deposited molten metal.
- For a constant WFS and TS, there is a significant difference in the first layer of the entire wall built up when comparing to the subsequent ones. This first layer is constantly narrower in width and greater in height. The ratio of height/width is very significant, unlike the other layers which tend towards a constant. This is influenced by the fact that the first layer was deposited on a flat and cold surface of a base plate but width and height profiles change to a quasi-steady state condition after the first and second layers.

9.3 Machining process

The summary of the main conclusion from the machining process of WAAM is as shown:

- In WAAM process, removing the base plate can have a significant effect on the stresses induced into the deposited wall and this also alters the physical geometries of the wall structure, and the effects on the machining of thin walls can be desirable. It was discovered that it is always better to remove the base plate prior to machining in order to have a less desirable effect on wall straightness.
- It was discovered that the deposited WAAM wall can be in four different shapes apart from being straight and each of these shapes has a significant effect on the machinability of WAAM wall.
- Deposition parameters is the key to the control of the effective wall width in machining of WAAM walls in order to achieve the required EWW, as any significant deviation from the shape and profile of the deposited wall will result in an increase in the material removal and wastage, and thereby contributing unnecessary costs.
- The major problem associated with machining of WAAM structures is the inability to machine parts with hollow shapes. A sequential process of both welding deposition and machining was introduced with an integrated system in which the structure was built in a sequential manner which entails machining after some layers of deposition and this process continues until the final part of the structure is machined.
- Study into the interaction between sequential weld deposit of WAAM and machining process using a solid lubricant was investigated. The result showed that the microstructures of samples were contaminated with the introduction of a solid lubricant.
- Cleaning of a deposited wall sample with acetone during welding was discovered to have an effect on the microstructure and hardness during sequential deposition of samples. There is an increase in the grain size of the microstructure when cleaned. Hence, this reduces the material hardness.

- Machining of WAAM parts Minimum Quantity Lubrication demonstrated to have a less significant effect on the microstructure and hardness of the WAAM parts.

9.4 Recommended future work

This research can be further extended into the following research directions:

- This study has been conducted on mild steel (because of its usefulness in automobile and construction industries) using WAAM, but a further study could be conducted using various engineering materials such as titanium and aluminium, because of their wide use in the aircraft industry. Different materials behave differently under the same conditions and it would be useful to conduct the same experiment using the commonly used industrial materials.
- The deposition can be further extended to include hot machining of samples using both sequential and non-sequential machining /additive manufacturing, investigating the mechanical property of the sample made from hot sequentially and non-sequential WAAM and a comparison can be made with the sample manufactured from cold sequential and non-sequential method. Different kinds of lubricants (i.e. Minimum Quantity Lubrication and solid lubricants) could also be applied during machining.

REFERENCES

Almeida-Sequeira, P. M, and Williams, S. (2010), Innovative process model of Ti-6Al-4V additive layer manufacturing using Cold Metal Transfer (CMT). In: Proceedings of the 21st Annual International Solid Freeform Fabrication Symposium, University of Texas at Austin, TX, USA, August 9-11, 2010, pp. 25-36.

App, R. L., Gourd L.M and Lelson K.A (1963), Effect of welding variables upon bead shape and size in submerged-arc welding, Welding and Metal Fabrication, vol. 31, no. 11, pp. 453-457.

Bart, J. (1999), Lubricants and the Environment, Tribology International, vol.3, no1-3, pp. 35-47.

Battersby, N. (2004), Base Fluids for Environmentally Acceptable Lubricants-What Does Biodegradable Really Mean? 14th International Colloquium Tribology, 13th-15th January 2004. Ostfildern, Germany, pp.735 - 742.

Baufeld, B. and Van Der Biest, O. (2009), Mechanical properties of Ti-6Al-4V specimens produced by shaped metal deposition. Science and Technology of Advanced Materials, vol.10, no.1, pp. 10-14.

Baufeld, B., Biest, O. V. D. and Gault, R. (2010), Additive manufacturing of Ti-6Al-4V components by shaped metal deposition: Microstructure and mechanical properties. Materials and Design, vol. 31, no. 1, pp. S106-S111.

Beck, M., Berger, P., Dausinger, F. and Hugel, H. (1990), Gas flow and chemical lasers. Proceedings of the 8th international symposium, International Society for Optical Engineering, Madrid, pp.769 - 774.

Bradstreet, B.J. (1968), Effects of surface tension and metal flow on bead formation, Welding Journal, vol. 47, no 7, pp. s314 - s322.

Bradstreet, B.J. (1969), Effect of welding conditions on cooling rate and hardness in the heat-affected zone, Welding Journal, vol. 48, no. 11, pp. 499s - 504s.

Brinksmeier, E. and Brockhoff, T. (1997), Minimum Quantity Lubrication in Grinding, 2nd International Machining and Grinding Conference Dearborn, MI, Society of Manufacturing Engineers, Dearborn, Michigan, vol.2, no MR97-230, pp. 1 - 14.

Byrne, G., Dornfeld, D. and Denkena, B. (2003), Advancing Cutting Technology, CIRP Annals - Manufacturing Technology, vol. 52, no. 2, pp. 483 - 507.

Byrne, G. and Scholta, E. (1993), Environmentally Clean Machining Processes — A Strategic Approach, CIRP Annals - Manufacturing Technology, vol. 42, no. 1, pp. 471 - 474.

Cao, Y., Zhu, S., Wang, T. and Wang, W. (2009), Modelling of welded bead profile for rapid prototyping by robotic MAG welding, China Welding (English Edition), vol. 18, no. 1, pp. 18 - 22.

Carry, B. (2002), Modern welding technology, 5th edition, Prentice Hall Canada, Toronto, pp. 477.

Chen, K. S., Huang, M. L. and Li, R. K. (2001), Process capability analysis for an entire product, International Journal of Production Research, vol. 39, no. 17, pp. 4077 - 4087.

Chen, Y. H., and Song, Y. (2001), Development of a layer based machining system, CAD Computer Aided Design, vol. 33, no. 4, pp. 331 - 342.

Cho, M.H. and Farson D.F. (2007), Understanding bead hump formation in gas metal arc welding using a numerical simulation, Metallurgical and Materials Transactions B: Process metallurgical and material processing science, vol. 38, no 2, pp. 305 - 319.

Choi, J. and Chang, Y. (2005), Characteristics of laser aided direct metal/material deposition process for tool steel, International Journal of Machine Tools and Manufacture, vol. 45, no. 4-5, pp. 597 - 607.

Cobb, R.C, Spenser, J.D. and Dicken, P.M (1993), Better surface finishing techniques is a must, Proceedings of the second Scandinavian Rapid Prototyping Conference, 4th – 6th october, 1993, Danish Technological institute, Aarhus, Denmark, pp. 34-37.

Colegrove, P., Ikeagu, C., Thistlethwaite, A., Williams, S., Nagy, T., Suder, W., Steuwer, A. and Pirling, T. (2009), Welding process impact on residual stress and distortion, Science and Technology of Welding and Joining, vol. 14, no. 8, pp. 717 - 725.

Comley, P, Walton, I., Jin, T., and Stephenson, D.J. (2006), A High Material Removal Rate Grinding Process for the Production of Automotive Crankshafts, CIRP Annals-Manufacturing Technology, vol. 55, no.1 pp.456 – 460.

Comley, P., (2005), Grinding processes and their effects on surface integrity PhD thesis, Cranfield University, Cranfield.

Deleryd, M. (1999), A pragmatic view on process capability studies, International Journal of Production Economics, vol. 58, no. 3, pp. 319 - 330.

Dickens, P. M., Pridham, M. S., Cobb, R. C., Gibson, I. (1992), 3-D Welding, in: Proceedings of the First European Conference on Rapid Prototyping, 6-7th July, University of Nottingham, England, pp. 81 - 93.

Ding. J (2012), Thermo-mechanical Analysis of Wire and Arc Additive Manufacturing Process, PhD thesis, Cranfield University, Cranfield

Ding, J., Colegrove, P., Mehnen, J., Ganguly, S., Sequeira Almeida, P. M., Wang, F. and Williams, S. (2011), Thermo-mechanical analysis of Wire and Arc Additive Layer Manufacturing process on large multi-layer parts, Computational Materials Science, vol. 50, no. 12, pp. 3315 - 3322.

Ezugwu, E. O. (2005), Key improvements in the machining of difficult-to-cut aerospace super alloys, International Journal of Machine Tools and Manufacture, vol. 45, no. 12, pp. 1353 - 1367.

Farad, K. and Mehdi, H. (2011), A new approach for predicting and optimising weld bead geometries in GWAN, International Journal of Aerospace and Mechanical Engineering, vol. 5, no 2. pp 56 - 62

Farr, J. P. G. (1975), Molybdenum disulphide in lubrication, A review, Wear Journal, vol. 35, no. 1, pp. 1 - 22.

Field, M. and Kahles, J.F. (1964), The surface integrity of machined and ground high strength steel, DMIC report, pp. 54 - 77.

Fuchs Lubricants (UK) Plc. (2007), Ecocool Ultra life; New water-soluble coolant technology. http://www.fuchslubricants.com/, accessed on the 12th January, 2012.

Geldart, M., Webb, P., Larsson, H., Backstrom, N., Gindy, N., and Rask, K. (2003), A direct comparison of the machining performance of a variax 5 axis parallel kinetic machining centre with convectional 3 and 5 axis machine tools, International Journal of Machine Tools & Manufacture, Vol 43, no 3, pp.1107 - 1116.

Gratzket, U., Kapadiat, P., Dowdent, J., Simon, J. and Krooss, G., (1992), Theoritical approach of the humping phenomenum in welding processes. Journal of Physic D: Applied Physics., vol 25, no 2, pp.1640 - 1647.

Griffith, M. L., Ensz, M. T., Puskar, J. D., Robino, C. V. et al. (2001), Understanding the microstructure and properties of components fabricated

by Laser Engineered Net Shaping (LENS), Proceedings of Materials Research Society Symposium, Vol.625, San Francisco, CA, pp. 9-20.

Gunter, K. L. and Sutherland, J.W. (1999), An Experimental Investigation into the Effect of Process Conditions on the Mass Concentration of Cutting Fluid Mist in Turning, Journal of Cleaner Production, vol. 7, no 4, pp 341 - 350.

Gurev H. S. and Stout, R. D (1963), Solidification phenomena in inert-gas metal arc welding. Welding Journal, vol. 42, no. 7, pp. 298s - 310s.

Gray, P.,Bedi, S., Ismail, F.,Rao, N., and Morphy, G., (2001), Comparison of 5 axis and 3 axis finish machining of hydro forming die insert. International Journal of Advanced Manufacturing Technology, vol 17, no 2, pp. 562 - 568.

Hassold, R. (1995), CNC machining as a rapid prototyping technique, Modern Machine Shop, vol. 68, no. 5, pp. 68 - 73.

Hobart Institute of Welding Technology, (1997), What is ailing that weld?. Welding Journal, vol. 76, no. 8, pp.45 - 48.

Hope, R. L., Jacobs, P. A. and Roth, R. N. (1997), Rapid prototyping with sloping surfaces, Rapid Prototyping Journal, vol. 3, no. 1, pp. 12 - 19.

Howes, T. D., Tönshoff, H. K., Heuer, W. and Howes, T. (1991), Environmental Aspects of Grinding Fluids, CIRP Annals - Manufacturing Technology, vol. 40, no. 2, pp. 623 - 630.

Juran, J.M. (1974), Juran's quality control handbook. 3rd edition, McGraw-Hill, New York.

Kane, V. E. (1986), Process capability indices, Journal of Quality Technology, Vol. 18, no 1, pp. 41 - 52.

Karunakaran, K. P., Suryakumar, S., Pushpa, V. and Akula, S. (2010), Low cost integration of additive and subtractive processes for hybrid layered manufacturing, Robotics and Computer-Integrated Manufacturing, vol. 26, no. 5, pp.67 - 77.

Kelly, S. M. and Kamper, S. L. (2004), Microstructural evolution in laser-deposited multilayer Ti-6Al-4V builds: Part 1. Microstructural characterization, Metallurgical and Materials Transactions A: Physical Metallurgy and Materials Science, vol.35 no.6, p. 1861 - 1867.

Kim, Y. S., Son, J., Kim, I. J., Kim, J. Y. and Kim, O. S. (2003), A study on relationship between process variable and bead penetration for robotic

carbon dioxide arc welding. Journal of Materials Processing Technology, vol. 136, no. 1, pp. 139 - 145.

Klocke, F. and Eisenblätter, G. (1997), Dry Cutting, CIRP Annals - Manufacturing Technology, vol. 46, no. 2, pp. 519 - 526.

Kobryn, P. A. and Semiatin, S. L. (2000), The laser additive manufacture of Ti-6Al-4V, Journal of the Minerals, Metals and Materials Society, vol. 53, no 9, pp. 40 - 42.

Koc, T. (2007), The impact of ISO 9000 quality management systems on manufacturing, Journal of Materials Processing Technology, vol. 186, no. 1-3, pp. 207 - 213.

Koren, Y., Heisel, U., Jovane, F., Moriwaki, T. et al. (1999), Reconfigurable manufacturing systems, CIRP Annals - Manufacturing Technology, vol. 48, no 2, pp. 527 - 540.

Krishna, P.V., Srikant, R.R. and Nageswara R.(2011), Solid lubricants in machining, Proceedings of the Institution of Mechanical Engineers, Part J: Journal of Engineering Tribology, vol. 225, no. 5, pp. PG213 - 227.

Kruth, J. Leu, M. C. and Nakagawa, T. (1998), Progress in Additive Manufacturing and Rapid Prototyping, CIRP Annals - Manufacturing Technology, vol. 47, no. 2, pp. 525 - 540.

Kulkarni, P. and Dutta, D. (2000), On the integration of layered manufacturing and material removal processes, Journal of Manufacturing Science and Engineering, Transactions of the ASME, vol. 122, no. 1, pp. 100 - 108.

Leggatt, R.H (2008), Residual stresses in welded structures, International Journal of Pressure Vessels and Piping, vol. 85, no. 3, pp. 144 - 151.

Levy, G. N., Schindel, R. and Kruth, J. P. (2003), Rapid manufacturing and rapid tooling with layer manufacturing (LM) technologies, state of the art and future perspectives, CIRP Annals - Manufacturing Technology, vol. 52, no. 2, pp. 589 - 609.

Li, K. and Liang, S. Y. (2006), Modelling of cutting temperature in near dry machining, Journal of Manufacturing Science and Engineering, Transactions of the ASME, vol. 128, no. 2, pp. 416 - 424.

Liu, M. Y.,Shi, B.,Wang, C., Ji, S. K., Cai, X. and Song,H. W.,(2003), Normal hall-petch behaviour of mild steel with submicron grains. Materials letter, Vol. 57, no. 19, pp. 2798 - 2802.

Lorant, E. (2010), Effect of microstructure on mechanical properties of Ti-6Al-4V structures made by Additive Layer Manufacturing , Phd thesis, Cranfield University, Cranfield.

Lucas, B., Verhaeghe, G. and Leggatt, R.,(1998), Job knowledge for welders 33: Distortion - types and causes (TWI, available from: http://www.twi.co.uk/content/jk33.html, accessed 4th February 2012.

Malkin, S. and Guo, C. (2007), Thermal Analysis of Grinding, CIRP Annals - Manufacturing Technology, vol. 56, no. 2, pp. 760 - 782.

Massam, M. (2008), Thermal characteristics of grinding fluids, PhD thesis, Cranfield University.Cranfield.

Mathers, G. (2002), The welding of aluminium and its alloys, First Edition, CRC Press, England.

McBrearty, K. (2005), Visibility analysis and consideration for computer numerical controlled rapid prototyping, PhD thesis, Pennsylvania State University, Pennsylvania.

Mendez, P and Eagar T., (2000), Humping formation in high current GTA welding. International conference on joining of advanced and specialty materials II. Cincinnati, OH, USA, pp22 - 30.

Mendez, P and Eagar T., (2003), Penetration and defect formation in high-current arc welding. Welding journal, vol. 82, no. 10, pp.296s - 306s.

Morris, T. (2011), Abrasive Machining with MQSL, PhD thesis, Cranfield University, Cranfield, Cranfield.

Nagesh, D. S. and Datta, G. L. (2002), Prediction of weld bead geometry and penetration in shielded metal-arc welding using artificial neural networks, Journal of Materials Processing Technology, vol. 123, no. 2, pp. 303 - 312.

Nageswara, R. D. and Vamsi, K. P. (2008), The influence of solid lubricant particle size on machining parameters in turning, International Journal of Machine Tools and Manufacture, vol. 48, no. 1, pp. 107 - 111.

Nguyen, T. C., Weckman, D. C., Johnson, D. A., and Kerr, H. W. (2005), The humping phenomenon during high-speed gas metal arc welding, Science and Technology of Welding and Joining, vol. 10, no. 4, pp. 447 - 459.

Ohashi, R., Fujimoto, M., Mironov, S., Sato, Y. S., and Kokawa, H. (2006), Effect of contamination on microstructure in friction stir welded DP590 steel.

Science and Technology of Welding and Joining, vol. 14, no. 3, pp. 221 - 227.

Oshima, K., Xiang, X and Yamane S. (2004), Effects of power source characteristic on carbon dioxide short circuiting arc welding. Science and Technology of Welding and Joining, vol. 13, no. 3, pp. 345 - 352.

Paul, S. and Chattopadhyay, A.B. (1995), A Study of Effect of Cryogenic-Cooling in Grinding, International Journal of Machine Tools and Manufacture, vol. 35, No.1, pp.109 - 117.

Pearn, W. L. (1997), Multiprocess performance analysis: a case study, Quality Engineering, vol. 10, no. 1, pp. 1-8.

Radhakrishnan, V. and Shaji, S. (2005), Elimination of cutting fluids in grinding: An investigation on the application of solid lubricants, Transactions of the North American Manufacturing Research Institute of SME, vol. 33, pp. 359 - 368.

Rajkumar, S., Muralidharan, C. and Balasubramanian, V. (2011), Influence of friction stir welding process and tool parameters on strength properties of AA7075-T_6 aluminium alloy joints, Materials and Design, vol. 32, no. 2, pp. 535 - 549.

Rao, N. D. and Krishna, V.P. (2006), The influence of solid lubricant particle size on machining parameters in turning, International Journal of Machine Tools and Manufacture, vol. 48, no. 1, pp. 107-111.

Rombouts, M., Kruth, J. P., Froyen, L. and Mercelis, P. (2006), Fundamentals of Selective Laser Melting of alloyed steel powders, CIRP Annals - Manufacturing Technology, vol. 55, no. 1, pp. 187 - 192.

Salmond, S.C (2000), Customise your Grinding Fluids, Manufacturing Engineering, vol. 124, no. 2, pp. 42 - 49.

Santos, E. C., Shiomi, M., Osakada, K. and Laoui, T. (2006), Rapid manufacturing of metal components by laser forming, International Journal of Machine Tools and Manufacture, vol. 46, no. 12-13, pp. 1459 - 1468.

Savage, W. F., Nippes, E. F. and Agusa, K. (1979), Effect of arc force on defect formation in GTA welding, Welding Journal, vol. 59, no. 7, pp. 212.

Savvatimskiy, A. I. (2005), Measurements of the melting point of graphite and the properties of liquid carbon (a review for 1963–2003), Carbon, vol. 43, no. 6, pp. 1115 - 1142.

Sequeira Almeida, P.M (2012), Process Control and Development in Wire and Arc Additive Manufacturing, PhD thesis, Cranfield University, Cranfield.

Shaji, S. and Radhakrishnan, V. (2002), Investigations on the application of solid lubricants in grinding, Proceedings of the Institution of Mechanical Engineers, Part B: Journal of Engineering Manufacture, vol. 216, no. 10, pp. 1325 - 1343.

Shaji, S. and Radhakrishnan, V. (2003), Application of solid lubricants in grinding: Investigations on graphite sandwiched grinding wheels, Machining Science and Technology, vol. 7, no. 1, pp. 137 - 155.

Shaw, M. C. (1996), Metal cutting principles, first edition, Oxford, Clarendon Press, New York.

Shewhart, W.A. (1980), Economic control of quality of manufactured product, Van Nostrand, New York. Republished in 1980, as a 50th Anniversary Commemorative Reissue by American Society for Quality Control, Milwaukee, WI. BookCrafters, Inc., Chelsea, MI, 1931.

Shumovsky, A. (1952), Controlling weld shrinkage and distortion, The Canadian Welder, vol. 6, no. 4, pp. 179 - 182.

Soderstrom, E. and Mendez, P. (2006), Humping mechanisms present in high speed welding, Science and Technology of Welding and Joining, vol. 11, no. 5, pp. 572 - 579.

Song, Y and Chen, Y. H (2001), Feature-based robot machining for prototyping. Proceedings of Institute of Mechanical Engineers - Part B, vol. 213, no. 3, pp. 451-459.

Sreejith, P. S. and Ngoi, B. K. A. (2000), Dry machining: Machining of the future, Journal of Materials Processing Technology, vol. 101, no. 1-3, pp. 287 - 291.

Suban, M. and Tusek J., (2002), Dependence of melting rate in MIG/MAG welding on the type of shielding gas used. Journal of Materials Processing Technology, vol. 119, no. 1, pp.185 - 192.

Suresh, R. K. N. and Venkateswara,, R. P. (2006), Experimental investigation to study the effect of solid lubricants on cutting forces and surface quality in end milling, International Journal of Machine Tools and Manufacture, vol. 46, no. 2, pp. 189 - 198.

Suresh R. K. N., Nouari, M. and Yang, M. (2010), Development of electrostatic solid lubrication system for improvement in machining process performance,

International Journal of Machine Tools and Manufacture, vol. 50, no. 9, pp. 789 - 797.

Sutherland, J.W. and Kulur, V.N. (2000), An Experimental Investigation of Air Quality in Wet and Dry Turning, CIRP Annals – Manufacturing Technology,, vol.49, No 1, pp. 61 - 64.

Syed, W. U. H., Pinkerton, A. J. and Li, L. (2005), A comparative study of wire feeding and powder feeding in direct diode laser deposition for rapid prototyping, Applied Surface Science, vol. 247, no. 1-4, pp. 268 - 276.

Tangelder, J.W.H. and Vergeest, J.S.M. (1994), Robust NC path generation for rapid shape prototyping, Journal of Design and Manufacturing, vol. 4, no. 4, pp. 281 - 292.

Teer, D. G.,Renevier, N. M., Hamphire, J., Fox, V. C., Witts, J., and Allen, T. (2001), Advantages of using self-lubricating, hard, wear-resistant MoS_2-based coatings, Surface and Coatings Technology, vol. 142–144, no. 10, pp. 67 - 77.

Thomas, A.W. (2005), Parameters development for MIG welding of high strength aerospace aluminium alloy, Ph.D. thesis, Cranfield University, Cranfield.

Venugopal, A.Q. and Rao, P.V (2004), Performance improvement of grinding of SiC using graphite as a solid lubricant, Materials and Manufacturing Processes, vol. 19, no. 2, pp. 177 - 186.

Wall, M. B., Ulrich, K. T. and Flowers, W. C. (1992), Evaluating prototyping technologies for product design, Research in Engineering Design, vol. 3, no. 3, pp. 163 - 177.

Wang, Z. Y. and Rajurkar, K. P. (2000), Cryogenic machining of hard-to-cut materials, Wear, vol. 239, no. 2, pp. 168 - 175.

Weinert, K., Inasaki, I., Sutherland, J. W. and Wakabayashi, T. (2004), Dry Machining and Minimum Quantity Lubrication, CIRP Annals - Manufacturing Technology, vol. 53, no. 2, pp. 511 - 537.

Williams, J. (2005), Engineering tribology, Cambridge University Press, Cambridge.

Williams, R. E. and Melton, V. L. (1998), Abrasive flow finishing of stereo lithography prototypes, Rapid Prototyping Journal, vol. 4, no. 2, pp. 56 - 67.

Wohlers, T. (2010), Additive manufacturing state of the industry, in Wohlers associates, USA. , available from: http://www.wohlersassociates.com/technical-articles, accessed 20th February 2013.

Yang, Z. Y., Chen, Y. H. and Sze, W. S. (2002a), Determining build orientation for layer-based machining, International Journal of Advanced Manufacturing Technology, vol. 18, no. 5, pp. 313 - 322.

Yang, Z. Y., Chen, Y. H. and Sze, W. S. (2002b), Layer-based machining: Recent development and support structure design, Proceedings of the Institution of Mechanical Engineers, Part B: Journal of Engineering Manufacture, vol. 216, no. 7, pp. 979 - 991.

Zhang, Y., Chen, Y., Li, P. and Male, A. T. (2003), Weld deposition-based rapid prototyping: A preliminary study, Journal of Materials Processing Technology, vol. 135, no. 2, pp. 347-357.

Appendices

Appendix A – Process capability analysis chart

Appendix B – Humping data

Appendix C – WAAM part manufacturing

Appendix D – Machine specifications

LEFT BLANK INTENTIONALLY

Appendix A - Process Capability Analysis Charts

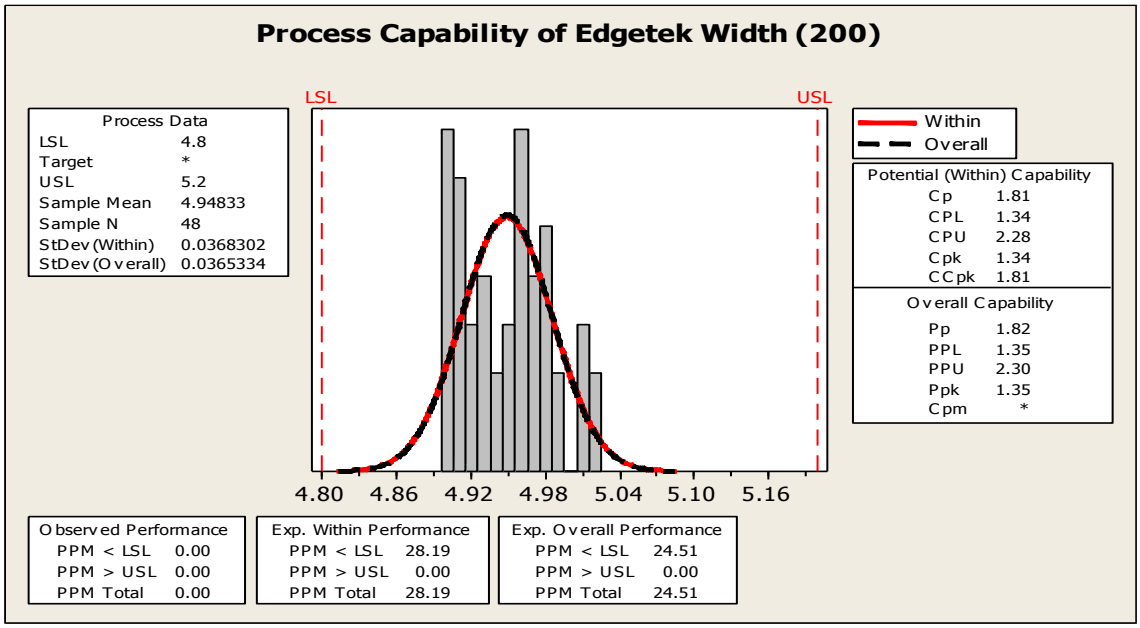

(a)

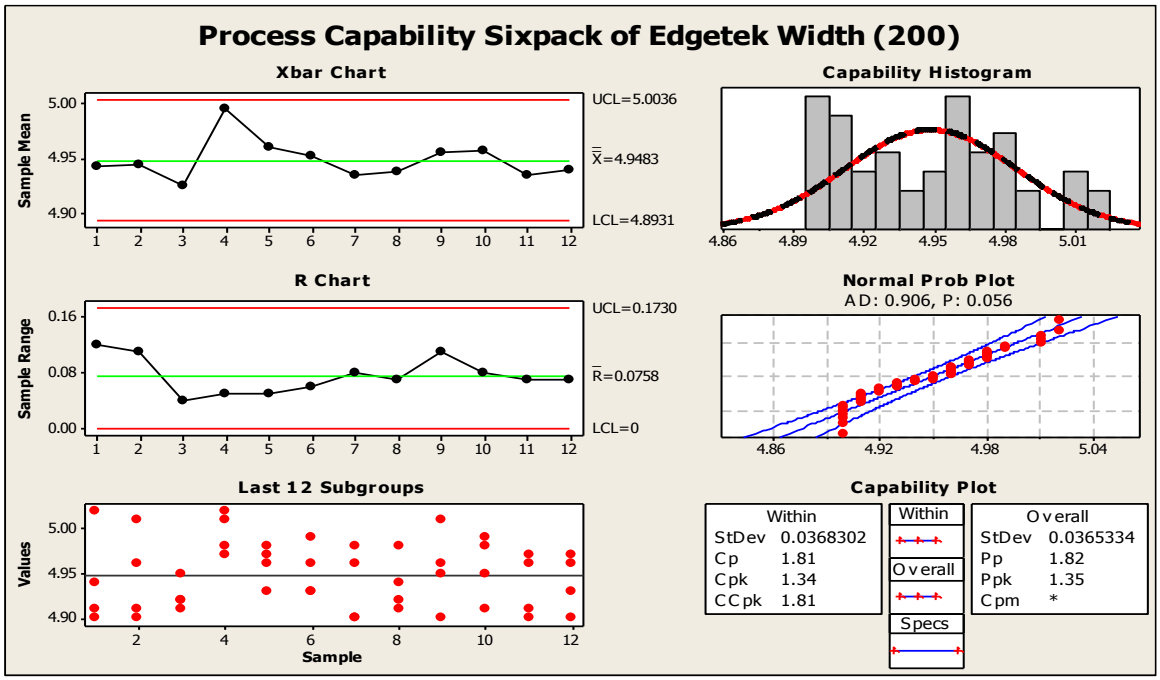

(b)

Figure A-1 (a) Process capability and (b) process capability six pack result for the width of the test sample using SAM Edgetek platform for TS of 0.2m/min

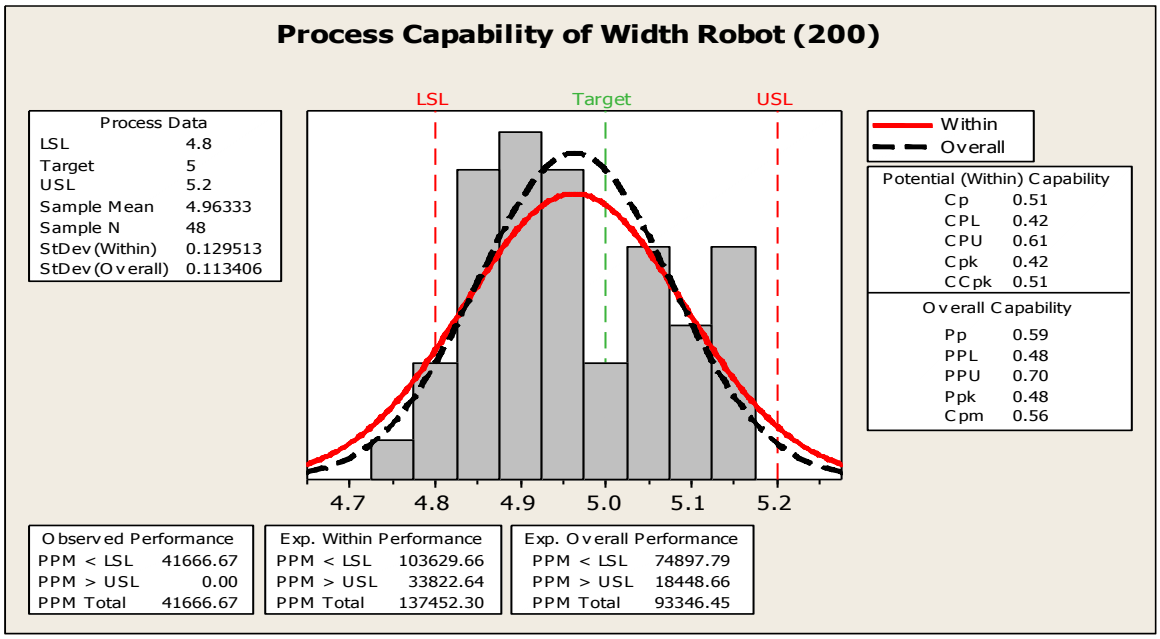

(a)

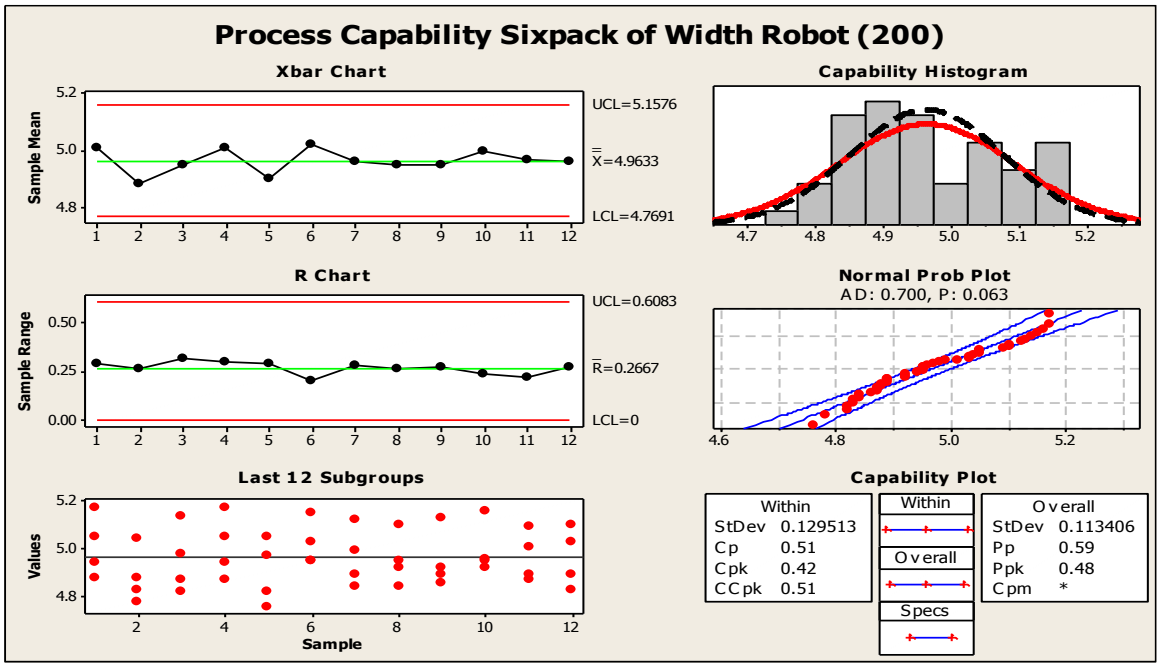

(b)

Figure A-2: (a) Process capability and (b) process capability six pack result for the width of the test sample using ABB Robot platform for TS of 0.2m/min

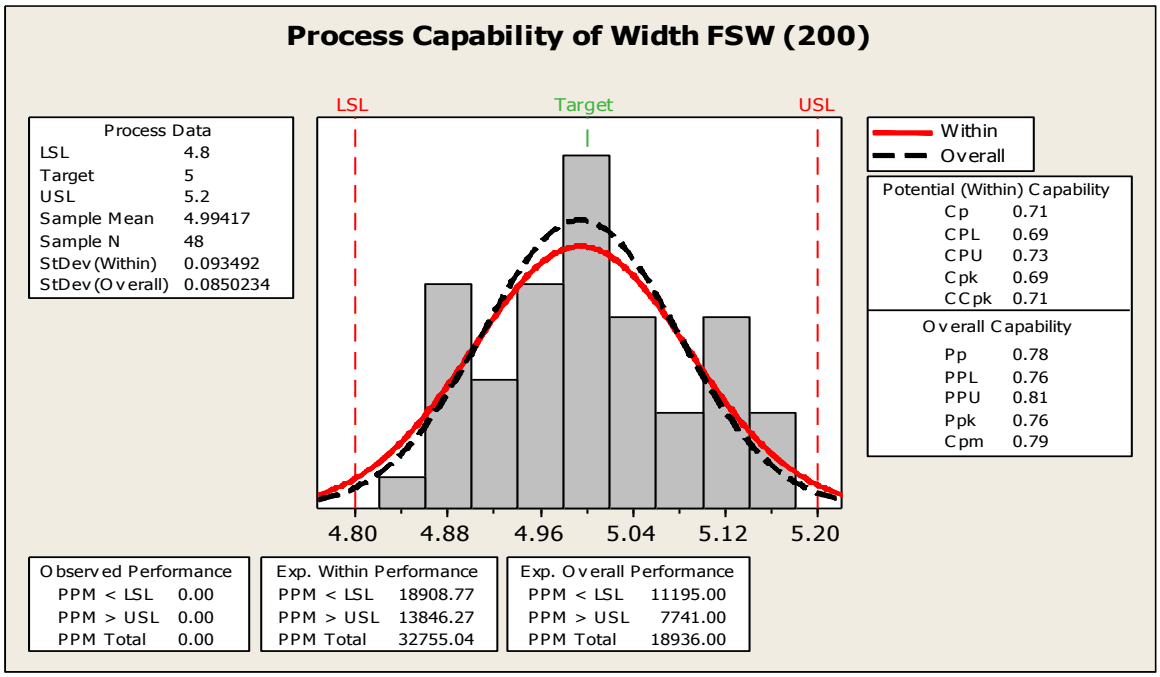

(a)

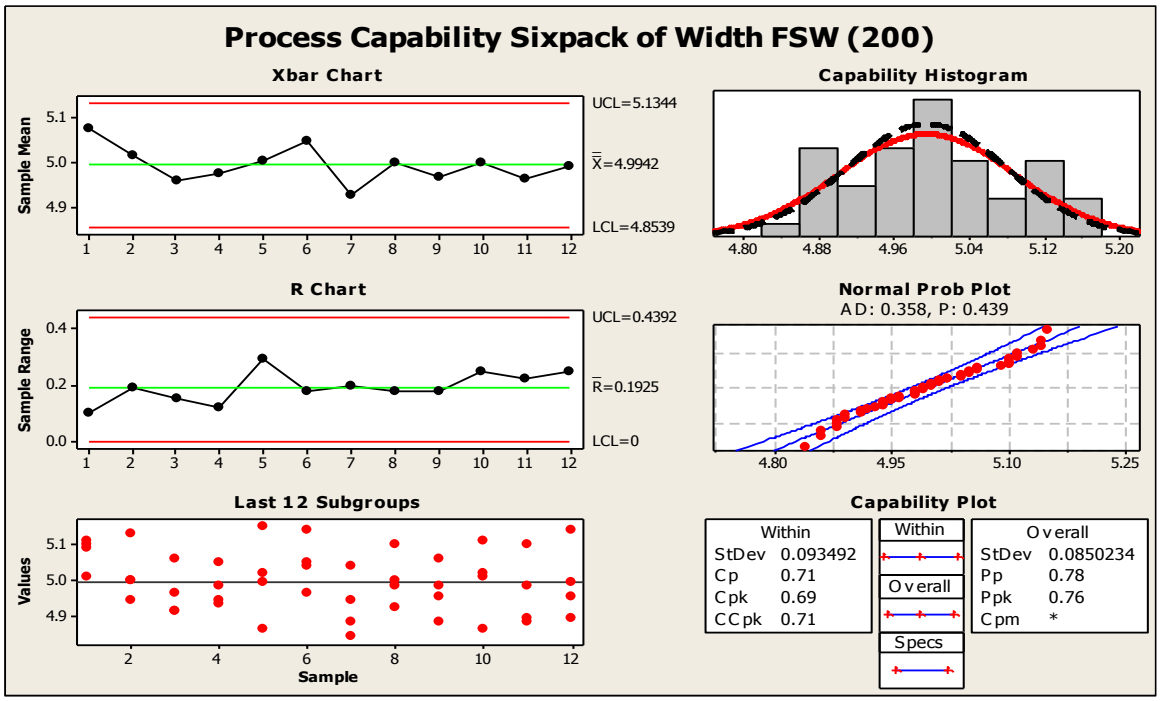

(b)

Figure A-3: (a) Process capability and (b) process capability six pack result for the width of the test sample using FSW platform for TS of 0.2m/min

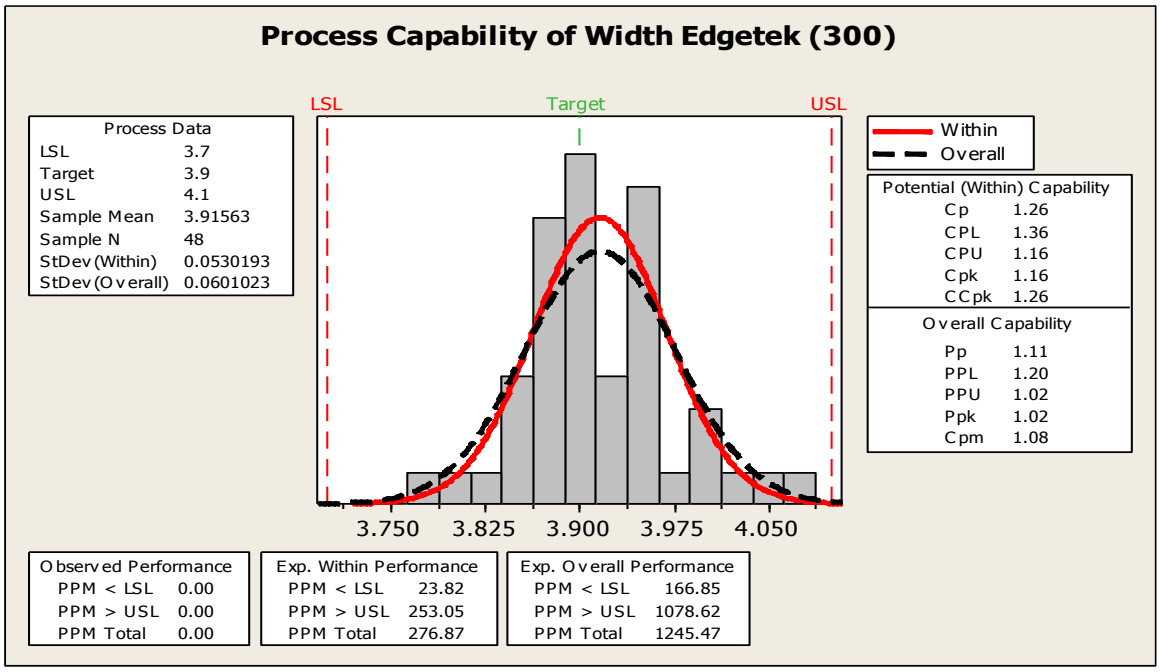

(a)

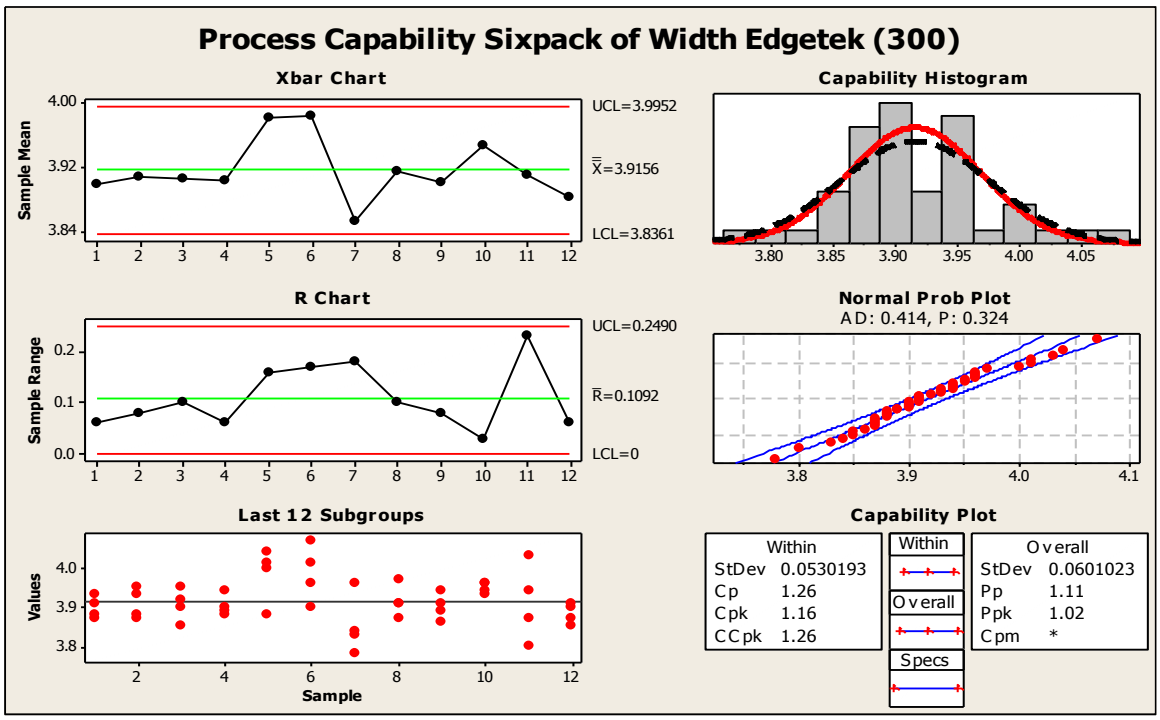

(b)

Figure A-4: (a) Process capability and (b) process capability six pack result for the width of the test sample using SAM Edgetek platform for TS of 0.3m/min

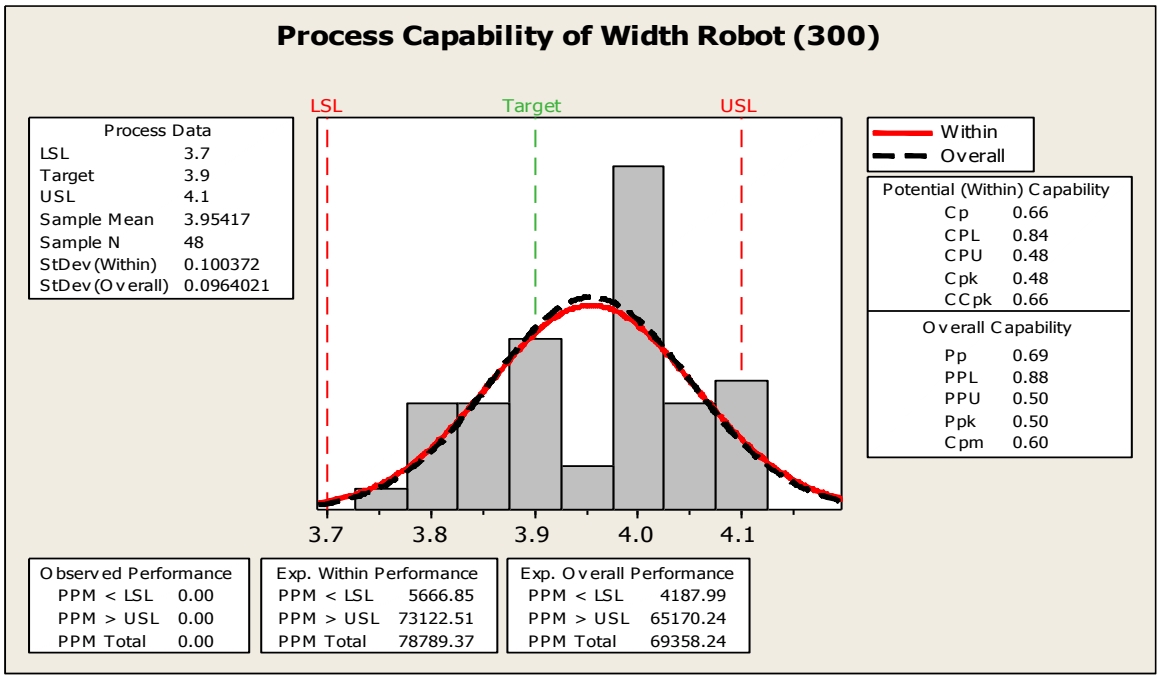

(a)

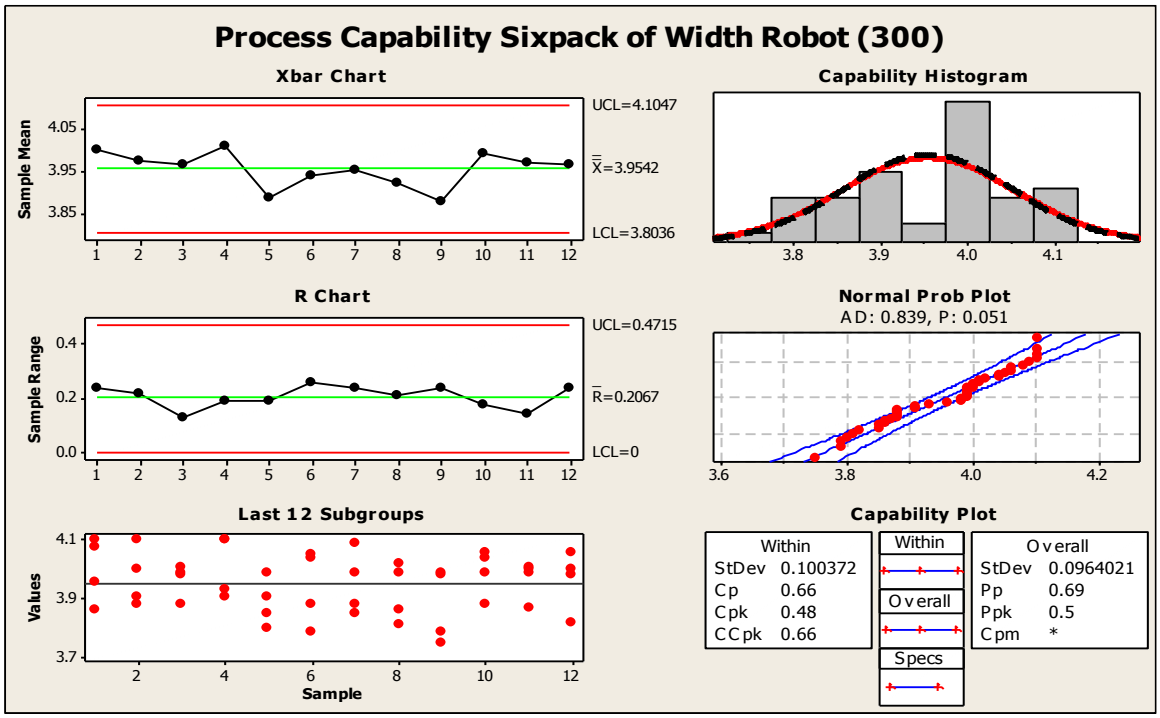

(b)

Figure A-5: (a) Process capability and (b) process capability six pack result for the width of the test sample using ABB robot platform for TS of 0.3m/min

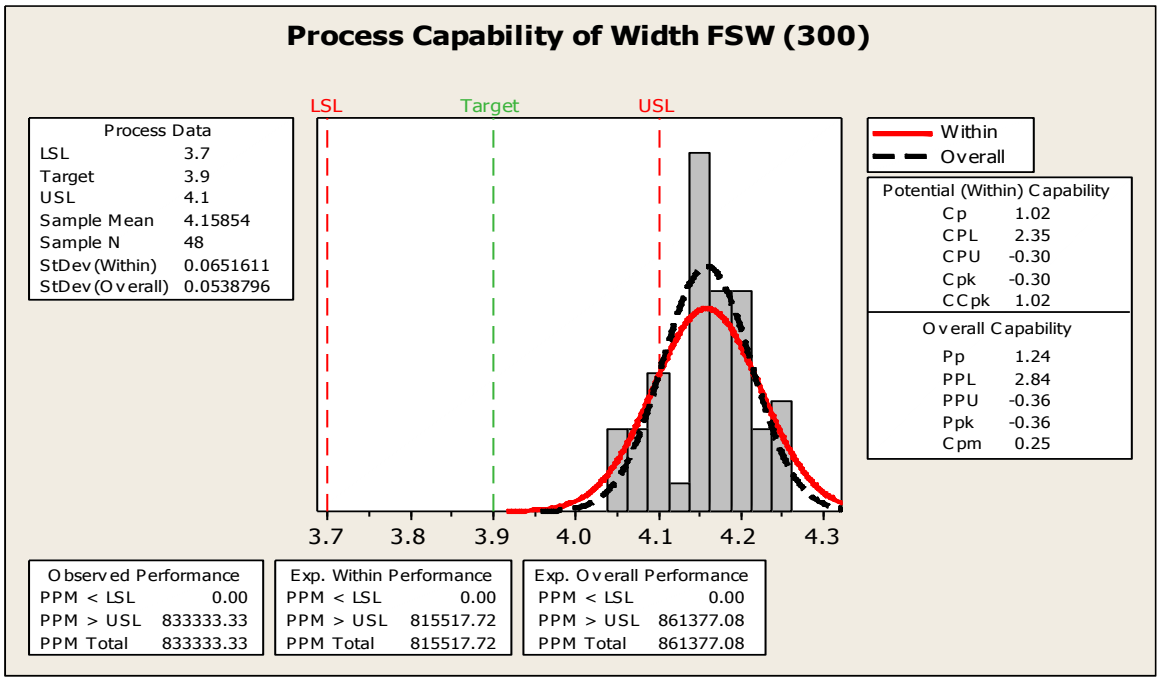

(a)

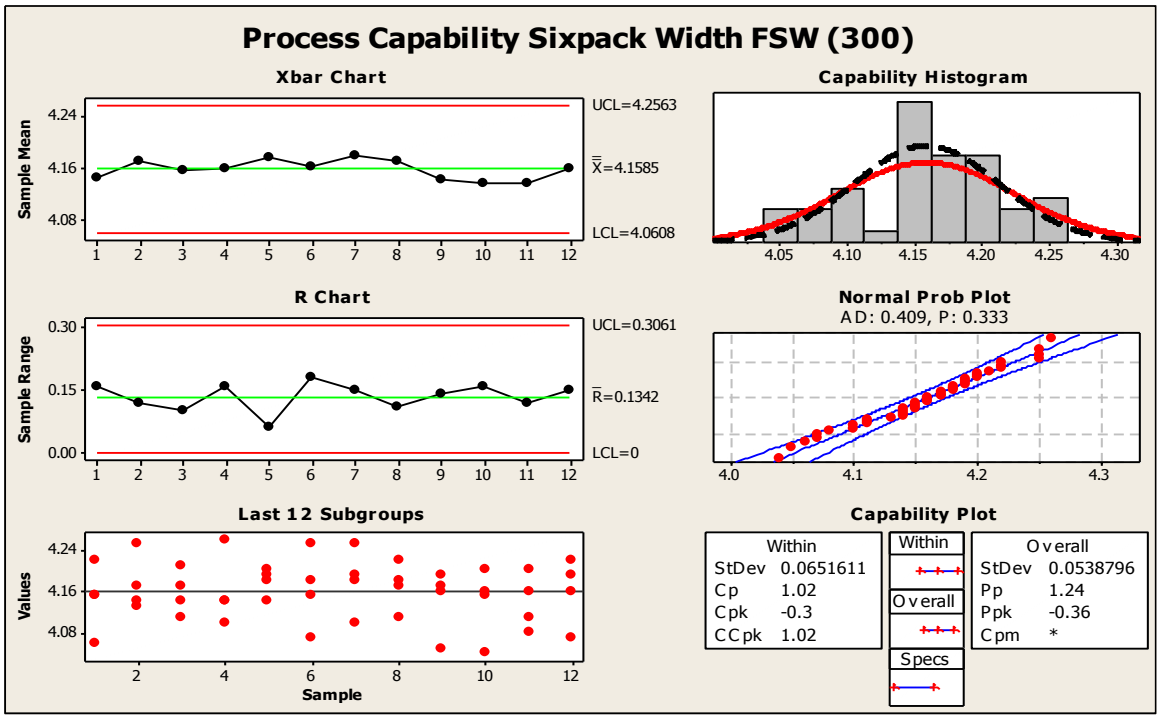

(b)

Figure A-6: (a) Process capability and (b) process capability six pack result for the width of the test sample using FSW platform for TS of 0.3m/min

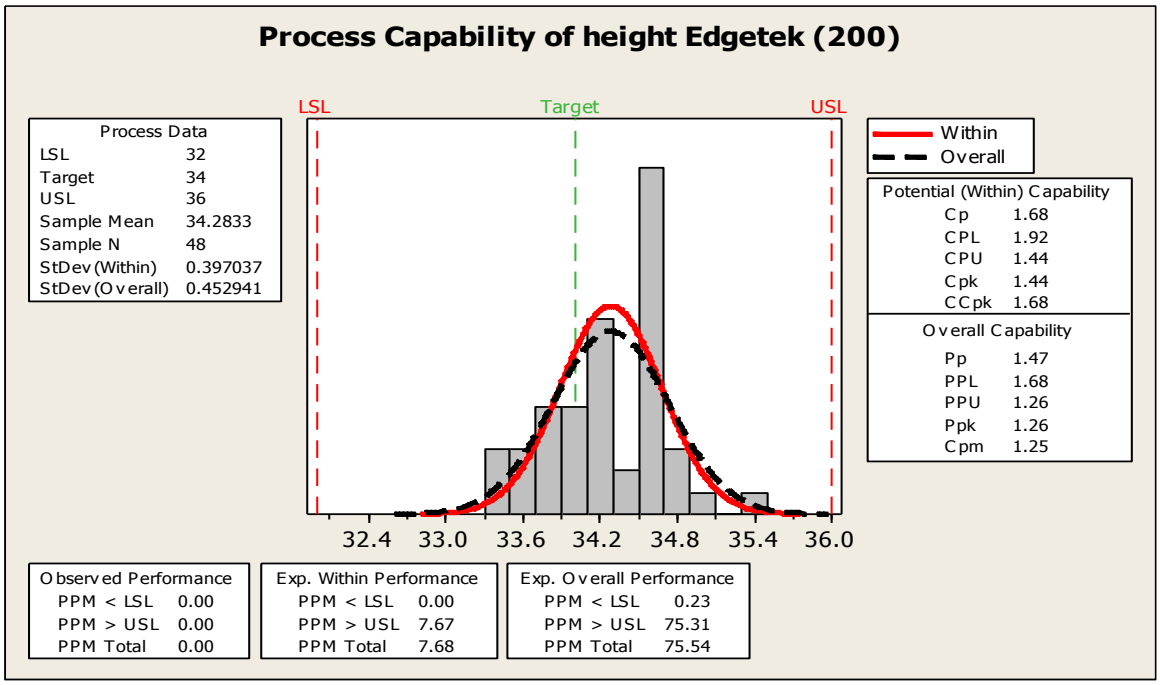

(a)

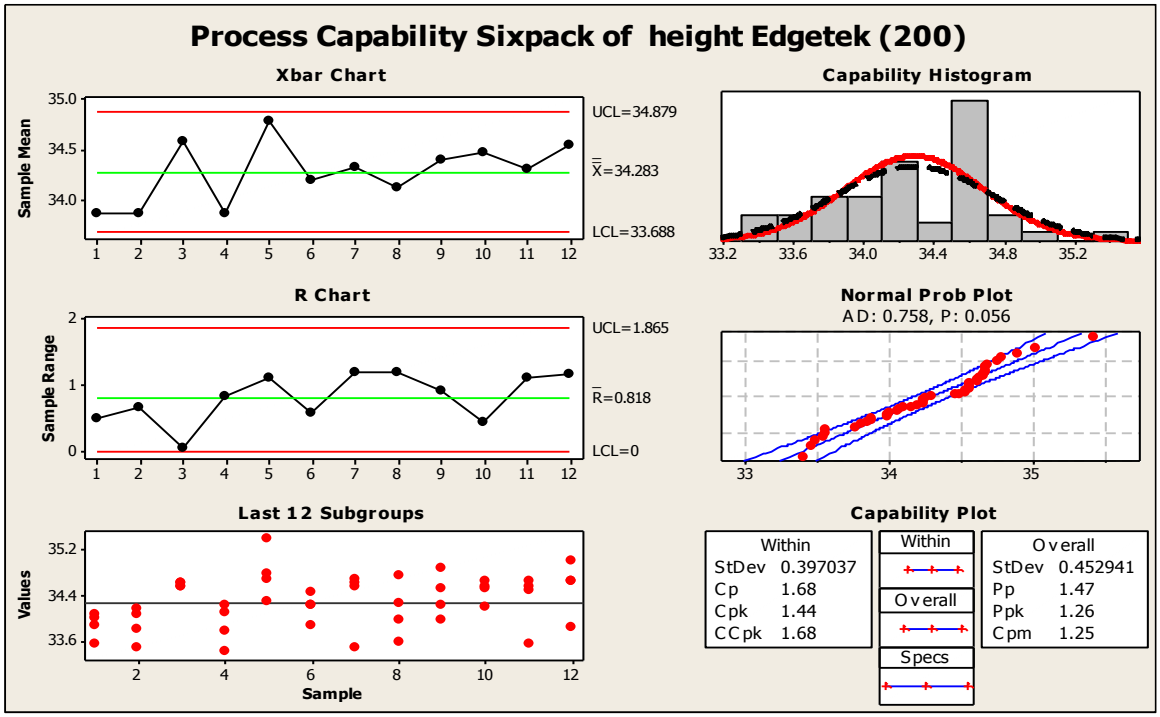

(b)

Figure A-7: (a) Process capability and (b) process capability six pack result for the height of the test sample using SAM Edgetek platform for TS of 0.2m/min

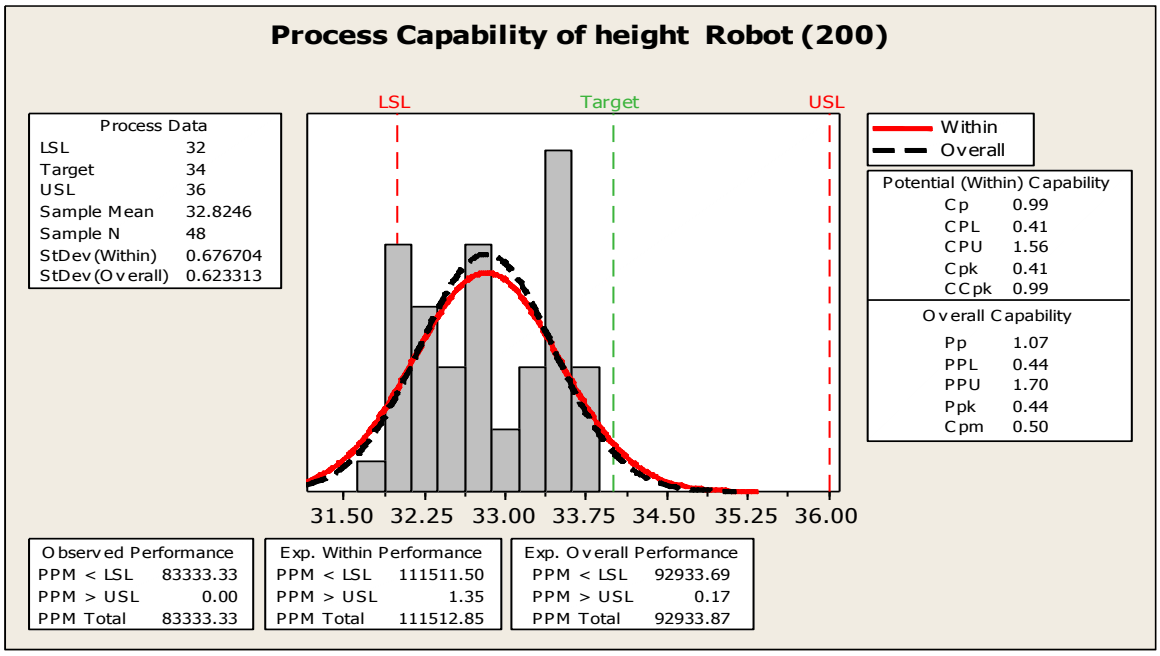

(a)

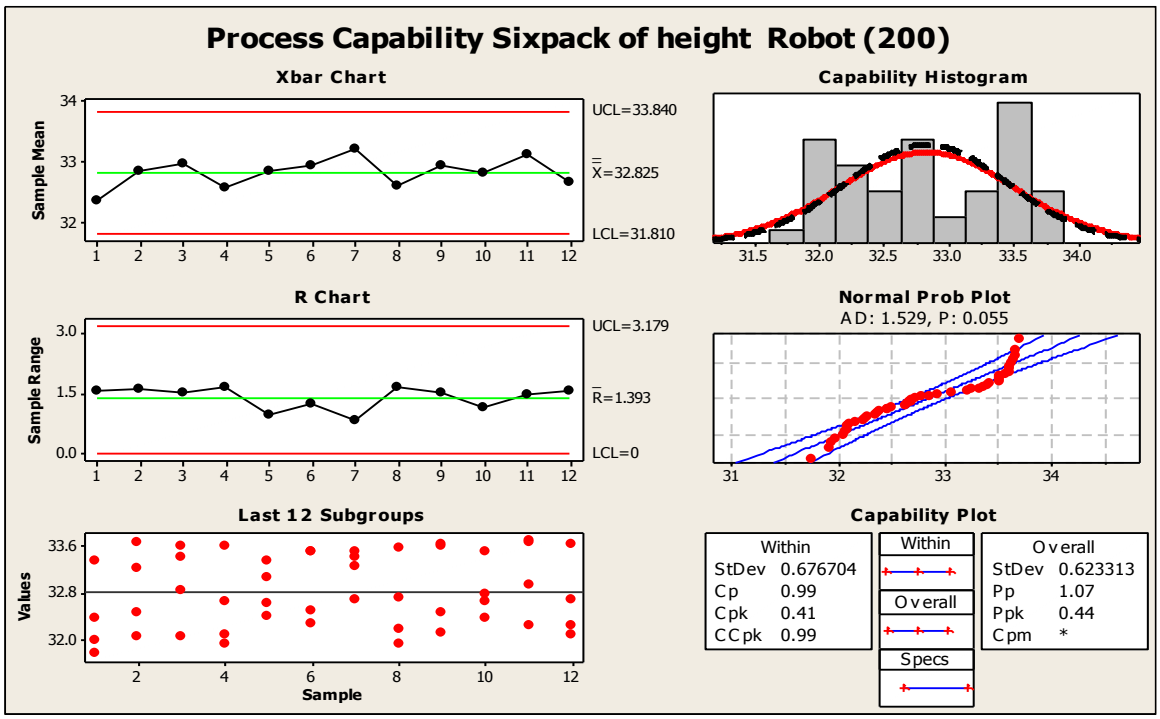

(b)

Figure A-8: (a) Process capability and (b) process capability six pack result for the height of the test sample using ABB robot platform for TS of 0.2m/min

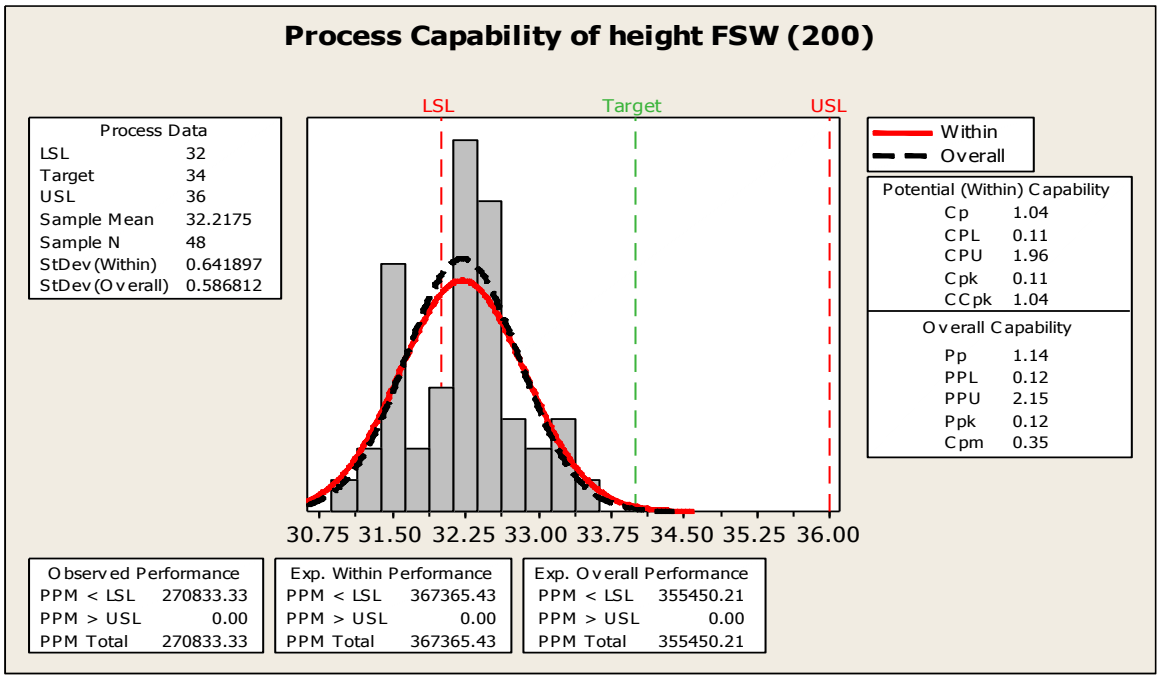

(a)

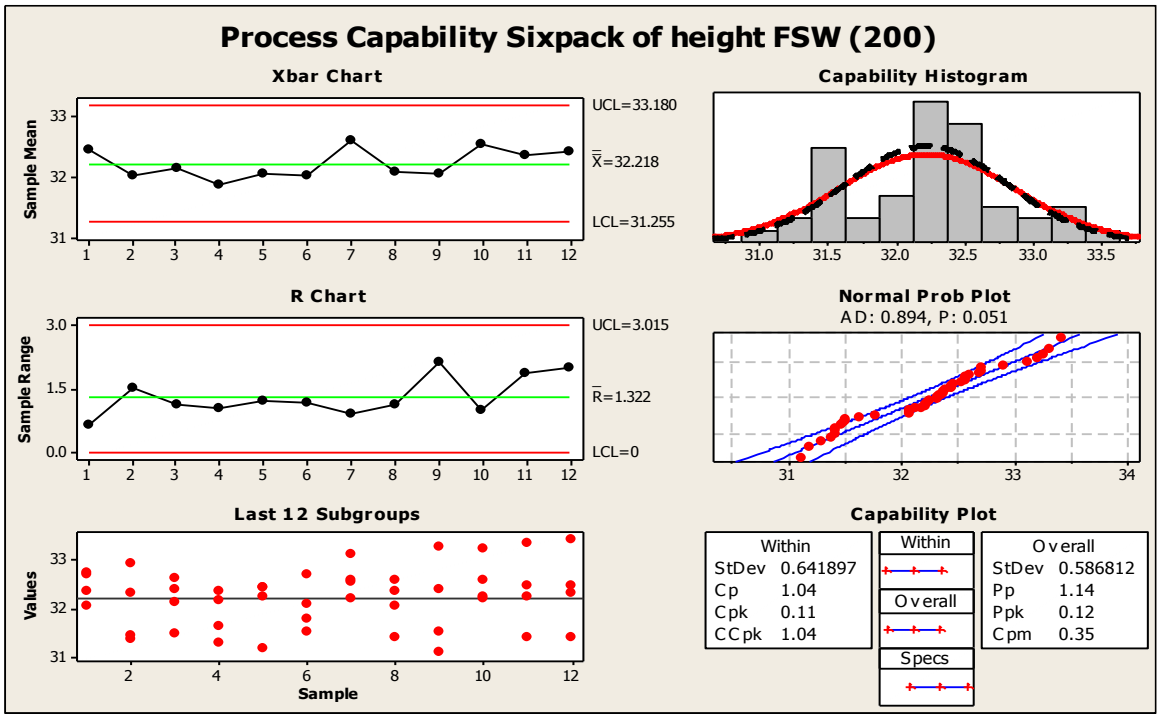

(b)

Figure A-9: (a) Process capability and (b) process capability six pack result for the height of the test sample using FSW platform for TS of 0.2m/min

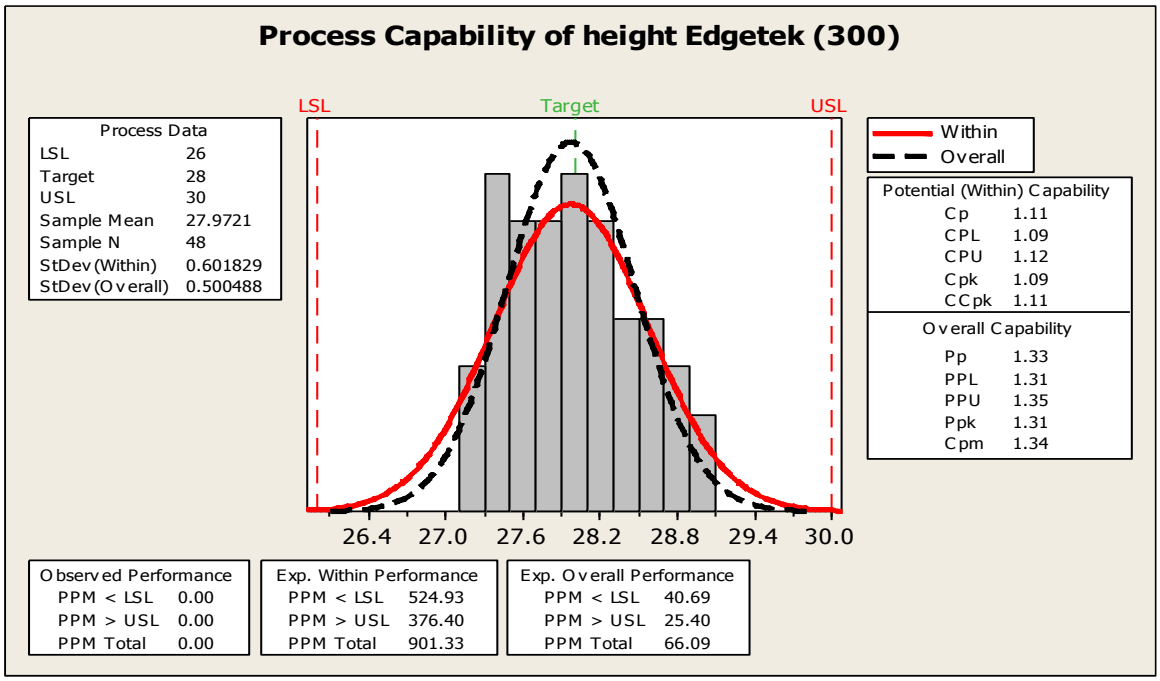

(a)

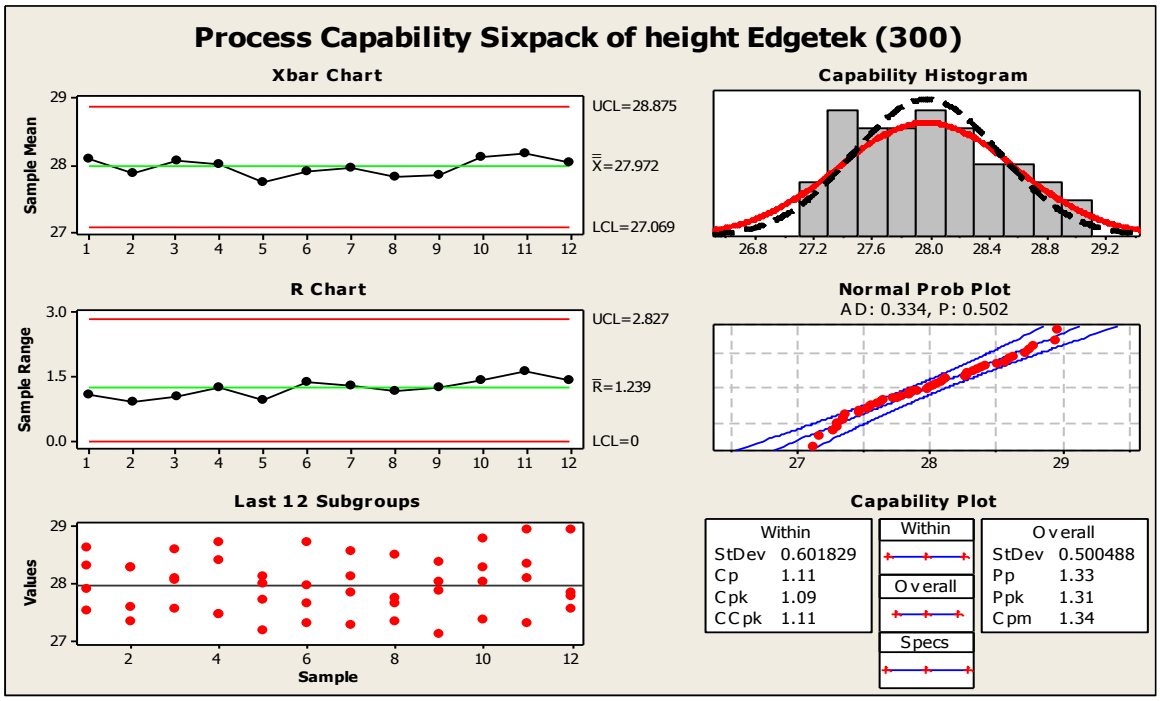

(b)

Figure A-10: (a) Process capability and (b) process capability six pack result for the height of the test sample using SAM Edgetek platform for TS of 0.3m/min

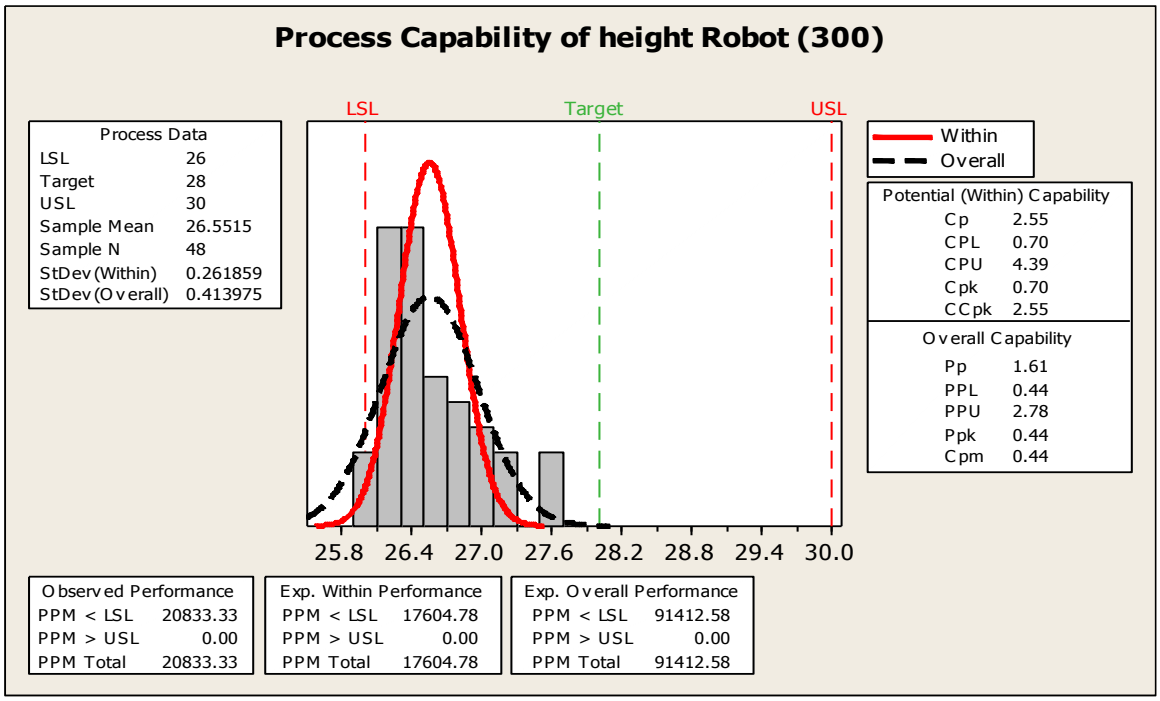

(a)

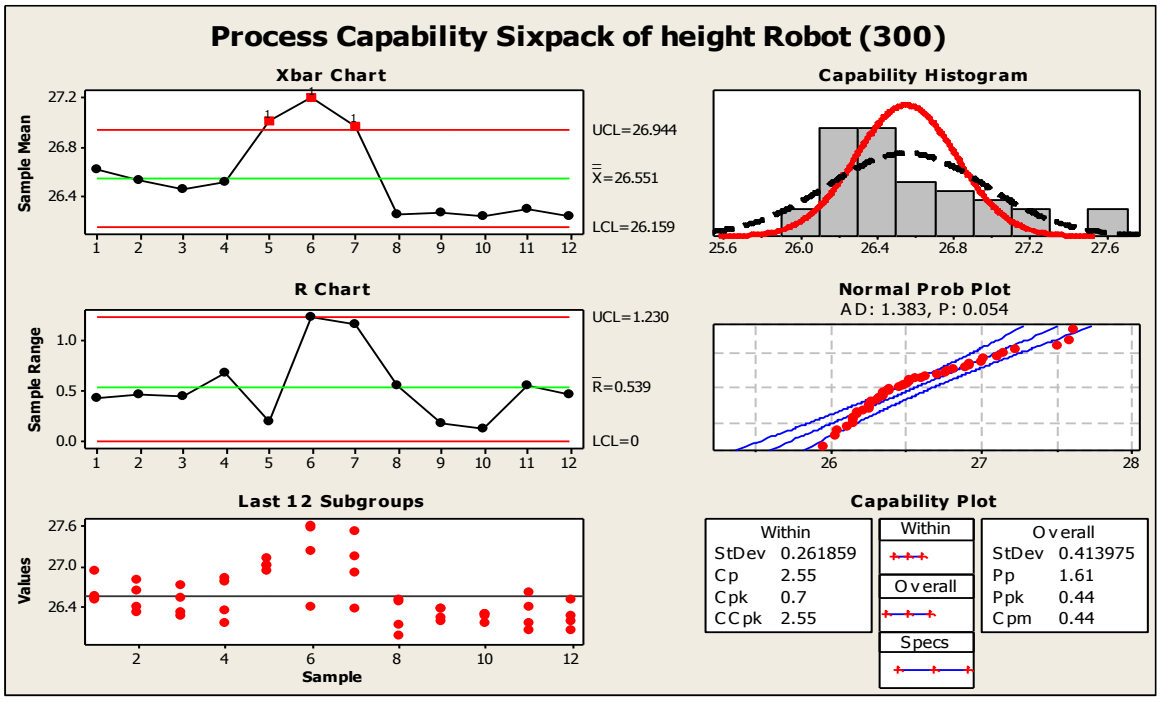

(b)

Figure A-11: (a) Process capability and (b) process capability six pack result for the height of the test sample using ABB robot platform for TS of 0.3m/min

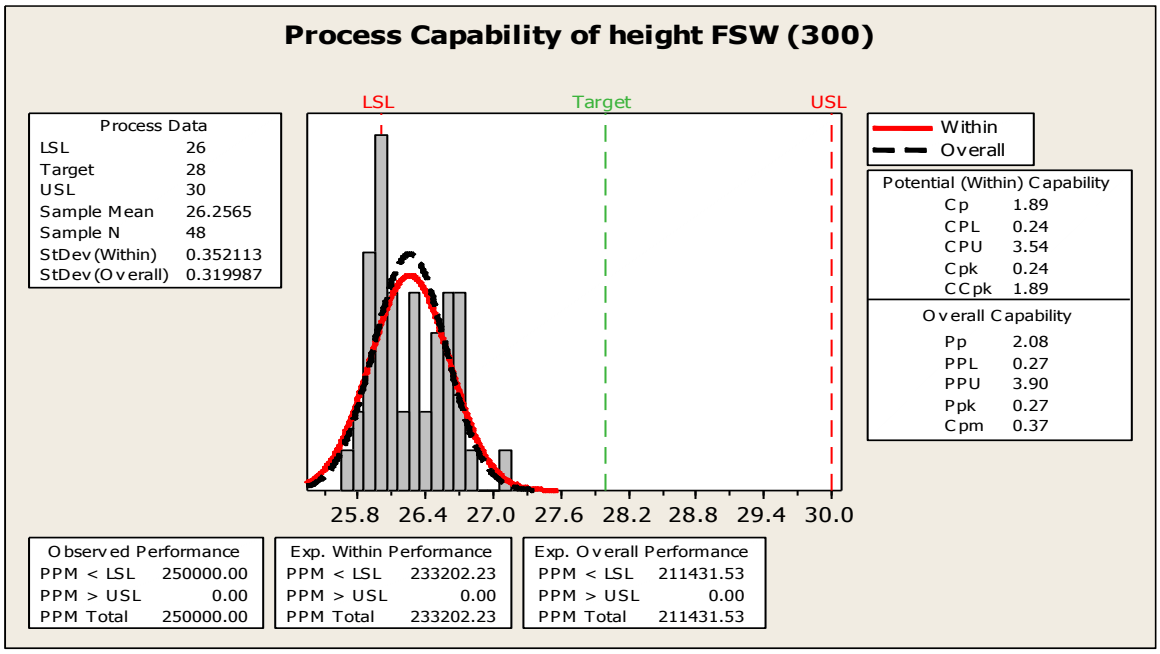

(a)

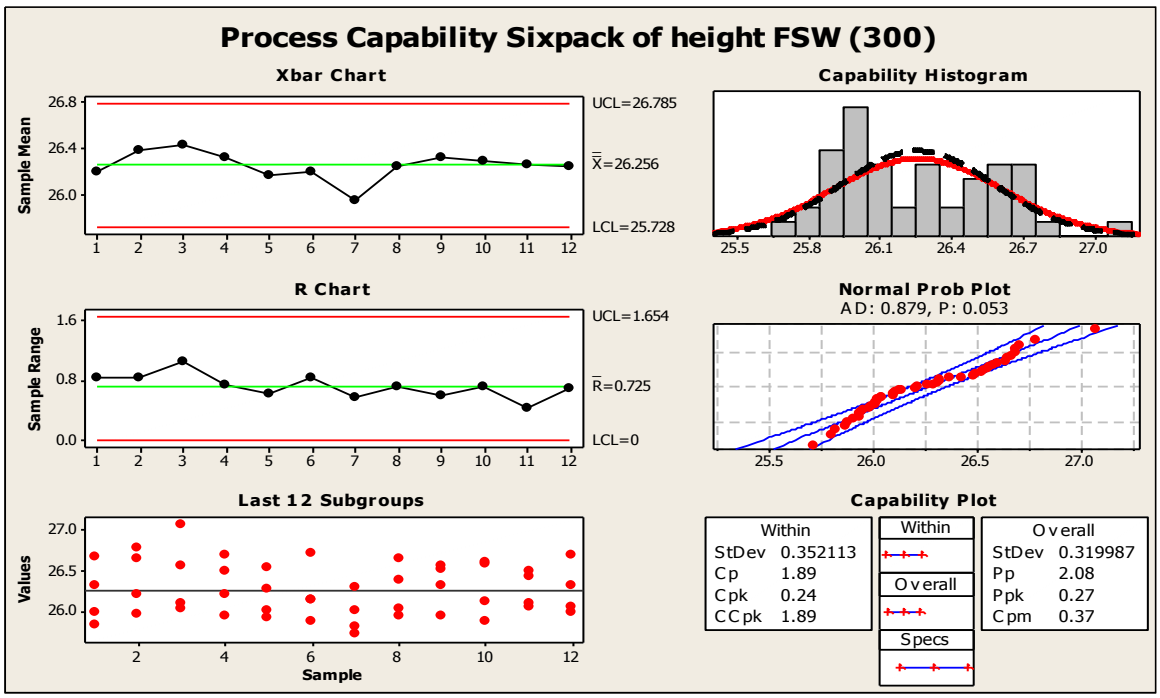

(b)

Figure A-12: (a) Process capability and (b) process capability six pack result for the height of the test sample using FSW platform for TS of 0.3m/min:

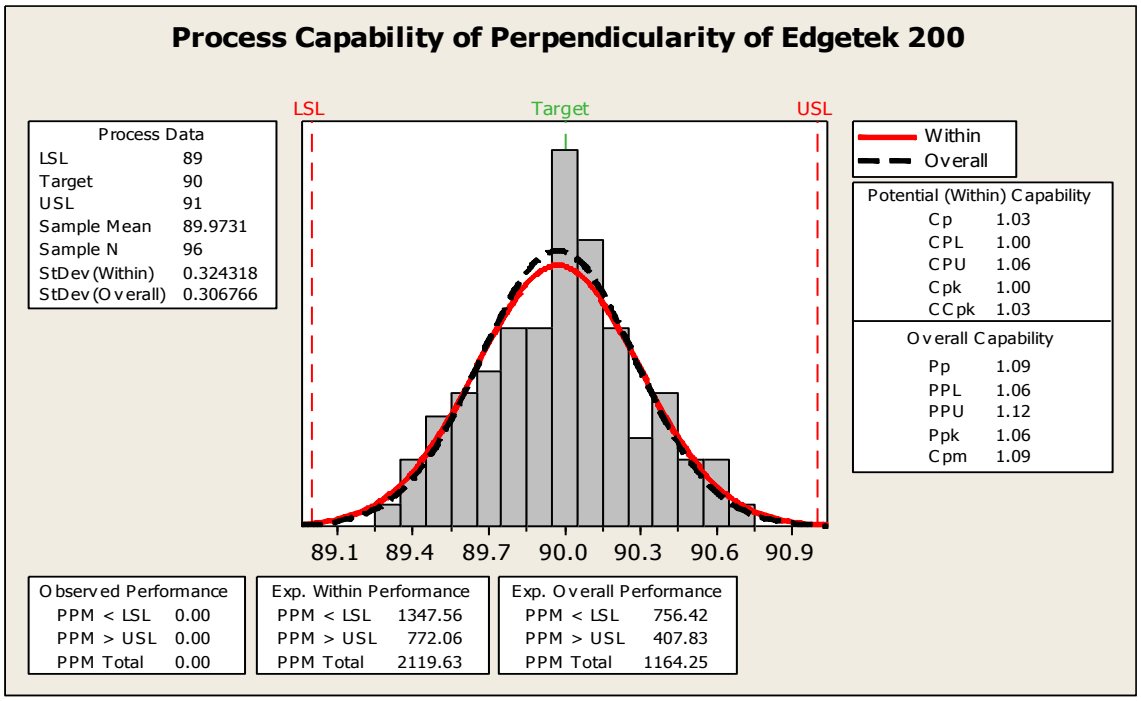

(a)

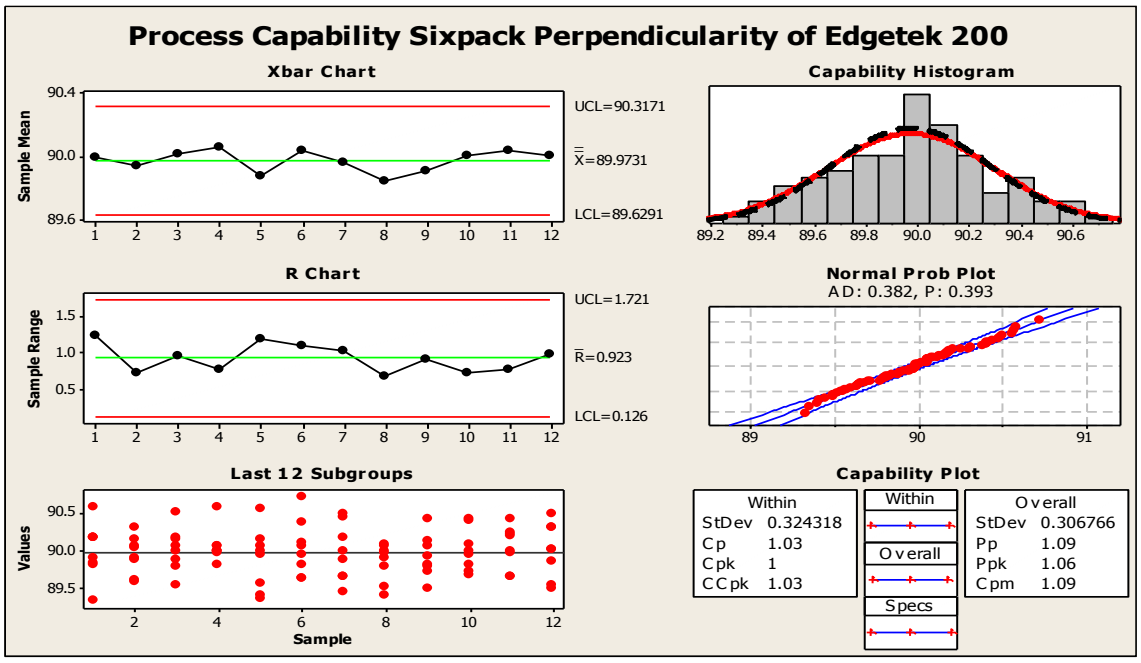

(b)

Figure A-13: (a) Process capability and (b) process capability six pack result for the perpendicularity of the test sample using SAM Edgetek platform for TS of 0.2m/min:

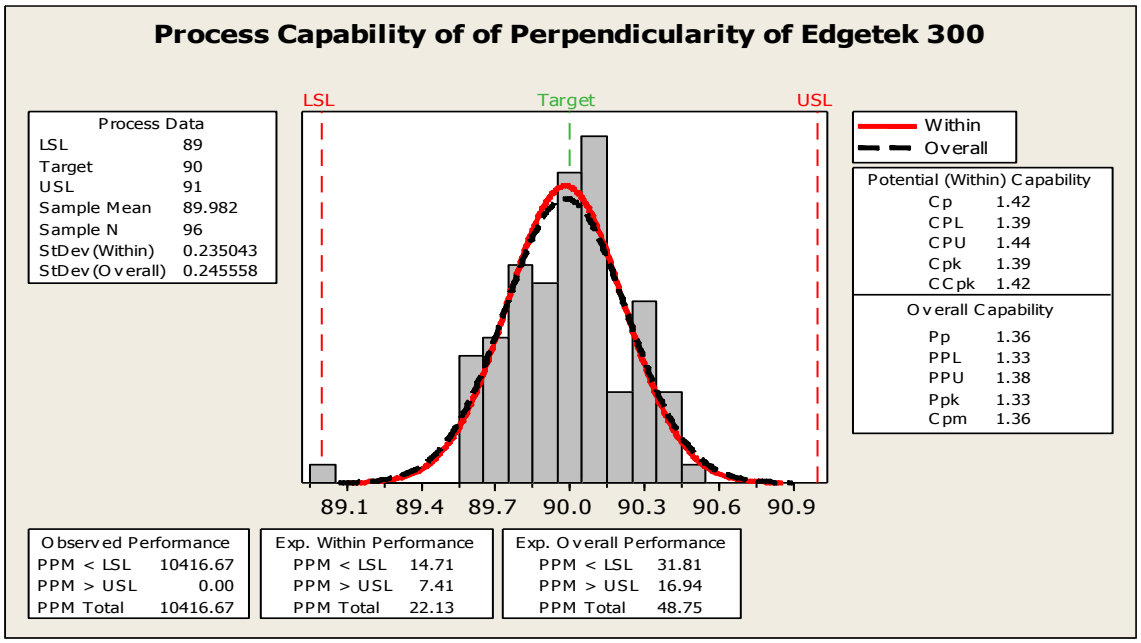

(a)

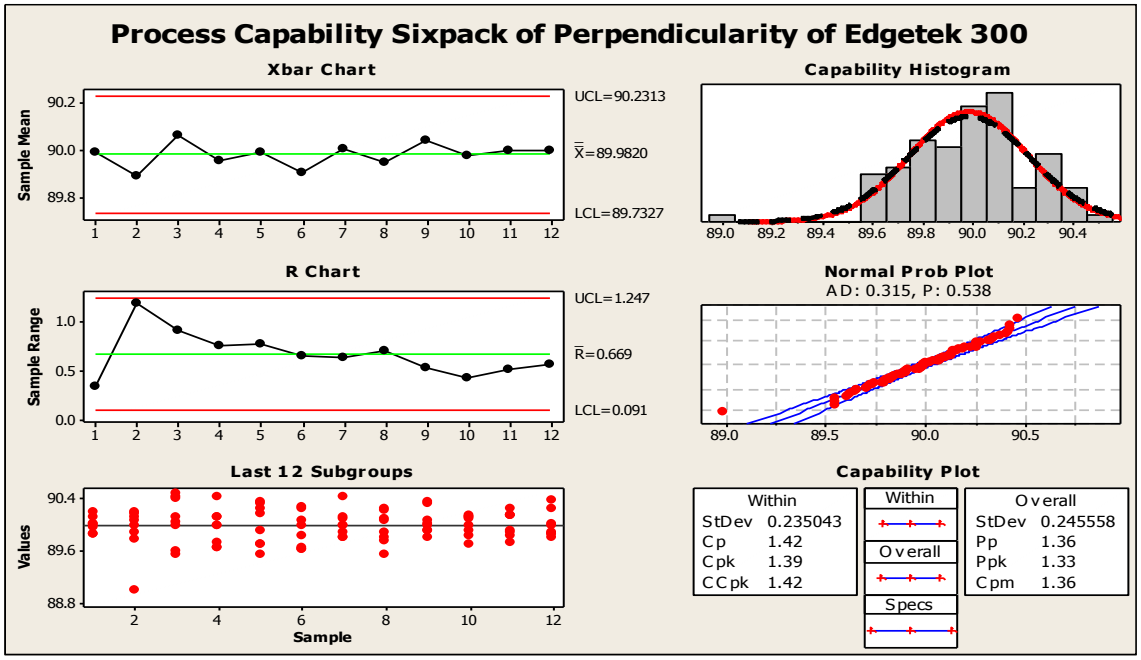

(b)

Figure A-14: (a) Process capability and (b) process capability six pack result for the perpendicularity of the test sample using SAM Edgetek platform for TS of 0.3m/min:

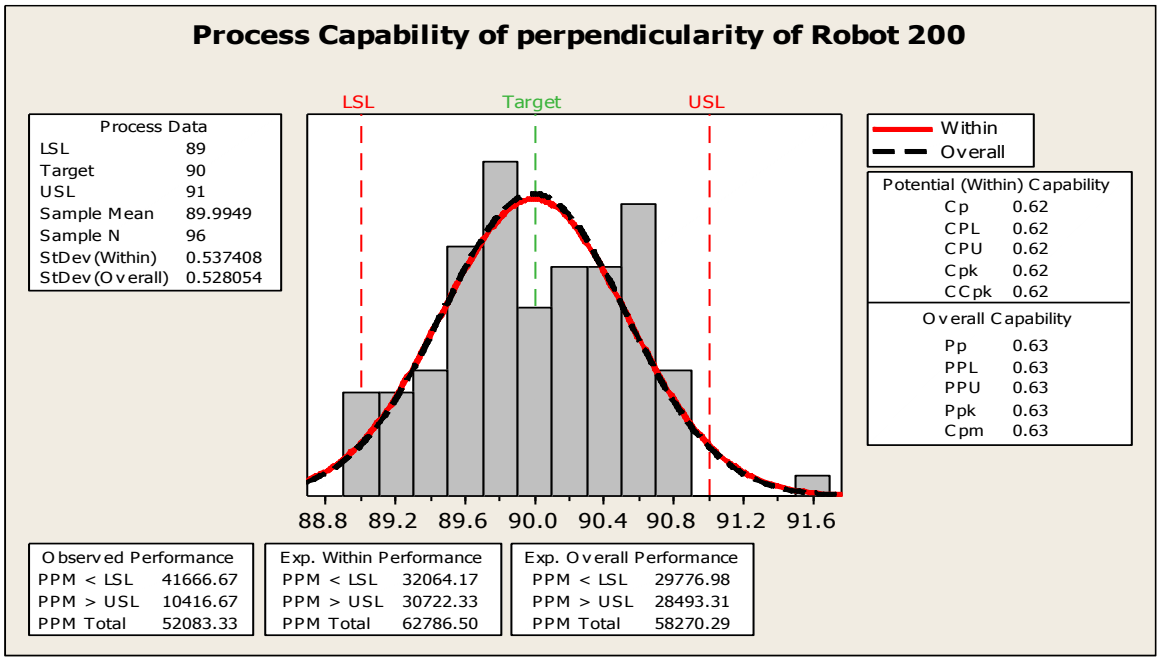

(a)

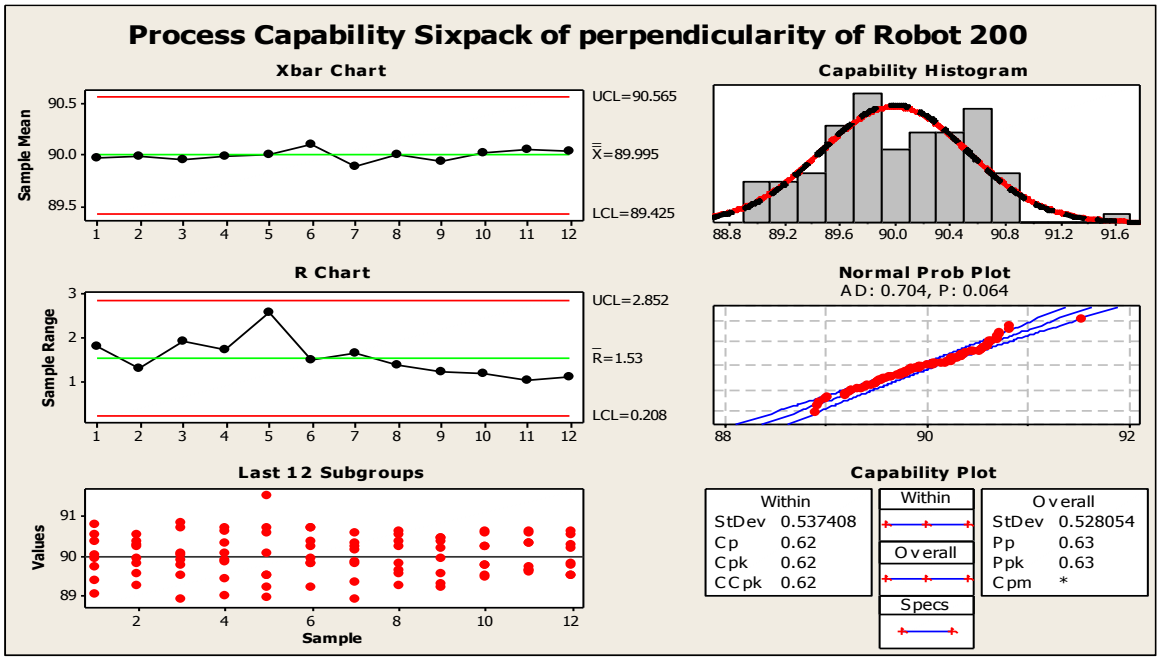

(b)

Figure A-15: (a) Process capability and (b) process capability six pack result for the perpendicularity of the test sample using ABB robot platform for TS of 0.2m/min:

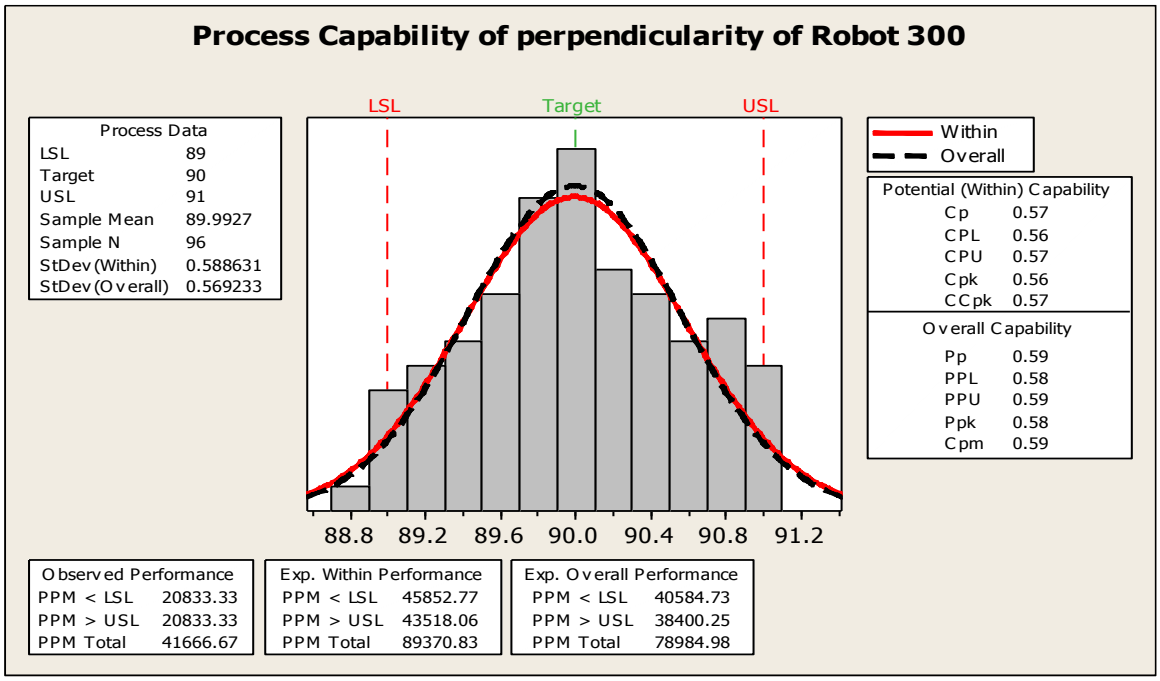

(a)

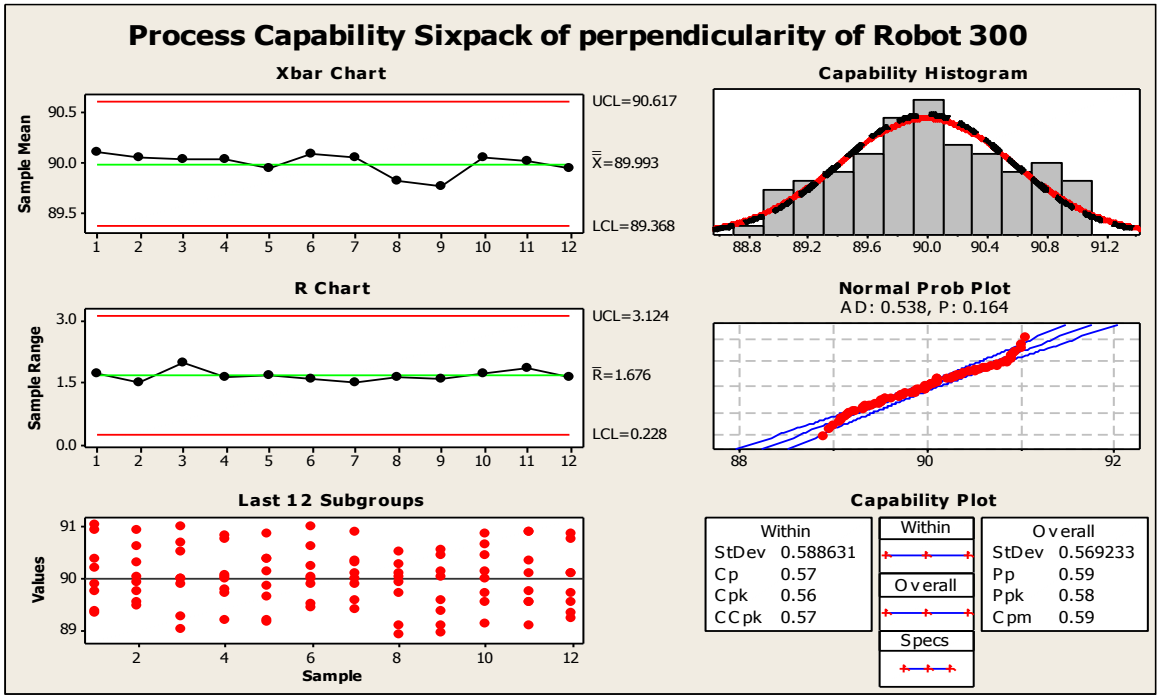

(b)

Figure A-16: (a) Process capability and (b) process capability six pack result for the perpendicularity of the test sample using ABB robot platform for TS of 0.3m/min:

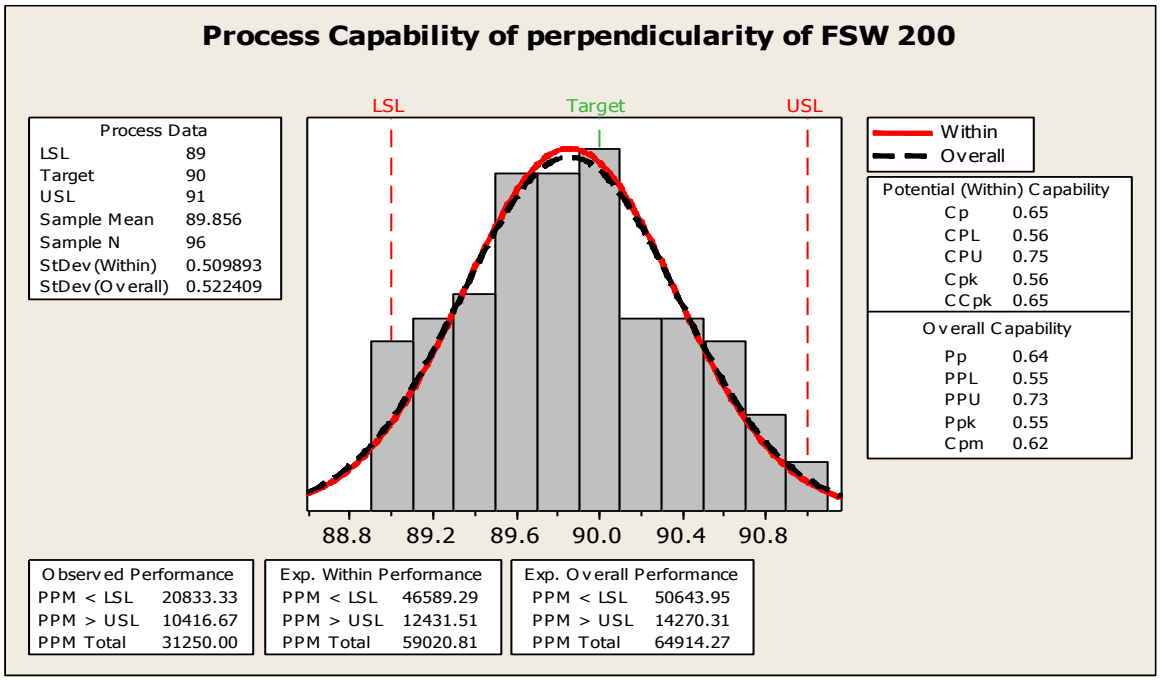

(a)

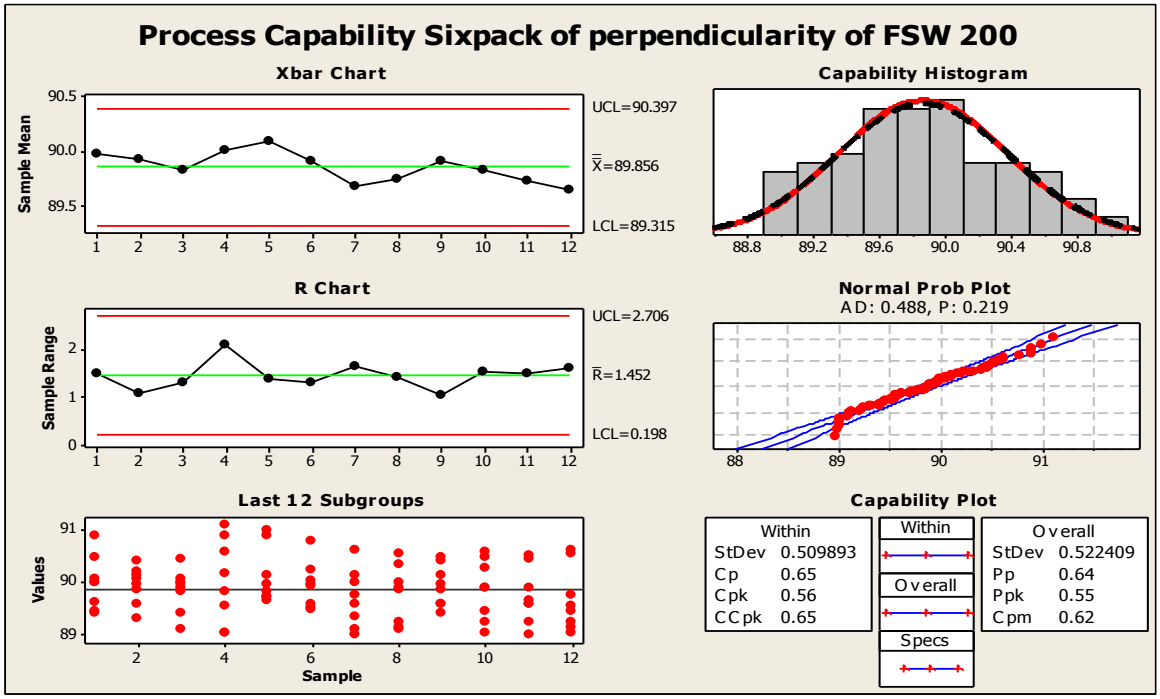

(b)

Figure A-17 : (a) Process capability and (b) process capability six pack result for the perpendicularity of the test sample using FSW platform for TS of 0.2m/min:

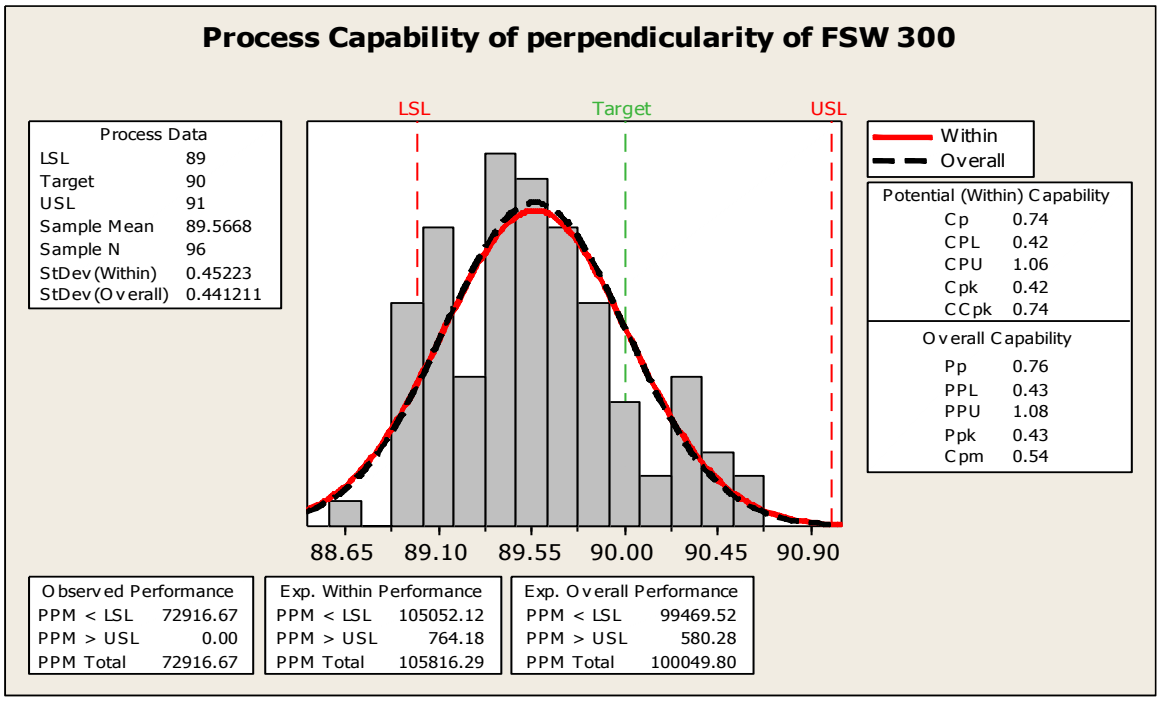

(a)

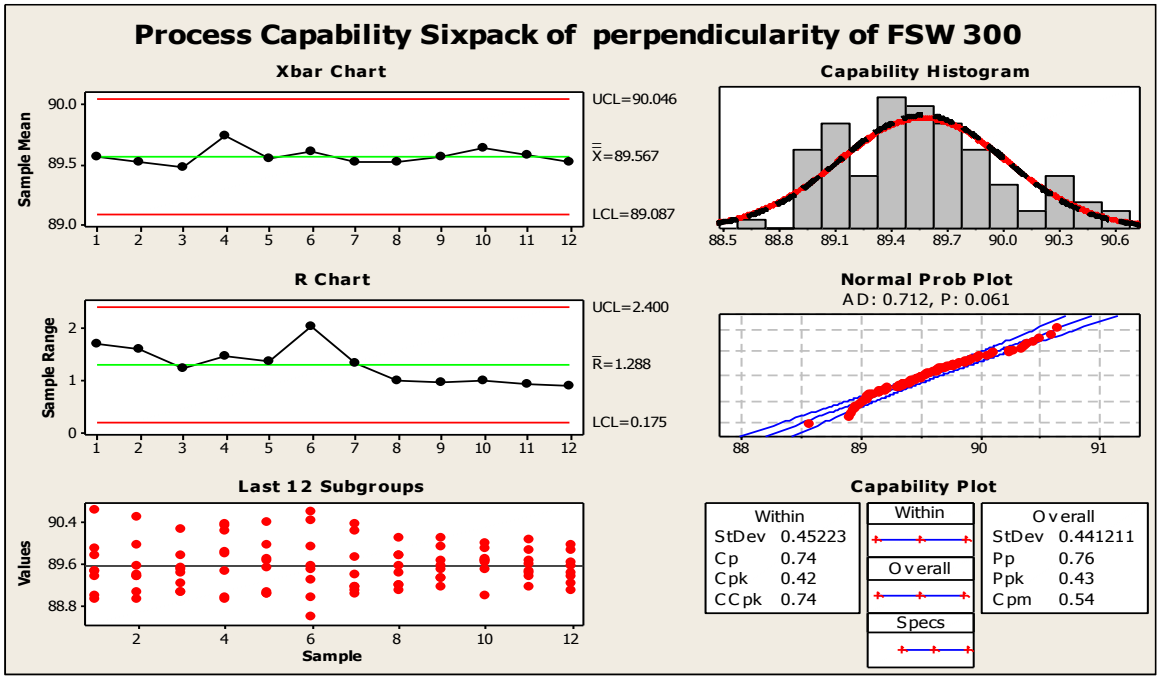

(b)

Figure A-18: (a) Process capability and (b) process capability six pack result for the perpendicularity of the test sample using FSW platform for TS of 0.3m/min:

Appendix B – Humping data

Table B- 1: Experimental design used for modelling SW_{wav}, W_{eff}, and MDE of multi-layer welds in steel for 0.8 mm wire diameter (10 layers high) (Almeida, 2012).

Trial n.	WFS_{set} (m/min)	WFS_{actual} (m/min)	WFS/TS	ΔSW (μm)	ΔSW CI (95%)	W_{eff} (mm)	W_{eff} CI (95%)	[4] TS
1a	3	1.98	30	657.31	45.45	4.26	0.03	0.10
1b	3	1.98	15	214.59	7.33	3.63	0.01	0.20
1c	3	1.98	10	205.4	40.59	2.99	0.02	0.30
1d	3	1.98	7.5	141.78	10.1	2.63	0.03	0.40
1e	3	1.98	6	101.73	4.76	2.32	0.02	0.50
1f	3	1.98	5	129.49	15.37	2.13	0.03	0.60
1g	3	1.98	4.29	-	-	-	-	0.70
1h	3	1.98	3.75	-	-	-	-	0.80
1i	3	1.98	3.33	-	-	-	-	0.90
1j	3	1.98	3	-	-	-	-	1.00
2a	5	3.77	50	833.5	41.34	6.55	0.08	0.10
2b	5	3.77	25	287.45	17.82	5.12	0.06	0.20
2c	5	3.77	16.67	270.67	48.11	4.49	0.05	0.30
2d	5	3.77	12.5	268.65	33.11	3.8	0.05	0.40
2e	5	3.77	10	250.62	21.88	3.34	0.03	0.50
2f	5	3.77	8.33	196.5	16.98	3.16	0.04	0.60
2g	5	3.77	7.14	341.17	22.15	2.58	0.01	0.70
2h	5	3.77	6.25	-	-	-	-	0.80
2i	5	3.77	5.56	-	-	-	-	0.90
2j	5	3.77	5	-	-	-	-	1.00
3a	7.5	6	75	797.17	50.48	8.11	0.07	0.10
3b	7.5	6	37.5	289.11	25.65	6.11	0.12	0.20
3c	7.5	6	25	325.98	60.27	5.22	0.07	0.30
3d	7.5	6	18.75	267.64	19.53	4.63	0.02	0.40
3e	7.5	6	15	283.46	27.48	4.34	0.09	0.50
3f	7.5	6	12.5	225.78	13.91	3.66	0.01	0.60
3g	7.5	6	10.71	255.67	22.42	3.23	0.09	0.70
3h	7.5	6	9.38	232.35	33.95	2.93	0.03	0.80
3i	7.5	6	8.33	-	-	-	-	0.90
3j	7.5	6	7.5	-	-	-	-	1.00
4a	10	8.24	100	1602.09	61.16	9.56	0.09	0.10

[4] TS in red showing the process with humps that agrees with the studies on humping.

4b	10	8.24	50	413.94	52.47	7.45	0.08	0.20
4c	10	8.24	33.33	309.7	24	6.21	0.03	0.30
4d	10	8.24	25	315.67	17.88	5.63	0.03	0.40
4e	10	8.24	20	180.66	37.79	5.24	0.06	0.50
4f	10	8.24	16.67	195.47	16.61	4.52	0.01	0.60
4g	10	8.24	14.29	178.31	4.88	4.13	0.03	0.70
4h	10	8.24	12.5	229.09	21.79	3.35	0.01	0.80
4i	10	8.24	11.11	-	-	-	-	0.90
4j	10	8.24	10	-	-	-	-	1.00
5a	12.5	10.47	125	2300	45.98	12.27	0.01	0.10
5b	12.5	10.47	62.5	646.29	14.49	9.47	0.01	0.20
5c	12.5	10.47	41.67	511	10.08	7.36	0.02	0.30
5d	12.5	10.47	31.25	431.07	20.59	6.73	0.05	0.40
5e	12.5	10.47	25	361.36	16.45	5.88	0.04	0.50
5f	12.5	10.47	20.83	232.34	5.63	5.22	0.01	0.60
5g	12.5	10.47	17.86	206.92	12.02	5.13	0.02	0.70
5h	12.5	10.47	15.63	245.65	29.26	4.73	0.04	0.80
5i	12.5	10.47	13.89	-	-	-	-	0.90
5j	12.5	10.47	12.5	-	-	-	-	1.00
6a	15	12.71	150	4300	58.56	13.35	0.05	0.10
6b	15	12.71	75	968.3	24.97	10.07	0.04	0.20
6c	15	12.71	50	740.26	33.51	8.79	0.01	0.30
6d	15	12.71	37.5	400.42	6.96	7.66	0.03	0.40
6e	15	12.71	30	272.41	17.73	6.65	0.03	0.50
6f	15	12.71	25	564.94	15.1	6	0.02	0.60
6g	15	12.71	21.43	456.65	24.16	5.43	0.07	0.70
6h	15	12.71	18.75	435.23	29.49	4.72	0.04	0.80
6i	15	12.71	16.67	517.9	54.11	4.42	0.02	0.90
6j	15	12.71	15	-	-	-	-	1.00

Appendix C – WAAM part manufacturing

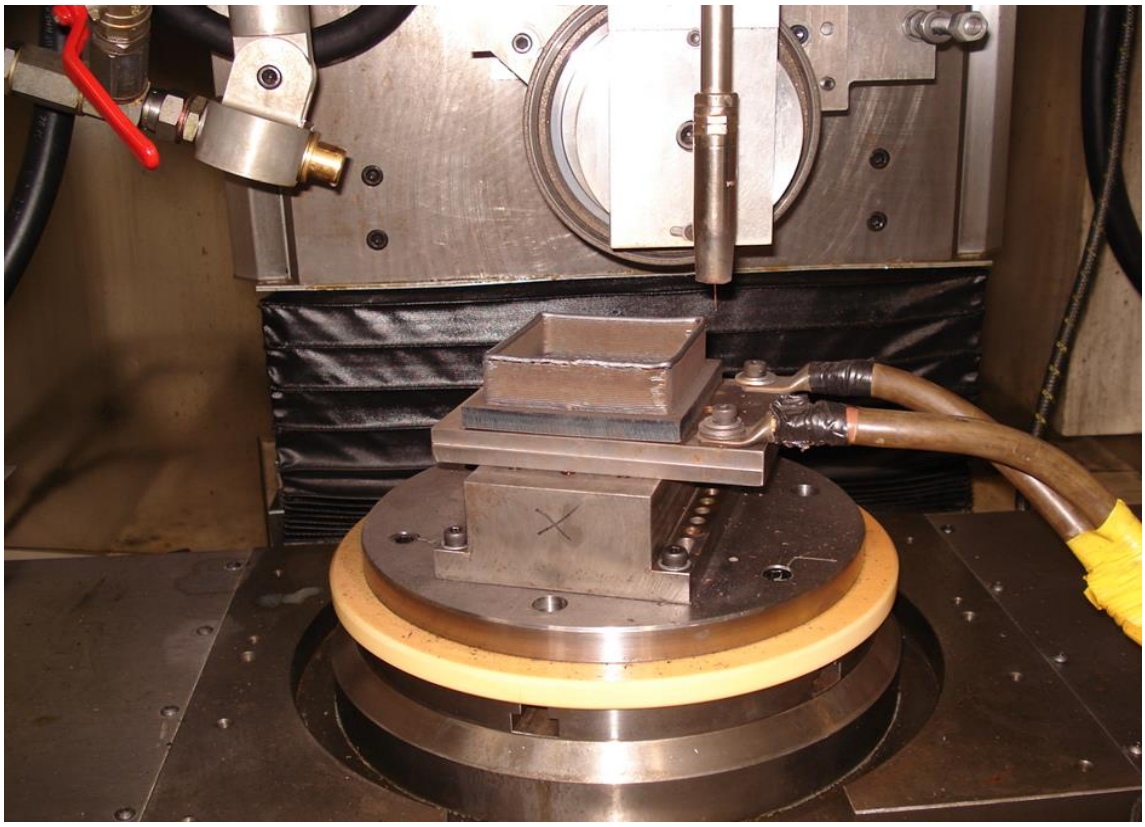

Figure C-1: Manufacturing of a sample on SAM Edgetek platform

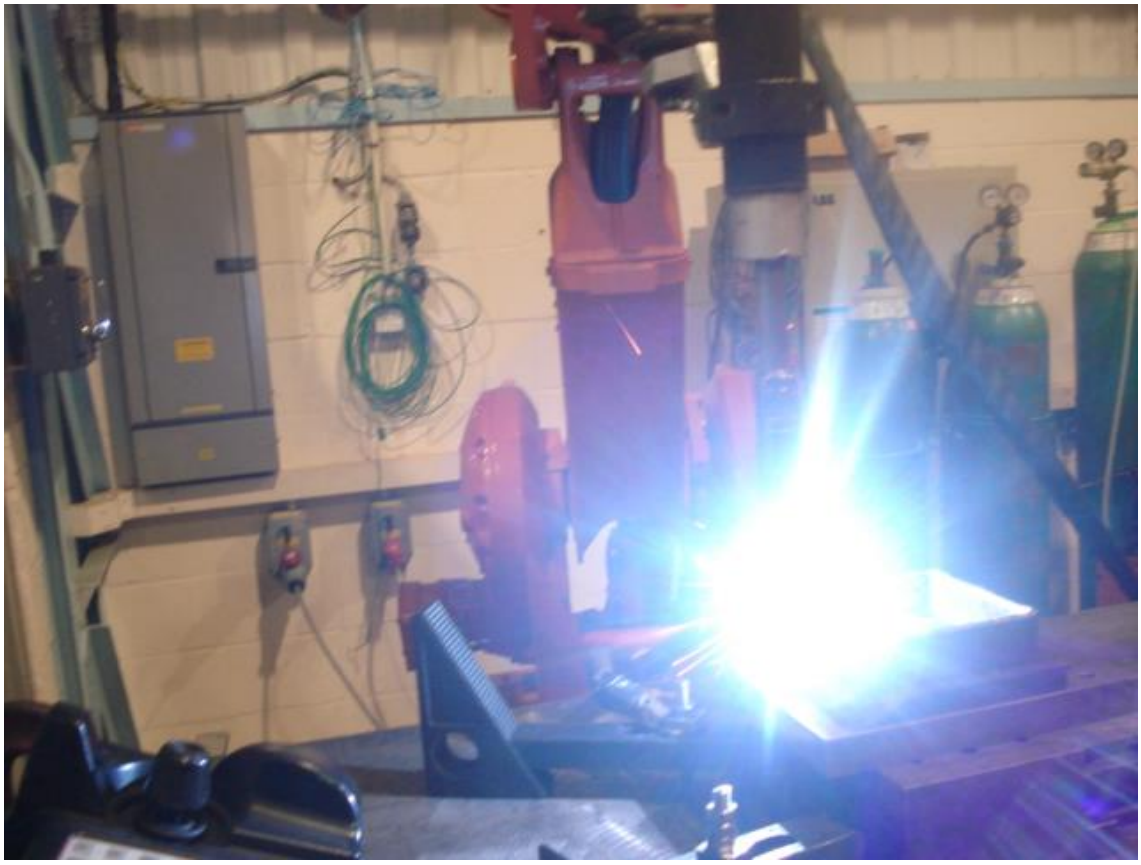

Figure C-2: Deposition of sample on ABB robot platform

Figure C-3: Some of the deposited samples in the platform comparison

LEFT BLANK INTENTIONALLY

Appendix D - Machine specifications

ABB robot specification

IRB 2400

Main applications

Arc welding, cutting/deburring, glueing/sealing, grinding/polishing, machine tending, material handling

Specification

Variants	Reach	Payload	Protection
IRB 2400-10	1.55 m	12 kg	FoundryPlus
IRB 2400-16	1.55 m	20 kg	FoundryPlus

Number of axes	6	
Mounting	Floor and inverted all versions.	
	Wall IRB 2400-10	
Supplementary load	IRB 2400-10	IRB 2400-16
Upper arm		
-wrist end	2 kg	2 kg
-rear end	10 kg	10 kg
Base unit	35 kg	35 kg

Physical

Dimensions	IRB 2400-10	IRB 2400-16
Total height	1564 mm	1564 mm
Robot base	723x600 mm	723x600 mm
Robot weight	380 kg	380 kg

Performance (according to ISO 9283)

Position repeatability (RP)	0.03 mm
Path repeatability	0.11-0.15 mm depending on variant

Movements

Axis	IRB 2400-10	IRB 2400-16
Working range		
Axis 1	360°**	360°
Axis 2	210°	210°
Axis 3	125°	125°
Axis 4	400°	400°
Axis 4, Option	Unlimited	Unlimited
Axis 5	240°	240°
Axis 6	800°	800°
Axis 6, Option	Unlimited	Unlimited
Max. speed		
Axis 1	150°/s 90° **	150°/s
Axis 2	150°/s 90° **	150°/s
Axis 3	150°/s 90° **	150°/s
Axis 4	360°/s	360°/s
Axis 5	360°/s	360°/s
Axis 6	450°/s	450°/s

**) For wall mounted version
*) ± 30° for wall mounted robot

Electrical Connections

Supply voltage	200–600 V, 50/60 Hz
Power consumption	ISO-Cube at max speed 0.67 kW

Environment

Ambient temperature for mechanical unit:

During operation	+5°C (41°F) to + 45°C (113°F)
Relative humidity	Max. 95%

Degree of protection	IRB 2400-10	IRB 2400-16
Standard	IP54	IP54
Foundry Plus 2 version	IP67	IP67

Noise level	Max. 70 dB (A)
Emission	EMC/EMI-shielded

Data and dimensions may be changed without notice

Working range

IRB 2400-10, IRB 2400-16

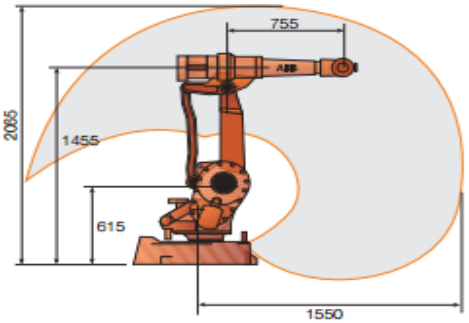

© Copyright ABB Robotics. PR10034 EN_R7 June 2012.

www.abb.com/robotics

Power and productivity for a better world™

FSW machine specification

MACHINE SPECIFICATION

CAPACITY

Max. Component height :	500mm
X axis traverse :	3,500mm
Y axis traverse:	2,000mm (2,500mm when disconnected from ballscrew)
Z axis traverse :	400mm.
Ram swivel (manual):	+/- 5°
Max. Spindle speed :	1,000 rpm
Machine weight:	33 Tonnes
Power supply:	415V, 50 Hz, 3ph
Control Voltage:	110 volts AC for contactors, Mains control Circuit & solenoids. 220 volts for panel lighting and heat exchanger. 24 volts DC for relays, limit & proximity switches and solenoids.
Control System:	GE Fanuc 18i MA

Environmental Requirements

Location	Indoors, dry location
Ambient Air Temperature	+5°C to +40°C
Humidity	35% to 95% (non condensing)
Ambient Light Level	300 lux minimum
Maximum Altitude	1000m above mean sea level

X AXIS.

Stroke	-	3,500 mm
Axis thrust	-	60 kn
Axis traverse rate (Welding)	-	Up to 1 m/min
Axis traverse rate (Rapid)	-	8 m/min
Ballscrew	-	100mm DIA x 20mm pitch
Mechanical Drive	-	Motor connected via timing belt to ballscrew. Motor pulley: 40 tooth. Ballscrew pulley: 192 tooth. Drive ratio: 4.8:1
Motor	-	Fanuc Alpha Servo Motor Model α 100/2000 100Nm at 2,000 rpm Type A06B -0332 – B077 / 7000
Motor Drive	-	Fanuc Alpha Servo Amplifier Type A06B - 6069 – H108
Feedback	-	Motor fitted with pulse encoder.

Y AXIS.

Stroke	-	2,000mm (working), 2,500 mm (manual traverse)
Axis thrust	-	60 kn
Axis traverse rate (Welding)	-	Up to 1 m/min
Axis traverse rate (Rapid)	-	8 m/min
Ballscrew	-	100mm DIA x 20mm pitch
Mechanical Drive	-	Motor connected via timing belt to ballscrew. Motor pulley: 40 tooth. Ballscrew pulley: 192 tooth. Drive ratio: 4.8:1
Motor	-	Fanuc Alpha Servo Motor Model α 100/2000 100Nm at 2,000 rpm Type A06B -0332 – B077 / 7000
Motor Drive	-	Fanuc Alpha Servo Amplifier Type A06B - 6069 – H108
Feedback	-	Motor fitted with pulse encoder.

Z AXIS.

Stroke	-	400mm
Axis thrust	-	100 kn
Axis traverse rate (Welding)	-	Up to 1 m/min
Axis traverse rate (Rapid)	-	2 m/min
Ballscrew	-	100mm DIA x 10mm pitch
Mechanical Drive	-	Motor connected via timing belt to ballscrew. Motor pulley: 48 tooth. Ballscrew pulley: 144 tooth. Drive ratio: 3:1
Motor	-	Fanuc Alpha Servo Motor with brake. Model α 100/2000 100Nm at 2,000 rpm Type A06B -0332 – B077 / 7000
Motor Drive	-	Fanuc Alpha Servo Amplifier Type A06B - 6069 – H108
Feedback	-	Motor fitted with pulse encoder.

B AXIS.

Manual Swivel	-	+/- 5°
Clamping	-	4 point jacking system
Feedback	-	Heidenhain rotary encoder (mounted inside left-hand trunnion).

SPINDLE AXIS

Mechanical Drive	-	Timing belt Motor pulley: 56 tooth Spindle pulley: 56 tooth Drive ratio : 1:1
Motor	-	Thrige Scott 60 KW 500 – 1000 rpm F.L.C 156 Amp
Motor drive	-	Controls Techniques MENTOR DRIVE STACK 4 QUAD M155-R 56KW